Mathematical and algorithmic analysis of modified Langevin dynamics

Zofia Trstanova

Communauté
UNIVERSITÉ Grenoble Alpes

THÈSE

Pour obtenir le grade de

DOCTEUR DE L'UNIVERSITÉ DE GRENOBLE

Spécialité : **Mathématiques appliquées**

Arrêté ministérial : 7 août 2006

Présentée par

Zofia Trstanova

Thèse dirigée par **Stephane Redon**
et codirigée par **Gabriel Stoltz**

préparée au sein **INRIA Grenoble Rhônes-Alpes**
et Laboratoire Jean Kuntzmann
et de **Ecole Doctorale Mathématiques, Sciences et Technologies de l'Information, Informatique**

Mathematical and Algorithmic Analysis of Modified Langevin Dynamics

Thèse soutenue publiquement le **25 novembre 2016**,
devant le jury composé de :

M. Jean-Louis Barrat
Professeur à l'Université Joseph Fourier, Président

M. Benedict Leimkuhler
Professeur à l'Université d'Edimbourg, Rapporteur

M. Grigorios A. Pavliotis
Professeur à l'Imperial College London, Rapporteur

M. Mathias Rousset
Chargé de Recherche à l'Inria Rennes, Examinateur

M. Stephane Redon
Chargé de Recherche à l'Inria Rhônes-Alpes Grenoble, Directeur de thèse

M. Gabriel Stoltz
Professeur l'Ecole des Ponts ParisTech, Co-Directeur de thèse

Summary

In statistical physics, the macroscopic information of interest for the systems under consideration can be inferred from averages over microscopic configurations distributed according to probability measures μ characterizing the thermodynamic state of the system. Due to the high dimensionality of the system (which is proportional to the number of particles), these configurations are most often sampled using trajectories of stochastic differential equations or Markov chains ergodic for the probability measure μ, which describes a system at constant temperature. One popular stochastic process allowing to sample this measure is the Langevin dynamics. In practice, the Langevin dynamics cannot be analytically integrated, its solution is therefore approximated with a numerical scheme. The numerical analysis of such discretization schemes is by now well-understood when the kinetic energy is the standard quadratic kinetic energy.

One important limitation of the estimators of the ergodic averages are their possibly large statistical errors. Under certain assumptions on potential and kinetic energy, it can be shown that a central limit theorem holds true. The asymptotic variance may be large due to the metastability of the Langevin process, which occurs as soon as the probability measure μ is multimodal.

In this thesis, we consider the discretization of modified Langevin dynamics which improve the sampling of the Boltzmann–Gibbs distribution by introducing a more general kinetic energy function U instead of the standard quadratic one. We have in fact two situations in mind:

(a) Adaptively Restrained (AR) Langevin dynamics, where the kinetic energy vanishes for small momenta, while it agrees with the standard kinetic energy for large momenta. The interest of this dynamics is that particles with low energy are restrained. The computational gain follows from the fact that the interactions between restrained particles need not be updated. Due to the separability of the position and momenta marginals of the distribution, the averages of observables which depend on the position variable are equal to the ones computed with the standard Langevin dynamics. The efficiency of this method lies in the trade-off between the computational gain and the asymptotic variance on ergodic averages which may increase compared to the standard dynamics since there are a priori more correlations in time due to restrained particles. Moreover, since the kinetic energy vanishes on some open set, the associated Langevin dynamics fails to be hypoelliptic. In fact, a first task of this thesis is to prove that the Langevin dynamics with such modified kinetic energy is ergodic. The next step is to present a mathematical analysis of the asymptotic variance for the AR-Langevin dynamics. In order to complement the analysis of this method, we estimate the algorithmic speed-up of the cost of a single iteration, as a function of the parameters of the dynamics.

(b) We also consider Langevin dynamics with kinetic energies growing more than quadratically at infinity, in an attempt to reduce metastability. The extra freedom provided by the choice of the kinetic energy should be used in order to reduce the metastability of the dynamics. In this thesis, we explore the choice of the kinetic energy and we demonstrate on a simple low-dimensional example an improved convergence of ergodic averages.

An issue with the situations we consider is the stability of discretized schemes. In order to obtain a weakly consistent method of order 2 (which is no longer trivial for a general kinetic energy), we rely on the recently developped Metropolis schemes.

Résumé

En physique statistique, l'information macroscopique d'intérêt pour les systèmes considérés peut être déduite à partir de moyennes sur des configurations microscopiques réparties selon des mesures de probabilité μ caractérisant l'état thermodynamique du système. En raison de la haute dimensionnalité du système (qui est proportionnelle au nombre de particules), les configurations sont le plus souvent échantillonnées en utilisant des trajectoires d'équations différentielles stochastiques ou des chaînes de Markov ergodiques pour la mesure de Boltzmann-Gibbs μ, qui décrit un système à température constante. Un processus stochastique classique permettant d'échantillonner cette mesure est la dynamique de Langevin. En pratique, les équations de la dynamique de Langevin ne peuvent pas être intégrées analytiquement, la solution est alors approchée par un schéma numérique. L'analyse numérique de ces schémas de discrétisation est maintenant bien maîtrisée pour l'énergie cinétique quadratique standard. Une limitation importante des estimateurs des moyennes sont leurs éventuelles grandes erreurs statistiques. Sous certaines hypothèses sur les énergies cinétique et potentielle, il peut être démontré qu'un théorème de limite central est vrai. La variance asymptotique peut être grande en raison de la métastabilité du processus de Langevin, qui se produit dès que la mesure de probabilité μ est multimodale.

Dans cette thèse, nous considérons la discrétisation de la dynamique de Langevin modifiée qui améliore l'échantillonnage de la distribution de Boltzmann-Gibbs en introduisant une fonction cinétique plus générale à la place de la formulation quadratique standard. Nous avons en fait deux situations en tête : (a) La dynamique de Langevin Adaptativement Restreinte, où l'énergie cinétique s'annule pour les faibles moments, et correspond à l'énergie cinétique standard pour les forts moments. L'intérêt de cette dynamique est que les particules avec une faible énergie sont restreintes. Le gain vient alors du fait que les interactions entre les particules restreintes ne doivent pas être mises à jour. En raison de la séparabilité des positions et des moments marginaux de la distribution, les moyennes des observables qui dépendent de la variable de position sont égales à celles calculées par la dynamique de Langevin standard. L'efficacité de cette méthode réside dans le compromis entre le gain de calcul et la variance asymptotique des moyennes ergodiques qui peut augmenter par rapport à la dynamique standards car il existe a priori plus des corrélations dans le temps en raison de particules restreintes. De plus, étant donné que l'énergie cinétique est nulle sur un ouvert, la dynamique de Langevin associé ne parvient pas à être hypoelliptique. La première tâche de cette thèse est de prouver que la dynamique de Langevin avec une telle énergie cinétique est ergodique. L'étape suivante consiste à présenter une analyse mathématique de la variance asymptotique de la dynamique AR-Langevin. Afin de compléter l'analyse de ce procédé, on estime l'accélération algorithmique du coût d'une seule itération, en fonction des paramètres de la dynamique. (b) Nous considérons aussi la dynamique de Langevin avec des énergies cinétiques dont la croissance est plus que quadratique à l'infini, dans une tentative de réduire la métastabilité. La liberté supplémentaire fournie par le choix de l'énergie cinétique doit être utilisée afin de réduire la métastabilité de la dynamique. Dans cette thèse, nous explorons le choix de l'énergie cinétique et nous démontrons une convergence améliorée des moyennes ergodiques sur un exemple de faible dimension.

Un des problèmes avec les situations que nous considérons est la stabilité des régimes discrétisés. Afin d'obtenir une méthode de discrétisation faiblement cohérente d'ordre 2 (ce qui n'est plus trivial dans le cas de l'énergie cinétique générale), nous nous reposons sur les schémas basés sur des méthodes de Metropolis.

List of publications

Journal publications

(1) S. Redon, G. Stoltz, **Z. Trstanova**. Error analysis of modified Langevin dynamics. J. Stat. Phys., 164(4):735–771, 2016.

(2) **Z. Trstanova**, S. Redon, Estimating the speed-up of Adaptively Restrained Langevin Dynamics, arXiv:1607.01489, submitted to J. Comput. Phys., 2016.

(3) G. Stoltz, **Z. Trstanova**, Stable and accurate schemes for Langevin dynamics with general kinetic energies, arXiv:1609.02891, 2016.

Conference talks

(1) SIAM Conference on Mathematical Aspects of Materials Science, Philadelphia, USA, 2016.

(2) Congrès SMAI, Les Karellis, France, 2015

Posters

(1) Stochastic Numerical Algorithms, Multiscale Modeling and High-dimensional Data Analytics, ICERM, Providence, USA, July 2016

(2) Computational Statistics and Molecular Simulation, Paris, France, February 2016

(3) Numerical Analysis of Stochastic PDEs, Inria Sofia-Antipolis, France, September 2015

(4) Multiscale Modeling of Materials, Ecole de Physique Les Houches, France, May 2015

(5) Multiscale Computational Methods in Materials Modeling Meeting, Edinburgh, UK, June 2014

Acknowledgments

First and foremost, I would like to thank both of my Ph.D. advisers: I am deeply grateful to Stephane Redon for giving me the opportunity to work on such an exciting project, for his enthusiasm and encouragement in the research. Stephane has never doubted my scientific skills, which was very important for my thesis and he has always been open and supportive to deviate the research towards more mathematical aspects. I want to thank him for introducing to me the world of algorithms, software development and research management, which made my thesis so colorful.

I would like to express my sincere gratitude to Gabriel Stoltz, for accepting to advise my research, the path of my thesis would have surely been different without his leading. I want to thank Gabriel for his dedication as adviser, for his continuous support and patience, for sharing his immense mathematical knowledge with me, for always demanding the highest quality of work and providing the most constructive criticism, while being at the same time very positive, kind and pedagogic.

I would like to thank the reviewers for carefully reading the manuscript and for their thoughtful comments and suggestions, and the members of the jury for their questions and comments during the defense, it was an honor to defend my work in front of them. I must acknowledge the European Research Council and Inria for funding my thesis project.

Next, I want to thank Sergei Grudinin, for sharing his interdisciplinary knowledge and his constructive criticism, which led to many interesting discussions. I have been extremely lucky to have met Svetlana Artemova, she has not only made my thesis possible by introducing the ARPS method in her thesis, but has also been advising me in many practical aspects of molecular dynamics and algorithms. I found in her a valuable friend who made my years in Grenoble unforgettable. Thank you, Sveta. My thanks go to Léonard Jaillet and Marc Piuzzi for sharing their experience as researchers, mostly in the beginning of my thesis. I also owe thanks to all the current and former members of NANO-D team at Inria, most importantly, Krishna Kant-Singh, François Rousse, Alexandre Hoffmann, Jocelyn Gaté, Petr Popov, Semeho Edorh, Emilie Neuveu, Silvia C. Dias Pinto, Khoa Nguyen, Guillaume Pages, and all the others, for working with me during these years. I am very grateful to our assistants, Imma Presseguer and Julie Bourget, who have been very helpful with the practical aspects of the life of a researcher.

I would like to thank the researchers from CERMICS, for making me feel welcome at their laboratory where I used to come to discuss mathematics, my special thanks to Julien Roussel,Tom Hudson, Giacomo Di Gesù, Athmane Bakhta and François Madiot.

I would like to thank Ralf Everaers, Nima Hamidi Siboni and other physicists from the Ecole de Physique Les Houches, who wanted to prove my thesis wrong, and while trying to do so, they taught me how fascinating physics can be. These discussions inspired the very last chapter of this work.

I wish I could express how lucky I was to have met all the friends from Grenoble and Paris, who made these cities my new home. My special thanks go to Bérengère, Marie and Antoine, Katka, Sofia, Diogo, Dharam, George, Fabrice, Violeta, Alexandros, Mara and, Fabian and François (F&F), who had the door of their apartment always open and full of movies, pizza and true friendship.

I am very grateful to my family, who gave me the opportunity to study and have always been the biggest support in all my projects. Last, but for the greatest contribution, I must thank Giacomo, who has supported me unconditionally during these years and has proven his strength (and stubbornness) overcoming any distance to always get back to me. Grazie.

Contents

1

Introduction

Computer simulations are widely used in many scientific domains. Performing “numerical experiments”, also known as *"in silico"*, has become an important part of the research methodology. Molecular simulations allow to bridge the gap between microscopic details and macroscopic observations. They have become a natural step for verification or development of new theories serving as a "microscope" and a virtual laboratory. Computer simulations reduce the number of experimental probes when searching for certain properties. For example in drug design, molecular simulations allow to explore pharmacologically relevant binding conformations and to choose some promising set of molecules which may then be tested experimentally [42]. In materials science, simulations are used to suggest new materials with desired properties, especially under experimental conditions that are inaccessible or expensive, such as high pressure or temperature [51].

Molecular simulations are very challenging because of the high dimensionality of simulated systems. The amount of substance is measured in molar mass: the number of atoms in one mole is given by the Avogadro number, a constant equal to 6.02×10^{23}. The typical time step used to integrate the equations is of the order of $10^{-15}s$ which corresponds to a fraction of usual periods of molecular vibrations (whose frequencies often are in the range $10^{12} - 10^{14}$ Hz). The distance is measured in Angstroms (recall that $1\mathring{A} = 10^{-10}$m). Despite increasing computational capacity, it will not be possible to reach time and dimension scales that are necessary for a sufficient exploration of many systems in the next decades. The challenge of molecular simulations is therefore to find simplified physical models which are sufficiently accurate but also feasible from the computational point of view. Their utility is evidenced by the awarding of the 2013 Nobel Prize in Chemistry "for the development of multi-scale models for complex chemical systems" to Arieh Warshel, Michael Levitt and Martin Karplus [131, 65].

In many systems, the interest lies in retrieving static, thermodynamic properties (pressure as a function of temperature and density) or dynamical properties (transport coefficients, Arrhenius constant). The most accurate description is provided by quantum mechanics. Numerical simulations based on quantum theory [30] are computationally very complex and nowadays it is not possible to simulate the dynamics of a system larger than a few hundreds of atoms- for typical wavefunctions based methods (Hartree-Fock or Kohn-Sham[83]). Molecular dynamics (MD) was pioneered by Alder and Wainwright in the late 1950s [5] in their study of the interactions of hard spheres. It approximates the quantum mechanical model by a classical framework allowing to capture many physical features relevant for understanding of the processes in the nature. The connection between the micro and macro scales is provided by statistical physics [12]. There are many introductory books for molecular simulations as for example [6, 48, 97, 76].

The limitation arising from of the time-scale motivated the development of methods increasing the efficiency of molecular dynamics simulations. This remains an active research area. There are basically three aspects which define the total computational time: the variance or the statistical error arising from the usually slow and difficult exploration of the physical system, the time step in the discretization and the computational cost per time step. One of the methods accelerating molecular simulations are Adaptively Restrained Particle Simulations (ARPS) proposed by [9]. This method modifies the physical model, more precisely the kinetic energy, such that the computational cost per time step is reduced. The computational gain lies in a temporarily freezing of a part of particles which is due to a modified definition of the kinetic energy of each particle. Consequently, it is possible to avoid the update of interactions between the frozen particles. Since the computation of the interactions at each time step is the bottleneck of particle simulations, this method can provide a significant speed-up. One purpose of this thesis is to perform a mathematical and algorithmic analysis of the ARPS method.

The introduction of this thesis is organized as follows: we first describe molecular dynamics in Section 1.1. In Section 1.2 we review sampling methods that allow the computation of macroscopic properties from microscopic configurations. We then focus in Section 1.3 on Langevin dynamics, stating some results about the convergence of continuous and discretized versions of this dynamics. We review computational challenges

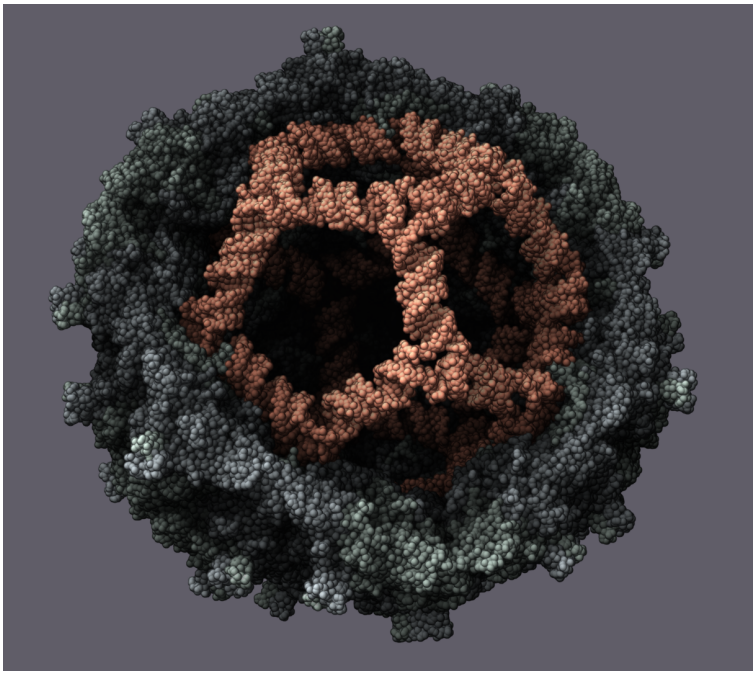

Fig. 1.1: *An example of molecular simulations in biology- simulation of pariacoto virus* [119, 37]: structural studies of viruses are very important to understand protein-protein and protein-RNA interactions as well as to understand assembly pathways in RNA viruses. This model was visualized in SAMSON, a software developed at NANO-D team in Inria.

of the computation of thermodynamics properties in Section 1.4 as well as computational methods which has been proposed as a remedy. Finally, in Section 1.5 we review Adaptively Restrained Particle Simulations, a method which has been the motivation of this thesis, and we highlight our contributions.

1.1 Molecular Dynamics

We introduce molecular dynamics in Section 1.1.1. We start by stating microscopic description of matter as a system of interacting particles. We then explain in Section 1.1.2 how macroscopic properties can be retrieved from the microscopic description by defining thermodynamic ensembles.

1.1.1 Microscopic description of matter

In molecular dynamics, matter consists of particles[1] which obey laws of classical mechanics. They interact with each other by forces which are usually described by potential energies initially derived from a quantum mechanical model or from empirical models based on experiments (see Section 1.1.1.1 below).

Each particle is characterized by its position, momentum and mass. The momentum of a particle is equal to the product of its mass and its velocity. Throughout this thesis, we denote by N the number of

[1] Particles as it will be used in this thesis.

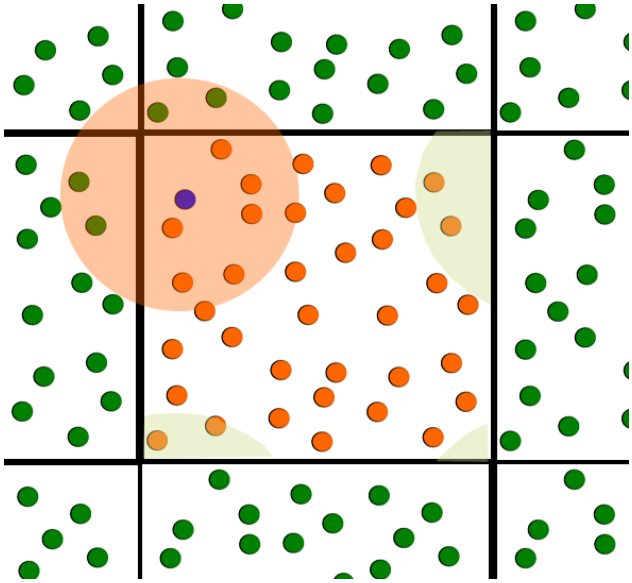

Fig. 1.2: *Periodic boundary conditions:* the central simulation box is extended to infinite dimensional system by considering its periodic images. For instance, the blue particle has neighbors within a radius (light orange circle) which are periodic images of particles from the central box (light green circle cuts).

particles and by d the spatial dimension. The total dimension being $d = N \times D$, we consider a set of $N \geqslant 1$ particles in the periodic box $\mathscr{D} = (L\mathbb{T})^{DN}$ where $\mathbb{T} = \mathbb{R}\backslash\mathbb{Z}$ is the one-dimensional unit torus and $L > 0$ the size of the simulation box. We denote by $q = (q_1, \ldots, q_N) \in \mathscr{D}$ the vector of all positions, by $p = (p_1, \ldots, p_N) \in \mathbb{R}^{DN}$ the vector of all momenta and by $M = \mathrm{diag}\,(m_1, \ldots, m_N)$ the diagonal matrix of the masses. The vector $(q, p) \in \mathcal{E} := \mathscr{D} \times \mathbb{R}^{DN}$ is called the microstate or point in phase space which is the set of all positions and momenta for which the energy is finite.

Let us recall some commonly used boundary conditions. Periodic boundary conditions are usually used in systems where all possible configurations can be obtained by a representative bulk portion of the system (see Figure 1.2). This portion is the central simulation box which is then extended into an infinite dimensional system by considering its periodic images. In this case, each particle interacts not only with its direct neighbors in the box but also with its periodic images. This has been found to work in practice, "despite its artificiality". Infinite boundary conditions, *i.e.* setting the configuration space to $\mathbb{R}^{DN}$, correspond to an isolated system. Open systems with inflows or outflows of energy or particles can also be considered, with additional exchanges or forcings at the boundaries.

The rest of this section is organized as follows: we introduce models for particle-interactions by introducing potential energies in Section 1.1.1.1. We illustrate this on an example of a solvent-solute model. In Section 1.1.1.2 we provide differential equations based on a Hamiltonian system which gives molecular dynamics and we recall some basic properties.

1.1.1.1 Particle interactions

The physical model of the system under study is encoded by the choice of the potential energy function which defines the interactions between particles. Interaction potentials should ideally be obtained from quantum mechanical computations based on an approximate numerical solution of the Schrödinger equation [30, 27]. In practice, due to the high computational complexity of the quantum models, this approach is complemented by the development of computationally less expensive empirical potentials, which are implemented in popular molecular dynamics packages such as AMBER, CHARMM, GROMACS, LAMMPS and NAMD.

For instance, chemical bonds such as covalent bonds are sometimes treated as springs which are described by a harmonic oscillator potential with frequency ω given by:

$$V_{\mathrm{HO}}(r) = \frac{\omega^2}{2}\left(r - r_0\right)^2,$$

where r denotes the distance between two particles, *i.e.* $r = |q_i - q_j|$ for some $i, j = 1, \ldots, N$, and $r_0 > 0$ is a rest-length.

For another example consider a dimer model which is a simple solvent-solute toy-model (see Figure 1.3 for an illustration). In this example, atoms of the solute are linked through bonded interactions, while the surrounding fluid particles are governed by non-bonded interactions. In this toy model, interactions between the atoms of the central molecule never break, while the solvent particles can interact only with other particles within some distance. The interaction potential between the particles of the central molecule can be modeled, for example, by a double well potential (depicted in Figure 1.4(Left)):

$$V_{\mathrm{D}}(r) = h\left[1 - \frac{(r - r_0 - w)^2}{w^2}\right]^2, \tag{1.1}$$

where h and w are two positive parameters. There are two stable states: the first one, at $r = r_0$, corresponds to the compact state and the second one, at $r = r_0 + 2w$, corresponds to the stretched state. Solvent particles interact through a Lennard-Jones pair potential [115], which is a model to describe fluids such as Argon:

$$V_{\mathrm{LJ}}(r) = 4\varepsilon\left[\left(\frac{\sigma}{r}\right)^{12} - \left(\frac{\sigma}{r}\right)^{6}\right], \tag{1.2}$$

where ε and σ are two positive parameters.

The total energy of the system is therefore a sum of potential energies due to the three kinds of interactions:

$$V(q) = V_{\mathrm{D}}(|q_1 - q_2|) + V_{\mathrm{SS}}(q_3, \ldots, q_N) + V_{\mathrm{DS}}(q), \tag{1.3}$$

where $q \in (L\mathbb{T})^{DN}$ and the solvent-solvent and dimer-solvent potential energies respectively read

$$V_{\mathrm{SS}}(q_3, \ldots, q_N) = \sum_{3 \leqslant i < j \leqslant N} V_{\mathrm{LJ}}(|q_i - q_j|), \qquad V_{\mathrm{DS}}(q) = \sum_{i=1,\ldots,2} \sum_{3 \leqslant j \leqslant N} V_{\mathrm{LJ}}(|q_i - q_j|).$$

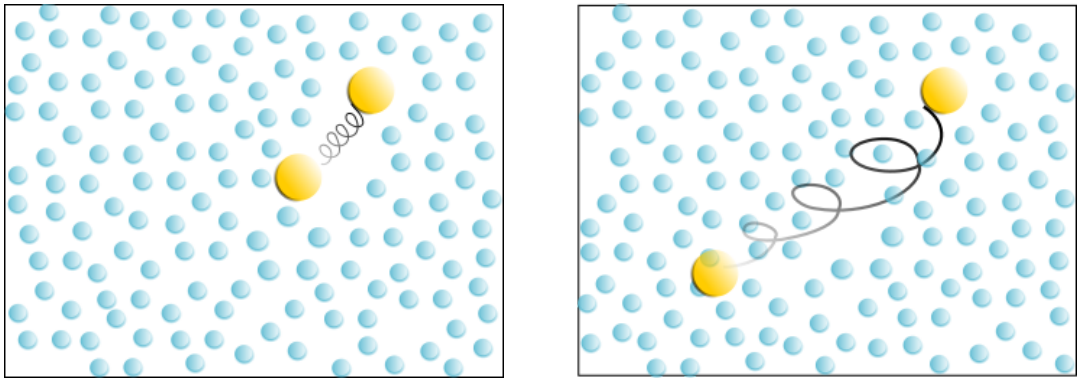

Fig. 1.3: Illustration of the dimer-solvent model: compact and stretched state of the dimer.

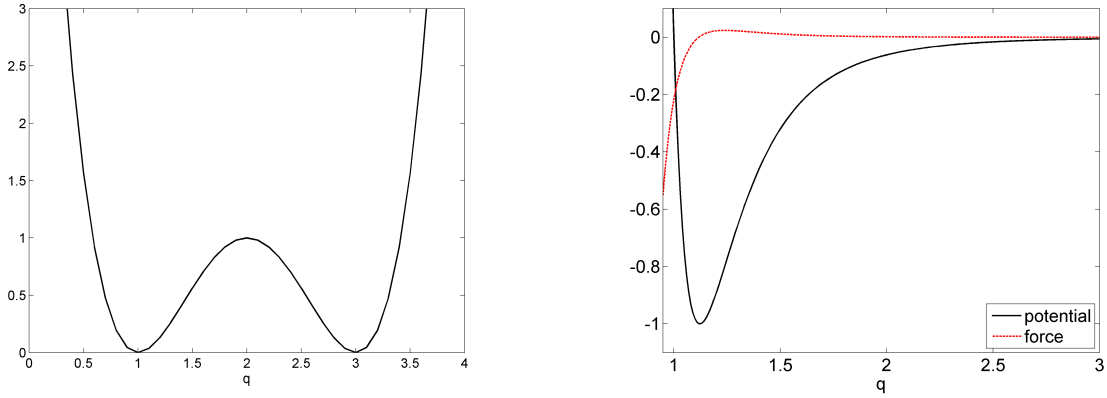

Fig. 1.4: (Left) Double-well potential. (Right) Lennard-Jones potential and the corresponding force.

The force acting on particle i is then $f_i = -\partial_{q_i} V(q)$. See Figure 1.4(Right) for a plot of the Lennard-Jones potential given by (1.2) and its derivative, with the two parameters ε and σ chosen equal to 1. In the WCA (Weeks-Chandler-Andersen) model, which models a fluid of purely repulsive particles [36, 15], the Lennard-Jones potential is moreover truncated at the radius $r_0 = 2^{1/6}\sigma$:

$$V_{\mathrm{WCA}}(r) = \begin{cases} 4\varepsilon \left[\left(\frac{\sigma}{r}\right)^{12} - \left(\frac{\sigma}{r}\right)^{6} \right] + \varepsilon & \text{if } r \leqslant r_0, \\ 0 & \text{if } r > r_0. \end{cases} \tag{1.4}$$

In the solvent-solute model, the interest lies in studying properties of the protein. However, the presence of the solvent is representative of environments usually encountered in biological systems, such as water. The protein might stabilize into different configurations with and without the correct surrounding medium. Unfortunately, the solvent adds additional degrees of freedom which require care in modeling and significantly increase the system size.

1.1.1.2 Hamiltonian dynamics

In classical mechanics, the time evolution of the positions and momenta is governed by the following system of differential equations:

$$\begin{cases} \dot{q}(t) = \nabla_p H\left(q(t), p(t)\right) \\ \dot{p}(t) = -\nabla_q H\left(q(t), p(t)\right), \end{cases} \tag{1.5}$$

where the initial condition is $(q(0), p(0)) = (q^0, p^0) \in \mathcal{E}$. The Hamiltonian function $H : \mathcal{E} \to \mathbb{R}$ corresponds to the total energy of the system:

$$H(q, p) = V(q) + U(p), \tag{1.6}$$

with the kinetic energy usually given by

$$U(p) = U_{\text{std}}(p) = \sum_{i=1}^{N} \frac{p_i^2}{2m_i}. \tag{1.7}$$

Recall that $p_i \in \mathbb{R}^D$ for $i = 1, \ldots, N$. The Hamiltonian is preserved by the dynamics. In other words, this dynamical model describes a system isolated from any external influence: a system containing a constant number of particles, with constant energy. The trajectories of the particles hence belong to a manifold determined by the initial value of the energy.

Let us recall some properties of the Hamiltonian system (1.5). We denote by ϕ_t the flow of the Hamiltonian dynamics as an application which associates to some initial condition (q_0, p_0) the solution $(q(t), p(t)) = \phi_t(q_0, p_0)$ to (1.5) at time t. Assume that ϕ_t exists for any $t \in \mathbb{R}$. The following mathematical and structural properties hold for Hamiltonian dynamics [53]:

- *Symmetry*. It holds that $\phi_{-t} = \phi_t^{-1}$.
- *Time-reversibility*. The Hamiltonian flow is reversible up to the momenta reversal, *i.e.*

  $$\phi_{-t} = S \circ \phi_t \circ S,$$

  where the momentum reversal function is given by $S(q, p) = (q, -p)$.
- *Energy conservation*. It holds that $H(q(t), p(t)) = H(q(0), p(0))$ for all $t \in \mathbb{R}$.
- *Volume preservation*. For any measurable set $B \subset \mathcal{E}$, and for all $t \in \mathbb{R}$, the following holds

  $$\int_{\phi_t(B)} dqdp = \int_B dqdp.$$

- *Symplecticity*. For $H \in C^2$, the flow ϕ_t is a symplectic mapping, *i.e.* $\nabla\phi_t^T J \nabla\phi_t = J$ where

  $$J = \begin{pmatrix} 0 & \mathrm{Id}_d \\ -\mathrm{Id}_d & 0 \end{pmatrix}.$$

From a practical point of view, the equations (1.5) cannot be solved analytically due to the high dimensionality of the system and due to the nonlinearity of the potentials. The solutions are hence approximated by a numerical integration of (1.5). We refer to [53] for an introduction to structure-preserving integration of Hamiltonian schemes. Symplectic methods are used for the integration of Hamiltonian systems since, when applied to Hamiltonian evolutions, they admit a modified equation which is Hamiltonian at all orders and the energy is very well preserved over very long times. For this reason, symplectic schemes are relevant for molecular dynamics, where the goal is to compute average properties at fixed energy.

The most common numerical scheme for (1.5), which is symplectic and has an error of second order with respect to the time step size Δt, is the Verlet scheme [126]: for an initial condition $(q^0, p^0) \in \mathcal{E}$, the solution of (1.5) at time $T = n\Delta t$ denoted as $(q_{n\Delta t}, p_{n\Delta t})$, is approximated by (q^n, p^n). The values (q^{n+1}, p^{n+1}) are obtained starting from the configurations at the previous time step (q^n, p^n) in the following way:

$$\Phi_{\Delta t}(q^n, p^n) = \begin{cases} p^{n+1/2} = p^n - \nabla V(q^n)\dfrac{\Delta t}{2}, \\ q^{n+1} = q^n + M^{-1}p^{n+1/2}\Delta t, \\ p^{n+1} = p^{n+1/2} - \nabla V(q^{n+1})\dfrac{\Delta t}{2}. \end{cases} \tag{1.8}$$

At each time step, the forces $-\nabla V$ acting on each particle need to be evaluated according to the new positions. Despite the form of the Verlet method, it only needs one new force evaluation per timestep. This implies that, at each time step, the evaluation of $-\nabla V(q^{n+1})$ is of order N^2 a priori for bonded interactions, while the update of positions and momenta is of order N. Therefore, *the computation of the forces at each time step is the computational bottleneck of particle simulations.*

1.1.1.3 Computation of interactions

An important feature in most relevant molecular models is the presence chemical (covalent) bonds describing the sharing of electrons between nuclei. *The bonded interactions* are complex and in a classical model would need to incorporate potential energy terms involving atomic pairs, triples, 4-tuples, 5-tuples, etc., but in practice are limited to length bonds (modelled by pair potentials), angle bonds (involving triples) and sometimes dihedral bonds involving groups of four atoms. *Non-bonded interactions* include short-range and long-range interactions and might disappear if the two particles get far enough from each other. Non-bonded interactions can be treated using *neighborlist* algorithms, which decrease the computational complexity of the computation of interactions [48]. Since in this case the potentials vanish behind the cut-off radius, each particle only interacts with its neighbors, *i.e.* particles within the cut-off radius. The computational complexity then becomes linear instead of quadratic in the number of particles. The most used neighborlists are Verlet lists [126, 48], linked-cell lists [58] and a combination of both [11]. Verlet lists are based on the distances between particles and then on creating lists of neighbors within some radius, usually taken bigger than the cut-off radius of the short-range interactions. The linked-cell lists algorithm divides the simulation box into sub-boxes bigger than the cut-off radius. Particles are then characterized according to

which sub-box they belong to. The interactions between particles are only updated among adjacent sub-boxes. The most efficient approach combines both algorithms: the box is divided into sub-cells, and the lists of neighbors are reduced by taking into account inter-particle distances. This algorithm is the most efficient since distances do not have to be computed between all particles thanks to the division of the simulation box into sub-cells of size r_C (the cut-off radius), and the volume in which neighbors might be present is refined from the volume given by $(2r_C)^3$ to $\frac{4}{3}\pi r_C^3$.

1.1.2 Macroscopic description

A fundamental purpose of molecular simulation is the computation of macroscopic quantities, typically through averages of functions of some variables of the system with respect to a given probability measure μ, which defines the macroscopic state of the system [12]:

$$\mathbb{E}_\mu(\varphi) = \int_{\mathcal{E}} \varphi \, d\mu \,. \tag{1.9}$$

In this setting, the function φ is called an observable and the set of all possible microscopic configurations $\mathcal{E}$ is called the phase space. We call the measure μ the *macroscopic state* of the system or the *thermodynamic ensemble*.

In the following section, we present some commonly used thermodynamics ensembles.

1.1.2.1 Microcanonical ensemble

The purely deterministic molecular dynamics as described in the previous section by equation (1.5) is naturally associated with the microcanonical ensemble, also called the NVE ensemble, which describes a system with constant number of particles (N) in a constant volume (V) and at constant energy (E). Because the energy is conserved, the stationary distribution $\mu_{\mathrm{NVE}} = Z_E^{-1}\delta_{H(q,p)-E}(dqdp)$ corresponds to the normalized uniform probability measure on the set $\mathcal{M}(E)$ of configurations according to the energy level E:

$$\mathcal{M}(E) = \{(q,p) \in \mathcal{E} \,|H(q,p) = E\} \,.$$

More precisely, the measure $\delta_{H(q,p)-E}(dqdp)$ is defined through the expectations for an observable φ as

$$\int_{\mathcal{M}(E)} \varphi(q,p)\delta_{H(q,p)-E}(dqdp) = \lim_{\Delta E \to 0} \frac{1}{\Delta E} \int_{\mathcal{N}_{\Delta E}} \varphi(q,p) dqdp,$$

where

$$\mathcal{N}_{\Delta E} = \{(q,p) \in \mathcal{E} \,|E \leqslant H(q,p) \leqslant E + \Delta E\} \,.$$

The normalization constant then reads

$$Z_E = \int_{\mathcal{M}(E)} \delta_{H(q,p)-E}(dqdp).$$

For more details we refer for instance to [81].

1.1.2.2 Canonical ensemble

Unlike in the microcanonical ensemble, most systems in the nature are not strictly isolated but usually interact with their environment, so that the energy varies. The environment can be modeled by a thermostat, which keeps the energy constant in average and hence imposes a constant temperature. This corresponds to the canonical ensemble, or the NVT ensemble, which is a system of N particles in a constant volume at a constant temperature T. The invariant distribution is the Boltzmann distribution

$$\mu(dq\,dp) = Z_\mu^{-1}\mathrm{e}^{-\beta H(q,p)}\,dq\,dp, \qquad Z_\mu = \int_{\mathcal{E}} \mathrm{e}^{-\beta H(q,p)}\,dq\,dp < +\infty, \tag{1.10}$$

where the normalization constant Z_μ is called the partition function and $\beta > 0$ is proportional to the inverse temperature: $\beta = (k_B T)^{-1}$, where k_B is the Boltzmann constant and T is the thermodynamical temperature. An important property is that when the Hamiltonian is separable, the canonical measure is

$$\mu\left(dqdp\right) = \nu\left(dq\right)\kappa\left(dp\right), \tag{1.11}$$

where κ and ν are the momentum and position marginal probability measures given by:

$$\nu(dq) = Z_\nu^{-1}\mathrm{e}^{-\beta V(q)}dq, \quad Z_\nu = \int_{\mathscr{D}} \mathrm{e}^{-\beta V(q)}dq, \tag{1.12}$$

and

$$\kappa(dp) = Z_\kappa^{-1}\mathrm{e}^{-\beta U(p)}dp, \quad Z_\kappa = \int_{\mathbb{R}^{DN}} \mathrm{e}^{-\beta U(p)}dp. \tag{1.13}$$

Note that due to the form of the kinetic energy (1.7) which is separable among the particles, the normalization constant of the momenta marginal distribution can be simply computed:

$$Z_\kappa = \prod_{i=1}^{N}\int_{\mathbb{R}^d} \mathrm{e}^{-\beta\frac{p_i^2}{2m_i}}dp = \left(\frac{2\pi}{\beta}\right)^{DN/2}\prod_{i=1}^{N} m_i^{D/2}.$$

Therefore, *the sampling of the canonical distribution can be performed by independently sampling positions from $\nu(dq)$ and momenta according to $\kappa(dp)$.*

To complete the understanding of the canonical ensemble, we provide some elements of its derivation. We refer to [12] for a more detailed discussion. The basic idea is that the Boltzmann distribution can be obtained by maximizing the entropy under the constraint that the energy is fixed in average. More precisely, we consider some probability measure with a density $\rho(q,p)$ with respect to the Lebesgue measure and such that

$$\rho \geqslant 0, \quad \int_{\mathcal{E}} \rho(q,p)dqdp = 1, \quad \int_{\mathcal{E}} H(q,p)\rho(q,p)dqdp = E,$$

for some energy level E. The first two conditions ensure that ρ is the density of a probability measure and the last condition fixes a constant energy in average. The statistical entropy is defined as

$$\mathcal{G}(\rho) = -\int_{\mathcal{E}} \rho(q,p) \ln \rho(q,p) dq\, dp.$$

The entropy quantifies the amount of information or disorder of the system. The canonical measure maximizes the entropy under all admissible probability measures on the phase space which conserve the energy in average, *i.e.* the canonical measure is a solution of:

$$\sup \left\{ \mathcal{G}(\rho), \rho \in L^1(\mathcal{E}), \rho \geqslant 0, \int_{\mathcal{E}} \rho = 1, \int_{\mathcal{E}} H\rho = E \right\}. \tag{1.14}$$

Denoting by λ, γ the Lagrange multipliers associated with the constraints in (1.14), the Euler-Lagrange equation corresponding to the optimization problem (1.14) reads

$$\mathcal{G}'(\rho) + \lambda + \gamma H = 0.$$

Since $\mathcal{G}'(\rho) = -1 - \ln \rho$, a possible minimizer is the measure with density $\exp(1 + \lambda + \gamma H(q,p))$. The Lagrange multiplier γ associated with the energy constraint is denoted by $-\beta$, while $\exp(1+\lambda)$ becomes the normalization constant Z_μ^{-1}. It can be proved that it is also the unique minimizer [81, Section 1.2.3.2].

For example, the *configurational temperature* can be obtained as the ratio of macroscopic observables which depend on the positions,

$$k_B T = \frac{\mathbb{E}_\mu \left[|\nabla V(q)|^2 \right]}{\mathbb{E}_\mu \left[\Delta V(q) \right]}, \tag{1.15}$$

and the *kinetic temperature* which is obtained as an average of a function of momenta:

$$k_B T = \mathbb{E}_\mu \left[p \cdot \nabla U(p) \right]. \tag{1.16}$$

1.1.2.3 Other ensembles

This work is focused on the canonical ensemble and we therefore only mention other possible ensembles (see for instance [121] for an introduction).

In the isobaric-isothermal ensemble or the NPT ensemble, the temperature and pressure are conserved. The volume of the simulations is held constant in average by the action of a piston, which keeps the pressure constant [7, 46].

Finally, we mention the grand-canonical ensemble, denoted by μVT (constant chemical potential[2] μ, volume V and temperature T). In this ensemble, the number of particles is preserved in average, which is controlled by the constant chemical potential μ.

[2] Not to be confused with the canonical distribution (1.10).

1.2 Sampling methods

One of the main challenges of computational statistical physics is the computation of macroscopic quantities as given by (1.9). In the most common setting, the distribution μ corresponds to the canonical ensemble (1.10). Due to the high dimensionality of the system at hand, the averages (1.9) cannot be computed directly. A remedy is to use the ergodic properties of the dynamics, which allow the approximation of (1.9) by a time integral over trajectories of the dynamics. More precisely, the ergodic average of an observable φ is computed as

$$\lim_{n\to+\infty} \frac{1}{n} \sum_{i=0}^{n-1} \varphi\left(q^i, p^i\right) = \int_{\mathcal{E}} \varphi \, d\mu, \tag{1.17}$$

where $(q^i, p^i)_{i\geqslant 0}$ is a sequence of microscopic configurations obtained by an appropriate numerical method.

Basically, three types of numerical methods can be distinguished: discretizations of continuous stochastic differential equations, Markov chain methods based on the Metropolis-Hastings algorithm and deterministic dynamics on an extended phase-space. In this thesis we focus on the first two classes of methods.

This section is organized as follows: in Section 1.2.1 we introduce methods based on continuous stochastic differential equations, the overdamped Langevin dynamics and Langevin dynamics. Since we focus on Langevin dynamics in Section 1.3, we only briefly discuss in Section 1.2.1 how these SDEs can be used to sample μ. In Section 1.2.2 we recall some basic properties of Markov chains and in Section 1.2.3 we introduce methods based on the Metropolis-Hastings algorithm. Finally, in the last section we mention some methods based on deterministic dynamics.

1.2.1 Continuous stochastic dynamics

Let us first consider a general stochastic differential equation (SDE) on $\mathbb{R}^d$

$$dx_t = b(x_t)dt + \sigma(x_t)dW_t \tag{1.18}$$

where $dW_t \in \mathbb{R}^m$ is the standard Brownian motion and $b : \mathbb{R}^d \to \mathbb{R}^d$ and $\sigma : \mathbb{R}^d \to \mathbb{R}^{d\times m}$ are such that there exists a unique (strong) solution (see for instance [99] for concrete assumptions). Then if there exists an invariant probability measure π and the SDE is ergodic with respect to this measure π (this property requiring appropriate assumptions on b and σ), the stochastic dynamics can be used as a sampling device in the following sense: for an observable $\varphi : \mathbb{R}^d \to \mathbb{R}$,

$$\lim_{t\to\infty} \frac{1}{t} \int_0^t \varphi(x_s)ds = \int_{\mathbb{R}^d} \varphi(x)\pi(dx), \text{ almost surely (a.s.).}$$

By this principle, the Boltzmann distribution (1.10) can be sampled using pathwise realizations of stochastic differential equations such as Langevin dynamics or the overdamped Langevin dynamics, which we introduce in this section.

Langevin dynamics can be interpreted as a stochastic perturbation of the Hamiltonian system (1.5), which models a coupling to a heat bath. It is defined by the following SDE:

$$\begin{cases} dq_t = M^{-1} p_t \, dt, \\ dp_t = -\nabla V(q_t) \, dt - \gamma M^{-1} p_t \, dt + \sigma \, dW_t, \end{cases} \tag{1.19}$$

where dW_t is a standard DN-dimensional Wiener process and $\gamma > 0$ is the friction. The friction γ can be a matrix and moreover it can depend on positions. For simplicity, we consider it to be a positive constant in this work. The term $\sigma \, dW_t$ is a fluctuation term bringing energy into the system. This energy is dissipated through the viscous friction term $-\gamma M^{-1} p_t \, dt$. These two terms are connected through the fluctuation-dissipation relation

$$\sigma \sigma^T = \frac{2\gamma}{\beta}, \tag{1.20}$$

which ensures that the canonical measure (1.10) with temperature $k_B T = \beta^{-1}$ is preserved (see Section 1.3.1).

In view of the separability of the Hamiltonian, the position and momenta marginals can be sampled individually. When considering only the marginal of the distribution μ in the position variable as given by (1.12), the overdamped Langevin dynamics (also called Brownian dynamics) can be used as a sampling device since it leaves the distribution ν invariant. The overdamped Langevin dynamics is

$$dq_t = -\nabla V(q_t) dt + \sqrt{\frac{2}{\beta}} dW_t. \tag{1.21}$$

As discussed in [81, Section 2.2.4], overdamped Langevin dynamics can be obtained from Langevin dynamics by two limiting processes: either as a large friction limit $\gamma \to +\infty$ with time rescaled as γt, or as a small mass limit $m \to 0$.

From a practical point of view, equations (1.19) and (1.21) cannot be solved exactly in general and need to be discretized by introducing a finite time step Δt such that the numerical solution x^n approximates $x_{n\Delta t}$ with $x = (q, p)$ or $x = q$ and for $n = 0, \dots T/\Delta t$. The resulting Markov chain (see Section 1.2.2), which is used to compute (1.17) is hence obtained by numerical approximations at each time step. The discretization of stochastic differential equations introduces a bias in the invariant distribution. This approach therefore generates samples from a modified distribution $\mu_{\Delta t} \neq \mu$, which can be shown to be close to μ for small time step sizes. We discuss the properties of the continuous and discretized Langevin dynamics in Section 1.3.

1.2.2 Markov chains

A time-homogeneous Markov chain $(x_n)_{n \geqslant 0}$ on $\mathcal{E}$ is a sequence of random variables sampled from a probability transition kernel $P(x, dx')$: at each iteration n, the new state x^{n+1} is sampled knowing only x^n, according to the probability distribution $P(x^n, dx')$. The fact that each new configuration x^{n+1} only depends on the previous one x^n is called the Markov property. In other words, given the present, past and future are conditionally independent. Since $P(x^n, dx')$ is a probability distribution, the following normali-

zation condition is satisfied:

$$\forall x \in \mathcal{E}, \quad \int_{\mathcal{E}} P(x, dx') = 1.$$

The study of the convergence of time homogeneous Markov chains is based on three concepts: stationarity, reversibility and irreducibility.

(1) A probability distribution π is a *stationary (or invariant) probability distribution* of P when

$$\int_{\mathcal{E}} P(x, dx')\pi(dx) = \pi\left(dx'\right). \tag{1.22}$$

If the distribution π possesses a density with respect to the Lebesgue measure, we write, with a slight abuse of notation, $\pi(dy) = \pi(y)dy$.

(2) A chain P satisfies the *detailed balance condition* if

$$P\left(x, dx'\right)\pi\left(dx\right) = P\left(x', dx\right)\pi\left(dx'\right).$$

This is equivalent to the *reversibility* with respect to π, *i.e.* the law of $(x_0, x_1, \ldots, x_n)$ when $x_0 \sim \pi$ is the same as the law of $x_n, \ldots, x_0$. The reversibility of the chain with kernel P with respect to the measure π implies the stationarity of π. Let us emphasize that reversibility is a sufficient, but not necessary condition for the invariance.

(3) A Markov chain P is said to be (aperiodically) *irreducible* with respect to π, if for any measurable set A such that $\pi\left(A\right) > 0$, and π-almost all initial condition x^0, there exists $n^0 \geqslant 0$ such that for any $n \geqslant n^0$,

$$P^n\left(x^0, A\right) > 0,$$

where the nth step transition probability is defined as

$$P^n\left(x^n, dx'\right) = \int_{y \in \mathcal{E}} P(x, dy)P^{n-1}\left(y, dx'\right), \quad P^1\left(x, dx'\right) := P\left(x, dx'\right).$$

A Markov chain, which satisfies the stationarity condition (1.22) and is aperiodically irreducible, is pathwise ergodic [89, Theorem 17.1.7]:

Theorem 1.1. *Let $\left(x^n\right)_{n\geqslant 0}$ be a Markov chain with stationary probability measure π. If $\left(x^n\right)_{n\geqslant 0}$ is aperiodically irreducible, then it is pathwise ergodic: for any bounded measurable function φ and π-almost all initial conditions x^0,*

$$\lim_{n\to+\infty} \frac{1}{n}\sum_{i=0}^{n-1} \varphi\left(x^i\right) = \mathbb{E}_\pi\left(\varphi\right) \quad \text{a.s.}$$

1.2.3 Metropolis-Hastings algorithm

Sampling methods based on Metropolis-Hasting algorithm are very popular in computational statistical physics. The Metropolis-Hasting algorithm was introduced in [56, 87]. It generates a Markov chain which

is invariant under the distribution π, and consists of two steps: first, a *proposal* for the new configuration is generated; then a decision to accept or reject the proposal is taken according to some probability rule. The generation of the proposal as well as the acceptance rule are at the core of the concrete method.

Starting from some initial state x^n, the Metropolis-Hastings algorithm generates a new configuration x^{n+1} as follows:

(1) Propose a state $\tilde{x}^{n+1}$ according to the proposition kernel $T(x^n, \cdot)$

(2) Accept the proposal with probability $\min\left(1, r(x^n, \tilde{x}^{n+1})\right)$, where the Metropolis-Hastings ratio reads

$$r(x, y) = \frac{\pi(y)T(y, x)}{\pi(x)T(x, y)}.$$

In this case, set $x^{n+1} = \tilde{x}^{n+1}$. Otherwise set $x^{n+1} = x^n$.

The probability transition kernel of the Metropolis-Hastings chain can be written as

$$P(x, dy) = \min\left(1, r(x, y)\right) T(x, y)dy + \left(1 - \int_{\mathcal{E}} \min\left(1, r(x, y')\right) T(x, y')dy'\right) \delta_x(dy).$$

The first term corresponds to the accepted transitions while the second term encodes all the rejected states.

It can be easily proven that the resulting Markov chain satisfies the detailed balance condition with respect to the distribution π, and hence is invariant under π (for the complete proof we refer to [81, Section 2.1.2]). Let us mention that a non-reversible Metropolis-Hastings algorithm was proposed recently, by means of a modification of the acceptance probability, using the notion of vorticity matrix [18]. The resulting Markov chain is non-reversible, which allows to improve the convergence of the sampled chain.

The crucial part of the algorithm is the generation of the proposal. As we explain in the following section, one common approach for generating a proposal is by numerical integration of some differential equation reversible with respect to π with finite time step. The smaller the time step, the more accurate the numerical approximation is and so the proposal is accepted with a higher probability. On the other hand, in order to explore the whole phase space efficiently, the time step size should not be too small. In conclusion, the efficiency of the Metropolis-Hastings algorithm is a trade-off between large moves that decorrelate the iterates when they are accepted and small moves that are less rejected but do not decorrelate the iterates much. In practical applications, the average rejection rate is usually chosen around 0.5. In some limiting regimes it is possible to find the optimal rejection rate (see [104, 103] and the many extensions of this approach).

In the following sections, we introduce three Metropolis-based methods for sampling the position marginal of the Boltzmann distribution (constructing Markov chains of the positions q): the random walk, the Hybrid Monte-Carlo method and the Metropolis Adjusted Langevin dynamics.

1.2.3.1 Random walk

The simplest proposals for Metropolis-Hastings algorithm as in the original work [87] are based on symmetric moves. More precisely, consider the following proposition of the new configuration

$$q' = q + G, \quad G \sim \mathcal{N}\left(0, \sigma^2 \mathrm{Id}_d\right),$$

where d is the dimension of the sampled space. The proposal probability kernel is in this case

$$T(q, dq') = (2\pi)^{-d} \exp\left(-\frac{|q-q'|^2}{2\sigma^2}\right) dq'.$$

Another option would be to consider a uniformly distributed random variable on the interval $[-\sigma, \sigma]^d$, instead. In this case the transition probability kernel becomes

$$T(q, dq') = (2\sigma)^{-d} \mathbb{1}_{(q'-q)\in(-\sigma,\sigma)^d} \, dq'.$$

Both proposals might not be very well suited for the sampled distribution, since for small values of σ they might create correlated successive moves or, for a large σ, the new configurations might be very unlikely.

1.2.3.2 Hybrid Monte-Carlo

Hybrid Monte-Carlo was first introduced in [40]. This method has been analyzed from a mathematical view-point in [111, 31, 16, 24, 84]. Hybrid Monte Carlo[3] is a Metropolis-Hastings type Markov chain method based on a proposal generated by the numerical integration of the deterministic dynamics (1.5). Since the deterministic dynamics is energy preserving, the momenta are initially re-sampled according to the canonical distribution, which allows exploration of all energy levels. The proposal is accepted or rejected with a probability given by the Metropolis ratio:

$$A^H_{\Delta t}\left(q^n, p^n, \tilde{q}^{n+1}, \tilde{p}^{n+1}\right) = \min\left(1, \mathrm{e}^{-\beta\left(H\left(\tilde{q}^{n+1}, \tilde{p}^{n+1}\right) - H(q^n, p^n)\right)}\right), \tag{1.23}$$

where the energy H is given by (1.6).

The update of Markov chain of positions q^n can be summarized as follows: for $\tau > 0$,

(1) Draw p^n according to the momenta marginal of the distribution (1.10), *i.e.* $p^n \sim \mathcal{N}(0, \beta/m)$.
(2) Propose $(\tilde{q}^{n+1}, \tilde{p}^{n+1})$ according to $(\Phi_{\Delta t}(q^n, p^n))^{\lfloor \tau/\Delta t \rfloor}$ given by (1.8) and compute $H(\tilde{q}^{n+1}, \tilde{p}^{n+1})$.
(3) Draw $\mathcal{U}^n \sim U[0,1]$. If $\mathcal{U}^n \leqslant A^H_{\Delta t}\left(q^n, p^{n+1}, \tilde{q}^{n+1}, \tilde{p}^{n+1}\right)$, set $q^{n+1} = \tilde{q}^{n+1}$.
Otherwise set $q^{n+1} = q^n$.

This method relies on the (believed) good properties of the deterministic dynamics: a fast exploration of the phase space at constant energy levels together with a preservation of the Boltzmann distribution. The rejection of the proposal occurs due to the discretization errors. The efficiency of the method is therefore given by a trade-off between larger time step sizes and a tolerable rejection rate. In order to improve the rejection rate, a method proposed by [63] uses an acceptance criterion based on a modified Hamiltonian, which is preserved by the flow generated by the Verlet scheme at order Δt^4 and can formally be obtained

[3] In the statistics community Hybrid Monte Carlo is called Hamiltonian Monte Carlo. The acronym HMC is however unchanged.

through backward error analysis. The samples are then re-weighted in order to be distributed according to the canonical distribution. However, in most cases, it is difficult or expensive to compute the modified (Shadow) Hamiltonian, since it involves the Hessian of the potential.

1.2.3.3 Metropolis-Adjusted Langevin Algorithm

The Metropolis-Adjusted Langevin Algorithm (MALA) was introduced in the chemistry literature under the name "Smart Monte Carlo" [108] and was rediscovered later on in the computational statistics literature [102].

It is a Metropolis-Hastings algorithm whose proposal function is obtained by an Euler-Maruyama discretization of the overdamped Langevin dynamics (1.21). For a given time step $\Delta t > 0$ and a configuration q^n, the proposed move $\tilde{q}^{n+1}$ reads

$$\tilde{q}^{n+1} = q^n - \nabla V(q^n)\Delta t + \sqrt{\frac{2\Delta t}{\beta}} G^n,$$

where G^n are identically and independently distributed (*i.i.d.*) standard d-dimensional Gaussian random variables. The proposal is then accepted or rejected according to the Metropolis-Hastings ratio

$$A_{\Delta t}\left(q^n, \tilde{q}^{n+1}\right) = \min\left(1, \frac{\mathrm{e}^{-\beta V\left(\tilde{q}^{n+1}\right)} T_{\Delta t}\left(q^n, \tilde{q}^{n+1}\right)}{\mathrm{e}^{-\beta V(q^n)} T_{\Delta t}\left(\tilde{q}^{n+1}, q^n\right)}\right),$$

where the probability transition reads

$$T_{\Delta t}\left(q, q'\right) = \left(\frac{1}{4\pi\Delta t}\right)^{d/2} \exp\left(-\frac{\beta\left|q' - q + \Delta t \nabla V(q)\right|^2}{4\Delta t}\right).$$

The generated Markov chain is irreducible with respect to the Lebesgue measure with ν as an invariant probability measure. It is therefore ergodic, and reversible with respect to ν. We refer to [81, Section 2.2.1] and references therein for further precisions.

When the drift function ∇V is globally Lipschitz and the time step size Δt is small enough, MALA is geometrically ergodic [102]. For non-globally Lipschitz drifts, the strong convergence of MALA to the overdamped Langevin dynamics was proved in [25, 26]. Exponential convergence rates towards the invariant measure (uniformly in the time step) up to exponentially small errors were stated in [22].

1.2.4 Deterministic dynamics

For a comprehensive review of deterministic methods we refer the reader to [76] for instance. Even though these approaches are quite popular among some practitioners, their ergodicity has not been rigorously proved. On the contrary, a non-ergodic behavior was proved in [73] for harmonic oscillators and perturbations of such system. The advantage of deterministic methods is, their fast convergence when they are ergodic: for

observables in $\mathrm{Ran}\mathcal{L}$, the associated error is of order $1/\tau$ (where τ is the physical time), instead of $1/\sqrt{\tau}$ as given by the CLT for stochastic processes. More precisely, for $\phi \in \mathrm{Ran}\mathcal{L}$ and $\psi = \mathcal{L}^{-1}\phi$,

$$\frac{1}{\tau}\int_0^\tau (\mathcal{L}\psi)\left(q(t),p(t)\right) dt = \frac{1}{\tau}\int_0^\tau \frac{d}{dt}\psi\left(q(t),p(t)\right) dt = \frac{1}{\tau}\left(\psi\left(q(\tau),p(\tau)\right) - \psi\left(q(0),p(0)\right)\right).$$

The issue is that the condition $\phi \in \mathrm{Ran}\mathcal{L}$ is very restrictive. Note that $\mathcal{L}$ is a generator of purely Hamiltonian dynamics. The proof of convergence cannot be extended to any observable since $\mathcal{L}^{-1}$ is not easily defined.

The simplest deterministic dynamics admitting the canonical measure as an invariant measure is the Nosé dynamics [60, 91, 92, 93]. It is based on the Hamiltonian system (1.5) which is extended with an auxiliary variable modeling the thermostat:

$$\begin{cases} \dot{q} = M^{-1}p, \\ \dot{p} = -\nabla V(q) - \xi p, \\ \dot{\xi} = Q^{-1}\left(p^T M^{-1} p - N k_B T\right), \end{cases}$$

where ξ is an additional variable with parameter $Q > 0$ ensuring that the measure $\mathrm{e}^{-\beta H(q,p)}\mathrm{e}^{-\beta Q\xi^2/2}$ is a stationary state.

Note however that the ergodicity of deterministic methods can be restored by incorporating a stochastic process [109, 79].

1.3 Langevin dynamics

We present Langevin dynamics in this section, since it is the fundamental dynamics used in this work. We first discuss the convergence of the continuous dynamics in Section 1.3.1. We then present discretization schemes in Section 1.3.2, together with results of numerical analysis.

1.3.1 Properties of the continuous dynamics

Langevin dynamics associated with a general Hamiltonian reads

$$\begin{cases} dq_t = \nabla_p H(q_t,p_t)\, dt, \\ dp_t = -\nabla_q H(q_t,p_t)\, dt - \gamma \nabla_p H(q_t,p_t)\, dt + \sqrt{\dfrac{2\gamma}{\beta}}\, dW_t, \end{cases} \tag{1.24}$$

where dW_t is a standard d-dimensional Wiener process and $\gamma > 0$ is the friction. As mentioned in Section 1.2.1, it would possible to choose the matrices γ and σ as position-dependent in order to restrict the action of the thermostat to the boundaries. In this thesis γ and σ are constant. As we have already mentioned, the fluctuation-dissipation relation (1.20) ensures that the dynamics preserves the invariant measure, see (1.27) below. For the separable Hamiltonian (1.6), and since the standard kinetic energy as already mentioned in (1.7) reads $U_{\mathrm{std}}(p) = p^T M^{-1} p/2$, Langevin dynamics simplifies to

$$\begin{cases} dq_t = M^{-1} p_t \, dt, \\ dp_t = -\nabla V(q_t) \, dt - \gamma M^{-1} p_t \, dt + \sqrt{\dfrac{2\gamma}{\beta}} \, dW_t. \end{cases} \tag{1.25}$$

The core of this work consists of considering a general kinetic energy function instead of the standard one, *i.e.* a more general Langevin dynamics than the standard one (1.25), based on the formulation (1.24). In the next section, we review some properties of Langevin dynamics (1.25).

1.3.1.1 Generator of the dynamics

Consider the general stochastic differential equation (1.18). Many properties of stochastic differential equations can be inferred from a differential operator, the infinitesimal generator (see for instance [99]). To define it, introduce the semi-group $P_{s,t}$, which is the transition function $P_{s,t}$ of a Markov process $t \mapsto x_t$ defined for any $0 \leqslant s \leqslant t$ and any test function φ as

$$P_{s,t}(\varphi)(x) = \mathbb{E}\left(\varphi(x_t) \, | x_s = x\right) .$$

The infinitesimal generator can then be defined by the following strong limit: for $t \geqslant 0$,

$$\lim_{s \to 0} \frac{P_{t,t+s} - \mathrm{Id}}{s} \varphi = \mathcal{L}\varphi.$$

The infinitesimal generator of the process $(x_t)_{t \geqslant 0}$, which is the solution of the stochastic differential equation (1.18), reads

$$\mathcal{L} = b \cdot \nabla_x + \frac{1}{2} \sigma\sigma^T : \nabla_x^2 \, ,$$

where the symbol : denotes the Frobenius inner product. The following property is a direct consequence of the Itô formula and it shows the link between the generator $\mathcal{L}$ and the SDE: for any compactly supported C^∞ function φ,

$$\frac{d}{dt} \, \mathbb{E}\left[\varphi(x_t) \, | x_0 = x\right] |_{t=0} = \mathcal{L}\varphi(x).$$

The generator of Langevin dynamics (1.25) reads

$$\mathcal{L} = M^{-1} p \cdot \nabla_q - \nabla V \cdot \nabla_p + \gamma \left(-M^{-1} p \cdot \nabla_p + \frac{1}{\beta} \Delta_p \right). \tag{1.26}$$

A simple computation shows that the canonical distribution (1.10) is invariant under the dynamics (1.25), *i.e.* for all C^∞ functions ϕ with compact support,

$$\int_{\mathcal{E}} \mathcal{L}\phi \, d\mu = 0. \tag{1.27}$$

The generator of the dynamics $\mathcal{L}$ also appears in the Fokker-Planck equation, which is the partial differential equations that governs the evolution of the law ψ of x_t:

$$\partial_t \psi = \mathcal{L}^\dagger \psi, \quad \psi(0) = \psi_0,$$

where $\mathcal{L}^\dagger$ is the L^2 adjoint of the operator $\mathcal{L}$. The analysis of the convergence to the canonical measure of the solution ψ can be studied in terms of the semi-group representation where it is reformulated as the convergence of $\mathrm{e}^{t\mathcal{L}^\dagger}\psi_0$ to the invariant measure μ. Moreover, by a dual viewpoint, we can study the convergence of observables towards their expectations with respect to μ. More precisely, we consider the average value at time t of a given observable, expressed using the semi-group $\mathrm{e}^{t\mathcal{L}}$ as

$$\left(\mathrm{e}^{t\mathcal{L}}\varphi\right)(x) = \mathbb{E}\left[\varphi(x_t)\,\middle|\, x^0 = x\right].$$

Furthermore, the infinitesimal generator $\mathcal{L}$ appears in the Poisson equation for the asymptotic variance of estimators based on time averages (see (1.48) below). The following framework can be used to study the solutions of this equation. Let us consider the vector space $\mathcal{B}(E)$, which is a space of bounded linear operators on a Banach space E with the operator norm

$$\|\mathcal{A}\|_{\mathcal{B}(E)} = \sup_{f\neq 0} \frac{\|\mathcal{A}f\|_E}{\|f\|_E}.$$

The Banach space E is typically a subspace of functions with average 0 with respect to the invariant measure, *i.e.* $\int_{\mathcal{E}} \varphi d\mu = 0$, which implies that $\mathrm{e}^{t\mathcal{L}}\varphi \to 0$ as $t \to \infty$. A very useful result is the invertibility of the generator $\mathcal{L}$, and bounds on its inverse in $\mathcal{B}(E)$. Such results can be deduced from decay estimates on the semi-group:

$$\|\mathrm{e}^{t\mathcal{L}}\|_{\mathcal{B}(E)} \leqslant C\mathrm{e}^{-\lambda t}, \tag{1.28}$$

since this allows to write

$$\mathcal{L}^{-1} = -\int_0^\infty \mathrm{e}^{t\mathcal{L}} dt.$$

In conclusion, the bound (1.28) implies that the operator $\mathcal{L}$ is invertible on E with

$$\|\mathcal{L}^{-1}\|_{\mathcal{B}(E)} \leqslant \frac{C}{\lambda}.$$

1.3.1.2 Convergence of ergodic averages

We recall in this section the basic components needed for proving the convergence of ergodic averages over one trajectory for Langevin dynamics, *i.e.*

$$\lim_{t\to\infty} \hat{\varphi}_t = \mathbb{E}_\mu(\varphi) = \int_{\mathcal{E}} \varphi \, d\mu, \text{ a.s.}, \quad \hat{\varphi}_t = \frac{1}{t}\int_0^t \varphi(q_s, p_s)\, ds\,. \tag{1.29}$$

This property is automatically ensured by the existence of an invariant probability measure and the irreducibility of the dynamics (see for instance [67, 88] for results on such convergences for possibly degenerate diffusions). Since, by construction, an invariant probability measure is known (namely the canonical mea-

sure (1.10)), it suffices to show that the process generated by the modified Langevin equation is irreducible to deduce the convergence of ergodic averages.

As reviewed in [99], the most standard argument to prove the irreducibility of degenerate diffusions is to prove the controllability of the dynamics relying on the Stroock-Varadhan support theorem (any open set of the phase space can be reached with positive probability), and the regularity of the transition kernel thanks to the hypoellipticity property. These conditions are satisfied for standard Langevin dynamics (see for instance [85]).

- The *controllability* argument shows that

$$\mathbb{P}\left((q_t, p_t) \in A \,|(q_0, p_0) = (q, p)\right) > 0 \tag{1.30}$$

when $t > 0$ and the set A is open. This approach was considered for Langevin dynamics in [99, 85, 117]. Consider an end point $(q^*, p^*) \in A$ and fix $t^* > 0$. The main idea is to construct a realization of the Brownian motion such that the dynamics started at (q, p) ends in (q^*, p^*). This can be achieved by considering a polynomial interpolation path $Q(t)$ such that $Q(0) = q, \dot{Q}(t) = M^{-1}p$ and $Q(t_0) = q^*, \dot{Q}(t_0) = M^{-1}p^*$. The corresponding control $u(t)$ is defined as $u(0) = 0$ and

$$M\ddot{Q}(t) = -\nabla V(Q(t)) - \gamma\dot{Q}(t) + \sqrt{\frac{2\gamma}{\beta}}\dot{u}(t).$$

It holds then

$$u(t) = \sqrt{\frac{\beta}{2\gamma}}\left(M\dot{Q}(t) - p + \gamma\left(Q(t) - q\right) + \int_0^t \nabla V(Q(s))ds\right). \tag{1.31}$$

By continuity of the solutions of the SDE with respect to the realizations of the Brownian motion, we can conclude to (1.30). We refer the reader to [85, Lemma 3.4] for more details. Note that the construction of the control is simple because there is a linear relationship between $\dot{Q}$ and P.

- To extend 1.30 to any set A of positive measure, the second step is to prove the *regularity of the transition kernel*. The following theorem allows to prove that, even though the generator of Langevin dynamics and its adjoint are not elliptic, they have some regularizing properties. This property is known as hypoellipticity.

  In order to state the result, we denote by $[A, B] = AB - BA$ the commutator of two operators A, B.

  Theorem 1.2 (Hörmander [61, 62]). *Consider C^∞ vector fields on the d-dimensional space $\mathcal{Y}$*

$$A_j = \sum_{i=1}^{d} A_{j,i}(y)\partial_{y_i},$$

and introduce the operator

$$\mathcal{A} = A_0 + \sum_{j=1}^{J} A_j^\dagger A_j,$$

where $A_j^\dagger$ is the (formal) adjoint of A_j on $L^2(\mathcal{Y})$. Assume that the Lie algebra spanned by $\{A_j\}_{j=0,\dots,J}$, $\{[A_j, A_k]\}_{j,k=0,\dots,J}$, $\{[[A_j, A_k], A_l]\}_{j,k,l=0,\dots,J}$, $\dots$, has maximal rank d at every point $y \in \mathcal{Y}$. Then $\mathcal{A}$ is hypoelliptic: there exists $\varepsilon > 0$ such that $\mathcal{A}f \in H^s_{\mathrm{loc}}$ implies $f \in H^{s+\varepsilon}_{\mathrm{loc}}$.

In particular, solutions f of the equation $\mathcal{A}f = 0$ are C^∞.
For Langevin dynamics, the generator (1.26) of the process can be rewritten as

$$\mathcal{L} = X_0 - \sum_{j=1}^{d} X_j^\dagger X_j,$$

where

$$X_0 = M^{-1}p \cdot \nabla_q - \nabla V \cdot \nabla_p - \gamma M^{-1}p \cdot \nabla_p, \qquad X_j = \sqrt{\frac{\gamma}{\beta}}\, \partial_{p_j},$$

and $X_j^\dagger = -X_j$ is the adjoint of X_j on the flat space $L^2(\mathcal{E})$. We next compute, for $j = 1, \dots, d$, the commutators

$$[X_0, X_j] = X_0 X_j - X_j X_0 = \sqrt{\frac{\gamma}{\beta}}\, \frac{1}{m_j} \left(\partial_{q_j} - \gamma \partial_{p_j}\right). \tag{1.32}$$

It is possible to recover the full algebra of derivatives by an appropriate combination of $X_1, \dots, X_d$ and $[X_0, X_1], \dots, [X_0, X_d]$, since the standard kinetic energy (1.7) is such that $\partial^2_{p_j} U_{\mathrm{std}}(p) = \frac{1}{m_j}$. This proves that the generator of Langevin dynamics $\mathcal{L}$ is hypoelliptic. In fact, the result can be extended to prove that $\partial_t - \mathcal{L}$ and $\partial_t - \mathcal{L}^\dagger$ are hypoelliptic on $\mathbb{R} \times \mathcal{E}$. This allows to show that the transition kernel of Langevin dynamics admits a C^∞ density for $t > 0$.

1.3.1.3 Convergence of the law

In this section we provide some methods for proving the convergence to equilibrium of Langevin dynamics in terms of the law of the process, *i.e.* $\mathrm{e}^{t\mathcal{L}}\varphi \to \mathbb{E}_\mu(\varphi)$ when $t \to \infty$, implied by estimates similar to (1.28) in appropriate spaces.

Hypocoercivity

Hypocoercivity shows the convergence in $H^1(\mu)$ which can be turned to a convergence in $L^2(\mu)$ using hypoelliptic regularization. The main idea is to introduce some mixed derivatives in q and p in a modified scalar product in order to retrieve some dissipation in the q direction. This idea was already present in the computations performed in [117, Section 3], and was later generalized by Villani in [127]. An application of the general hypocoercivity framework to Langevin dynamics was performed in [55] (see also [82]).

More precisely, the coercivity is obtained in the Hilbert space $H^1(\mu) \cap L^2_0(\mu)$, where

$$H^1(\mu) = \left\{ \varphi \in L^2(\mu) \,\middle|\, \nabla_p \varphi, \nabla_q \varphi \in L^2(\mu) \right\}$$

is endowed with a scalar product different from the canonical one:

$$\langle \varphi_1, \varphi_2 \rangle_{H^1(\mu)} = \langle \varphi_1, \varphi_2 \rangle_{L^2(\mu)} + \langle \nabla_q \varphi_1, \nabla_q \varphi_2 \rangle_{L^2(\mu)} + \langle \nabla_p \varphi_1, \nabla_p \varphi_2 \rangle_{L^2(\mu)}.$$

Although hypocoercivity eventually provides decay estimates in $H^1(\mu)$, we introduce the following scalar product:

$$\langle\langle u, v \rangle\rangle = \langle u, v \rangle + a \langle \nabla_p u, \nabla_p v \rangle - b \langle \nabla_p u, \nabla_q v \rangle - b \langle \nabla_q u, \nabla_p v \rangle + c \langle \nabla_q u, \nabla_q v \rangle, \tag{1.33}$$

where, for simplicity of notation, we denote by $\langle \cdot, \cdot \rangle$ the standard scalar product on $L^2(\mu)$. This scalar product is equivalent to the canonical scalar product on $H^1(\mu)$ if and only if the following condition is satisfied:

$$a, c > 0, \quad ac - b^2 > 0. \tag{1.34}$$

Hypocoercivity provides decay estimates of the evolution semi-group in the following sense: there exist $C \geqslant 1$ and $\kappa > 0$ such that for any $t \geqslant 0$,

$$\| \mathrm{e}^{t\mathcal{L}} \|_{\mathcal{B}(H^1(\mu) \cap L^2_0(\mu))} \leqslant C \, \mathrm{e}^{-\kappa t}, \quad \forall t \geqslant 0. \tag{1.35}$$

The interest of the hypocoercive approach is that the final optimal constants C and κ can be made quite explicit in terms of the various factors.

The passage from bounds in $H^1(\mu)$ to bounds in $L^2(\mu)$ follows from hypoelliptic regularization results (see [127, Theorem A.8] or [55, Section 6.1]). For $\nabla^2 V \in L^\infty(\mathcal{D})$, it can be proved that there exists $K > 0$ such that, for any $\varphi \in L^2(\mu)$,

$$\| \nabla_p \mathrm{e}^{t\mathcal{L}} \varphi \|_{L^2(\mu)} + \| \nabla_q \mathrm{e}^{t\mathcal{L}} \varphi \|_{L^2(\mu)} \leqslant \frac{K}{t^{3/2}} \| \varphi \|_{L^2(\mu)}, \quad \forall 0 < t \leqslant 1.$$

Combining this inequality and (1.35) with $t_0 = 1$, for instance, we can conclude that, for $t \geqslant 1$ and $\varphi \in L^2_0(\mu)$,

$$\| \mathrm{e}^{t\mathcal{L}} \varphi \|^2_{L^2(\mu)} \leqslant \langle\langle \mathrm{e}^{t\mathcal{L}} \varphi, \, \mathrm{e}^{t\mathcal{L}} \varphi \rangle\rangle \leqslant \mathrm{e}^{-2\kappa(t-t_0)} \langle\langle \mathrm{e}^{t_0\mathcal{L}} \varphi, \, \mathrm{e}^{t_0\mathcal{L}} \varphi \rangle\rangle \leqslant \widetilde{C} \, \mathrm{e}^{-2\kappa t} \| \varphi \|^2_{L^2(\mu)},$$

which gives the claimed exponential decay in $L^2(\mu)$.

In fact, it is possible to directly obtain exponential convergence in L^2 by the approach recently presented in [39] (for more details see also Chapter 5).

Weighted L^∞ spaces

An alternative functional framework for proving the exponential convergence is provided by weighted L^∞-spaces. This method is based on the elementary derivation provided in [54], with similar results already obtained in [89] and reviewed in [99]. This result is less quantitative in terms of the convergence rates than

the approach by hypocoercivity. However, it can be applied in many situations where the hypocoercivity approach fails; for instance for proving the ergodicity of discrete dynamics [78], non-reversible dynamics [64] or non-hypoelliptic dynamics (see Chapter 2).

In order to state the exponential convergence result, we introduce the weighted L^∞ space:

$$L^\infty_{\mathcal{K}} = \left\{ f \text{ measurable} \;\middle|\; \|f\|_{L^\infty_{\mathcal{K}}} := \left\| \frac{f}{\mathcal{K}} \right\|_{L^\infty} < +\infty \right\} \tag{1.36}$$

for some Lyapunov function $\mathcal{K} : \mathcal{E} \to [1, +\infty)$. We define Lyapunov functions $\mathcal{K}_n$ such that

$$\mathcal{K}_n \leqslant \mathcal{K}_{n+1}, \quad \forall n \geqslant 0.$$

We introduce the space $\mathscr{S}$ of smooth functions $\varphi \in C^\infty(\mathcal{E})$ for which, for any $k \in \mathbb{N}^d$, there exists $m_k \in \mathbb{N}$ such that $\partial^k \varphi \in L^\infty_{\mathcal{K}_{m_k}}(\mathcal{E})$. An example for previously defined functions is $\mathcal{K}_n(x) = 1 + |x|^n$ for some $n \geqslant 2$. In this case, the functions in $\mathscr{S}$ and their derivatives, grow at most polynomially. We define the space $\widetilde{\mathscr{S}}$ as a subset of the space $\mathscr{S}$ which contains functions with average zero with respect to μ:

$$\widetilde{\mathscr{S}} = \left\{ f \in \mathscr{S} \;\middle|\; \int_{\mathcal{E}} f \, d\mu = 0 \right\}.$$

We introduce the general setting as proposed in [54] and in the sequel, we apply it on Langevin dynamics. In [54], two sufficient conditions for the exponential convergence are stated: a Lyapunov condition and a minorization condition.

We denote by P the evolution operator, here $P = \mathrm{e}^{t_0 \mathcal{L}}$ for some $t_0 > 0$. The Lyapunov condition makes sure that the dynamics returns to the region of the configuration space where the value of the Lyapunov function are not too large. It reads:

Assumption 1.3 (Lyapunov condition) *There exists a function $\mathcal{K} : X \to [1, +\infty)$ and constants $b \geqslant 0$ and $a \in (0, 1)$ such that*

$$(P\mathcal{K})(x) \leqslant a\mathcal{K}(x) + b, \quad \forall x \in X. \tag{1.37}$$

The second necessary condition is the minorization condition:

Assumption 1.4 (Minorization condition) *There exists a constant $\eta \in (0, 1)$ and a probability measure λ such that*

$$\inf_{x \in \mathcal{C}} P(x, \mathrm{d}y) \geqslant \eta \, \lambda(dy),$$

where $\mathcal{C} = \{x \in X \mid \mathcal{K}(x) \leqslant C_{\max}\}$ for some $C_{\max} > 1 + 2b/(1 - \alpha)$, where a, b are introduced in Assumption 1.3.

This condition ensures that there is a sufficiently strong coupling of the evolution in the region where the Lyapunov function is bounded by $C_{\max}$. When the configuration space is compact, or when the set $\mathcal{C}$ is compact, this condition is easy to prove for SDEs since it is implied by the irreducibility property and some

regularity results on the density of the transition kernel. As we have already mentioned, the latter result is provided by hypoellipticity, which holds for Langevin dynamics.

When the Lyapunov and minorization conditions hold true, the following convergence result is obtained [54]:

Theorem 1.5 (Exponential convergence in weighted L^∞-spaces). *Suppose that Assumptions 1.3 and 1.4 hold. Then P admits a unique invariant probability measure π. This measure is such that*

$$\int_X \mathcal{K} d\pi < +\infty. \tag{1.38}$$

Moreover, there exist $C > 0$ and $r \in (0,1)$ such that, for any $\varphi \in L^\infty_{\mathcal{K}}(X)$ and any $n \in \mathbb{N}$,

$$\left\| P^n \varphi - \int_X \varphi d\pi \right\|_{L^\infty_{\mathcal{K}}} \leqslant C r^n \left\| \varphi - \int_X \varphi d\pi \right\|_{L^\infty_{\mathcal{K}}}. \tag{1.39}$$

For the standard Langevin dynamics where $X = \mathcal{E}$ (recall that the position space is compact) and $\pi = \mu$, the Lyapunov condition holds with the Lyapunov function

$$\mathcal{K}_n(q,p) = 1 + |p|^{2n} \tag{1.40}$$

for $n \geqslant 1$, since

$$\begin{aligned} \mathcal{L}\mathcal{K}_n(q,p) &= -p^T \nabla V(q) - \gamma n \left(p^T M^{-1} p - \frac{n+d-2}{\beta} \right) |p|^{n-2} \\ &\leqslant -\frac{\gamma n}{m_+} |p|^n + \|\nabla V\|_{L^\infty} |p| + \frac{\gamma n (n+d-2)}{\beta} |p|^{n-2}, \end{aligned}$$

with $m_+ = \max(m_1, \ldots, m_d)$. Therefore there exists $b_n \geqslant 0$ such that

$$\mathcal{L}\mathcal{K}_n \leqslant -\frac{\gamma n}{2m_+} \mathcal{K}_n + b_n.$$

This inequality implies (1.37) (see [82] for more details). Moreover, we have already discussed why the minorization condition is satisfied, so this allows to state the following convergence result.

Theorem 1.6 (Langevin dynamics: Exponential convergence of the law). *Consider Langevin dynamics* (1.25)*. The invariant measure μ is unique. Moreover, for any $n \geqslant 2$ there exist constants C_n and $\lambda_n > 0$ such that*

$$\forall f \in L^\infty_{\mathcal{K}_n}, \quad \forall\, t \geqslant 0, \qquad \left\| \mathrm{e}^{t\mathcal{L}} f - \int_{\mathcal{E}} f d\mu \right\|_{L^\infty_{\mathcal{K}_n}} \leqslant C_n \mathrm{e}^{-\lambda_n t} \|f\|_{L^\infty_{\mathcal{K}_n}}. \tag{1.41}$$

We define the projection on the functions with zero average with respect to the measure μ by

$$\Pi_\mu f = f - \int_{\mathcal{E}} f d\mu \tag{1.42}$$

and the space $\widetilde{L^\infty_{\mathcal{K}_s}} = \Pi_\mu \left(L^\infty_{\mathcal{K}_s}\right)$. The ergodicity result of Theorem 1.6 allows us to conclude that the operator $\mathcal{L}$ is invertible on $\widetilde{L^\infty_{\mathcal{K}_s}}$ since the following operator equality holds on $\mathcal{B}\left(\widetilde{L^\infty_{\mathcal{K}_s}}\right)$, the Banach space of bounded operators on $\widetilde{L^\infty_{\mathcal{K}_s}}$:

$$\mathcal{L}^{-1} = \int_0^{+\infty} \mathrm{e}^{t\mathcal{L}}\, dt. \tag{1.43}$$

Corollary 1.1. *For any $n \geqslant 2$ it holds that*

$$\left\|\mathcal{L}^{-1}\right\|_{\mathcal{B}\left(\widetilde{L^\infty_{\mathcal{K}_n}}\right)} \leqslant \frac{C_n}{\lambda_n}, \tag{1.44}$$

where λ, C are the constants introduced in Theorem 1.6.

1.3.1.4 A Central Limit theorem for ergodic averages

Recall that the estimator $\widehat{\cdot}$ of a given observable φ is defined (see (1.29)) as

$$\widehat{\varphi}_t = \frac{1}{t}\int_0^t \varphi(q_s, p_s) ds.$$

We have explained in Section 1.3.1.1 how to prove that the almost sure convergence (1.29) holds for Langevin dynamics. The Central limit theorem (CLT) then provides convergence rates parametrized by the asymptotic variance. In order show that a CLT holds, we first show that the asymptotic variance is well-defined. This quantity reads

$$\sigma^2_\varphi = \lim_{t\to+\infty} t\,\mathrm{Var}_\mu(\widehat{\varphi}_t), \tag{1.45}$$

where

$$t\,\mathrm{Var}_\mu(\widehat{\varphi}_t) = t\,\mathbb{E}_\mu[(\widehat{\varphi}_t)^2 - (\mathbb{E}_\mu\widehat{\varphi}_t)^2] = t\,\mathbb{E}_\mu\left[\left(\frac{1}{t}\int_0^t \Pi_\mu\varphi(q_s,p_s)\mathrm{d}s\right)^2\right].$$

The expectations are with respect to initial conditions $(q_0, p_0) \sim \mu$ and for all realizations of the stochastic dynamics. Note that the invariance of μ allows to write $\mathbb{E}_\mu\widehat{\varphi}_t = \mathbb{E}_\mu\varphi$. In the following we rewrite (1.45) in terms of the semi-group $\mathrm{e}^{t\mathcal{L}}$ and we use the estimates obtained in the previous section in order to show that the variance is well-defined.

We expand $t\,\mathrm{Var}_\mu(\widehat{\varphi}_t)$ as

$$
\begin{aligned}
t\,\mathrm{Var}_\mu(\widehat{\varphi}_t) &= \frac{1}{t}\int_0^t\int_0^t \mathbb{E}_\mu\left[\Pi_\mu\varphi(q_s,p_s)\Pi_\mu\varphi(q_r,p_r)\right] ds\, dr \\
&= \frac{2}{t}\int_0^t\int_0^s \mathbb{E}_\mu\left[\Pi_\mu\varphi(q_s,p_s)\Pi_\mu\varphi(q_r,p_r)\right] ds\, dr, \\
&= 2\int_0^t\left(1-\frac{s}{t}\right)\mathbb{E}_\mu\left[\Pi\varphi(q_s,p_s)\Pi_\mu\varphi(q_0,p_0)\right] ds \\
&= 2\int_0^t\left(1-\frac{s}{t}\right)\int_{\mathcal{E}}\left(\mathrm{e}^{s\mathcal{L}}\Pi_\mu\varphi\right)\Pi_\mu\varphi\, d\mu\, ds,
\end{aligned}
\tag{1.46}
$$

where we used

$$
\mathbb{E}_\mu\left[\Pi_\mu\varphi(q_s,p_s)\Pi_\mu\varphi(q_r,p_r)\right] = \mathbb{E}_\mu\left[\Pi_\mu\varphi(q_{s-r},p_{s-r})\Pi_\mu\varphi(q_0,p_0)\right]
$$

which is implied by the stationarity of μ. We assume the following decay estimates of the semi-group $\mathrm{e}^{s\mathcal{L}}$ in a functional space $\mathscr{E} \subset L^2_0(\mu)$:

$$
\|\mathrm{e}^{s\mathcal{L}}\|_{\mathcal{B}(\mathscr{E})} \leqslant C\,\mathrm{e}^{-\kappa s}, \quad \forall t \geqslant 0, \tag{1.47}
$$

for some constant $C \in \mathbb{R}_+$ and $\kappa > 0$. We have shown in the previous section how to obtain such estimates: by hypocoercivity techniques where $\mathscr{E}$ is $L^2_0(\mu)$ or $H^1(\pi) \cap L^2_0(\pi)$, or by the techniques for weighted-L^∞ spaces where $\mathscr{E}$ is $\widetilde{L^\infty_{\mathcal{K}}}(\mathcal{E})$. Then the dominated convergence theorem shows for $\varphi \in \mathscr{E}$ that

$$
t\,\mathrm{Var}_\mu(\widehat{\varphi}_t) \xrightarrow[t\to+\infty]{} \sigma^2_\varphi,
$$

with

$$
\sigma^2_\varphi = 2\int_0^{+\infty}\int_{\mathcal{E}}(\mathrm{e}^{s\mathcal{L}}\Pi_\mu\varphi)\Pi_\mu\varphi\, d\mu\, ds = -2\int_{\mathcal{E}}(\mathcal{L}^{-1}\Pi_\mu\varphi)\Pi_\mu\varphi\, d\mu. \tag{1.48}
$$

Note that the integral on the right hand side is well-defined if and only if the solution Φ of the Poisson equation

$$
\mathcal{L}\Phi = \Pi_\mu\varphi \tag{1.49}
$$

belongs to $\mathscr{E} \subset L^2(\mu)$. By Corollary 1.1, the operator $\mathcal{L}^{-1}$ is a well-defined bounded operator on $\widetilde{L^\infty_{\mathcal{K}_n}}(\mathcal{E})$ for $n \geqslant 2$ (and an equivalent result holds on $L^2_0(\mu)$ or $H^1(\pi) \cap L^2_0(\pi)$ by hypocoercivity results).

If the Poisson equation (1.49) has a solution in $L^2(\mu)$ and the initial conditions are distributed according to μ, the results obtained in [17] show that a CLT holds, *i.e.*

$$
\sqrt{t}\,\widehat{\Pi_\mu\varphi_t} \xrightarrow[t\to+\infty]{\text{law}} \mathcal{N}(0,\sigma^2_\varphi).
$$

In order to conclude this section, let us introduce a notion of correlation time in order to compare the asymptotic variance (1.48) and the asymptotic variance obtained by averages of independent and identically distributed (i.i.d.) random variables $(q^n,p^n)_{n\geqslant 1}$ with common law μ. For $\varphi \in L^2(\mu)$, a CLT holds for the estimator

$$\widehat{\varphi^{\mathrm{iid}}_{N_{\mathrm{iter}}}} = \frac{1}{N_{\mathrm{iter}}} \sum_{n=1}^{N_{\mathrm{iter}}} \varphi(q^n, p^n), \tag{1.50}$$

whose asymptotic variance is given by

$$\sigma^2_{\varphi,\mathrm{iid}} = \lim_{N_{\mathrm{iter}} \to +\infty} N_{\mathrm{iter}} \mathbb{E}_\mu \left[\left(\widehat{\Pi_\mu \varphi^{\mathrm{iid}}_{N_{\mathrm{iter}}}} \right)^2 \right] = \int_{\mathcal{E}} (\Pi_\mu \varphi)^2 d\mu.$$

We define $\theta_{\mathrm{corr},\varphi}$ as some correlation time and express the asymptotic variance (1.48) for time averages estimates with ergodic SDEs as

$$\sigma^2_\varphi = \theta_{\mathrm{corr},\varphi} \sigma^2_{\varphi,\mathrm{iid}}. \tag{1.51}$$

In other words, in order to have an estimator of the same quality as the one based on N_{iter} i.i.d. samples, integration times of order $t = N_{\mathrm{iter}} \theta_{\mathrm{corr},\varphi}$ should be considered.

1.3.2 Discretization of Langevin dynamics

The Hamiltonian dynamics can be recovered as the limit $\gamma \to 0$ of Langevin dynamics. Therefore, many discretization schemes for Langevin dynamics are obtained by appropriate modifications of the schemes for Hamiltonian dynamics (1.5). One of the first and most popular schemes for the integration of Langevin dynamics (1.25) is the so-called Brünger-Brooks-Karplus (BBK) scheme proposed by [28]. Even though there exist schemes with better properties, it is widely implemented in numerous simulation packages. Many others schemes have been proposed for Langevin dynamics, see for instance [76]. We focus here on schemes based on a splitting of the generator of the dynamics in the case where the position space is compact. In this situation, the ergodicity of the discretized process can be proven, and hence there is no need for implicit schemes or a Metropolization of the dynamics in order to ensure the existence of an invariant probability measure.

1.3.2.1 Splitting strategies

A systematic way of designing a discretization scheme of (1.25) is by splitting the generator (1.26). This technique is based on the approach used for the discretization of deterministic dynamics (see [53]). The most common splitting schemes for Langevin dynamics are of order 1 or 2. It is theoretically possible to design schemes of an arbitrary order. However, an order higher than two is often not an option for particle simulations, not only because such schemes require multiple forces evaluation per time step (which may be unacceptable due to the system size), but more importantly because the time step size is limited by the stability properties of the dynamics.

Consider an operator X such that $X = A_1 + A_2$. The evolution operator of the dynamics with generator X is $\mathrm{e}^{\Delta t X}$. Its discrete counterpart is the operator associated with the one-step numerical scheme under consideration. It is characterized by the action on a test function φ:

$$P_{\Delta t} \varphi(x) = \mathbb{E}\left(\varphi\left(x^{n+1} \right) | x^n = x \right).$$

It is possible to infer the weak order from the error after one step (see also [90] and Section 1.3.2.2 below): under some technical conditions, the numerical scheme has a weak order $\alpha \geqslant 1$ if

$$P_{\Delta t}\varphi = \mathrm{e}^{\Delta t X}\varphi + O\left(\Delta t^{\alpha+1}\right). \tag{1.52}$$

The Lie-Trotter splitting is a first-order splitting, whose evolution operator reads

$$P_t^{\mathrm{Lie}}\varphi = \mathrm{e}^{tA_1}\mathrm{e}^{tA_2}\varphi.$$

A second order in the time step size can be achieved by the Strang splitting which has the evolution operator

$$P_t^{\mathrm{Strang}}\varphi = \mathrm{e}^{tA_1/2}\mathrm{e}^{tA_2}\mathrm{e}^{tA_1/2}\varphi.$$

The order of the splitting is obtained through the Baker-Campbell-Hausdorff (BCH) formula [53], which states that for two operators A_1 and A_2 there exists an operator Z_t such that

$$\mathrm{e}^{tA_1}\mathrm{e}^{tA_2} = \mathrm{e}^{Z_t},$$

with

$$Z_t = t\left(A_1 + A_2\right) + \frac{t^2}{2}\left[A_1, A_2\right] + \mathrm{O}\left(t^2\right), \quad [A_1, A_2] = A_1A_2 - A_2A_1.$$

By comparing the formal expansion of the operator $\mathrm{e}^{\Delta t X}$ one can easily see that the Lie-Trotter splitting formally is first order accurate in the time step size Δt:

$$\mathrm{e}^{\Delta t X} = \mathrm{e}^{\Delta t A_1}\mathrm{e}^{\Delta t A_2} + \mathrm{O}\left(\Delta t^2\right).$$

By the same principle we can see that the Strang splitting has order 2:

$$\mathrm{e}^{\Delta t X} = \mathrm{e}^{\Delta t A_1/2}\mathrm{e}^{\Delta t A_2}\mathrm{e}^{\Delta t A_1/2} + \mathrm{O}\left(\Delta t^3\right).$$

This approach can be applied to the stochastic differential equation (1.25). For a fixed time step size $\Delta t > 0$, we denote the evolution operator of the discretization scheme by $P_{\Delta t}$. This operator is defined for the Markov chain (q^n, p^n) as follows: for any smooth observable φ,

$$P_{\Delta t}\varphi(q,p) = \mathbb{E}\left(\varphi(q^{n+1}, p^{n+1}) \mid (q^n, p^n) = (q,p)\right).$$

In this framework, the formal equality (1.52) should be understood in the following sense: there is $\alpha \in \mathbb{N}$ such that for a given $\varphi \in \mathscr{S}$ (recall that $\mathscr{S}$ is a space of functions and their derivatives growing at most polynomially, that we introduced in Section 1.3.1.3), there exist $K, \Delta t^* > 0$ for which

$$P_{\Delta t}\varphi = \mathrm{e}^{\Delta t \mathcal{L}}\varphi + \Delta t^{\alpha+1} r_{\Delta t,\varphi}, \quad \text{for any } 0 < \Delta t \leqslant \Delta t^*, \tag{1.53}$$

with the remainder $\|r_{\Delta t,\varphi}\|_{L^\infty_{\mathcal{K}}} \leqslant K$ for some scale function $\mathcal{K}$, and the operator $\mathcal{L}$ is given by (1.26).

The generator (1.26) can be decomposed into three operators:

$$A := M^{-1}p \cdot \nabla_q, \qquad B := -\nabla V(q) \cdot \nabla_p, \qquad \mathcal{L}_{\mathrm{FD}} := -M^{-1}p \cdot \nabla_p + \frac{1}{\beta}\Delta_p\,, \tag{1.54}$$

The generator of the fluctuation-dissipation part is denoted by $\gamma\mathcal{L}_{\mathrm{FD}}$, while the generator of the Hamiltonian part is $\mathcal{L}_{\mathrm{Ham}} = A + B$. Note that $\mathcal{L} = \mathcal{L}_{\mathrm{Ham}} + \gamma\mathcal{L}_{\mathrm{FD}}$. The elementary dynamics associated with $\mathcal{L}_{\mathrm{FD}}$ is the following Ornstein-Uhlenbeck process:

$$dp_t = -\gamma M^{-1}p_t\,dt + \sqrt{\frac{2\gamma}{\beta}}\,dW_t, \tag{1.55}$$

which can be solved analytically as

$$p_t = \alpha_t p_0 + \sqrt{\frac{2\gamma}{\beta}}\int_0^t \alpha_{t-s}dW_s\,, \quad \alpha_t := \mathrm{e}^{-\gamma M^{-1}t}. \tag{1.56}$$

A Lie-Trotter splitting of the elementary evolutions generated by $A, B, \gamma\mathcal{L}_{\mathrm{FD}}$ provides six possible first-order splitting schemes of the general form

$$P_{\Delta t}^{Z,Y,X} = \mathrm{e}^{\Delta t Z}\,\mathrm{e}^{\Delta t Y}\,\mathrm{e}^{\Delta t X},$$

with all possible permutations (Z, Y, X) of $(A, B, \gamma\mathcal{L}_{\mathrm{FD}})$. For instance, the numerical scheme associated with $P_{\Delta t}^{B,A,\gamma\mathcal{L}_{\mathrm{FD}}}$ reads

$$\begin{cases} \widetilde{p}^{n+1} = p^n - \Delta t\,\nabla V(q^n), \\ q^{n+1} = q^n + \Delta t\,M^{-1}\widetilde{p}^{n+1}, \\ p^{n+1} = \alpha_{\Delta t}\widetilde{p}^{n+1} + \sqrt{\dfrac{1-\alpha_{\Delta t}^2}{\beta}M}\,G^n, \end{cases} \tag{1.57}$$

where $(G^n)_{n\geqslant 0}$ are i.i.d. Gaussian random vectors with identity covariance. Second-order splitting schemes are obtained by a Strang splitting of the elementary evolutions generated by $A, B, \gamma\mathcal{L}_{\mathrm{FD}}$. There are again six possible schemes, which are of the general form

$$P_{\Delta t}^{Z,Y,X,Y,Z} = \mathrm{e}^{\Delta t Z/2}\,\mathrm{e}^{\Delta t Y/2}\,\mathrm{e}^{\Delta t X}\,\mathrm{e}^{\Delta t Y/2}\,\mathrm{e}^{\Delta t Z/2},$$

with the same possible orderings as for first-order schemes.

Another class of methods which may be useful can also be obtained through a Lie-Trotter splitting between the Hamiltonian and the fluctuation-dissipation provided the Hamiltonian part is discretized at order 2 at least [23, 3]:

$$P_{\Delta t} = \mathrm{e}^{\Delta t A/2}\mathrm{e}^{\Delta t\gamma B}\mathrm{e}^{\Delta t A/2}\mathrm{e}^{\Delta t\gamma\mathcal{L}_{\mathrm{FD}}}, \tag{1.58}$$

where the Hamiltonian part is integrated by a Strang splitting of the operator $\mathrm{e}^{\Delta t \mathcal{L}_{\mathrm{Ham}}}$, such as the one correspondingly to the Verlet scheme (1.8). This scheme is called Geometric Langevin algorithm (GLA), and it reads:

$$\begin{cases} p^{n+1/2} = p^n - \nabla V(q^n)\dfrac{\Delta t}{2}, \\ q^{n+1} = q^n + M^{-1}p^{n+1/2}\Delta t, \\ \tilde{p}^{n+1} = p^{n+1/2} - \nabla V(q^{n+1})\dfrac{\Delta t}{2}, \\ p^{n+1} = \alpha_{\Delta t}\tilde{p}^{n+1} + \sqrt{\dfrac{1-\alpha_{\Delta t}^2}{\beta}M}G^n. \end{cases} \tag{1.59}$$

1.3.2.2 Numerical analysis

The standard numerical analysis of SDEs traditionally distinguishes two types of discretization errors [90, 68]:

(1) *Weak error estimates.* There exists $\alpha \in \mathbb{R}_+$ such that, for any compactly supported C^∞ test function φ and finite time horizon $T > 0$, there are $C \geqslant 0$ and $\Delta t^* > 0$ for which, for any $0 < \Delta t \leqslant \Delta t^*$,

$$\sup_{0 \leqslant n \leqslant T/\Delta t} |\mathbb{E}[\varphi(x^n)] - \mathbb{E}[\varphi(x_{n\Delta t})]| \leqslant C\Delta t^\alpha.$$

As stated in Theorem 2.1 of [90], the order α in these error estimates is determined by the error over one time step and some control of the moments of the numerical scheme and the continuous dynamics, *i.e.* the formal equality (1.53).

(2) *Strong error estimates in L^p-norm.* There exists $\alpha \in \mathbb{R}_+$ for which, for any time horizon T, there is $C \geqslant 0$ and $\Delta t^* > 0$ such that, for any $0 < \Delta t \leqslant \Delta t^*$,

$$\sup_{0 \leqslant n \leqslant T/\Delta t} (\mathbb{E}|x^n - x_{n\Delta t}|^p)^{1/p} \leqslant C\Delta t^\alpha.$$

The constants C and $\Delta t^* > 0$ depend on φ and T. In fact, the constant C is obtained via some (discrete) Gronwall estimate, as in the standard numerical analysis of ordinary differential equations. It hence, in general, increases exponentially with time. The above error estimates are therefore not relevant to long-time convergence since the prefactor C is not uniformly controlled in time.

1.3.2.3 Ergodicity of the discretized dynamics

For molecular dynamics, the interest is rather on the error behavior in the ergodic limit. The discretized Langevin dynamics provides samples (q^n, p^n) for the approximations of ergodic averages (1.9) by the estimator

$$\widehat{\varphi}_{N_{\mathrm{iter}},\Delta t} = \frac{1}{N_{\mathrm{iter}}} \sum_{n=0}^{N_{\mathrm{iter}}-1} \varphi\left(q^n, p^n\right). \tag{1.60}$$

Once the irreducibility and the invariance of a probability measure $\mu_{\Delta t}$ ($\neq \mu$) of the Markov chain are proved, the Law of Large Numbers ensures that

$$\lim_{N_{\text{iter}} \to \infty} \widehat{\varphi}_{N_{\text{iter}}} = \int_{\mathcal{E}} \varphi(q,p)\, d\mu_{\Delta t}\,(q,p) = \mathbb{E}_{\mu_{\Delta t}}\,(\varphi) \quad \text{a.s.}$$

The total error can be decomposed into two error terms:

$$\widehat{\varphi}_{N_{\text{iter}}} - \mathbb{E}_{\mu}\,(\varphi) = \Big(\mathbb{E}_{\mu_{\Delta t}}\Big(\varphi\Big) - \mathbb{E}_{\mu}\,(\varphi)\Big) + \Big(\widehat{\varphi}_{N_{\text{iter}}} - \mathbb{E}_{\mu_{\Delta t}}\,(\varphi)\Big). \tag{1.61}$$

The first term corresponds to the systematic error (bias) determined by the error on the invariant measure due to the finite time step used for the discretization (see Section 1.3.2.4). The second term corresponds to the statistical error, which we address in Section 1.3.2.5.

The ergodicity of the splitting schemes presented in Section 1.3.2.1 can be proved for compact position spaces [78]. For unbounded position spaces, a geometric convergence has been shown only for implicit schemes (see [85, 71]).

The proof of the ergodicity of the splitting schemes for compact position spaces provided in [78] is, similarly to the continuous dynamics, based on the fact that a minorization and a Lyapunov condition hold for the discretization scheme (described by an evolution operator $P_{\Delta t}$).

- *Uniform minorization condition*: for any $T > 0$ large enough and any fixed $p^* > 0$, there exist $\Delta t^* > 0, \kappa > 0$ and a probability measure ν such that, for any bounded, measurable non-negative function f, for any $0 < \Delta t \leqslant \Delta t^*$ and any $(q,p) \in \mathcal{E}$,

$$\inf_{|p| \leqslant p^*} \left[(P_{\Delta t})^{\lceil T/\Delta t \rceil}\, f\right](q,p) \geqslant \kappa \int_{\mathcal{E}} f \mathrm{d}\nu.$$

- *Uniform Lyapunov condition*: there exists $\Delta t^* > 0$ such that for any $s^* \in \mathbb{N}$ and $0 < \Delta t \leqslant \Delta t^*$, there exist $b > 0$ and $a \in [0,1)$ such that for any $0 < s \leqslant s^*$

$$P_{\Delta t} \mathcal{K}_s \leqslant \mathrm{e}^{-a\Delta t} \mathcal{K}_s + b,$$

  where $\mathcal{K}_s(p) = 1 + |p|^{2s}$ has already been introduced in (1.40).

This approach was used in [78] in order to prove the ergodicity of first and second order splitting schemes for compact position spaces, and obtain resolvent bounds uniform with respect to Δt.

Theorem 1.7. *Consider one of the discretization schemes with the evolution operator $P_{\Delta t}$ obtained through splitting of order 1 or 2 as introduced in Section 1.3.2.1. Then for any $\gamma > 0$, there exists Δt^* for which there is a unique invariant measure $\mu_{\Delta t}$ with finite moments: for any $s \geqslant 1$ and $0 < \Delta t < \Delta t^*$,*

$$\int_{\mathcal{E}} \mathcal{K}_s d\mu_{\Delta t} < \infty.$$

Moreover the following exponential convergence holds: for any $s \geqslant 1$, there exist $\lambda, K > 0$ such that for all $\varphi \in L^\infty_{\mathcal{K}_s}$ and $0 < \Delta t \leqslant \Delta t^*$,

$$\forall n \geqslant 0, \quad \left\| P^n_{\Delta t}\varphi - \int_{\mathcal{E}} \varphi \, d\mu_{\Delta t} \right\|_{L^\infty_{\mathcal{K}_s}} \leqslant K \mathrm{e}^{-\lambda n \Delta t} \left\| \varphi \right\|_{L^\infty_{\mathcal{K}_s}}. \tag{1.62}$$

In particular,

$$\left\| \Big(\frac{\mathrm{Id} - P_{\Delta t}}{\Delta t} \Big)^{-1} \right\|_{\mathcal{B}\left(L^\infty_{\mathcal{K}_s}\right)} \leqslant \frac{K}{\lambda}.$$

In general, in order to ensure the existence of an invariant measure, the numerical method can be connected to a Metropolis-Hastings step.

1.3.2.4 Error on the invariant measure

The discretized Langevin dynamics based on splitting schemes in compact position spaces admits a unique invariant measure $\mu_{\Delta t}$ (see Theorem 1.7), which is different from the canonical measure μ. The difference between μ and $\mu_{\Delta t}$ can be estimated from the weak error of the discretization schemes provided the numerical scheme induces an ergodic Markov chain. In the following section, we recall the framework reviewed in [82], which can be used to study splitting schemes for Langevin dynamics (1.25) as in [78].

More specifically, we assume that the continuous dynamics, with generator $\mathcal{L}$, admits a unique invariant measure μ and that the numerical scheme with discrete evolution operator $P_{\Delta t}$ admits an invariant measure $\mu_{\Delta t}$. Moreover suppose that, for a C^∞ function φ and a given integer α, the evolution operator can be expanded as

$$P_{\Delta t}\varphi = \varphi + \Delta t \, \mathcal{A}_1\varphi + \Delta t^2 \mathcal{A}_2\varphi + \cdots + \Delta t^{\alpha+1}\mathcal{A}_{\alpha+1}\varphi + \Delta t^{\alpha+2} r_{\varphi,\Delta t}, \tag{1.63}$$

for some remainder term $r_{\varphi,\Delta t}$ such that $\left\| r_{\Delta t,\varphi} \right\|_{L^\infty_{\mathcal{K}}} \leqslant K$ and a scale function $\mathcal{K}$ with values in $[1, +\infty)$. The operators $\mathcal{A}_k$ are identified in practice by Taylor expansions with an integral remainder and an average over the randomness.

The following theorem characterizes the error on the invariant measure.

Theorem 1.8 ([82]). *Suppose that the operators $\mathcal{A}_1^{-1}$ and $(\mathcal{A}_1^*)^{-1}$ leave $\widetilde{\mathscr{S}}$ invariant, and that an expansion such as* (1.63) *holds for any $\varphi \in \mathscr{S}$ and $\alpha \in \mathbb{N}$, with a remainder $r_{\varphi,\Delta t}$ for which there exist $K \geqslant 0$, $m \in \mathbb{N}$ and $\Delta t^* > 0$ (all depending on φ and α) such that*

$$\left\| r_{\varphi,\Delta t} \right\|_{L^\infty_{\mathcal{K}_m}} \leqslant K, \quad \forall \Delta t \leqslant \Delta t^*.$$

Assume in addition that the operators $\mathcal{A}_k$ leave $\mathscr{S}$ invariant for any $k \geqslant 1$, that there exists $\alpha \geqslant 1$ such that, for any $\varphi \in \mathscr{S}$,

$$\int_{\mathcal{E}} \mathcal{A}_k\varphi \, d\mu = 0, \quad \forall k \in \{1, \ldots, \alpha\}, \tag{1.64}$$

and that $g_{\alpha+1} = \mathcal{A}_{\alpha+1}^* \mathbf{1} \in \widetilde{\mathscr{S}}$. *Finally, assume that the numerical scheme admits an invariant measure* $\mu_{\Delta t}$ *which integrates all scale functions:*

$$\int_{\mathcal{E}} \mathcal{K}_n \, d\mu_{\Delta t} < +\infty, \quad \forall n \geqslant 0.$$

Then, there exists $L > 0$ *such that, for any* $0 < \Delta t \leqslant \Delta t^*$,

$$\int_{\mathcal{E}} \varphi \, d\mu_{\Delta t} = \int_{\mathcal{E}} \varphi \, d\mu + \Delta t^{\alpha} \int_{\mathcal{E}} \varphi f_{\alpha+1} \, d\mu + \Delta t^{\alpha+1} R_{\varphi,\Delta t}, \tag{1.65}$$

with $|R_{\varphi,\Delta t}| \leqslant L$ *and where*

$$f_{\alpha+1} = -\left(\mathcal{A}_1^*\right)^{-1} g_{\alpha+1} \in \widetilde{\mathscr{S}}. \tag{1.66}$$

Note that for a method of weak order α it holds $\mathcal{A}_k = \mathcal{L}^k/k!$ for $1 \leqslant k \leqslant \alpha$. However, the previous theorem suggests that, if the operators in the expansion are such that $\mathcal{A}_k = a_k \mathcal{L}^k$ with some prefactor $a_k \neq 1/k!$ for some $1 \leqslant k \leqslant \alpha$, the dynamics might preserve the invariant measure up to error terms of order $\Delta t^{\alpha+1}$, even though its weak order is not α. We also refer to [3], where Langevin dynamics is discretized by schemes for which the operators $\mathcal{A}_k$ are quite different from $\mathcal{L}^k$ although the invariant measure $\mu_{\Delta t}$ is still close to μ.

The application of the previous theorem on the GLA scheme (1.59) immediately gives that, even though this scheme has a weak error 1, the resulting error on the invariant measure is of order 2 (since the generators $\mathcal{L}_{\mathrm{FD}}$ and $\mathcal{L}_{\mathrm{Ham}}$ preserve the measure as needed for (1.64)).

The leading order (1.66) in the expansion (1.65) can be explicitly computed and estimated as an integrated correlation function thanks to the following connection: for $\varphi \in \widetilde{\mathscr{S}}$,

$$\int_{\mathcal{E}} \varphi f_{\alpha+1} \, d\mu = -\int_{\mathcal{E}} (\mathcal{L}^{-1} \Pi \varphi) g_{\alpha+1} \, d\mu = \int_0^{+\infty} \int_{\mathcal{E}} \left(\mathrm{e}^{t\mathcal{L}} \Pi \varphi\right) g_{\alpha+1} \, d\mu \, dt = -\int_0^{\infty} \mathbb{E}\left[\varphi(q_t, p_t) g_{\alpha+1}(q_0, p_0)\right] dt.$$

This approach was proposed and applied to Langevin dynamics in [78]. An alternative option to eliminate the leading-order error term is to use Romberg extrapolation [118].

1.3.2.5 Asymptotic variance of trajectorial averages

The statistical error $\widehat{\varphi}_{N_{\mathrm{iter}}} - \mathbb{E}_{\mu_{\Delta t}}(\varphi)$ usually dominates the error on the computation of ergodic averages (1.61). As for the continuous dynamics, a Central Limit Theorem holds true for an ergodic Markov chain once the asymptotic variance is well-defined. The statistical error of an observable $\varphi \in L^\infty_{\mathcal{K}}(\mu_{\Delta t}) \subset L^2(\mu_{\Delta t})$ therefore behaves in the limit $N_{\mathrm{iter}} \to \infty$ as a Gaussian random variable with asymptotic variance given by

$$
\begin{aligned}
\sigma^2_{\Delta t} &= \lim_{N_{\rm iter}\to\infty} N_{\rm iter} \mathrm{Var}_{\mu_{\Delta t}}\left(\widehat{\varphi}_{N_{\rm iter},\Delta \rm t}\right) \\
&= \mathbb{E}_{\mu_{\Delta t}}\left([\Pi_{\Delta t}\varphi]^2\right) + 2\sum_{n=1}^{\infty} \mathbb{E}_{\mu_{\Delta t}}\left[\Pi_{\Delta t}\varphi(q^n,p^n)\Pi_{\Delta t}\varphi(q^0,p^0)\right] \\
&= \int_{\mathcal{E}} \Pi_{\Delta t}\varphi\left[\left(2\left(\mathrm{Id}-P_{\Delta t}\right)^{-1}-\mathrm{Id}\right)\Pi_{\Delta t}\varphi\right]\, d\mu_{\Delta t}
\end{aligned}
\tag{1.67}
$$

where

$$
\Pi_{\Delta t}\varphi := \varphi - \int_{\mathcal{E}} \varphi d\mu_{\Delta t}.
$$

The above limit is obtained from the dominated convergence theorem, once the Poisson equation

$$
\left(\mathrm{Id}-P_{\Delta t}\right)\Phi = \Pi_{\Delta t}\varphi
$$

has a solution in $L^2(\mu_{\Delta t})$. This result is provided by estimates similar to (1.62) where an exponential decay rate uniform with respect to the time step Δt is obtained. For more details we refer to [82]. In conclusion, for $N_{\rm iter}$ simulation steps, the statistical error is of order

$$
\frac{\sigma_{\Delta t}}{\sqrt{N_{\rm iter}}} = \frac{\sigma_{\Delta t}\sqrt{\Delta t}}{\sqrt{T}}.
$$

Note that the variance can be rewritten as

$$
\Delta t\sigma^2_{\varphi,\Delta t} = 2\int_{\mathcal{E}} (\Pi_{\Delta t}\varphi)\left[\left(\frac{\mathrm{Id}-P_{\Delta t}}{\Delta t}\right)^{-1}\Pi_{\Delta t}\varphi\right]\, d\mu_{\Delta t} - \Delta t\int_{\mathcal{E}} |\Pi_{\Delta t}\varphi|^2\, d\mu_{\Delta t}\,.
$$

Since weakly consistent numerical methods are such that

$$
\frac{\mathrm{Id}-\mathrm{P}_{\Delta \rm t}}{\Delta t}\varphi = \mathcal{L}\varphi + O\left(\Delta t\right),
$$

it suggests that

$$
\lim_{\Delta t\to 0} \Delta t\sigma^2_{\varphi,\Delta t} = \sigma^2_{\varphi},
$$

i.e. the variance of the discretized process converges to the variance of the continuous process σ^2 as Δt tends to 0 (see [82] for a rigorous proof).

1.4 Computational challenges

The main computational challenges in molecular dynamics arise from the time and space scales under consideration. In order to achieve sufficient precision in the computation of thermodynamics averages, the simulation needs to capture relevant physical phenomena, which occur at long physical times (of the order of a micro-second (10^{-6}s) up to several hours and more [110]). On the other hand, at the atomistic level, the simulation time steps are of the order of a femto-second (10^{-15} s) due to stability limitations on the

Verlet integration [130]. Moreover, performing a single step is already computationally expensive due to the number of degrees of freedom under consideration.

There are three main factors that influence the speed of convergence measured in terms of computational time: the asymptotic variance of time averages, the maximal admissible time step size for the discretization and the computational effort per time step. In the next sections we discuss these three aspects.

1.4.1 Stability and accuracy

One of the limiting factors for molecular dynamics simulations is *the maximal admissible time step size*. It is usually limited by the highest frequency mode in the model. From a mathematical point of view, the maximal time step size is determined by the stability threshold of the discretization scheme. For pedagogical purpose, we consider the dynamics (1.5) in the case of a harmonic potential with unit mass and pulsation ω in dimension one, for which the Hamiltonian reads

$$H(q,p) = \frac{1}{2}\omega^2 q^2 + \frac{1}{2}p^2.$$

The quadratic form of the harmonic potential allows us to write the one-step iteration of the Verlet scheme (1.8) as the following linear update:

$$\begin{pmatrix} q^{n+1} \\ p^{n+1} \end{pmatrix} = A \begin{pmatrix} q^n \\ p^n \end{pmatrix}, \quad A = \begin{pmatrix} 1 - \dfrac{(\omega\Delta t)^2}{2} & \Delta t \\ -\omega^2 \Delta t \left(1 - \dfrac{(\omega\Delta t)^2}{4}\right) & 1 - \dfrac{(\omega\Delta t)^2}{2} \end{pmatrix}. \tag{1.68}$$

In order to obtain a trajectory $(q^n, p^n)_{n\geqslant 0}$ which is bounded, the eigenvalues of the matrix A must have moduli smaller than 1. This is the case if and only if

$$\omega\Delta t < 2. \tag{1.69}$$

For discretizations of Langevin dynamics (1.25), the stability of the scheme is understood as the existence of an invariant measure $\mu_{\Delta t}$. The stability conditions of discretization schemes for Langevin dynamics can be studied for harmonic problems using a spectral analysis of the matrices encoding the transition operators similar to (1.69) [76, 75].

An alternative option is for instance the application of an implicit method which can be unconditionally stable in the step size. The issue is that such schemes are unconditionally stable in the linear case, but not in the non-linear case. There are also other problems, such as the cost of iterations due to the fix-point method used to solve non-linear systems [76].

Multiple time-stepping methods allow to reduce the instability in molecular dynamics. The RESPA method achieves an increase in the total integration time step by separating fast and slow degrees of freedom and integrating them with different time step size [124, 123, 122, 125]. Another widely used group of methods corresponds to constrained dynamics [32, 35], where stiff bond stretches are removed. For more details we

refer to [81, 76] and references therein. In [13, 95] a method based on changing the mass matrix in order to increase the time steps used in the simulation was proposed.

Finally, a careful analysis of the leading-order error terms of the splitting schemes for Langevin dynamics shows that the order of the splitting operators matters: in the limit of infinite friction, the BAOAB scheme[4] has a leading order correction whose average with respect to momentum vanishes. This property provides accuracy of effective order 2 on the configurational sampling instead of effective order 1 as in other splittings (for instance ABOBA) [74]. This method was also recently combined with constrained Langevin dynamics, allowing a substantial increase of the maximal admissible time step size [77].

1.4.2 Metastability

In many practical applications, potentials which govern the dynamics of the system are very complicated and the sampling process is metastable. Metastability is characterized by the multi-modality of the position marginal of the sampled distribution. A distribution is called multi-modal when it possesses regions of high probability separated from each other by regions with very low probability. In molecular simulations, this implies that the dynamics remains trapped in some region for a long time due to energetic or entropic barriers. In order to illustrate the metastability due to energetic barriers, the complicated energy landscape is usually compared to a mountain range, which must be explored entirely in order to obtain correct averages of observables of interest. The transitions between the valleys require bigger "climbing" effort, and occur rarely. Most of the simulation time is therefore spent in the valleys, which are "over-explored". The main interest is therefore the passage to another valley, which provides new information necessary for the correctness of the computed average.

A simple example which illustrates a metastable dynamics is Langevin dynamics with a double-well potential, which can be[5] given by the following function in dimension 1:

$$V_{\mathrm{DW}}(q) = \frac{h}{\frac{1}{(q-w)^2} + \frac{1}{(q+w)^2}}, \tag{1.70}$$

where h is the height and $\pm w$ are the positions of the wells. Figure 1.5(Left) presents a plot of V_{DW}. The potential possess two energy minima separated by a possibly high energy region. Figure 1.5(Right) shows the temporal evolution of the positions which oscillate around two values with only rare transitions in-between.

Another cause of the metastability are entropic barriers. A paradigmatic example of this situation are two boxes with periodic boundary conditions except in one direction, and connected by a very narrow channel. The potential energy is zero and the stochastic process $(q_t)_{t\geqslant 0}$ is thefore a simple random walk. There are no energetic barriers in this direction, metastability solely arises from entropic effects: it takes a long time for

[4] Recall the construction of the discretization scheme based on the splitting of the generator as for instance (1.58). Note that "O" corresponds to $\mathcal{L}_{\mathrm{FD}}$ in this manuscript.

[5] We use this function since it is very simple to modify it for more modes. A more common double-well function is given by $(q^2 - w^2)^2$ with some parameter w as presented in Section 1.1.1.1.

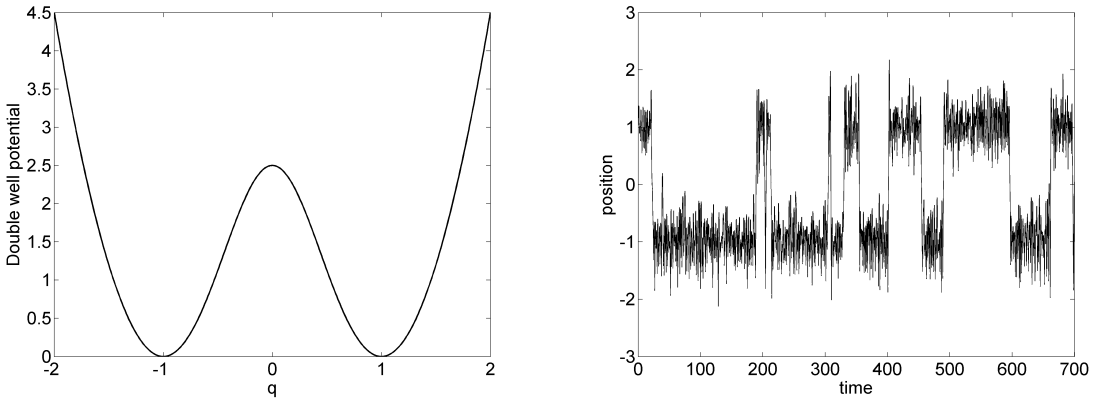

Fig. 1.5: (Left) One-dimensional double-well potential (1.70) with $h = 5$ and $w = 1$. (Right) Evolution of the position as a function of time ($\gamma = 1$ and $\beta = 1$).

a particle to pass from one box into another since the accessible space for the system to leave a metastable state is very small.

These two causes of metastability (energetic and entropic) can be distinguished according to the scaling of the transition rates with respect to the temperature: when the temperature decreases (*i.e.* β increases), the typical time scale to leave a metastable region grows exponentially fast with respect to β for energetic barriers, in accordance with results from large deviation theory [47]; while for an entropic barrier, a change in temperature is (asymptotically) equivalent to a linear rescaling in time.

The metastability implies that the asymptotic variance σ_φ^2 of the time averages defined in (1.48) is relatively high. Since the statistical error is of order $\frac{\sigma_\varphi}{\sqrt{N_{\rm iter}}}$, the number of the simulation steps $N_{\rm iter}$ which are necessary for achieving a certain statistical precision might be very large.

Variance reduction techniques

Many techniques were introduced to reduce the variance of trajectory averages computed with discretizations of SDEs and hence to decrease the statistical error in the estimated averages [29]. These methods can be characterized according to whether they (i) target a given observable, *i.e.* try to reduce σ_φ^2 for a given φ; or (ii) all possible observables, *i.e.* the objective is to decrease

$$\sup_{\varphi \in L^2(\pi)} \frac{\sigma_\varphi^2}{\|\varphi\|_{L^2(\pi)^2}} = \sup_{\|\varphi\|_{L^2(\pi)} \leqslant 1} 2 \int_{\mathcal{X}} \Pi\varphi(-\mathcal{L}^{-1}\Pi\varphi) d\pi.$$

Control variate techniques[6] belong to the first class of variance reduction methods. This approach was proposed in the computational statistics literature [8, 57] and in the statistical physics literature [10]. Instead of computing the ergodic average $\mathbb{E}_\mu[\varphi]$ of the observable φ, it is based on the estimator $\mathbb{E}_\mu[\varphi - \phi]$, where

[6] Also known as known as the zero-variance principle in the statistical physics literature.

an additional observable ϕ was introduced such that $\mathbb{E}[\phi] = 0$. The suggestion is to find ϕ such that the variance $\sigma^2_{\varphi-\phi}$ is smaller than σ^2_φ.

Stratification is a general-purpose variance reduction method. It decomposes the difficult sampling problem into easier sampling problems. The local averages are then re-weighted according to the canonical weight of the region itself [112]. This method can be made practical by using approaches developed in statistics [49, 86, 69] or by thermodynamic integration, which constrains the dynamics on the levels sets and varies the level set constant to sample the full space. See [81] for an introduction to this method.

The key idea of *importance sampling* is to change the measure which is sampled into a measure which is easier to sample. This is most commonly done by replacing the potential energy function V in the dynamics by a modified potential $V + \widetilde{V}$. The modified Langevin dynamics associated with the potential $V + \widetilde{V}$, namely

$$\begin{cases} d\widetilde{q}_t = M^{-1}\widetilde{p}_t dt, \\ d\widetilde{p}_t = -\nabla\Big(V + \widetilde{V}\Big)(\widetilde{q}_t)\mathrm{d}t - \gamma\, M^{-1}\widetilde{p}_t dt + \sqrt{\dfrac{2\gamma}{\beta}} dW_t, \end{cases}$$

is ergodic for the modified canonical probability measure $\mu_{\widetilde{V}} = Z_{\widetilde{V}}^{-1}\, \mathrm{e}^{-\beta\widetilde{V}}\mu$. The fundamental observation to retrieve averages with respect to μ with realizations of the modified dynamics is that

$$\int_{\mathcal{E}} \varphi(q)\, \mu(dq\, dp) = \frac{\displaystyle\int_{\mathcal{E}} \varphi\, \mathrm{e}^{\beta\widetilde{V}} d\mu_{\widetilde{V}}}{\displaystyle\int_{\mathcal{E}} \mathrm{e}^{\beta\widetilde{V}} d\mu_{\widetilde{V}}}. \tag{1.71}$$

In the practice, instead of the estimator

$$\widehat{\varphi}^{\widetilde{V}}_t = \frac{\displaystyle\int_0^t \varphi(\widetilde{q}_s)\, \mathrm{e}^{\beta\widetilde{V}(\widetilde{q}_s)} ds}{\displaystyle\int_0^t \mathrm{e}^{\beta\widetilde{V}(\widetilde{q}_s)} ds}, \tag{1.72}$$

its discretized version is used

$$\widehat{\varphi}^{\widetilde{V}}_{N_{\mathrm{iter}},\Delta t} = \frac{\displaystyle\sum_{n=0}^{N_{\mathrm{iter}}} \varphi(\widetilde{q}^n)\, \mathrm{e}^{\beta\widetilde{V}(\widetilde{q}^n)}}{\displaystyle\sum_{n=0}^{N_{\mathrm{iter}}} \mathrm{e}^{\beta\widetilde{V}(\widetilde{q}^n)}}, \tag{1.73}$$

where $\widetilde{q}^n$ is an approximation of $\widetilde{q}_{n\Delta t}$. In order for importance sampling to be efficient, the weights $\mathrm{e}^{\beta\widetilde{V}(q^n)}$ should not be too degenerate. For a fixed observable, it is possible to optimize the modified potential [33].

Non-reversible dynamics

Methods based on adding non-reversible terms into the dynamics allow to keep the same measure invariant while possibly decreasing the asymptotic variance. For an application to overdamped Langevin dynamics see [41, 100].

Sampling reactive paths

In order to improve the efficiency of the simulation of paths over long times in terms of improved transition rates, *accelerated dynamics* techniques are usually applied. There are three basic methods: Parallel Replica method [129], Hyperdynamics [128] and the Temperature Accelerated Dynamics [113]. See [4, 80] for reviews on these methods.

1.4.3 Computational cost per time step

Many methods focus on reducing the dimensionality of the simulated system in order to lower the computational cost per time step and hence accelerate the simulations in terms of wall-clock time. In some cases, reducing the number of degrees of freedom even allows to increase the stability threshold on the time step. This is the purpose for example of coarse-graining techniques. These methods, as for example dissipative particle dynamics [59, 44], model groups of particles (for instance a molecule) by some effective particles. The interactions between such particles are determined by averaging over the fully detailed system. We also refer to [66, 106] for a few selected works on the coarse-graining methods. Many methods couple multiple-scales models into multi-resolution simulations [96, 43].

Incremental algorithms allow in certain cases to reduce the algorithmic cost per time step by reusing some part of the information from the previous step. This approach was applied in several contexts, *e.g.* for modeling hydrocarbon systems ([20]), proteins ([107]), and for electronic structure calculations ([21]).

In order to conclude this section let us remark that due to the dimensionality of molecular simulations the parallelization of simulations is necessary and therefore all methods should be designed in a way such that the parallelization is possible and efficient.

1.5 Adaptively Restrained Particle Simulations

Adaptively Restrained Particle Simulations (ARPS) is a method proposed in [9] with the aim of accelerating particle simulations. The key idea is to modify the dynamics in order to reduce the computational cost per time step by decreasing the cost of the force computation, which is the most expensive part. This is achieved by "restraining" some particles temporarily: a particle is *restrained* if its position has not changed between two successive time steps. Since particle interactions typically depend on relative positions, this makes it possible to skip the computation of interactions between restrained particles in the update of the force. On Figure 1.6 we illustrate this by a cartoon of a simulation of particles: the left picture represents a simulation of some solute (orange) particles surrounded by solvent particles (blue) and the picture on the right hand

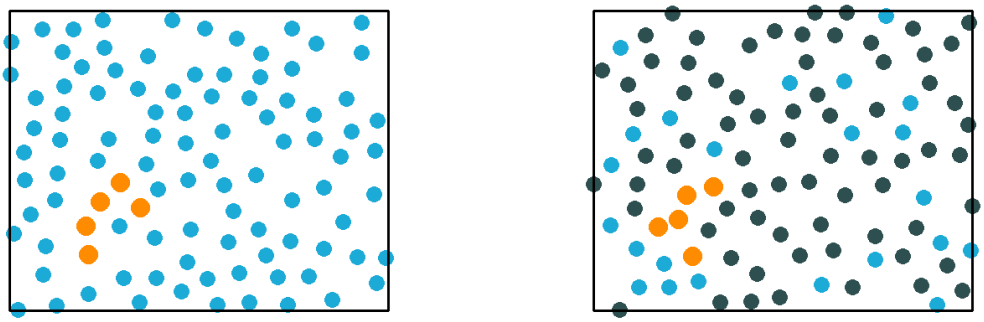

Fig. 1.6: Particle simulation: standard one (left) and ARPS method (right).

size shows a modification of the solvent particles by the ARPS method. The restrained particles are colored in grey. One can easily imagine that skipping all interactions between the restrained particles dramatically reduces the amount of interactions which need to be computed.

The restraining of the particles is achieved by modifying the kinetic energy function. More precisely, the standard kinetic energy function (which is a quadratic function of the momenta) is replaced by a function which is zero for small values of momenta. Looking at the Verlet scheme (1.8), one can immediately see that if the kinetic energy of the particle i vanishes in the neighborhood of a value p_i^n at step n, so does its gradient and the position remains unchanged, *i.e.* $q_i^{n+1} = q_i^n$. In the ARPS method, the kinetic energy function is a sum of individual contributions

$$U_{\mathrm{AR}}(p) = \sum_{i=1}^{N} u(p_i)$$

which are parameterized by two constants $0 \leqslant e_{\min} < e_{\max}$. For large values of momenta, the modified individual kinetic energies are equal to the standard kinetic energy of one particle, but they vanish for small momenta:

$$u(p_i) = \begin{cases} 0 & \text{for } \dfrac{p_i^2}{2m_i} \leqslant e_{\min}, \\ \dfrac{p_i^2}{2m_i} & \text{for } \dfrac{p_i^2}{2m_i} \geqslant e_{\max}, \\ s\left(\dfrac{p_i^2}{2m_i}\right) & \text{for } \dfrac{p_i^2}{2m_i} \in [e_{\min}, e_{\max}]\,. \end{cases}$$

A spline s smoothly interpolates between these two limiting regimes. The Hamiltonian of this dynamics reads

$$H_{\mathrm{AR}}(q,p) = V(q) + U_{\mathrm{AR}}(p),$$

and the invariant measure of the associated Langevin dynamics (assuming $\mathrm{e}^{-\beta H_{\mathrm{AR}}} \in L^1(\mathcal{E})$) is therefore

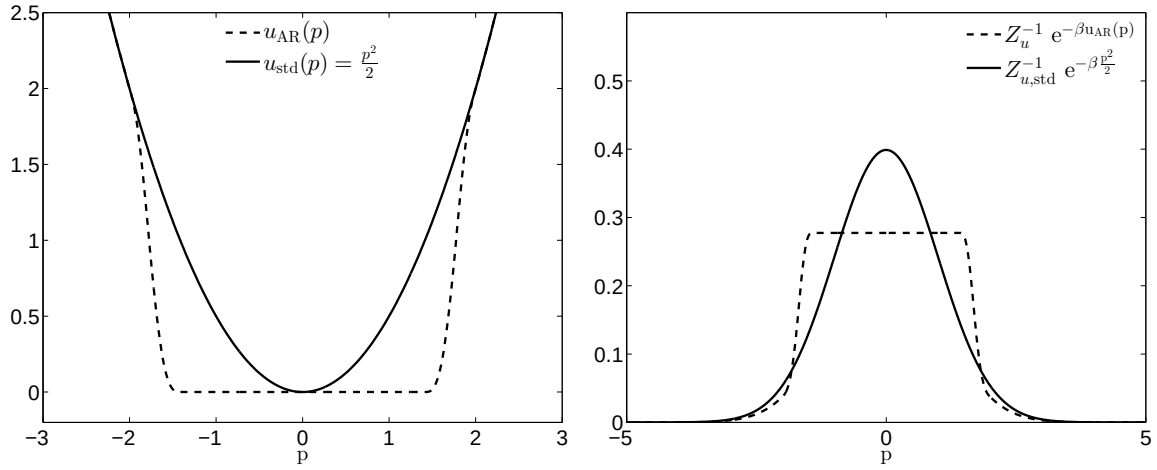

Fig. 1.7: (Left) Standard quadratic kinetic energy function U_{std} (solid lines), and an example of an AR kinetic energy function u with parameters $e_{\max} = 2$ and $e_{\min} = 1$ (dashed line). (Right) The corresponding marginal canonical densities associated with the kinetic energy function.

$$\mu(dq\,dp) = Z_\mu^{-1} \mathrm{e}^{-\beta H_{\mathrm{AR}}(q,p)}\,dq\,dp, \qquad Z_\mu = \int_{\mathcal{E}} \mathrm{e}^{-\beta H_{\mathrm{AR}}(q,p)}\,dq\,dp < +\infty.$$

Due to the separability of the position and momenta marginals of the distribution, the averages of observables which depend on the position variable are equal to the ones computed with the standard Langevin dynamics, *i.e.*

$$\mathbb{E}_{\mu_{\mathrm{AR}}}\left[\varphi(q)\right] = \mathbb{E}_{\mu_{\mathrm{std}}}\left[\varphi(q)\right],$$

where $\mu_{\mathrm{std}}(q,p) = Z_{\mathrm{std}}^{-1} \mathrm{e}^{-\beta U_{\mathrm{std}}(p)} \mathrm{e}^{-\beta V(q)} dpdq$ is the canonical distribution with the standard kinetic energy U_{std} given by (1.7). A possible choice of the values of the parameters in the individual AR kinetic energy u, as well as the associated canonical distribution of momenta $Z_u^{-1} \mathrm{e}^{-\beta u(p)}\,dp$ are depicted in Figure 1.7 when the dimension is 1.

Note that, due to the additive structure of the kinetic energy, the momenta p_i are independent and identically distributed (i.i.d.) under the canonical measure. It is however possible to choose different parameters $e_{\min}$ and $e_{\max}$ for different particles, for example to focus calculations on a specific part of the particle system, in which case the momenta are still independent but not longer identically distributed. Such a situation is for example the solvent solute model already mentioned in Section 1.1.1.1.

1.6 Contributions

The main contributions of this thesis can be summarized as follows:

- The content of Chapter 2 was published in [98]. Motivated by the ARPS method which introduces a modified general kinetic energy, we consider general modified Langevin dynamics with Hamiltonian $H(q,p) = V(q) + U(p)$. We prove the ergodicity both in terms of almost-sure convergence of time averages along a single realization, and convergence of the law of the process, in the case where the kinetic energy is a perturbation of the standard kinetic energy, *i.e.* under the assumption that there exists $C > 0$ such that
$$\forall p \in \mathbb{R}^d, \quad \left| M^{-1}p - \nabla U(p) \right| \leqslant C. \tag{1.74}$$
We also provide a result on the regularity of the evolution semi-group, adapted from similar estimates for standard Langevin dynamics in [117]. These results hold even if U vanishes on some open set. Such estimates allow us to analyze the statistical error. We state in particular a Central Limit Theorem for $\widehat{\varphi}_t$, and perform a perturbative study of the asymptotic variance of the AR-Langevin dynamics in some limiting regime. Our theoretical findings are illustrated by numerical simulations, both in a simple one-dimensional case where the variance can be accurately computed using an appropriate Galerkin approximation, as well as for a more realistic system for which we resort to Monte-Carlo simulations.
- In Chapter 3 we again consider Langevin dynamics with general kinetic energy and focus on the case when the kinetic energy is a local perturbation of the standard kinetic energy (see (1.74)). We study the discretization of such dynamics in order to achieve a second order accuracy on the average properties and construct algorithms which are numerically stable. We metropolize such dynamics and use this approach to quantify the stability of the dynamics in terms of the average rejection rate. Moreover, we propose an alternative definition to [9] of the AR-kinetic energy function which has better stability properties. This work is preprinted as [114].
- In Chapter 4, we study the parametrization of the Adaptively Restrained (AR) Langevin dynamics. We propose an analysis of the influence of the parameters on the total achievable speed-up. A previous work [9] has shown numerically that there exists a choice of parameters for which this method is efficient. We consider all factors which determine the total speed-up with respect to (1.19). We show that from the average properties of the AR-Langevin dynamics, which depend on the choice of the parameters, it is possible to estimate the computational cost. By adding information about the variance, it is also possible to predict the total speed-up as a function of the chosen parameters. We therefore complement the understanding of the method and propose a strategy for finding optimal parameters in practical applications on various systems. This work corresponds to the preprint [120].
- Finally, in the last chapter, we consider Langevin dynamics with general kinetic energies. We present numerical examples where a special form of the kinetic energy improves the sampling of metastable systems. This work is currently in progress, but some preliminary results are presented in the preprint [114].

2

Error Analysis of Modified Langevin Dynamics

Summary. In this chapter we consider Langevin dynamics associated with a modified kinetic energy vanishing for small momenta. This allows us to freeze slow particles, and hence avoid the re-computation of inter-particle forces, which leads to computational gains. On the other hand, the statistical error may increase since there are a priori more correlations in time. The aim of this chapter is first to prove the ergodicity of the modified Langevin dynamics (which fails to be hypoelliptic), and next to analyze how the asymptotic variance on ergodic averages depends on the parameters of the modified kinetic energy. Numerical results illustrate the approach, both for low-dimensional systems where we resort to a Galerkin approximation of the generator, and for more realistic systems using Monte Carlo simulations.

The results presented in this chapter were published in [98].

We consider the computation of macroscopic quantities through averages of functions of the variables of the system with respect to the Boltzmann-Gibbs probability measure μ introduced in (1.10). Numerically, high-dimensional averages (1.9) with respect to μ are often approximated as ergodic averages over realizations of appropriate stochastic differential equations (SDEs):

$$\lim_{t\to\infty} \widehat{\varphi}_t = \mathbb{E}_\mu(\varphi) \quad \text{a.s.}, \qquad \widehat{\varphi}_t := \frac{1}{t}\int_0^t \varphi(q_s, p_s)\, ds\,. \tag{2.1}$$

A typical dynamics to this end is the Langevin dynamics (1.24). As we explained in Section 1.3.2.3, there are two main sources of error in the computation of average properties such as $\mathbb{E}_\mu(A)$ through time averages as in (1.29): a systematic bias and statistical errors. In this chapter, we focus on the statistical error, the systematic bias being discussed in Chapter 3. Statistical errors may be large when the dynamics is metastable, *i.e.* when the system remains trapped for a very long time in some region of the configuration space (called a metastable region) before hopping to another metastable region. As we discussed in Section 1.4.2, many techniques have been introduced in order to reduce the variance.

The mathematical analysis we provide is inspired by the ARPS method introduced in Section 1.5, where the kinetic energy of each particle is more drastically modified in order to reduce the variance for a given computational effort in wall-clock time: it is set to 0 when the particle's momenta are small, while it remains unchanged for larger momenta. Adaptively restrained particle simulations may yield a significant algorithmic speed-up $S_{\rm a}$ when a sufficiently large number of particles are restrained at each time step (see Chapter 4). Unfortunately, restraining particles even temporarily may lead to more correlated iterates, which may translate into an increase of the statistical error $\sigma^2_{\rm mod}$ compared to the statistical error $\sigma^2_{\rm std}$ observed for standard Langevin dynamics. The actual speed-up of the method (see Chapter 4), in terms of the total wall-clock time needed to achieve a given precision in the estimation of an observable, should therefore be expressed as:

$$S_{\rm total} = S_{\rm a}\frac{\sigma^2_{\rm std}}{\sigma^2_{\rm mod}}\,. \tag{2.2}$$

Our aim here is to quantify the increase in the variance as a function of the parameters of the modified kinetic energy. In fact, a first task is to prove that the Langevin dynamics with modified kinetic energy is indeed ergodic, and that the variance is well defined. This is unclear at first sight since the modified dynamics fails to be hypoelliptic (see Section 1.3.1.2 and the discussion in Section 2.2.1).

This chapter is organized as follows. In Section 2.1, we introduce the modified Langevin dynamics we consider, and present the particular case of the AR-Langevin dynamic. The ergodicity of these dynamics is proved in Section 2.2, both in terms of almost-sure convergence of time averages along a single realization, and convergence of the law of the process. We also provide a result on the regularity of the evolution semigroup, adapted from similar estimates for standard Langevin dynamics in [117]. Such estimates allow us to analyze the statistical error in Section 2.3. We state in particular a Central Limit Theorem for $\widehat{\varphi}_t$, and perform a perturbative study of the asymptotic variance of the AR-Langevin dynamics in some limiting regime. Our

theoretical findings are illustrated by numerical simulations in Section 2.4, both in a simple one-dimensional case where the variance can be accurately computed using an appropriate Galerkin approximation, as well as for a more realistic system for which we resort to Monte-Carlo simulations. The proofs of our results are gathered in Section 2.5.

2.1 Modified Langevin dynamics

We consider a system of N particles with periodic conditions as described in Section 1.1.1. Recall that the spatial dimension is D, so that the total dimension of the system is $d := D \times N$.

In order to possibly increase the rate of convergence of the ergodic averages (2.1), we modify the Langevin dynamics (1.19) by changing the kinetic energy. More precisely, instead of the standard quadratic kinetic energy U_{std} given by (1.7), we introduce a general kinetic energy function $U : \mathbb{R}^d \to \mathbb{R}$. The total energy of the system is then characterized by the Hamiltonian

$$H(p, q) = U(p) + V(q). \tag{2.3}$$

In order to ensure that the measure $\mathrm{e}^{-\beta H(q,p)}\, dq\, dp$ can be normalized, and in order to simplify the mathematical analysis, we make in the sequel the following assumption.

Assumption 2.1 *The potential energy function V belongs to $C^\infty(\mathcal{D}, \mathbb{R})$, and $U \in C^\infty(\mathbb{R}^d, \mathbb{R})$ grows sufficiently rapidly at infinity in order to ensure that $\mathrm{e}^{-\beta U} \in L^1(\mathbb{R}^d)$.*

The Langevin dynamics (1.24) simplifies, for the separable Hamiltonian (2.3),

$$\begin{cases} dq_t = \nabla U(p_t)\, dt, \\ dp_t = -\nabla V(q_t)\, dt - \gamma \nabla U(p_t)\, dt + \sqrt{\dfrac{2\gamma}{\beta}}\, dW_t. \end{cases} \tag{2.4}$$

The generator of the process (2.4) reads

$$\mathcal{L} = \nabla U \cdot \nabla_q - \nabla V \cdot \nabla_p + \gamma \left(-\nabla U \cdot \nabla_p + \frac{1}{\beta} \Delta_p \right). \tag{2.5}$$

Recall the canonical distribution (1.10) which is

$$\mu(dq\, dp) = Z_\mu^{-1} \mathrm{e}^{-\beta H(q,p)}\, dq\, dp, \qquad Z_\mu = \int_{\mathcal{E}} \mathrm{e}^{-\beta H(q,p)}\, dq\, dp < +\infty.$$

A simple computation shows that the distribution (1.10) is invariant under the dynamics (2.4), *i.e.* for all C^∞ functions ϕ with compact support,

$$\int_{\mathcal{E}} \mathcal{L}\phi\, d\mu = 0.$$

Note that, in view of the separability of the Hamiltonian, for any kinetic energy U, the marginal of the distribution μ in the position variables is ν given by (1.12). In particular, this marginal distribution coincides with the one of the standard Langevin dynamics (1.19) (we will show in Section 2.2 that the modified Langevin dynamics is ergodic). This allows to straightforwardly estimate canonical averages of observables depending only on the positions with the modified Langevin dynamics (2.4). In fact, there is no restriction in generality in considering observables depending only on the positions, since general observables $\varphi(q,p)$ depending both on momenta and positions can be reduced to functions of the positions only by a partial integration in the momentum variables. This partial integration is often very easy to perform since momenta are independent Gaussian random variables under the canonical measure associated with the standard kinetic energy.

2.2 Ergodicity of the modified Langevin dynamics

There are several notions of ergodicity for stochastic processes (see Section 1.3.1.2) and Section 1.3.1.3 for an introduction). We focus here on two of them: the convergence of ergodic averages over a single trajectory, and the convergence of the law of the process.

2.2.1 Convergence of ergodic averages

As explained in Section 1.3.1.2, the convergence of ergodic averages over one trajectory is automatically ensured by the existence of an invariant probability measure and the irreducibility of the dynamics. Since, by construction, an invariant probability measure is known (namely the canonical measure (2.1)), it suffices to show that the process generated by the modified Langevin equation is irreducible to be able to conclude the convergence of ergodic averages.

As reviewed in Section 1.3.1.2, the most standard argument to prove the irreducibility of degenerate diffusions is to prove the controllability of the dynamics relying on the Stroock-Varadhan support theorem, and the regularity of the transition kernel thanks to some hypoellipticity property. These conditions are satisfied for standard Langevin dynamics, but not for the modified Langevin dynamics we consider, since the Hessian of the kinetic energy function may not be invertible on an open set. This is the case for the AR kinetic energy function presented in Section 1.5.

To illustrate this point, let us show for instance how the standard way of proving hypoellipticity fails. As we explained in Section 1.3.1.2, in order to apply Theorem 1.2, the first task is to rewrite the generator (2.5) of the process as

$$\mathcal{L} = X_0 - \sum_{j=1}^{d} X_j^\dagger X_j,$$

where

$$X_0 = \nabla U \cdot \nabla_q - \nabla V \cdot \nabla_p - \gamma \nabla U \cdot \nabla_p, \qquad X_j = \sqrt{\frac{\gamma}{\beta}}\, \partial_{p_j},$$

and $X_j^\dagger$ is the adjoint of X_j on the flat space $L^2(\mathcal{E})$. We next compute, for $j = 1, \dots, d$, the commutators

$$[X_0, X_j] = X_0 X_j - X_j X_0 = \sqrt{\frac{\gamma}{\beta}} \nabla \left(\partial_{p_j} U\right) \cdot (\nabla_q - \gamma \nabla_p) .$$

When $\nabla^2 U$ is invertible (which is the case for U_{std}), it is possible to recover the full algebra of derivatives by an appropriate combination of $X_1, \dots, X_d$ and $[X_0, X_1], \dots, [X_0, X_d]$. Here, we consider a situation when this is not the case and, even more dramatically, where the Hessian may vanish on an open set. In this situation, $[X_0, X_j] = 0$ on the same open set, and in fact all iterated commutators $[X_0, [\dots [X_0, X_j]]]$ also vanish. Note that also the proof of the controllability based on the construction of a control (1.31) faces similar issues.

We solve this problem by a direct constructive approach, where we see the modified dynamics as a perturbation of the standard Langevin dynamics. We rely on the following assumption:

Assumption 2.2 *The kinetic energy function $U \in C^\infty$ of the modified Langevin dynamics is such that*

$$\|\nabla U - \nabla U_{\mathrm{std}}\|_{L^\infty} \leqslant G_{\mathrm{std}} \tag{2.6}$$

for some constant $G_{\mathrm{std}} < +\infty$, where U_{std} is defined in (1.7)*.*

Under this assumption, we can prove that the modified Langevin dynamics is irreducible by proving an appropriate minorization condition, which crucially relies on the compactness of the position space $\mathcal{D}$ (see Section 2.5.2 for the proof).

Lemma 2.1 (Minorization condition). *Suppose Assumption 2.2 holds. Then for any fixed $p^* > 0$ and $t > 0$, there exists a probability measure $\nu_{p^*,t}$ on $\mathcal{D} \times \mathbb{R}^d$ and a constant $\kappa > 0$ such that, for every Borel set $B \in \mathscr{B}(\mathcal{E})$,*

$$\mathbb{P}\left((q_t, p_t) \in B \,\middle|\, |p_0| \leqslant p^*\right) \geqslant \kappa\, \nu_{p^*,t}(B),$$

with $\nu_{p^*,t}(B) > 0$ when $|B| > 0$.

The minorization condition implies the irreducibility of the dynamics, so that the following convergence result readily follows.

Theorem 2.3 (Convergence of ergodic averages). *When Assumption 2.2 holds, ergodic averages over trajectories almost surely converge to the corresponding canonical average:*

$$\forall \varphi \in L^1(\mu), \qquad \lim_{t \to +\infty} \frac{1}{t} \int_0^t \varphi(q_s, p_s) ds = \int_{\mathcal{E}} \varphi \, d\mu \quad \text{a.s.}$$

2.2.2 Convergence of the law

As explained in Section 1.3.1.3, there are various functional frameworks to measure the convergence of the law of the process. The approach by hypocoercivity fails, since the generator of the modified Langevin dynamics is not hypoelliptic, and hence the condition (1.34) is not satisfied.

We consider here weighted L^∞ estimates on the semi-group $\mathrm{e}^{t\mathcal{L}}$ as described in Section 1.3.1.3. Recall the weighted L^∞ space $L^\infty_{\mathcal{K}}$ defined in (1.36). In order to prove the exponential convergence of the law, we rely on the result of [54], which states that if a Lyapunov condition and a minorization condition hold, then the sampled chain converges exponentially fast to its steady state in the following sense.

Theorem 2.4 (Exponential convergence of the law). *Suppose that Assumption 2.2 holds. Then the invariant measure μ is unique, and for any $s \in \mathbb{N}^*$, there exist constants $C_s, \lambda_s > 0$ such that*

$$\forall \varphi \in L^\infty_{\mathcal{K}_s}, \quad \forall\, t \geqslant 0, \qquad \left\| \mathrm{e}^{t\mathcal{L}}\varphi - \int_{\mathcal{E}} \varphi d\mu \right\|_{L^\infty_{\mathcal{K}_s}} \leqslant C_s \mathrm{e}^{-\lambda_s t} \left\|\varphi\right\|_{L^\infty_{\mathcal{K}_s}}. \tag{2.7}$$

The minorization condition is already stated in Lemma 2.1, while the appropriate Lyapunov condition reads as follows (see Section 2.5.1 for the proof, which uses the same strategy as [78] and [64]).

Lemma 2.2 (Lyapunov Condition). *Suppose that Assumption 2.2 holds. Then, for any $s \geqslant 1$ and $t > 0$, there exist $b > 0$ and $a \in [0, 1)$ such that*

$$\mathrm{e}^{t\mathcal{L}}\mathcal{K}_s \leqslant a\mathcal{K}_s + b.$$

2.2.3 Regularity results for the evolution semi-group

We provide in this section decay estimates for the spatial derivatives of $\mathrm{e}^{t\mathcal{L}}\varphi$, following the approach pioneered in [117] and further refined in [71]. These estimates can in fact be extended in a straightforward way to modified Langevin dynamics with Hessians bounded from below by a positive constant. Our aim in this section is to provide decay estimates for the spatial derivatives of $\mathrm{e}^{t\mathcal{L}}\varphi$ in the situation when $\nabla^2 U$ fails to be strictly convex, for instance because $\nabla^2 U$ vanishes on an open set as is the case for AR-Langevin dynamics.

In order to state our results, we first need to define the weighted Sobolev spaces $\mathscr{W}^{n,\infty}_{\mathcal{K}_s}$ for $n \in \mathbb{N}$:

$$\mathscr{W}^{n,\infty}_{\mathcal{K}_s} = \left\{ \varphi \in L^\infty_{\mathcal{K}_s} \,\middle|\, \forall k \in \mathbb{N}^{2d},\ |k| \leqslant n,\ \partial^k \varphi \in L^\infty_{\mathcal{K}_s} \right\}.$$

These spaces gather all functions which grow at most like $\mathcal{K}_s$, and whose derivatives of order at most n all grow at most like $\mathcal{K}_s$. Recall the space of smooth functions $\mathscr{S}$, which is the vector space of functions $\varphi \in L^2(\mu)$ such that, for any $n \geqslant 0$, there exists $r \in \mathbb{N}$ for which $\varphi \in \mathscr{W}^{n,\infty}_{\mathcal{K}_r}$.

We also make the following assumption on the kinetic energy function, which can be understood as a condition of "almost strict convexity" of the Hessian $\nabla^2 U$.

Assumption 2.5 *The kinetic energy $U \in \mathscr{S}$ has bounded second-order derivatives:*

$$\sup_{|j|=2} \left\| \partial^j U \right\|_{L^\infty} < \infty \,, \tag{2.8}$$

and there exist a function $U_\nu \in \mathscr{S}$ and constants $\nu > 0$ and $G_\nu \geqslant 0$ such that

$$\nabla^2 U_\nu \geqslant \nu > 0 \tag{2.9}$$

and

$$\left\| \nabla \left(U - U_\nu \right) \right\|_{L^\infty} \leqslant G_\nu. \tag{2.10}$$

Remark 2.1. *A natural choice for the function U_ν in Assumption 2.5 is $U_{\rm std}$. The condition* (2.9) *then holds with $\nu = 1/\max(m_1, \ldots, m_N)$. Moreover,* (2.8) *holds as soon as U is a local perturbation of $U_{\rm std}$. The most demanding condition is therefore* (2.10)*, especially if G_ν has to be small as in Lemma 2.3 below.*

By following the same strategy as in [71, Proposition A.1.] (which refines the results already obtained in [117]), and appropriately taking care of the lack of strict positivity of the Hessian $\nabla^2 U$ by assuming that G_ν is sufficiently small, we prove the following result in Section 2.5.3.

Recall the orthogonal projection $\mathit{\Pi}_\mu$ onto the orthogonal of the kernel of the operator $\mathcal{L}$ (with respect to the $L^2(\mu)$ scalar product) defined in (1.42).

Lemma 2.3. *Suppose that Assumptions 2.2 and 2.5 hold, and fix $\varphi \in \mathscr{S}$. For any $n \geqslant 1$, there exist $\widetilde{n}, s_n \in \mathbb{N}$ and $\lambda_n > 0$ such that, for $s \geqslant s_n$ and $G_\nu \leqslant \rho_s$, in Equation* (2.10)*, with $\rho_s > 0$ sufficiently small (depending on s but not on n), there is $r \in \mathbb{N}$ and $C > 0$ for which*

$$\forall t \geqslant 0, \quad \forall\, |k| \leqslant n, \qquad \left\| \partial^k \mathrm{e}^{t\mathcal{L}} \mathit{\Pi}_\mu \varphi \right\|_{L^\infty_{\mathcal{K}_s}} \leqslant C \left\| \varphi \right\|_{W^{\tilde{n},\infty}_{\mathcal{K}_r}} \mathrm{e}^{-\lambda_n t}. \tag{2.11}$$

The parameter ρ_s can in fact be made explicit, see (2.34) below. The decay estimate (2.11) shows that the derivatives of the evolution operator can be controlled in appropriate weighted Hilbert spaces. Note however that the Lyapunov functions entering the estimates are not the same a priori on both sides of the inequality (2.11). Let us emphasize, though, that we can obtain a control in all spaces $L^\infty_{\mathcal{K}_s}$ for s sufficiently large (depending on the order of derivation).

2.3 Analysis of the statistical error

The asymptotic variance characterizes the statistical error (see Section 1.3.1.4). In Section 2.3.1, we show that the asymptotic variance is well defined for the modified Langevin dynamics. We can in fact prove a stronger result, namely that a Central Limit Theorem (CLT) holds for ergodic averages over one trajectory. In a second step, we more carefully analyze in Section 2.3.2 the properties of the variance of the AR-Langevin dynamics by proving a linear response result in the limit of a vanishing lower bound on the kinetic energies. To obtain the latter results, we rely on the estimates provided by Lemma 2.3.

2.3.1 A Central Limit theorem for ergodic averages

Let us first write the asymptotic variance in terms of the generator of the dynamics. We have defined $\widetilde{L^\infty_{\mathcal{K}_s}} = \Pi_\mu\left(L^\infty_{\mathcal{K}_s}\right)$, since $L^\infty_{\mathcal{K}_s} \subset L^2(\mu)$. The ergodicity result (2.7) allows us to conclude that the operator $\mathcal{L}$ is invertible on $\widetilde{L^\infty_{\mathcal{K}_s}}$ since the operator equality (1.43) holds on $\mathcal{B}\left(\widetilde{L^\infty_{\mathcal{K}_s}}\right)$. This leads to the following resolvent bounds (the second part being a direct corollary of Lemma 2.3).

Corollary 2.1. *Suppose that Assumption 2.2 holds. Then, for any $s \in \mathbb{N}^*$,*

$$\left\|\mathcal{L}^{-1}\right\|_{\mathcal{B}\left(\widetilde{L^\infty_{\mathcal{K}_s}}\right)} \leqslant \frac{C_s}{\lambda_s}, \tag{2.12}$$

where λ_s, C_s are the constants introduced in Theorem 2.4. Suppose in addition that Assumption 2.5 holds, and fix $\varphi \in \mathscr{S}$. For any $n \geqslant 1$, there exist $\tilde{n}, s_n \in \mathbb{N}$ and $\lambda_n > 0$ such that, for $s \geqslant s_n$ and $G_\nu \leqslant \rho_s$ with $\rho_s > 0$ sufficiently small (depending on s but not on n), there is $r \in \mathbb{N}$ and $C > 0$ for which

$$\forall\, |k| \leqslant n, \qquad \left\|\partial^k \mathcal{L}^{-1} \Pi_\mu \varphi\right\|_{L^\infty_{\mathcal{K}_s}} \leqslant \frac{C}{\lambda_n} \left\|\varphi\right\|_{W^{\tilde{n},\infty}_{\mathcal{K}_r}}. \tag{2.13}$$

This already allows us to conclude that the asymptotic variance of the time average $\widehat{\varphi}_t$ defined in (2.1) is well defined for any observable $\varphi \in L^\infty_{\mathcal{K}_r}$ due to the computation provided in (1.46)-(1.48). The asymptotic variance reads

$$\sigma^2_\varphi = 2 \int_{\mathcal{E}} \left(\Pi_\mu \varphi\right) \left(-\mathcal{L}^{-1} \Pi_\mu \varphi\right)\, d\mu.$$

In fact, a Central Limit Theorem can be shown to hold for $\widehat{\varphi}_t$ using standard results (see *e.g.* [17]).

2.3.2 Perturbative study of the variance for the AR-Langevin dynamics

Our aim in this section is to better understand, from a quantitative viewpoint, the behavior of the asymptotic variance for the AR-Langevin dynamics (1.48), at least in some limiting regime where the parameter $e_{\min}$ is small. For larger values, we need to rely on numerical simulations (see Section 2.4).

The regime where both $e_{\min}$ and $e_{\max}$ go to 0 is somewhat singular since the transition from $U(p) = 0$ to $U(p) = U_{\rm std}(p)$ becomes quite abrupt, which prevents a rigorous theoretical analysis. The regimes where either $e_{\min}$ or $e_{\max}$ go to infinity are also of dubious interest since the dynamics strongly perturbs the standard Langevin dynamics. Therefore, we restrict ourselves to the situation where $e_{\min} \to 0$ with $e_{\max}$ fixed.

In order to highlight the dependence of the AR kinetic energy function on the restraining parameters $0 \leqslant e_{\min} < e_{\max}$, we denote it by $U_{e_{\min},e_{\max}}$ in the remainder of this section. Let us however first give a more precise definition of this function, having in mind that $e_{\max}$ is fixed while $e_{\min}$ eventually goes to 0. We introduce to this end an interpolation function $f_{0,e_{\max}} \in C^\infty(\mathbb{R})$ such that

$$0 \leqslant f_{0,e_{\max}} \leqslant 1, \qquad f_{0,e_{\max}}(x) = 1 \text{ for } x \leqslant 0, \qquad f_{0,e_{\max}}(x) = 0 \text{ for } x \geqslant e_{\max}, \tag{2.14}$$

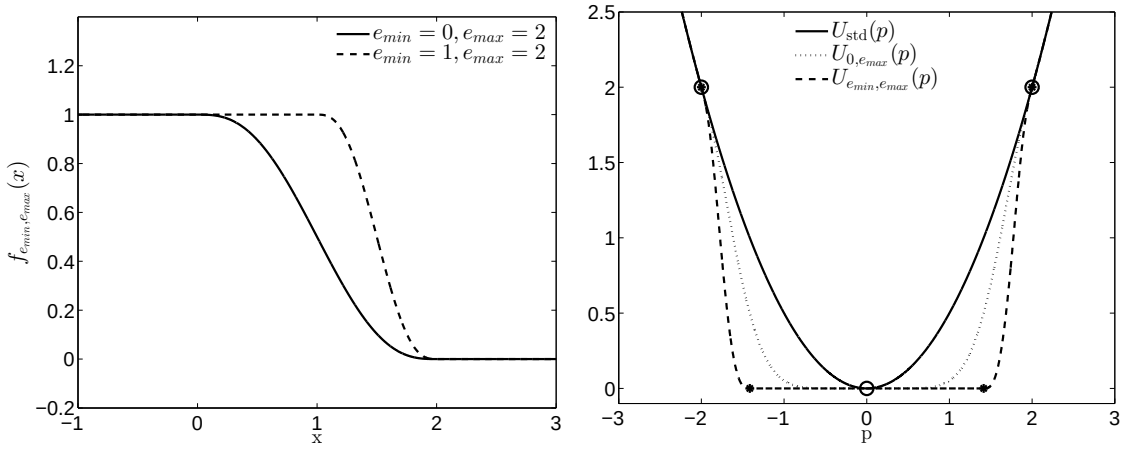

Fig. 2.1: (Left) Functions $f_{0,e_{\max}}$ and $f_{e_{\min},e_{\max}}$ for $e_{\max} = 2$ and $e_{\min} = 1$. (Right) Standard kinetic energy function U_{std}, as well as two AR kinetic energy functions $U_{e_{\min},e_{\max}}$ with $e_{\max} = 2$ and $e_{\min} = 0$ or 1.

and

$$\forall n \geqslant 1, \qquad f^{(n)}_{0,e_{\max}}(0) = f^{(n)}_{0,e_{\max}}(e_{\max}) = 0.$$

We next define an interpolation function $f_{e_{\min},e_{\max}}$ obtained from the function $f_{0,e_{\max}}$ by an appropriate shift of the lower bound and a rescaling. More precisely, $f_{e_{\min},e_{\max}}(x) = f_{0,e_{\max}}(\theta_{e_{\min}}(x))$ with

$$\theta_{e_{\min}}(x) := \begin{cases} x - e_{\min}, & \text{for } x \leqslant e_{\min}, \\ \dfrac{e_{\max}}{e_{\max} - e_{\min}}(x - e_{\min}), & \text{for } e_{\min} \leqslant x \leqslant e_{\max}, \\ x, & \text{for } x \geqslant e_{\max}. \end{cases} \tag{2.15}$$

A plot of $f_{e_{\min},e_{\max}}$ is provided in Figure 2.1(Left).

Definition 2.1 (AR kinetic energy function). *For two parameters $0 \leqslant e_{\min} < e_{\max}$, the AR kinetic energy function $U_{e_{\min},e_{\max}}$ is defined as*

$$U_{e_{\min},e_{\max}}(p) := \sum_{i=1}^{N} u_{e_{\min},e_{\max}}(p_i), \tag{2.16}$$

where the individual kinetic energy functions are

$$u_{e_{\min},e_{\max}}(p_i) := \begin{cases} 0, & \textit{for } \dfrac{p_i^2}{2m_i} \leqslant e_{\min}, \\ \left[1 - f_{e_{\min},e_{\max}}\left(\dfrac{p_i^2}{2m_i}\right)\right] \dfrac{p_i^2}{2m_i}, & \textit{for } \dfrac{p_i^2}{2m_i} \in [e_{\min}, e_{\max}], \\ \dfrac{p_i^2}{2m_i}, & \textit{for } \dfrac{p_i^2}{2m_i} \geqslant e_{\max}. \end{cases} \tag{2.17}$$

Of course, $U_{e_{\min},e_{\max}}(p)$ converges to $U_{0,e_{\max}}(p)$ as $e_{\min} \to 0$. The limiting kinetic energy function $U_{0,e_{\max}}$ corresponds to what we call the Zero-$e_{\max}$-AR-Langevin dynamics (see Figure 2.1(Right) for an illustration). Let us emphasize that the limiting dynamics is not the standard Langevin dynamics, so that the expansion in powers of $e_{\min}$ of the variance we provide is with respect to the limiting variance of the dynamics corresponding to $U_{0,e_{\max}}$. To simplify the notation, we denote by $\sigma^2(e_{\min})$ the variance associated with the kinetic energy $U_{e_{\min},e_{\max}}$.

Proposition 2.1. *There exist $e^*_{\max} > 0$ and $\mathscr{K} \in \mathbb{R}$ such that, for any $0 < e_{\max} \leqslant e^*_{\max}$,*

$$\forall 0 \leqslant e_{\min} \leqslant \frac{e_{\max}}{2}, \qquad \sigma^2(e_{\min}) = \sigma^2(0) + \mathscr{K}\, e_{\min} + \mathrm{O}(e_{\min}^2). \tag{2.18}$$

The proof can be read in Section 2.5.4. The assumption that $e_{\max}$ is sufficiently small ensures that Assumption 2.5 holds (see Section 2.5.4.3). The result is formally clear. The difficulty in proving it is that the kinetic energy is not a smooth function of $e_{\min}$ because the shift function is only piecewise smooth.

Remark 2.2. *An inspection of the proof of Proposition 2.1 shows that the linear response result can be generalized to non-zero values of $e_{\min}$ and in fact to linear responses in the parameter $e_{\max}$ as well. For the latter case, we consider $f_{0,e_{\max}}(x) = f_{0,1}(x/e_{\max})$. Denoting now by $\sigma^2(e_{\min}, e_{\max})$ the variance associated with the kinetic energy $U_{e_{\min},e_{\max}}$, it can be proved that, for $0 < e_{\min} < e_{\max}$ not too large, there are $a, b \in \mathbb{R}$ such that, for $\delta, \eta \in \mathbb{R}$ sufficiently small,*

$$\sigma^2(e_{\min} + \delta, e_{\max} + \eta) = \sigma^2(e_{\min}, e_{\max}) + a\delta + b\eta + \mathrm{O}(\eta^2 + \delta^2).$$

2.4 Numerical results

The aim of this section is to quantify the evolution of the variance of AR-Langevin dynamics as the parameters of the kinetic energy function are modified. We first consider in Section 2.4.1 a simple system in spatial dimension 1, for which the variance can be very precisely computed using a Galerkin-type approximation. We next consider more realistic particle systems in Section 2.4.2, relying on molecular dynamics simulations to estimate the variance. In this section, the function $f_{0,e_{\max}}(x)$ is chosen to be of the form $f_{0,1}(x/e_{\max})$, with $f_{0,1}$ a fifth-order spline function.

2.4.1 A simple one-dimensional system

We first consider a single particle in spatial dimension $d = 1$, in the periodic domain $\mathcal{D} = 2\pi\mathbb{T}$ and at inverse temperature $\beta = 1$. In this case, it is possible to directly approximate the asymptotic variance (1.48) using some Galerkin discretization, as in [101] or [72].

We denote by $\mathcal{L}_{e_{\min},e_{\max}}$ the generator of the modified Langevin dynamics associated with the AR kinetic energy function $U_{e_{\min},e_{\max}}$ defined in (2.16), by $\mu_{e_{\min},e_{\max}}$ the associated canonical measure, and by $\Pi_{e_{\min},e_{\max}}$ the projector onto functions of $L^2(\mu_{e_{\min},e_{\max}})$ with average 0 with respect to $\mu_{e_{\min},e_{\max}}$.

For a given observable φ, we first approximate the solution of the following Poisson equation:

$$-\mathcal{L}_{e_{\min},e_{\max}}\Phi_\varphi = \Pi_{e_{\min},e_{\max}}\varphi, \tag{2.19}$$

and then compute the variance as given by (1.48):

$$\sigma_\varphi^2 = 2\int_{\mathcal{E}} \Phi_\varphi\,\varphi\,d\mu_{e_{\min},e_{\max}}.$$

To achieve this, we introduce the basis functions $\psi_{nk}(q,p) := G_k(q)\,H_n(p)$, where $G_k(q) = (2\pi)^{-1/2}\mathrm{e}^{\mathrm{i}kq}$ (for $k \in \mathbb{Z}$) and $H_n(p)$ are the Hermite polynomials:

$$H_n(p) = (-1)^n \mathrm{e}^{p^2/2}\frac{d^n}{dp^n}\left(\mathrm{e}^{-p^2/2}\right), \forall n \in \mathbb{N}.$$

The choice of G_k is natural in view of the spatial periodicity of the functions under consideration, while Hermite polynomials are eigenfunctions of the generator associated with the Ornstein-Uhlenbeck process on the momenta for the standard quadratic kinetic energy $p^2/2$. Note however that, when the kinetic energy is modified as $U_{e_{\min},e_{\max}}$, the Hermite polynomials are no longer orthogonal for the $L^2(\mu_{e_{\min},e_{\max}})$ scalar product.

We approximate the Poisson equation (2.19) on the basis $\mathcal{V}_{N_G,N_H} = \mathrm{Span}\{\psi_{nk}\}_{0\leqslant n\leqslant N_H,\,-N_G\leqslant k\leqslant N_G}$ for given integers $N_G, H_H \geqslant 1$, and we look for approximate solutions of the form $\Pi_{e_{\min},e_{\max}}\Phi_\varphi^{N_G,N_H}$ with

$$\Phi_\varphi^{N_G,N_H} = \sum_{n=-N_H}^{N_H}\sum_{k=0}^{N_G}[b_{N_G,N_H}]_{nk}\,\psi_{nk},$$

where b_{N_G,N_H} is a vector of size $(2N_G+1)(N_H+1)$. Restricting (2.19) to $\mathcal{V}_{N_G,N_H}$ leads to

$$M_{N_G,N_H}b_{N_G,N_H} = a_{N_G,N_H}, \tag{2.20}$$

where M_{N_G,N_H} is a matrix of size $(2N_G+1)(N_H+1)\times(2N_G+1)(N_H+1)$ and a_{N_G,N_H} a vector of size $(2N_G+1)(N_H+1)$, whose entries respectively read

$$[M_{N_G,N_H}]_{nk,ml} = \langle\psi_{ml}, -\mathcal{L}_{e_{\min},e_{\max}}\psi_{nk}\rangle_{L^2(\mu_{e_{\min},e_{\max}})},$$
$$[a_{N_G,N_H}]_{ml} = \langle\psi_{ml}, \Pi_{e_{\min},e_{\max}}\varphi\rangle_{L^2(\mu_{e_{\min},e_{\max}})}.$$

The approximated solution $\Phi_\varphi^{N_G,N_H}$ of the Poisson equation (2.19) can therefore be computed by solving (2.20). Note however that some care is needed at this stage since $\mathcal{L}_{e_{\min},e_{\max}}$ is not invertible on $\mathcal{V}_{N_G,N_H}$, because the basis functions $\{\psi_{nk}\}_{0\leqslant n\leqslant N_H,\,-N_G\leqslant k\leqslant N_G}$ are not of integral 0 with respect to $\mu_{e_{\min},e_{\max}}$. We correct this by performing a singular value decomposition of M_{N_G,N_H}, removing the component of a_{N_G,N_H} associated with the singular value 0, and computing the inverse of M_{N_G,N_H} on the subspace generated

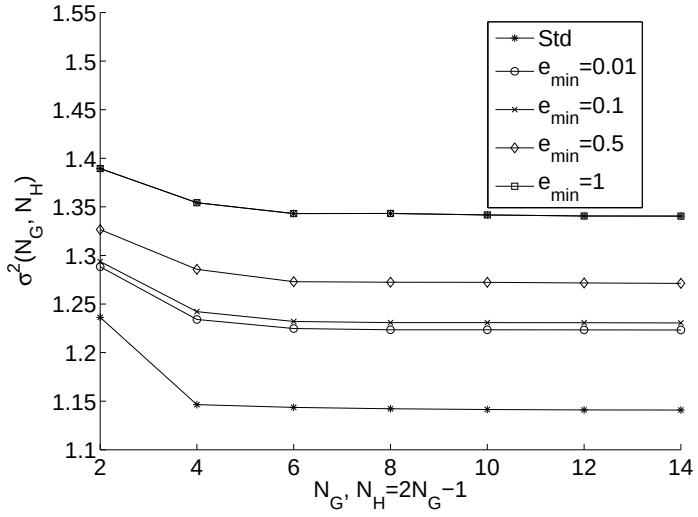

Fig. 2.2: Convergence of the Galerkin approximation in the basis size N_G and $N_H = 2N_G - 1$: approximation of the variance of observable $\varphi = V$ for the standard dynamics and the AR dynamics with fixed parameter $e_{\max} = 2$ and various values of $e_{\min}$.

by the eigenvectors associated with non-zero eigenvalues. In practice, we compute the entries of a_{N_G,N_H} and M_{N_G,N_H} by numerical quadrature. Since the Hermite polynomials are no longer orthogonal for the $L^2(\mu_{e_{\min},e_{\max}})$ scalar product, quadratures are required both in position and momentum variables. The variance is finally approximated as

$$\sigma_\varphi^2(N_G, N_H) = 2 \int_{\mathcal{E}} \varphi \, \Phi_\varphi^{N_G,N_H} \, d\mu_{e_{\min},e_{\max}} = 2 b_{N_G,N_H}^T a_{N_G,N_H}.$$

In the simulations presented in this section, the potential is $V(q) = \cos(q)$, the observable under study is $\varphi = V$, and we always set $N_H = 2N_G - 1$. Figure 2.2 presents the convergence of the variance with respect to the basis size, for the standard Langevin dynamics and the AR Langevin dynamics with $e_{\max} = 2$ and various values of $e_{\min}$. The results show that the choice $N_G = 12$ is sufficient in all cases to approximate the asymptotic value. We checked in addition in one case, namely for the standard dynamics, that the values we obtain are very close to a reference value obtained with $N_G = 30$: the relative variation is of order 10^{-8} for $N_G = 10$, 10^{-10} for $N_G = 12$ and 10^{-11} for $N_G = 14$. We therefore set $N_G = 12$ in the remainder of this section.

The variation of the computed variance for $\varphi = V$ is plotted in Figure 2.3 for various parameters $0 \leqslant e_{\min} < e_{\max}$ of the AR-Langevin dynamics. Note that, as expected, the variance increases with increasing values of $e_{\min}$ for fixed $e_{\max}$, but also with increasing values of $e_{\max}$ for fixed $e_{\min}$. We next illustrate the linear response results of Proposition 2.1 and Remark 2.2 in Figures 2.4 and 2.5: in both situations, the variance increases linearly when the parameter under consideration is varied in a sufficiently small

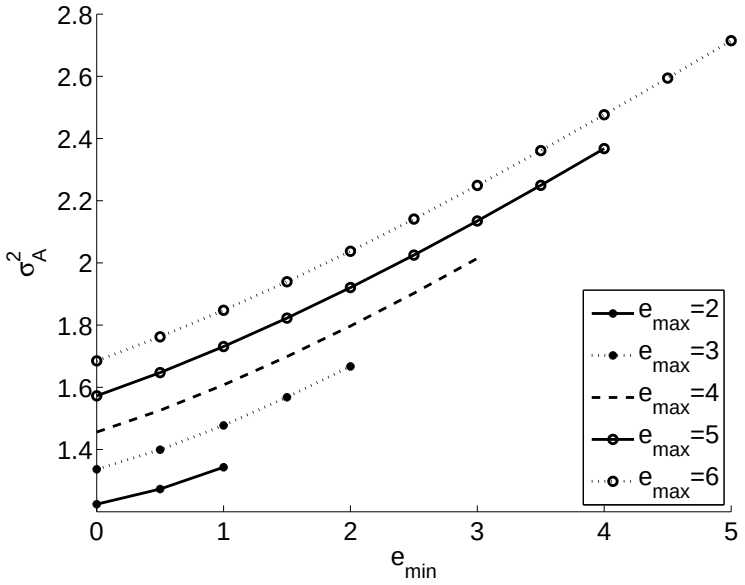

Fig. 2.3: Asymptotic variance of time averages for $\varphi = V$, approximated by the Galerkin method, as a function of $e_{\min}$ and for several values of $e_{\max}$.

neighborhood of its initial value. After that initial regime, nonlinear variations appear. Note also that the relative increase of the variance is more pronounced as a function of $e_{\max}$ than $e_{\min}$.

Remark 2.3. *In practice, the idea usually is to set the lower bound $e_{\min}$ sufficiently large when performing Monte Carlo simulations, in order to decrease as much as possible the computational cost (see Chapter 4). The gap $e_{\max} - e_{\min}$ should however not be too small in order to have a sufficiently smooth transition from a vanishing kinetic energy to a quadratic one. This requires therefore $e_{\max}$ to be quite large if $e_{\min}$ is large. The results presented in Figure 2.5 suggest that this may not be the optimal choice, unless the algorithmic speed-up is quite large.*

2.4.2 A more realistic system

In order to study the variation of the variance as a function of $e_{\min}$ and $e_{\max}$ in systems of higher dimensions, we resort to Monte Carlo simulations. This requires discretizing the AR-Langevin dynamics (5). We resort to a scheme of weak order 2 for the standard kinetic energy obtained by a splitting strategy where the generator of the modified Langevin dynamics (2.5) is decomposed into three parts:

$$A := \nabla U(p) \cdot \nabla_q, \qquad B := -\nabla V(q) \cdot \nabla_p, \qquad \mathcal{L}_{\mathrm{FD}} := -\nabla U(p) \cdot \nabla_p + \frac{1}{\beta} \Delta_p \, .$$

The transition kernel obtained by a Strang splitting reads $P_{\Delta t} = \mathrm{e}^{\gamma \Delta t \mathcal{L}_{\mathrm{FD}}/2} \mathrm{e}^{\Delta t B/2} \mathrm{e}^{\Delta t A} \mathrm{e}^{\Delta t B/2} \mathrm{e}^{\gamma \Delta t \mathcal{L}_{\mathrm{FD}}/2}$. Contrarily to the standard kinetic energy functions, the elementary evolution associated with $\mathcal{L}_{\mathrm{FD}}$ cannot be integrated analytically. We approximate $\mathrm{e}^{\gamma \Delta t/2 \mathcal{L}_{\mathrm{FD}}}$ by a midpoint rule, encoded by a transition kernel

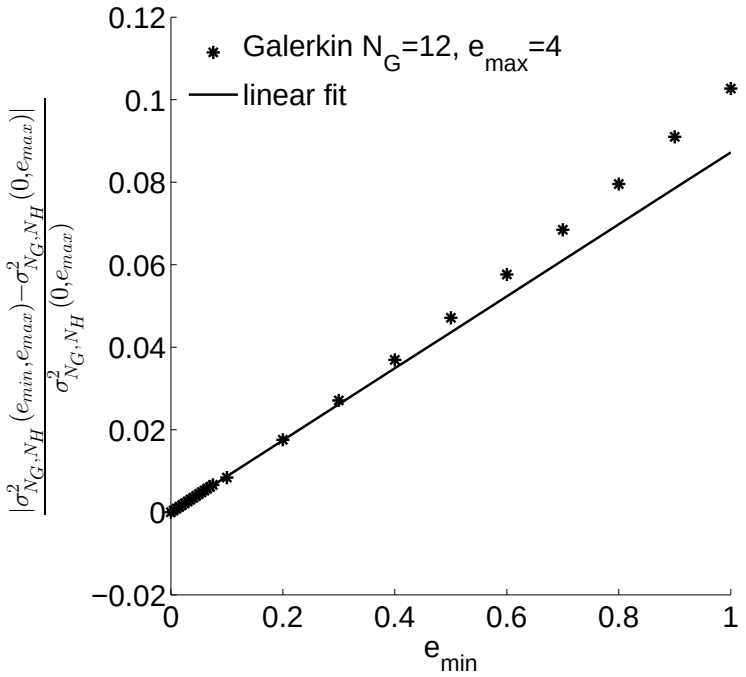

Fig. 2.4: Relative difference between the variance $\sigma^2_{N_G,N_H}(e_{\min}, e_{\max})$ and its initial value computed for reference parameters. Fixed upper bound $e_{\max} = 4$, and reference value $e_{\min} = 0$.

$P^{\gamma,\mathcal{L}_{\mathrm{FD}}}_{\Delta t}$. This gives the following discretization scheme:

$$\begin{cases} p^{n+1/4} = p^n - \gamma \nabla U \left(\dfrac{p^{n+1/4} + p^n}{2} \right) \dfrac{\Delta t}{2} + \sqrt{\dfrac{\gamma \Delta t}{\beta}} G^n, \\ p^{n+1/2} = p^{n+1/4} - \nabla V(q^n) \dfrac{\Delta t}{2}, \\ q^{n+1} = q^n + \nabla U(p^{n+1/2}) \Delta t, \\ p^{n+3/4} = p^{n+1/2} - \nabla V(q^{n+1}) \dfrac{\Delta t}{2}, \\ p^{n+1} = p^{n+3/4} - \gamma \nabla U \left(\dfrac{p^{n+1} + p^{n+3/4}}{2} \right) \dfrac{\Delta t}{2} + \sqrt{\dfrac{\gamma \Delta t}{\beta}} G^{n+1/2}, \end{cases} \tag{2.21}$$

where $G^n, G^{n+1/2}$ are i.i.d. standard d-dimensional Gaussian random variables. The first and the last line are obtained by implicit schemes, solved in practice by a fixed point strategy (the termination criterion being that the distance between successive iterates is smaller than 10^{-10}, and the initial iterate being provided by a Euler-Maruyama step). By following the same approach as in [78], it can indeed be proved that this scheme is of weak order 2 for the standard kinetic energy; see Chapter 3 for further precisions as well as for the construction of a scheme for the modified Langevin dynamics which has weak order 2 .

The ergodicity of some second-order schemes was proved for the standard Langevin dynamics in [78]. Since the AR-Langevin dynamics can be seen as a perturbation of the standard Langevin dynamics, it can

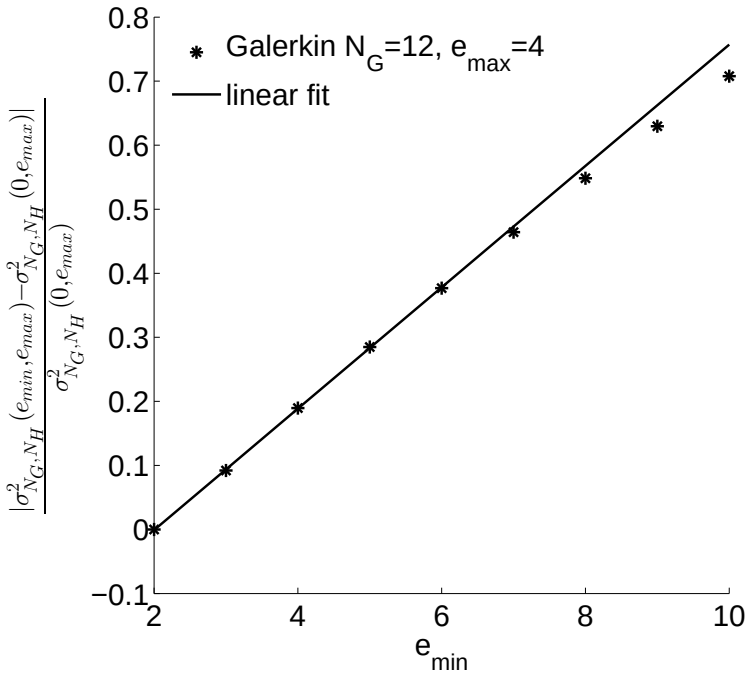

Fig. 2.5: Same as Figure 2.4. Fixed lower bound $e_{\min} = 0$, and reference value $e_{\max} = 2$.

be proved by combining the proofs from [78] and the proof of Theorem 2.4 that, when $0 \leqslant e_{\min} < e_{\max}$ are sufficiently small, the corresponding discretization of the AR-Langevin dynamics remains ergodic (see Chapter 3). The corresponding invariant measure is denoted by $\mu_{e_{\min},\Delta t}$. It also follows by the results of [78] that the error on averages of smooth observables $\varphi \in \mathscr{S}$ with respect to $\mu_{e_{\min},\Delta t}$ is of order 2 for the standard kinetic energy, i.e. there exists $a \in \mathbb{R}$ such that

$$\int_{\mathcal{E}} \varphi \, d\mu_{e_{\min},\Delta t} = \int_{\mathcal{E}} \varphi \, d\mu_{e_{\min}} + a\Delta t^2 + \mathrm{O}\left(\Delta t^3\right).$$

See Chapter 3 for error estimates for more general kinetic energies. As already mentioned in Remark 2.3, the reduction of the gap between the parameters $e_{\min}$ and $e_{\max}$ reduces the smoothness of the transition between the restrained dynamics and the full dynamics. This raises issues in the stability of the scheme, which can be partly cured by resorting to a Metropolis-Hastings correction ([87, 56] as done in Chapter 3.

We consider the system of dimer surrounded by solvent described in Section 1.1.1.1. It is composed of $N = 49$ particles in dimension 2, so that $d = 98$ and $\mathcal{D} = (L\mathbb{T})^{2N}$. The masses are set to 1 for all particles. Among these particles, two particles (numbered 1 and 2 in the following) are designated to form a dimer while the others are solvent particles. All particles, except the two particles forming the dimer, interact through a purely repulsive WCA pair potential (1.4) with two positive parameters $\varepsilon_{\mathrm{LJ}}$ and σ_{LJ} and $r_0 = 2^{1/6}\sigma_{\mathrm{LJ}}$. The interaction potential between the two particles of the dimer is a double-well potential given by (1.1). Recall that the potential V_{D} has two energy minima. The first one, at $r = r_0$, corresponds to the compact state. The second one, at $r = r_0 + 2w$, corresponds to the stretched state. The total energy of

the system is therefore, for $q \in (L\mathbb{T})^{dN}$ with $d = 2$, equal to (1.3). We choose $\beta = 1$, $\varepsilon_{\mathrm{LJ}} = 1$, $\sigma_{\mathrm{LJ}} = 1$, $h = 1$, $w = 1$, and set the particle density $\rho = N/L^2$ to 0.56 in the numerical results presented in this section, sufficiently high to ensure that the solvent markedly modifies the distribution of configurations of the dimer compared to the gas phase.

The source of metastability in the system is the double-well potential on the dimer. In such a system, it makes sense to restrain only solvent particles (since they account for most of the computational cost), and keep the standard kinetic energy for the particles forming the dimer (since the observable depends on their positions). As noted in Section 1.5, the method allows us to choose different individual kinetic energies for different particles. Since the solvent interacts with the dimer, we study how the variance of time averages of observables related to the configuration of the dimer, such as the dimer potential energy $\varphi = V_{\mathrm{D}}$, depends on the restraining parameters chosen for the solvent particles. We also estimate the variance of time averages based on observables depending only on the solvent degrees of freedom, such as the solvent-solvent potential energy $\varphi = V_{\mathrm{SS}}$.

The asymptotic variance of time averages for a given observable φ is estimated by approximating the integrated auto-correlation function

$$\sigma_\varphi^2 = 2 \int_0^\infty \mathbb{E}_{\mu_{e_{\min},e_{\max}}} \left[\left(\Pi_\mu \varphi\right)(q_0,p_0) \left(\Pi_\mu \varphi\right)(q_t,p_t) \right] dt,$$

where the expectation is with respect to initial conditions $(q_0, p_0) \sim \mu_{e_{\min},e_{\max}}$ and all realizations of the AR-Langevin dynamics. This is done by first truncating the upper bound in the integral by a sufficiently large time T_{corr}, and using a trapezoidal rule:

$$\sigma_\varphi^2 \approx \sigma_{\varphi,M,\Delta t}^2 := \Delta t \left(\frac{\widetilde{C}_0^M}{2} + \sum_{j=1}^{I_{\mathrm{corr}}} \widetilde{C}_j^M \right) \tag{2.22}$$

where $I_{\mathrm{corr}} = \left\lfloor \frac{T_{\mathrm{corr}}}{\Delta t} \right\rfloor$, and the empirical averages over M realizations of trajectories of I_{corr} steps are defined as

$$\widetilde{C}_j^M := C_j^M - \widehat{\varphi}_j^M \widehat{\varphi}_0^M, \quad j \in \{1, \ldots, I_{\mathrm{corr}}\} ,$$

with

$$C_j^M := \frac{1}{M} \sum_{m=1}^M \varphi(q_j^m, p_j^m)\varphi(q_0^m, p_0^m), \quad \widehat{\varphi}_j^M := \frac{1}{M} \sum_{m=1}^M \varphi(q_j^m, p_j^m) .$$

The initial condition (q_0^{m+1}, p_0^{m+1}) for the $(m+1)$th trajectory is obtained from the last configuration of the mth configuration, namely $(q_{I_{\mathrm{corr}}}^{m+1}, p_{I_{\mathrm{corr}}}^{m+1})$. Figure 2.6 presents the auto-correlation function obtained for $\varphi = V_{\mathrm{D}}$. The results show that the choice $T_{\mathrm{corr}} = 3$ is reasonable.

The results of [78] and Corollary (3.3) show that the errors on the approximation of the variance should be of order Δt^2 when $T_{\mathrm{corr}} \to +\infty$ for the standard kinetic energy. For more general kinetic energies we however expect that errors will be of order $a_1 \Delta t + a_2 \Delta t^2$ with a_1 small (see Chapter 3 for more details). This is illustrated in Figures 2.7, 2.8, 2.9 and 2.10, which present the convergence of $\sigma_{\varphi,M,\Delta t}^2$ as a function

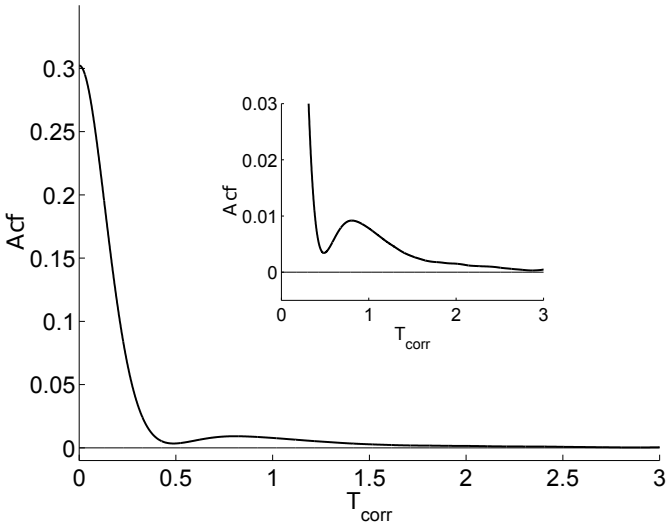

Fig. 2.6: Auto-correlation function $\mathbb{E}_\mu\left[\left(\Pi_\mu\varphi\right)\left(p_0,q_0\right)\left(\Pi_\mu\varphi\right)\left(p_t,q_t\right)\right]$ for $\varphi = V_D$ as a function of time.

of Δt for $M = 3 \times 10^6$. It is possible to extrapolate the value of the variance at $\Delta t = 0$ by fitting $\sigma^2_{\varphi,M,\Delta t}$ as $a_0 + a_1\Delta t^2$. It turns out that, for the specific observable under consideration, a convergence consistent with weak order 2 is observed (see also Figure (3.2b) which suggests that it is difficult to observe the lack of second order when the fluctuation-dissipation part has weak order 1). Note that the errors on the variance are bigger in the case $e_{\min} = 2.7$, which is expected due to the smaller gap between the parameters $e_{\max}, e_{\min}$. In the sequel, all the reported approximations of the variance are obtained by computing $\sigma^2_{\varphi,M,\Delta t}$ for 6 values of the time step Δt, and extrapolating to the limit $\Delta t \to 0$ as in Figures 2.7, 2.8, 2.9 and 2.10. More precisely, the time steps are chosen as $\Delta t_{0,k} = k \times 10^{-3}$ for $k = 1, \ldots, 6$ when $e_{\min} = 0$, and $\Delta t_{e^*_{\min},k} = k \times 10^{-4}$ for $e^*_{\min} = 2.7$. For intermediate values of $e_{\min}$, the time steps $\Delta t_{e_{\min},k}$ are obtained by a linear interpolation between $\Delta t_{0,k}$ and $\Delta t_{e^*_{\min},k}$.

The variations as a function of $e_{\min}$ of the approximations of the variances $\sigma^2_\varphi(e_{\min})$ for the solvent-solvent potential energy V_{SS} and the dimer potential energy V_{D} are reported in Figures 2.11 and 2.12. Surprisingly, even though the solvent particles are restrained, the variance of the solvent-solvent potential decreases linearly for moderately small values of $e_{\min}$; whereas, as expected, the variance of the dimer potential, which is only implicitly influenced by the restraining parameters, increases linearly for these values of $e_{\min}$. In order to more easily compare the impacts of the restraining procedure, we plot in Figure 2.13 the relative differences of the variance $\sigma^2(e_{\min})$ and the variance of Zero-$e_{\max}$-AR dynamics $\sigma^2_\varphi(0)$ as a function of $e_{\min}$. For the two observables under consideration, the impact of an increase of the parameter $e_{\min}$ on the variance associated with the dimer potential is much weaker than on the variance related to the solvent potential. We also provide in Figure 2.14 the percentage of restrained particles, which directly depends on the restraining parameter $e_{\min}$ and dictates the algorithmic speed-up (see Chapter 3). This supports the idea that the use of the AR-Langevin method for heterogeneous systems can be beneficial when

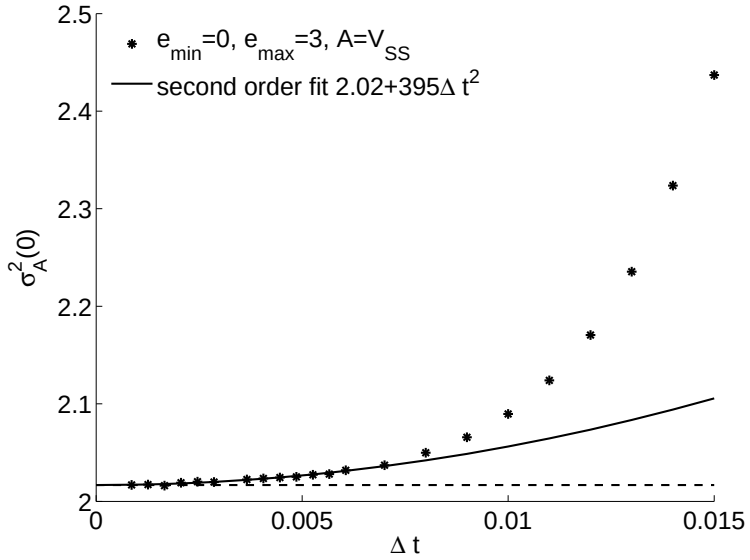

Fig. 2.7: Estimated variance $\sigma^2_{\varphi,M,\Delta t}$ for $\varphi = V_{\mathrm{SS}}$, as a function of the step size Δt, for $e_{\min} = 0$ and $e_{\max} = 3$.

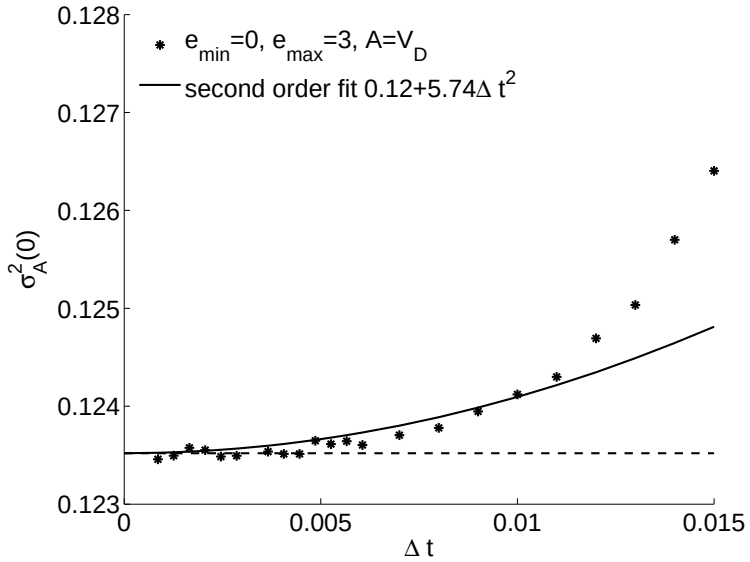

Fig. 2.8: Estimated variance $\sigma^2_{\varphi,M,\Delta t}$ for $\varphi = V_{\mathrm{D}}$, as a function of the step size Δt, for $e_{\min} = 0$ and $e_{\max} = 3$.

the AR parameters are set to non-zero values for the part of the system which is not directly of interest (e.g. the solvent), while the standard kinetic energy should be kept for the degrees of freedom that are directly involved in the observable (e.g. the dimer).

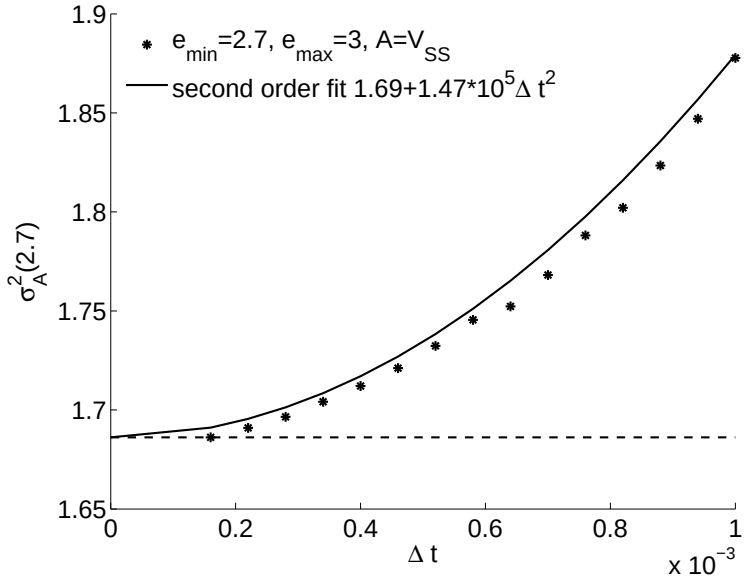

Fig. 2.9: Same as Figure 2.7, except that $e_{\min} = 2.7$.

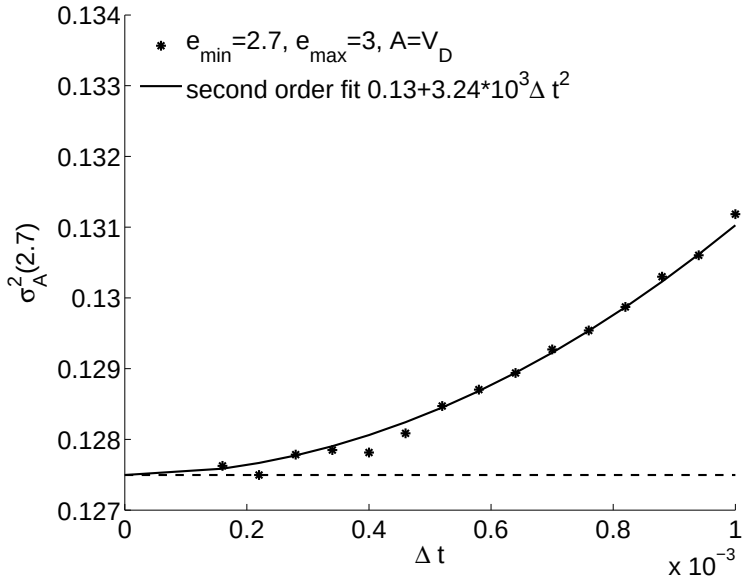

Fig. 2.10: Same as Figure 2.8, except that $e_{\min} = 2.7$.

2.5 Proofs of the results

2.5.1 Proof of Lemma 2.2

The modified Langevin equation can be written as a perturbation of the Langevin equation, namely

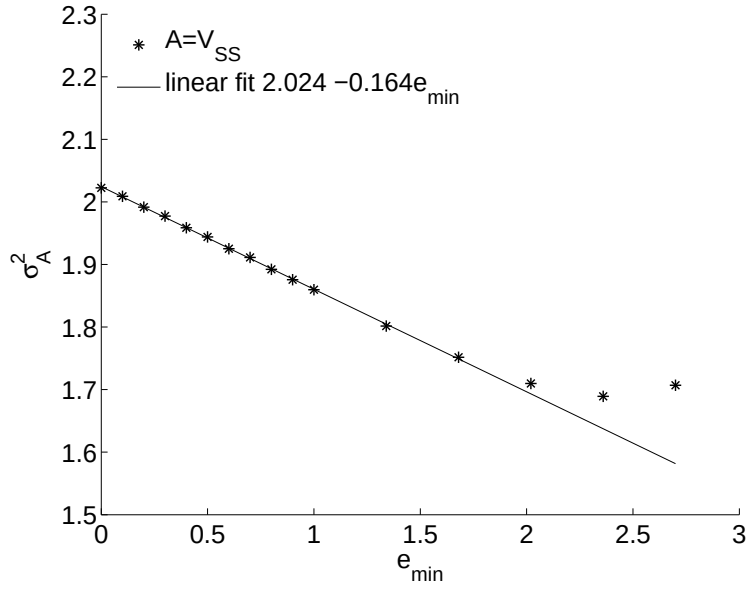

Fig. 2.11: Estimated variance σ^2_φ for $\varphi = V_{\rm SS}$ as a function of $e_{\min} \in [0, 2.7]$ for $e_{\max} = 3$.

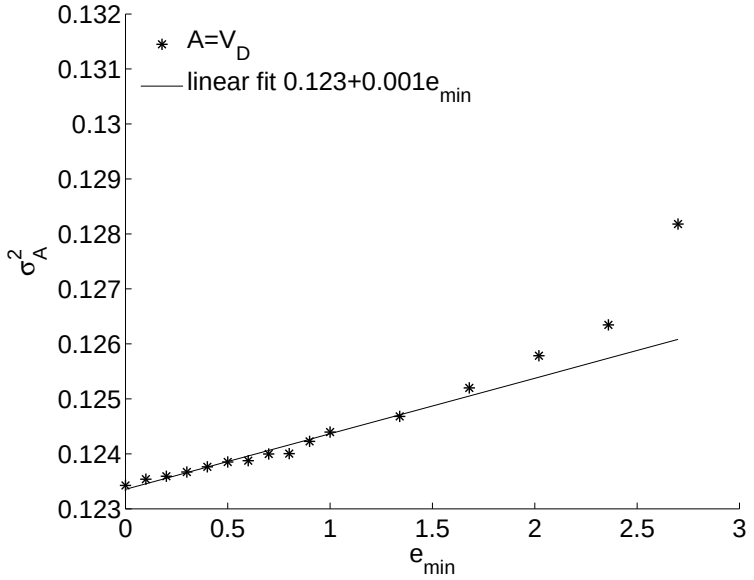

Fig. 2.12: Estimated variance σ^2_φ for $\varphi = V_{\rm D}$ as a function of $e_{\min} \in [0, 2.7]$ for $e_{\max} = 3$.

$$\begin{cases} dq_t = \left(M^{-1}p_t - \mathcal{Z}(p_t)\right) dt, \\ dp_t = -\nabla V(q_t)dt - \gamma \left(M^{-1}p_t - \mathcal{Z}(p_t)\right) dt + \sqrt{\dfrac{2\gamma}{\beta}}\, dW_t, \end{cases} \tag{2.23}$$

where $\mathcal{Z}(p) := \nabla U_{\rm std}(p) - \nabla U(p) = M^{-1}p - \nabla U(p)$ is uniformly bounded as $|\mathcal{Z}(p)| \leqslant G_{\rm std}$ in view of Assumption 2.2. By a direct integration in time of the momenta dynamics,

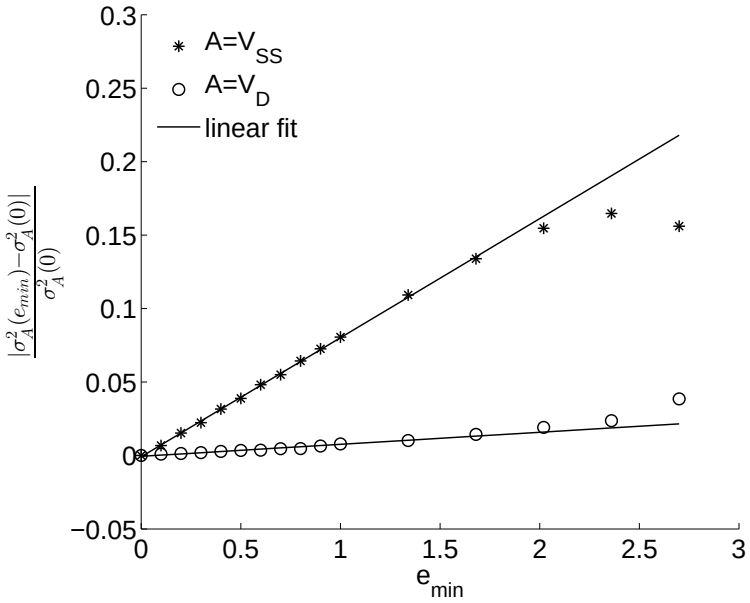

Fig. 2.13: Relative variation in the estimated variances $\sigma_\varphi^2(e_{\min})$ with respect to the reference variances $\sigma_\varphi^2(0)$.

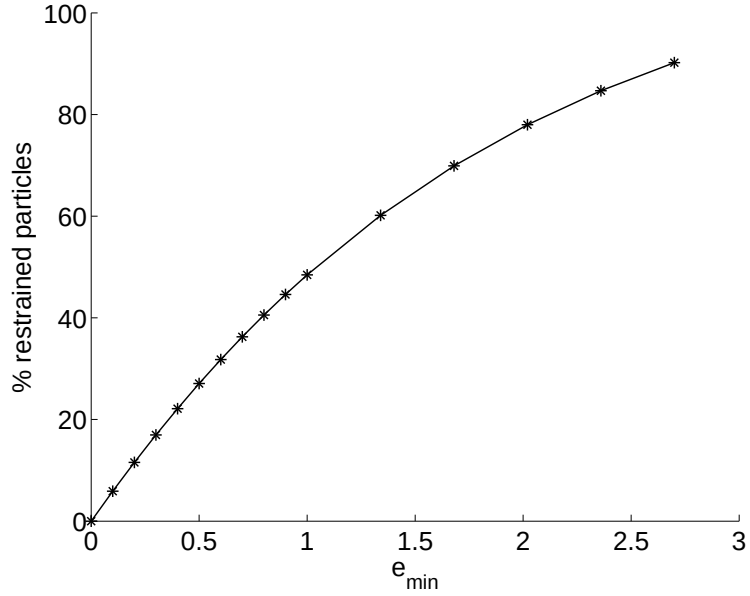

Fig. 2.14: Percentage of restrained particles as a function of $e_{\min}$.

$$p_t = \mathrm{e}^{-\gamma t} p_0 + \mathcal{F}_t + \mathcal{G}_t, \qquad \mathcal{F}_t = \int_0^t \Big(-\nabla V(q_s) + \gamma \mathcal{Z}(p_s) \Big) \mathrm{e}^{-\gamma(t-s)}\, ds, \tag{2.24}$$

where

$$\mathcal{G}_t = \sqrt{\frac{2\gamma}{\beta}} \int_0^t \mathrm{e}^{-\gamma(t-s)} dW_s$$

is a Gaussian random variable with mean zero and covariance $\left(1-\mathrm{e}^{-2\gamma t}\right)\beta^{-1}$. Note also that $\mathcal{F}_t$ is uniformly bounded; more precisely, $|\mathcal{F}_t| \leqslant \|\nabla V\|_{L^\infty}/\gamma + G_{\mathrm{std}}$.

Let us first consider the case $s = 1$. We introduce $\alpha_t := \mathrm{e}^{-\gamma t} < 1$ for a given time $t > 0$. With this notation,

$$\begin{aligned}|p_t|^2 = |\alpha_t p_0 + \mathcal{F}_t + \mathcal{G}_t|^2 &= \alpha_t^2 |p_t|^2 + 2\alpha_t p_t^T(\mathcal{F}_t + \mathcal{G}_t) + |\mathcal{F}_t|^2 + 2\mathcal{F}_t\mathcal{G}_t + |\mathcal{G}_t|^2 \\ &\leqslant \alpha_t^2(1+\varepsilon)\,|p_t|^2 + \left(2 + \frac{1}{4\varepsilon}\right)\mathcal{F}_t^2 + |\mathcal{G}_t|^2 + 2\alpha_t p_t^T \mathcal{G}_t,\end{aligned}$$

where we used Young's inequality to obtain the last line, with a constant $\varepsilon > 0$ sufficiently small so that $\alpha_t^2(1+\varepsilon) < 1$. We next take the expectation of the previous inequality, conditionally to the filtration of events up to time t. Since $\mathbb{E}\left[p_t^T \mathcal{G}_t \mid \mathscr{F}_t\right] = 0$, it follows

$$\mathbb{E}\left[\mathcal{K}_1(q_t,p_t)\middle|\mathscr{F}_t\right] \leqslant \alpha^2(1+\varepsilon)\mathcal{K}_1(q_t,p_t) + R,$$

for some constant $R > 0$. This shows the Lyapunov condition for $n = 1$. The higher order conditions ($n > 1$) can be proved as in [64, Section 5.1.5], by noting that $|p_t|^{2s}$ is equal to $\alpha_t^{2s}|p_0|^{2s}$ plus some lower order polynomial in p_0.

2.5.2 Proof of Lemma 2.1

The main idea is, as in [64, Section 5.1.5], to compare the modified Langevin dynamics to the standard Langevin dynamics with zero forces, for which a minorizing measure $\nu_{p^*,t}$ can be explicitly constructed. From the rewriting (2.23), we deduce, in view of the momenta evolution (2.24),

$$q_t = q_0 + \int_0^t \Big(p_s - \mathcal{Z}(p_s)\Big)ds = q_0 + \int_0^t \mathrm{e}^{-\gamma s} p_0\, ds + \widetilde{\mathcal{G}}_t + \widetilde{\mathcal{F}}_t,$$

where periodic boundary conditions are considered, and

$$\widetilde{\mathcal{F}}_t := \int_0^t \mathcal{F}_s\, ds - \int_0^t \mathcal{Z}(p_s)\, ds, \qquad \widetilde{\mathcal{G}}_t = \int_0^t \mathcal{G}_s\, ds.$$

Note that $\widetilde{\mathcal{F}}_t$ is bounded as

$$\left|\widetilde{\mathcal{F}}_t\right| \leqslant \left(\frac{\|\nabla V\|_{L^\infty}}{\gamma} + 2G_{\mathrm{std}}\right) t,$$

whereas $\widetilde{\mathcal{G}}_t$ is a Gaussian random variable, which is correlated to $\mathcal{G}_t$. A simple computation shows that

$$\mathcal{V} := \mathbb{E}\left[(\widetilde{\mathcal{G}}_t, \mathcal{G}_t)^T (\widetilde{\mathcal{G}}_t, \mathcal{G}_t)\right] = \begin{pmatrix} \mathcal{V}_{qq} & \mathcal{V}_{qp} \\ \mathcal{V}_{pq} & \mathcal{V}_{pp} \end{pmatrix}, \qquad \begin{cases} \mathcal{V}_{qq} = \dfrac{1}{\beta\gamma}\left(2t - \dfrac{1}{\gamma}\left(3 - 4\alpha_t + \alpha_t^2\right)\right), \\ \mathcal{V}_{qp} = \dfrac{1}{\beta\gamma}\left(1 - \alpha_t\right)^2, \\ \mathcal{V}_{pp} = \dfrac{1}{\beta}\left(1 - \alpha_t^2\right), \end{cases}$$

where $\alpha_t = \mathrm{e}^{-\gamma t}$ is the same constant as in Section 2.5.1. Therefore, for a given measurable set $B \in \mathscr{B}(\mathcal{E})$,

$$\mathbb{P}\left((q_t, p_t) \in B \,\middle|\, |p_0| \leqslant p_*\right) \geqslant \mathbb{P}\left(\left(\widetilde{\mathcal{G}}_t, \mathcal{G}_t\right) \in B - (\mathcal{Q}_t, \mathcal{P}_t) \,\middle|\, |p_0| \leqslant p_*\right), \tag{2.25}$$

where

$$\mathcal{Q}_t := q_0 + \frac{1 - \alpha_t}{\gamma} p_0 + \widetilde{\mathcal{F}}_t, \qquad \mathcal{P}_t := \alpha_t p_0 + \mathcal{F}_t,$$

are both bounded by some constant $R > 0$ (depending on p^* and t) when $|p_0| \leqslant p^*$. Note that there is an inequality in (2.25) since we neglect in fact the periodic images of q_t when writing it as $\mathcal{Q}_t + \widetilde{\mathcal{G}}_t$, the latter two quantities being interpreted as elements of $\mathbb{R}^d$. Since the matrix $\mathcal{V}$ is definite positive, we can finally consider the following minorizing measure:

$$\nu_{p^*,t}(B) := Z_R^{-1} \inf_{|\mathcal{Q}|, |\mathcal{P}| \leqslant R} \int_{B - (\mathcal{Q}, \mathcal{P})} \exp\left(-\frac{x^T \mathcal{V}^{-1} x}{2}\right) dx,$$

where $Z_R > 0$ is a normalization constant. The proof is concluded by defining $\kappa = (2\pi)^{-d} \det\left(\mathcal{V}\right)^{-1/2} Z_R$.

2.5.3 Proof of Lemma 2.3

2.5.3.1 General structure of the proof

The proof follows the strategy of [71, Proposition A.1]. We recall in this section the general outline of this proof, and highlight the required extensions. The proofs of these extensions are then provided in Section 2.5.3.2. Without restriction of generality, and in order to simplify the notation, we assume that $\varphi = \mathit{\Pi}_\mu \varphi$. We introduce weight functions

$$\pi_s(p) := \frac{1}{\mathcal{K}_s(p)},$$

where the Lyapunov functions $\mathcal{K}_s$ are defined in (1.40). We also define

$$u(t, q, p) = \left(\mathrm{e}^{t\mathcal{L}} \varphi\right)(q, p) = \mathbb{E}\left[\varphi(q_t, p_t) \mid (q_0, p_0) = (q, p)\right].$$

The following result, central in this proof, gives estimates on derivatives of $u(t)$ in the weighted spaces $L^2(\pi_s)$ (see Section 2.5.3.2 for the proof).

Lemma 2.4. *Suppose that Assumptions 2.2 and 2.5 hold. For any $n \geqslant 1$, there exists $\lambda_n > 0$ and $s_n \in \mathbb{N}$ such that, for $s \geqslant s_n$ and $G_\nu \leqslant \rho_s$ with $\rho_s > 0$ sufficiently small, there is $r \in \mathbb{N}$ and $C > 0$ for which*

$$\forall\, |k| \leqslant n, \qquad \int_{\mathcal{E}} \left|\partial^k u(t,q,p)\right|^2 \pi_s(p)\, dp\, dq \leqslant C\, \|\varphi\|^2_{W^{n,\infty}_{\mathcal{K}_r}} \exp(-\lambda t). \tag{2.26}$$

Assume in the sequel that $G_\nu \leqslant \rho_s$ for s sufficiently large. In view of the estimates (2.26), and using the fact that $\partial^j \pi_s(p) = \psi_{j,s}(p)\pi_s(p)$ with $\psi_{j,s}(p) \to 0$ as $|p| \to +\infty$, we obtain that, for any $n \geqslant 1$, there exist $s_n \in \mathbb{N}$ such that, for $s \geqslant s_n$, it is possible to find $r \in \mathbb{N}$ and $C > 0$ for which

$$\forall\, |k| + |\ell| \leqslant n, \quad \forall t \geqslant 0, \qquad \int_{\mathcal{E}} \left|\partial^\ell \Big(\partial^k u(t,q,p)\pi_s(p)\Big)\right|^2 dp\, dq \leqslant C\, \|\varphi\|^2_{W^{\tilde{n},\infty}_{\mathcal{K}_r}} \exp(-\lambda t).$$

By the Sobolev embedding theorem, we can conclude that, for any $n \geqslant 1$, there exist $s_n, \widetilde{n} \in \mathbb{N}$ such that, for $s \geqslant s_n$ and provided $G_\nu \leqslant \rho_s$, it is possible to find $r \in \mathbb{N}$ and $C > 0$ for which

$$\forall |k| \leqslant n, \qquad \left|\partial^k u(t,q,p)\right| \pi_s(p) \leqslant C\, \|\varphi\|^2_{W^{\tilde{n},\infty}_{\mathcal{K}_r}} \exp(-\lambda t).$$

This concludes the proof of Lemma 2.3.

2.5.3.2 Proof of Lemma 2.4

The main tool in the proof of Lemma 2.4 is the following estimate, which is the counterpart of [71, Lemma A.6] for our modified Langevin dynamics.

Lemma 2.5. *Let $\mathcal{A}$ be a linear operator. Assume that $U \in \mathscr{S}$ and $\Delta U \in L^\infty$. There exists an integer s_* such that, for all $s \geqslant s_*$, there is a constant $\omega_s > 0$ for which the following inequality holds true for any $\zeta, T > 0$:*

$$\begin{aligned}
&\exp(\zeta T) \int_{\mathcal{E}} |\mathcal{A}u(t)|^2\, \pi_s\, dq\, dp + \frac{2\gamma}{\beta} \int_0^T \exp(\zeta t) \left(\int_{\mathcal{E}} |\nabla_p \mathcal{A}u(t)|^2\, \pi_s\, dq\, dp \right) dt \\
&\quad \leqslant \int_{\mathcal{E}} |\mathcal{A}u(0)|^2\, \pi_s\, dq\, dp \\
&\qquad + (\omega_s + \gamma\, \|\Delta U\|_{L^\infty} + \zeta) \int_0^T \exp(\zeta t) \left(\int_{\mathcal{E}} |\mathcal{A}u(t)|^2\, \pi_s\, dp\, dq \right) dt \\
&\qquad + 2 \int_0^T \exp(\zeta t) \left(\int_{\mathcal{E}} [\mathcal{A}, \mathcal{L}]\, u(t)\ \mathcal{A}u(t) \pi_s\, dq\, dp \right) dt\ .
\end{aligned} \tag{2.27}$$

In fact, a careful inspection of the proof shows that, since $U \in \mathscr{S}$, it is possible to avoid the assumption $\Delta U \in L^\infty$ by appropriately increasing the Lyapunov index s. Since $\Delta U \in L^\infty$ for AR-Langevin dynamics, we however keep this assumption.

Proof. A simple computation shows that

$$2\mathcal{L}\mathcal{A}u(t)\,\mathcal{A}u(t) = \mathcal{L}\left(|\mathcal{A}u(t)|^2\right) - \frac{2\gamma}{\beta}\,|\nabla_p \mathcal{A}u(t)|^2\ . \tag{2.28}$$

The formal adjoint of the operator $\mathcal{L}$ in $L^2(\mathcal{E})$ is given by

$$\mathcal{L}^\dagger = -\left(\nabla U\cdot\nabla_q - \nabla V\cdot\nabla_p\right) + \gamma\left(\Delta U + \nabla U\cdot\nabla_p + \frac{1}{\beta}\Delta_p\right).$$

In view of Assumption 2.2, there exists therefore $\omega_s > 0$ such that

$$\begin{aligned}\mathcal{L}^\dagger\pi_s &= \left[-\left(\nabla V + \gamma\nabla U\right)\cdot\frac{\nabla\mathcal{K}_s}{\mathcal{K}_s} + \gamma\Delta U - \frac{\gamma}{\beta}\frac{\Delta\mathcal{K}_s}{\mathcal{K}_s} + \frac{2\gamma}{\beta}\frac{|\nabla\mathcal{K}_s|^2}{\mathcal{K}_s^2}\right]\pi_s \\ &\leqslant \left(\omega_s + \gamma\,\|\Delta U\|_{L^\infty}\right)\pi_s.\end{aligned} \tag{2.29}$$

With this estimation, we can follow exactly the proof of [71, Lemma A.6], *i.e.* write the expression for $\frac{d}{dt}\left[\exp(\zeta t)\,|\mathcal{A}u(t)|^2\right]$, use (2.28), integrate the resulting expression in time and with respect to $\pi_s\,dq\,dp$ (for s sufficiently large), and finally use (2.29) to deduce (2.27).

Let us now prove Lemma 2.4. The complete proof is done by induction on n. We provide here the complete proofs for $n = 0$ and $n = 1$, and only sketch the extension to higher orders of derivation since the proof follows the same lines as in [71, Appendix A].

Case $n = 0$.

Recall first that, in view of Assumption 2.2, the exponential convergence of the law provided by Theorem 2.4 holds. Denote by λ_ℓ the corresponding exponential rate of decay for a given $\ell \in \mathbb{N}^*$. For any $r \in \mathbb{N}$, we directly obtain the following decay estimates in $L^2(\pi_l)$ when $l > 2r + d/2$: there exists $\widetilde{C}_{l,r} > 0$ such that

$$\int_{\mathcal{E}} |u(t)|^2\,\pi_l \leqslant \widetilde{C}_{l,r}\,\mathrm{e}^{-2\lambda_r t}\,\|\varphi\|^2_{L^\infty_{\mathcal{K}_r}}\ .$$

Note that this corresponds to the case $n = 0$ in Lemma 2.4.

Case $n = 1$.

We now prove the estimates in the case $n = 1$. We first apply Lemma 2.5 with $\mathcal{A} = \mathrm{Id}$: there exists $s_* \in \mathbb{N}$ such that, for all $s \geqslant s_*$ and $\zeta < 2\lambda_r$, there is $C > 0$ and $r \in \mathbb{N}$ for which

$$\forall T \in \mathbb{R}_+, \qquad \int_0^T \exp(\zeta t)\left[\int_{\mathcal{E}} |\nabla_p u(t,q,p)|^2\,\pi_s(p)\,dq\,dp\right]dt \leqslant C\,\|\varphi\|^2_{L^\infty_{\mathcal{K}_r}}\ . \tag{2.30}$$

In order to control derivatives in q, the key idea, going back to [117], is to use mixed derivatives $\alpha\partial_{p_i} - \partial_{q_i}$ (for some parameter $\alpha > 0$). This allows indeed to retrieve some dissipation in the q direction when $\nabla^2 U$ is positive definite. The next lemma is the most important part of our proof since we show how to extend the use of mixed derivatives to the case when $\nabla^2 U$ is not positive definite.

Lemma 2.6. *Consider the operator $L_\alpha := \alpha\nabla_p - \nabla_q$ for some parameter $\alpha \in \mathbb{R}$. There exists $s_* \in \mathbb{N}$ such that, for $s \geqslant s_*$ and provided $G_\nu \leqslant \rho_s$ (for some constant $\rho_s > 0$ defined in* (2.34) *below), there is $r \in \mathbb{N}$, $\zeta < 2\lambda_r$, $\alpha > 0$ and $C > 0$ for which*

$$\begin{aligned} \forall T > 0,\ \int_0^T \exp(\zeta t) \left[\int_{\mathcal{E}} \left(|L_\alpha u(t,q,p)|^2 + |\nabla_p L_\alpha u(t,q,p)|^2 \right) \pi_s(p)\, dq\, dp \right] dt \\ \leqslant C \left\| \varphi \right\|^2_{W^{1,\infty}_{\mathcal{K}_r}} . \end{aligned} \tag{2.31}$$

Proof. Define $L_{\alpha,i} := \alpha\partial_{p_i} - \partial_{q_i}$ for $i \in \{1, \ldots, d\}$. The commutator of $L_{\alpha,i}$ and $\mathcal{L}$ is

$$\begin{aligned} [L_{\alpha,i}, \mathcal{L}] &= -\alpha \left(\nabla_p \partial_{p_i} U \right) \cdot (\gamma \nabla_p - \nabla_q) + \left(\nabla_q \partial_{q_i} V \right) \cdot \nabla_p \\ &= -\alpha \left(\nabla_p \partial_{p_i} U \right) \cdot L_\alpha - \alpha \left(\gamma - \alpha \right) \left(\nabla_p \partial_{p_i} U \right) \cdot \nabla_p + \left(\nabla_q \partial_{q_i} V \right) \cdot \nabla_p . \end{aligned}$$

Introducing $C_V := \sup_{i,j=1,\ldots,d} \left\| \partial^2_{q_i q_j} V \right\|_{L^\infty}$, a simple computation shows that

$$\begin{aligned} &2 \sum_{i=1}^d L_{\alpha,i} u(t) [L_{\alpha,i}, \mathcal{L}] u(t) = \\ &\quad = -2\alpha \sum_{i=1}^d \sum_{j=1}^d L_i u(t) \left(\partial_{p_j} \partial_{p_i} U \right) L_{\alpha,j} u(t) \\ &\qquad + 2\alpha(\alpha - \gamma) \sum_{i=1}^d L_{\alpha,i} u(t) \left(\nabla \partial_{p_i} U \right) \cdot \nabla_p u(t) + 2 \sum_{i=1}^d L_{\alpha,i} u(t) \nabla \left(\partial_{q_i} V \right) \cdot \nabla_p u(t) \\ &\quad \leqslant \left(\varepsilon_1 + \varepsilon_2 - 2\nu\alpha \right) |L_\alpha u(t)|^2 - 2\alpha \sum_{i=1}^d \sum_{j=1}^d L_{\alpha,i} u(t) \partial_{p_j} \partial_{p_i} (U - U_\nu) L_{\alpha,j} u(t) \\ &\qquad + \frac{\alpha^2 (\gamma - \alpha)^2}{\varepsilon_1} \left(\sup_{|j|=2} \left\| \partial^j U \right\|^2_{L^\infty} \right) |\nabla_p u(t)|^2 + \frac{C_V^2}{\varepsilon_2} |\nabla_p u(t)|^2 \end{aligned}$$

for any $\varepsilon_1, \varepsilon_2 > 0$. With this preliminary computation, we can now choose $\mathcal{A} = L_{\alpha,i}$ in Lemma 2.5 and sum over $i = 1, \ldots, d$: for $s \geqslant s_*$ with s_* sufficiently large,

$$
\begin{aligned}
&\exp(\zeta T)\int_{\mathcal{E}} |L_\alpha u(t)|^2\,\pi_s\,dq\,dp + \frac{2\gamma}{\beta}\int_0^T \exp(\zeta t)\left(\int_{\mathcal{E}}\sum_{i=1}^d |\nabla_p L_{\alpha,i}u(t)|^2\,\pi_s\,dq\,dp\right)dt \\
&\quad\leqslant \int_{\mathcal{E}} |L_\alpha u(0)|^2\,\pi_s\,dq\,dp \\
&\quad+ \left(\omega_s + \gamma\,\|\Delta U\|_{L^\infty}^2 + \zeta + \varepsilon_1 + \varepsilon_2 - 2\nu\alpha\right)\int_0^T \exp(\zeta t)\left(\int_{\mathcal{E}} |L_\alpha u(t)|^2\,\pi_s\,dq\,dp\right)dt \qquad (2.32)\\
&\quad- 2\alpha\int_0^T \exp(\zeta t)\left(\int_{\mathcal{E}} L_\alpha u(t)^T\left[\nabla^2(U-U_\nu)\right]L_\alpha u(t)\,\pi_s\,dq\,dp\right)dt \qquad (2.33)\\
&\quad+ \frac{\alpha^2(\gamma-\alpha)^2}{\varepsilon_1}\left(\sup_{|j|=2}\left\|\partial^j U\right\|_{L^\infty}^2\right)\int_0^T \exp(\zeta t)\left(\int_{\mathcal{E}} |\nabla_p u(t)|^2\,\pi_s\,dq\,dp\right)dt \\
&\quad+ \frac{C_V^2}{\varepsilon_2}\int_0^T \exp(\zeta t)\left(\int_{\mathcal{E}} |\nabla_p u(t)|^2\,\pi_s\,dq\,dp\right)dt\,.
\end{aligned}
$$

Since $L_\alpha u(0) = (\alpha\nabla_p - \nabla_q)\varphi \in \widetilde{\mathscr{W}}^{1,\infty}_{\mathcal{K}_r}$ for some integer $r \leqslant s_*$ (upon increasing s_*), and in view of (2.30), the first and the two last terms of the right hand side of the above inequality can be controlled uniformly in time for $\zeta < 2\lambda_r$.

It remains to take care of the terms (2.32) and (2.33). Our strategy is to prove that they are negative when $\zeta < 2\lambda_r$, and can hence be transfered to the left-hand side of the inequality. To simplify the notation, we denote $\widetilde{U} := U - U_\nu$. Recall that, by Assumption 2.5, it holds $\|\nabla\widetilde{U}\|_{L^\infty} \leqslant G_\nu$. An integration by parts shows that

$$
\begin{aligned}
-\int_{\mathcal{E}}\sum_{j=1}^d L_{\alpha,i}u(t)\,\left(\partial_{p_j}\partial_{p_i}\widetilde{U}\right)L_{\alpha,j}u(t)\,\pi_s\,dq\,dp &= \int_{\mathcal{E}}\left(\nabla\widetilde{U}\cdot L_\alpha u(t)\right)\mathrm{div}_p\left(L_\alpha u(t)\right)\,\pi_s\,dq\,dp \\
+\int_{\mathcal{E}}\sum_{j=1}^d\left(\partial_{p_i}\widetilde{U}\right)L_{\alpha,j}u(t)\Big(\partial_{p_j}L_{\alpha,i}u(t)\Big)\pi_s\,dq\,dp &+ \int_{\mathcal{E}}\sum_{j=1}^d\left(\nabla\widetilde{U}\cdot L_\alpha u(t)\right)\Big(\nabla\pi_s\cdot L_\alpha u(t)\Big)dq\,dp.
\end{aligned}
$$

With this expression we now bound the term (2.33) by

$$
\begin{aligned}
&-2\alpha\int_0^T \exp(\zeta t)\left(\int_{\mathcal{E}}\sum_{i=1}^d\sum_{j=1}^d L_i u(t)\left(\partial_{p_j}\partial_{p_i}\widetilde{U}\right)L_j u(t)\,\pi_s\,dq\,dp\right)dt \\
&\qquad\leqslant 2(1+\mathscr{G}_s)\alpha\varepsilon_3\left\|\nabla\widetilde{U}\right\|_{L^\infty}\int_0^T \exp(\zeta t)\left(\int_{\mathcal{E}}|Lu(t)|^2\,\pi_s\,dq\,dp\right)dt \\
&\qquad\quad+\frac{2\alpha}{\varepsilon_3}\left\|\nabla\widetilde{U}\right\|_{L^\infty}\int_0^T \exp(\zeta t)\left(\int_{\mathcal{E}}\sum_{i=1}^d|\nabla_p L_i u(t)|^2\,\pi_s\,dq\,dp\right)dt,
\end{aligned}
$$

where we have used Young's inequality and introduced a constant $\mathscr{G}_s \in \mathbb{R}_+$ such that $|\nabla_p\pi_s| \leqslant \mathscr{G}_s\pi_s$.

The following conditions are therefore sufficient to ensure that (2.32) and (2.33) are non-positive when $\zeta < 2\lambda_r$: there exists $\alpha > 0$ such that

$$\omega_s + \gamma \left\|\Delta U\right\|_{L^\infty}^2 + \zeta - 2\nu\alpha + 2\alpha\varepsilon_3(\mathscr{G}_s + 1) \left\|\nabla \widetilde{U}\right\|_{L^\infty} < 0$$

and

$$\frac{2\gamma}{\beta} > \frac{2\alpha}{\varepsilon_3} \left\|\nabla \widetilde{U}\right\|_{L^\infty}.$$

These conditions can be restated as

$$\frac{\omega_s + \gamma \left\|\Delta U\right\|_{L^\infty}^2 + \zeta}{2\left(\nu - \varepsilon_3(\mathscr{G}_s + 1) \left\|\nabla \widetilde{U}\right\|_{L^\infty}\right)} < \alpha < \frac{\gamma\varepsilon_3}{\beta \left\|\nabla \widetilde{U}\right\|_{L^\infty}}.$$

Since ζ can be chosen arbitrarily small (while still being positive), the latter condition holds provided $\left\|\nabla \widetilde{U}\right\|_{L^\infty}$:

$$\left\|\nabla \widetilde{U}\right\|_{L^\infty} < \frac{2\gamma\nu\varepsilon_3}{\beta(\omega_s + \gamma \left\|\Delta U\right\|_{L^\infty}^2 + \zeta) + 2\gamma(\mathscr{G}_s + 1)\varepsilon_3^2}.$$

After optimization with respect to ε_3, this leads to the final condition

$$\left\|\nabla \widetilde{U}\right\|_{L^\infty} < \sqrt{\frac{\nu^2\gamma}{2\beta(\omega_s + \gamma \left\|\Delta U\right\|_{L^\infty}^2 + \zeta)(\mathscr{G}_s + 1)}}.$$

In conclusion, defining

$$\rho_s = \sqrt{\frac{\nu^2\gamma}{2\beta(\omega_s + \gamma \left\|\Delta U\right\|_{L^\infty}^2)(\mathscr{G}_s + 1)}}, \tag{2.34}$$

we see that the estimate (2.31) holds when the constant G_ν from Assumption 2.5 satisfies $G_\nu \leqslant \rho_s$.

The remainder of the proof of Lemma 2.4 is very similar to the corresponding proof in [71]. We first combine (2.30) and Lemma 2.6: there exists $s_* \in \mathbb{N}$ such that for $s \geqslant s_*$ there exist an integer r, a sufficiently small $\zeta < 2\lambda_r$ and $\rho_s > 0$ such that if $G_\nu \leqslant \rho_s$, then there is a constant $C > 0$ for which

$$\forall T \geqslant 0, \qquad \int_0^T \exp(\zeta t) \left(\int_{\mathcal{E}} \left|\nabla_q u(t)\right|^2 \pi_s \, dq \, dp\right) dt \leqslant C \left\|\varphi\right\|_{W^{1,\infty}_{\mathcal{K}_r}}^2. \tag{2.35}$$

We can now again apply Lemma 2.5, and sum the estimates obtained with $\mathcal{A} = \partial_{p_i}$. Before stating the result, we bound the integrand of the term involving the commutator $[\partial_{p_i}, \mathcal{L}]$ (for $i = 1, \ldots, d$) as:

$$\begin{aligned}
\left|\sum_{i=1}^d [\partial_{p_i}, \mathcal{L}] \, u(t) \partial_{p_i} u(t)\right| &= \left|\sum_{i=1}^d \nabla_p(\partial_{p_i} U) \cdot (\nabla_q - \gamma\nabla_p) u(t) \, \partial_{p_i} u(t)\right| \\
&\leqslant d \left(\sup_{|j|=2} \left\|\partial^j U\right\|_{L^\infty}^2\right) \left|(\nabla_q - \gamma\nabla_p) u(t)\right| \, \left|\nabla_p u(t)\right| \\
&\leqslant d \left(\sup_{|j|=2} \left\|\partial^j U\right\|_{L^\infty}^2\right) \left[\frac{1}{2}|\nabla_q u(t)|^2 + \left(\gamma + \frac{1}{2}\right) |\nabla_p u(t)|^2\right].
\end{aligned}$$

Then, for $s \geqslant s_*$ (with s_* sufficiently large) and for all $T \geqslant 0$,

$$
\begin{aligned}
&\exp(\zeta T)\int_{\mathcal{E}}|\nabla_p u(t)|^2\,\pi_s\,dq\,dp\\
&\leqslant \int_{\mathcal{E}}|\nabla_p u(0)|^2\,\pi_s\,dq\,dp + d\left(\sup_{|j|=2}\left\|\partial^j U\right\|_{L^\infty}\right)\int_0^T\exp(\zeta t)\left(\int_{\mathcal{E}}|\nabla_q u(t)|^2\,\pi_s\,dq\,dp\right)dt\\
&\quad+\left(\omega_s+\zeta+\sup_{|j|=2}\left\|\partial^j U\right\|_{L^\infty}(d+2\gamma d+\gamma)\right)\int_0^T\exp(\zeta t)\left(\int_{\mathcal{E}}|\nabla_p u(t)|^2\,\pi_s\,dq\,dp\right)dt.
\end{aligned}
$$

In view of (2.30) and (2.35) and since $\nabla_p u(0)=\nabla_p A\in\widetilde{W}^{1,\infty}_{\widetilde{\mathcal{K}}_{\widetilde{r}}}$ for some integer $\widetilde{r}\in\mathbb{N}$, we see that there exists $s_*\geqslant 1$ sufficiently large such that, for any $s\geqslant s_*$ and $\zeta>0$ sufficiently small, and provided $G_\nu\leqslant\rho_s$, there is a constant $C>0$ and an integer r for which

$$
\int_{\mathcal{E}}|\nabla_p u(t)|^2\,\pi_s\,dq\,dp\leqslant C\,\|\varphi\|^2_{W^{1,\infty}_{\mathcal{K}_r}}\exp(-\zeta T).
$$

To conclude to Lemma 2.4 for $n=1$, it remains to apply Lemma 2.5 with $\mathcal{A}=\nabla_q$ in order to obtain an estimate similar to the one above, but for $|\nabla_q u(t)|^2$. This is possible in view of the following bounds on the commutator: for all $i=1,\dots,d$,

$$
\left|\left[\partial_{q_i},\mathcal{L}\right]u(t)\partial_{q_i}u(t)\right| = |\nabla\left(\partial_{q_i}V\right)\cdot\nabla_p u(t)\partial_{q_i}u(t)|\leqslant|\nabla_p u(t)|^2+C_V^2\,|\partial_{q_i}u(t)|^2\,.
$$

General n.

The remainder of the proof is done by induction of n and relies on the control of the commutators $\left[\partial_q^k,\mathcal{L}\right]$ with $|k|=n$, which are independent of U, as well as

$$
\left|\left[\partial_p^k,\mathcal{L}\right]\psi\right|\leqslant\sum_{\substack{i\in\mathbb{N}^{2d}\\|i|\leqslant n}}\mathcal{P}_i\left|\partial^i\psi\right|,
$$

where $\mathcal{P}_i$ are positive polynomial functions that depend on the polynomial growth of U and its derivatives. These polynomial functions can be controlled with Lyapunov weights for sufficiently large indices. In addition, the same approach as in the proof of Lemma 2.6 is used to estimate the extra term arising from missing positivity of $\nabla^2 U$, namely

$$
\begin{aligned}
&-2\alpha\int_0^T\exp(\zeta t)\left(\int_{\mathcal{E}}\sum_{i=1}^d\sum_{j=1}^d L_{\alpha,i}\left(\partial_q^n u(t)\right)\left[\partial^2_{p_ip_j}\left(U-U_\nu\right)\right]L_{\alpha,j}\left(\partial_q^n u(t)\right)\pi_s\,dq\,dp\right)dt\\
&\quad\leqslant 2(1+\mathscr{G}_s)\alpha\varepsilon_3\left\|\nabla\widetilde{U}\right\|_{L^\infty}\int_0^T\exp(\zeta t)\left(\int_{\mathcal{E}}\left|L_\alpha\left(\partial_q^n u(t)\right)\right|^2\pi_s\,dq\,dp\right)dt\\
&\qquad+\frac{2\alpha}{\varepsilon_3}\left\|\nabla\widetilde{U}\right\|_{L^\infty}\int_0^T\exp(\zeta t)\left(\int_{\mathcal{E}}\left|\nabla_p L_\alpha\left(\partial_q^n u(t)\right)\right|^2\pi_s\,dq\,dp\right)dt.
\end{aligned}
$$

Therefore, the result is obtained when the same condition (2.34) on G_ν is satisfied. Note however that this condition depends on s, hence on n since s has to be larger than some index s_n.

2.5.4 Proof of Proposition 2.1

2.5.4.1 General structure of the proof

We define the AR perturbation function as

$$D_{e_{\min}}(p) := \nabla U_{0,e_{\max}}(p) - \nabla U_{e_{\min},e_{\max}}(p)\,. \tag{2.36}$$

This allows to write the generator $\mathcal{L}_{e_{\min},e_{\max}}$ of the AR-Langevin dynamics (2.5) as a perturbation of the generator $\mathcal{L}_{0,e_{\max}}$:

$$\mathcal{L}_{e_{\min},e_{\max}} = \mathcal{L}_{0,e_{\max}} - D_{e_{\min}}(p)\cdot\tilde{\mathcal{L}}, \qquad \tilde{\mathcal{L}} := \nabla_q - \gamma\nabla_p.$$

For notational convenience we omit the subscript $e_{\max}$ and simply write $\mathcal{L}_{e_{\min}} := \mathcal{L}_{e_{\min},e_{\max}}$. We also denote by $\mu_{e_{\min}}$ the invariant measure associated with $\mathcal{L}_{e_{\min}}$, and by $\Pi_{e_{\min}}$ the projection

$$\Pi_{e_{\min}} f = f - \int_{\mathcal{E}} f\, d\mu_{e_{\min}}.$$

For a given observable $\varphi \in \mathscr{S}$, the asymptotic variance associated with the corresponding time averages reads, in view of (1.48):

$$\sigma^2_\varphi(e_{\min}) = -2\int_{\mathcal{E}} \Phi_{\varphi,e_{\min}}\varphi\, d\mu_{e_{\min}}, \tag{2.37}$$

where $\Phi_{\varphi,e_{\min}} \in \mathscr{S}$ is the unique solution in $L^\infty_{\mathcal{K}_s}$ (s being such that $\varphi \in L^\infty_{\mathcal{K}_s}$) of the following Poisson equation:

$$\mathcal{L}_{e_{\min}}\Phi_{\varphi,e_{\min}} = \Pi_{e_{\min}}\varphi, \qquad \Pi_{e_{\min}}\Phi_{\varphi,e_{\min}} = 0. \tag{2.38}$$

Similarly, the limiting variance for $e_{\min} = 0$ can be rewritten as

$$\sigma^2_\varphi(0) = -2\int_{\mathcal{E}} \Phi_{\varphi,0}\varphi\, d\mu_0, \qquad \mathcal{L}_0\Phi_{\varphi,0} = \Pi_0\varphi, \qquad \Pi_0\Phi_{\varphi,0} = 0. \tag{2.39}$$

In order to prove the convergence of (2.37) to (2.39) and to identify the linear term in $e_{\min}$, the idea is to expand $\mu_{e_{\min}}$ and $\Phi_{\varphi,e_{\min}}$ in powers of $e_{\min}$. To this end, we rewrite the Poisson equation (2.38) as

$$\Pi_0\left(\Pi_0 - \mathcal{L}_0^{-1}\Pi_0 D_{e_{\min}}\cdot\tilde{\mathcal{L}}\right)\Phi_{\varphi,e_{\min}} = \mathcal{L}_0^{-1}\Pi_0\varphi.$$

The operator $\mathcal{L}_0^{-1}\Pi_0 D_{e_{\min}}\cdot\tilde{\mathcal{L}}$ is not bounded (since $\tilde{\mathcal{L}}$ contains derivatives in q, which cannot be controlled by $\mathcal{L}_0$), so that it is not possible to write the inverse of $\Pi_0 - \mathcal{L}_0^{-1}\Pi_0 D_{e_{\min}}\cdot\tilde{\mathcal{L}}$ as some Neumann series. It is however possible to consider a pseudo-inverse operator by truncating the Neumann series at order n. This motivates the introduction of the following approximation of the solution of (2.38):

$$\Phi^n_{\varphi,e_{\min}} := \sum_{k=0}^{n} \left(\mathcal{L}_0^{-1}\Pi_0 D_{e_{\min}} \cdot \tilde{\mathcal{L}}\right)^k \mathcal{L}_0^{-1}\Pi_0\varphi\,.$$

The corresponding approximation of the variance reads

$$\sigma^2_{\varphi,n}(e_{\min}) := -2\int_{\mathcal{E}} \left(\Pi_{e_{\min}}\Phi^n_{\varphi,e_{\min}}\right)\varphi\, d\mu_{e_{\min}}. \tag{2.40}$$

The connection with the exact variance (2.37) is given by the following lemma, which is proved in Section 2.5.4.5. We introduce a critical value $e^*_{\max}$ such that Assumption 2.5 is satisfied for $0 \leqslant e_{\min} \leqslant e_{\max}/2$ and $e_{\max} \leqslant e^*_{\max}$ (see Section 2.5.4.3). This allows to resort to Lemma 2.3.

Lemma 2.7. *Fix $0 < e_{\max} \leqslant e^*_{\max}$. Then, for any $\varphi \in \mathscr{S}$ and for all $n \geqslant 1$, there exists a constant $C_{\varphi,n} > 0$ such that*

$$\forall\, 0 \leqslant e_{\min} \leqslant \frac{e_{\max}}{2}, \qquad \left|\sigma^2_{\varphi}(e_{\min}) - \sigma^2_{\varphi,n}(e_{\min})\right| \leqslant C_{\varphi,n} e^{n+1}_{\min}.$$

The key point in the proof of Lemma 2.7 are the following estimates (see Section 2.5.4.4 for the proof).

Lemma 2.8. *Fix $0 < e_{\max} \leqslant e^*_{\max}$ and $\varphi \in \mathscr{S}$. For any $n \geqslant 1$, there exist $s_n, l_n \in \mathbb{N}$ such that, for any $s \geqslant s_n$, there is $r_n \in \mathbb{N}$ and $\tilde{C}_n > 0$ for which*

$$\forall\, 0 \leqslant e_{\min} \leqslant \frac{e_{\max}}{2}, \qquad \left\|\left(\mathcal{L}_0^{-1}\Pi_0 D_{e_{\min}} \cdot \tilde{\mathcal{L}}\right)^n \Pi_0\varphi\right\|_{L^\infty_{\mathcal{K}_s}} \leqslant \tilde{C}_n e^n_{\min} \left\|\varphi\right\|_{W^{l_n,\infty}_{\mathcal{K}_{r_n}}}.$$

Proposition 2.1 now straightforwardly follows by combining Lemma 2.7 and the following expansion in powers of $e_{\min}$ of the truncated variance (whose proof can be read in Section 2.5.4.6).

Proposition 2.2. *Fix $0 < e_{\max} \leqslant e^*_{\max}$. There exists a constant $\mathscr{K} \in \mathbb{R}$ such that, for any $n \geqslant 1$ and $0 \leqslant e_{\min} \leqslant e_{\max}/2$ sufficiently small,*

$$\sigma^2_{\varphi,n}(e_{\min}) = \sigma^2_{\varphi}(0) + \mathscr{K}\, e_{\min} + \mathrm{O}(e^2_{\min}).$$

2.5.4.2 Technical results on expansions with respect to $e_{\min}$

Recall that the function $f_{0,e_{\max}}$ (with $f_{0,e_{\max}}$ defined in (2.14)) belongs to $C^\infty(\mathbb{R},[0,1])$. The next result shows that the same is true for

$$f_{e_{\min},e_{\max}} = f_{0,e_{\max}} \circ \theta_{e_{\min}},$$

with $\theta_{e_{\min}}$ defined in (2.15). This is not obvious a priori since $\theta_{e_{\min}}$ is only piecewise C^∞, with singularities on the first order derivative at $e_{\min}$ and $e_{\max}$. In fact, it can even be proved that $f_{e_{\min},e_{\max}} - f_{0,e_{\max}}$ and all its derivatives are small when $e_{\min}$ is small.

Lemma 2.9. *For any $0 \leqslant e_{\min} < e_{\max}$, the function $f_{e_{\min},e_{\max}}$ belongs to $C^\infty(\mathbb{R},[0,1])$. Moreover, its derivatives have a compact support in $[0,e_{\max}]$. Finally, for any $n_0 \in \mathbb{N}$ and $\delta > 0$, there exists a constant $C_{n_0,e_{\max},\delta} > 0$ such that*

$$\forall\, 0 \leqslant n \leqslant n_0, \quad \forall\, e_{\min} \in [0, e_{\max} - \delta], \qquad \left\| f^{(n)}_{e_{\min},e_{\max}} - f^{(n)}_{0,e_{\max}} \right\|_{L^\infty} \leqslant C_{n_0,e_{\max},\delta} e_{\min}. \tag{2.41}$$

Proof. The function $\theta_{e_{\min}}$ is defined piecewise on three intervals $[0,e_{\min})$, $(e_{\min},e_{\max})$ and $(e_{\max},+\infty)$. In the interior of each interval, both $f_{0,e_{\max}}$ and $\theta_{e_{\min}}$ are C^∞, and so is therefore their composition. In addition, $f_{e_{\min},e_{\max}}$ is constant on $(e_{\max},+\infty)$, hence all derivatives vanish on this interval. To prove that $f_{e_{\min},e_{\max}}$ is C^∞ with derivatives of compact support, it therefore suffices to prove that all derivatives can be extended by continuity at the points $e_{\min}$ and $e_{\max}$.

Since $f_{0,e_{\max}}$ is constant outside the interval $[e_{\min},e_{\max}]$, a simple computation shows that, for $n \geqslant 1$,

$$\left(f_{0,e_{\max}} \circ \theta_{e_{\min}}\right)^{(n)}(x) = \begin{cases} 0 & \text{for } 0 \leqslant x < e_{\min}, \\ \left(\dfrac{e_{\max}}{e_{\max}-e_{\min}}\right)^n f^{(n)}_{0,e_{\max}}(\theta_{e_{\min}}(x)) & \text{for } e_{\min} < x < e_{\max}, \\ 0 & \text{for } x > e_{\max}. \end{cases} \tag{2.42}$$

It is therefore obvious to check the continuity at $e_{\min}$ and $e_{\max}$ since all derivatives of $f_{0,e_{\max}}$ vanish at 0 and $e_{\max}$, and $\theta_{e_{\min}}(e_{\min}) = 0$ while $\theta_{e_{\min}}(e_{\max}) = e_{\max}$.

Moreover, it is easy to check that $|\theta_{e_{\min}}(x) - x| \leqslant e_{\min}$, so that the estimate (2.41) already follows in the case $n = 0$ since $f_{0,e_{\max}}$ is Lipschitz continuous. To obtain the same result for higher order derivatives, we note that the n-th order derivative can be rewritten as

$$f^{(n)}_{e_{\min},e_{\max}} = f^{(n)}_{0,e_{\max}} \circ \theta_{e_{\min}} + f^{(n)}_{0,e_{\max}} \circ \theta_{e_{\min}} \left(\left[\left(\frac{e_{\max}}{e_{\max}-e_{\min}} \right)^n - 1 \right] \mathbb{1}_{[e_{\min},e_{\max}]} \right).$$

Therefore, $f^{(n)}_{e_{\min},e_{\max}} - f^{(n)}_{0,e_{\max}}$ is the sum of (i) $f^{(n)}_{0,e_{\max}}(\theta_{e_{\min}}) - f^{(n)}_{0,e_{\max}}$, which is of order $e_{\min}$ in L^∞ norm by the same argument as before since $f^{(n)}_{0,e_{\max}}$ is Lipschitz continuous; and (ii) a remainder term of order $e_{\min}$ since $f^{(n)}_{0,e_{\max}} \circ \theta_{e_{\min}}$ is uniformly bounded; while for any $0 < \delta < e_{\max}$ there exists $R_{n,\delta} > 0$ such that

$$\forall\, e_{\min} \in [0, e_{\max} - \delta], \qquad \left| \left(\frac{e_{\max}}{e_{\max}-e_{\min}} \right)^n - 1 \right| \leqslant R_{n,\delta} e_{\min}\,.$$

This allows to obtain the desired result.

In view of the definition (2.16)-(2.17) of $U_{e_{\min},e_{\max}}(p) = \sum_{i=1}^N u_{e_{\min},e_{\max}}(p_i)$, we can deduce the following estimates on $U_{e_{\min},e_{\max}} - U_{0,e_{\max}}$ and its derivatives, which allow in particular to control $D_{e_{\min}}$. To state the result, we introduce

$$\mathscr{C}_K := \left\{ p \in \mathbb{R}^d \;\middle|\; \forall i = 1, \dots N,\ \frac{p_i^2}{2m_i} \leqslant K \right\} .$$

Corollary 2.2. *For any $0 \leqslant e_{\min} < e_{\max}$, the function $U_{e_{\min},e_{\max}}$ belongs to C^∞. For any $n \geqslant 0$ and $|\alpha| = n$, the function $\partial^\alpha \left(U_{e_{\min},e_{\max}} - U_{0,e_{\max}} \right)$ has a compact support in $\mathscr{C}_{e_{\max}}$. Moreover, for any $n_0 \geqslant 0$ and $\delta > 0$, there exists a constant $C_{n_0,\delta,e_{\max}} > 0$ such that*

$$\forall\, |\alpha| \leqslant n_0,\ \forall\, e_{\min} \in [0, e_{\max} - \delta], \quad \left\| \partial^\alpha U_{e_{\min},e_{\max}} - \partial^\alpha U_{0,e_{\max}} \right\|_{L^\infty} \leqslant C_{n_0,\delta,e_{\max}} e_{\min} . \tag{2.43}$$

In order to obtain more precise statements about the behavior of the functions $f_{e_{\min},e_{\max}}(x)$ for small values of $e_{\min}$, a natural idea would be to perform Taylor expansions with respect to this parameter. The difficulty is however that the derivatives with respect to $e_{\min}$ of the shift function $\theta_{e_{\min}}(x)$ are not continuous in x. This prevents to write directly remainders of order $e_{\min}^2$. Before stating the precise result in Lemma 2.11, we need another technical ingredient.

Lemma 2.10. *Fix $e_{\max} > 0$ and define $\tilde{\tau}(x) := \dfrac{x - e_{\max}}{e_{\max}}$. Then, for any $n \geqslant 0$ and $\delta > 0$, there exists $C_{n,\delta} > 0$ such that*

$$\forall\, e_{\min} \in [0, e_{\max} - \delta], \qquad \left\| \frac{f^{(n)}_{0,e_{\max}} \circ \theta_{e_{\min}} - f^{(n)}_{0,e_{\max}}}{e_{\min}} - f^{(n+1)}_{0,e_{\max}} \circ \tilde{\tau} \right\|_{L^\infty} \leqslant C_{n,\delta}\, e_{\min} . \tag{2.44}$$

Proof. Note that, formally, $\tilde{\tau}$ is the derivative of $\theta_{e_{\min}}$ on $[e_{\min}, e_{\max}]$ with respect to $e_{\min}$, evaluated at $e_{\min} = 0$. Recall also $|\theta_{e_{\min}}(x) - x| \leqslant e_{\min}$. Simple computations show that there exists $C_\delta > 0$ such that

$$\forall x \in \mathbb{R}^+, \qquad \left| \frac{\theta_{e_{\min}}(x) - x}{e_{\min}} - \tilde{\tau}(x) \right| \leqslant C_\delta e_{\min} .$$

Since $f_{0,e_{\min}} \in C^\infty$, there exists $t \in [0,1]$ such that

$$f^{(n)}_{0,e_{\max}}\big(\theta_{e_{\min}}(x)\big) - f^{(n)}_{0,e_{\max}}(x) = f^{(n+1)}_{0,e_{\max}}\Big(x + t\big(\theta_{e_{\min}}(x) - x\big)\Big)\big(\theta_{e_{\min}}(x) - x\big) . \tag{2.45}$$

Therefore, for $x \in [0, e_{\max}]$,

$$
\begin{aligned}
&\left| \frac{f^{(n)}_{0,e_{\max}}\left(\theta_{e_{\min}}(x)\right) - f^{(n)}_{0,e_{\max}}(x)}{e_{\min}} - f^{(n+1)}_{0,e_{\max}}(x)\tilde{\tau}(x) \right| \\
&= \left| f^{(n+1)}_{0,e_{\max}}\Big(x + t\big(\theta_{e_{\min}}(x) - x\big)\Big) \frac{\theta_{e_{\min}}(x) - x}{e_{\min}} - f^{(n+1)}_{0,e_{\max}}(x)\tilde{\tau}(x) \right| \\
&\leqslant \left| f^{(n+1)}_{0,e_{\max}}\Big(x + t\big(\theta_{e_{\min}}(x) - x\big)\Big) - f^{(n+1)}_{0,e_{\max}}(x) \right| \left| \frac{\theta_{e_{\min}}(x) - x}{e_{\min}} \right| + \left| f^{(n+1)}_{0,e_{\max}}(x) \right| \left| \frac{\theta_{e_{\min}}(x) - x}{e_{\min}} - \tilde{\tau}(x) \right| \\
&\leqslant \left(\left\| f^{(n+2)}_{0,e_{\max}} \right\|_{L^\infty([0,e_{\max}])} + C_\delta \left\| f^{(n+1)}_{0,e_{\max}} \right\|_{L^\infty([0,e_{\max}])} \right) e_{\min},
\end{aligned}
\tag{2.46}
$$

where we have used the following equality: there exists $\alpha \in [0,1]$ such that

$$
f^{(n+1)}_{0,e_{\max}}\Big(x + t\big(\theta_{e_{\min}}(x) - x\big)\Big) - f^{(n+1)}_{0,e_{\max}}(x) = t\, f^{(n+2)}_{0,e_{\max}}\Big(x + \alpha\big(\theta_{e_{\min}}(x) - x\big)\Big)\big(\theta_{e_{\min}}(x) - x\big),
$$

together with the bound $|\theta_{e_{\min}}(x) - x| \leqslant e_{\min}$.

Lemma 2.11. *Fix $e_{\max} > 0$. There exist functions $\mathscr{D}_i \in C^\infty(\mathbb{R}^d)$ (for $i = 1, \dots, N$), with compact support in $\mathscr{C}_{e_{\max}}$, such that, for $0 < \delta < e_{\max}$ and $r \in \mathbb{N}$, there is $C_{r,\delta} > 0$ such that*

$$
e_{\min} \in [0, e_{\max} - \delta], \quad \|D_{e_{\min},i} - e_{\min}\mathscr{D}_i\|_{W^{r,\infty}} \leqslant C_{r,\delta} e^2_{\min}. \tag{2.47}
$$

Proof. Recall that the functions $D_{e_{\min},i} : \mathbb{R}^D \to \mathbb{R}^D$ are defined, for $i = 1, \dots, N$, as

$$
\begin{aligned}
D_{e_{\min},i}(p) = &\left[f_{e_{\min},e_{\max}}\left(\frac{|p_i|^2}{2m_i}\right) - f_{0,e_{\max}}\left(\frac{|p_i|^2}{2m_i}\right) \right] \frac{p_i}{m_i} \\
&+ \frac{|p_i|^2}{2m_i} \left[f'_{e_{\min},e_{\max}}\left(\frac{|p_i|^2}{2m_i}\right) - f'_{0,e_{\max}}\left(\frac{|p_i|^2}{2m_i}\right) \right] \frac{p_i}{m_i}.
\end{aligned}
$$

We next define, for $i = 1, \dots, N$, the function

$$
\mathscr{D}_i(p) := \begin{cases} \left[f'_{0,e_{\max}}\left(\dfrac{|p_i|^2}{2m_i}\right) + \dfrac{|p_i|^2}{2m_i} f''_{0,e_{\max}}\left(\dfrac{|p_i|^2}{2m_i}\right) \right] \tilde{\tau}\left(\dfrac{|p_i|^2}{2m_i}\right) \dfrac{p_i}{m_i}, & \text{for } \dfrac{|p_i|^2}{2m_i} \in [0, e_{\max}], \\ 0, & \text{for } \dfrac{|p_i|^2}{2m_i} \geqslant e_{\max}, \end{cases}
$$

where $\tilde{\tau}$ is defined in Lemma 2.10. Recall that $f_{0,e_{\max}} \in C^\infty$ and $f^{(n)}_{0,e_{\max}}$ have compact support on $[0, e_{\max}]$ for $n \geqslant 1$. Therefore, $\mathscr{D}_i \in C^\infty$ also has compact support in $\mathscr{C}_{e_{\max}}$.

The case $r = 0$ of (2.47) follows directly from Lemma 2.10 with $n = 0$ and $n = 1$. Let us now consider the case $r = 1$ more carefully. To simplify the presentation, we consider separately the two terms in the sums defining the functions $D_{e_{\min},i}$ and $\mathscr{D}_i$, *i.e.* $D_{e_{\min},i} = D_{e_{\min},i,1} + D_{e_{\min},i,2}$ and $\mathscr{D}_i = \mathscr{D}_{i,1} + \mathscr{D}_{i,2}$ with

$$D_{e_{\min},i,1}(p) = \left[f_{e_{\min},e_{\max}}\left(\frac{|p_i|^2}{2m_i}\right) - f_{0,e_{\max}}\left(\frac{|p_i|^2}{2m_i}\right)\right]\frac{p_i}{m_i},$$

and

$$\mathscr{D}_{i,1}(p) := \begin{cases} f'_{0,e_{\max}}\left(\frac{|p_i|^2}{2m_i}\right)\tilde{\tau}\left(\frac{|p_i|^2}{2m_i}\right)\frac{p_i}{m_i}, & \text{for } \frac{|p_i|^2}{2m_i} \in [0, e_{\max}], \\ 0, & \text{for } \frac{|p_i|^2}{2m_i} \geqslant e_{\max}. \end{cases}$$

We present the estimates only for the difference $D_{e_{\min},i,1}/e_{\min} - \mathscr{D}_{i,1}$ since similar computations allows to control the difference $D_{e_{\min},i,2}/e_{\min} - \mathscr{D}_{i,2}$. For $\alpha, \alpha' \in \{1, \dots, D\}$, we denote by $p_{i,\alpha}$ the αth component of the momentum of the ith particle and by $D_{e_{\min},i,1,\alpha'}$ and $\mathscr{D}_{i,1,\alpha'}$ the α'th components of $D_{e_{\min},i,1}$ and $\mathscr{D}_{i,1}$. Then, for $p_i \in \mathscr{C}_{e_{\max}}$,

$$\begin{aligned}
&\left|\partial_{p_{i,\alpha}}\left(\frac{D_{e_{\min},i,1,\alpha'}}{e_{\min}} - \mathscr{D}_{i,1,\alpha'}\right)(p)\right| = \\
&\leqslant \frac{\delta_{\alpha,\alpha'}}{m_i}\left|\frac{f_{0,e_{\max}}\circ\theta_{e_{\min}}\left(\frac{|p_i|^2}{2m_i}\right) - f_{0,e_{\max}}\left(\frac{|p_i|^2}{2m_i}\right)}{e_{\min}} - f'_{0,e_{\max}}\left(\frac{|p_i|^2}{2m_i}\right)\tilde{\tau}\left(\frac{|p_i|^2}{2m_i}\right)\right| \\
&+ \frac{|p_{i,\alpha}p_{i,\alpha'}|}{m_i^2}\left|\frac{f'_{0,e_{\max}}\circ\theta_{e_{\min}}\left(\frac{|p_i|^2}{2m_i}\right)\theta'_{e_{\min}}\left(\frac{|p_i|^2}{2m_i}\right) - f'_{0,e_{\max}}\left(\frac{|p_i|^2}{2m_i}\right)}{e_{\min}}\right| \\
&+ \frac{|p_{i,\alpha}p_{i,\alpha'}|}{m_i^2}\left|f''_{0,e_{\max}}\left(\frac{|p_i|^2}{2m_i}\right)\tilde{\tau}\left(\frac{|p_i|^2}{2m_i}\right) - f'_{0,e_{\max}}\left(\frac{|p_i|^2}{2m_i}\right)\frac{1}{e_{\max}}\right| \\
&\leqslant \frac{\delta_{\alpha,\alpha'}}{m_i}\left|\frac{f_{0,e_{\max}}\circ\theta_{e_{\min}}\left(\frac{|p_i|^2}{2m_i}\right) - f_{0,e_{\max}}\left(\frac{|p_i|^2}{2m_i}\right)}{e_{\min}} - f'_{0,e_{\max}}\left(\frac{|p_i|^2}{2m_i}\right)\tilde{\tau}\left(\frac{|p_i|^2}{2m_i}\right)\right| \\
&\quad + \frac{|p_{i,\alpha}p_{i,\alpha'}|}{m_i^2}\left|\frac{f'_{0,e_{\max}}\circ\theta_{e_{\min}}\left(\frac{|p_i|^2}{2m_i}\right) - f'_{0,e_{\max}}\left(\frac{|p_i|^2}{2m_i}\right)}{e_{\min}} - f''_{0,e_{\max}}\left(\frac{|p_i|^2}{2m_i}\right)\tilde{\tau}\left(\frac{|p_i|^2}{2m_i}\right)\right| \\
&\quad + \frac{|p_{i,\alpha}p_{i,\alpha'}|}{m_i^2}\left|\left[f'_{0,e_{\max}}\circ\theta_{e_{\min}}\left(\frac{|p_i|^2}{2m_i}\right) - f'_{0,e_{\max}}\left(\frac{|p_i|^2}{2m_i}\right)\right]\frac{\theta'_{e_{\min}}\left(\frac{|p_i|^2}{2m_i}\right) - 1}{e_{\min}}\right| \\
&\quad + \frac{|p_{i,\alpha}p_{i,\alpha'}|}{m_i^2}\left|f'_{0,e_{\max}}\left(\frac{|p_i|^2}{2m_i}\right)\left[\frac{\theta'_{e_{\min}}\left(\frac{|p_i|^2}{2m_i}\right) - 1}{e_{\min}} - \frac{1}{e_{\max}}\right]\right|,
\end{aligned}$$

where we used $\tilde{\tau}'(x) = 1/e_{\max}$ for $x \in [0, e_{\max}]$. The first two terms in the last inequality can be bounded by $C^* e_{\min}$ for some constant $C^* \in \mathbb{R}_+$ in view of Lemma 2.10. For the last two terms, distinguish the cases $p_i \in \mathscr{C}_{i,e_{\min}}$ and $p_i \in \mathscr{C}_{i,e_{\max}} \backslash \mathscr{C}_{i,e_{\min}}$, where for $K \geqslant 0$ we define

$$\mathscr{C}_{i,K} := \left\{ p_i \in \mathbb{R}^D \;\middle|\; \frac{|p_i|^2}{2m_i} \leqslant K \right\}.$$

When $p_i \in \mathscr{C}_{i,e_{\min}}$, the third term disappears since $\theta'_{e_{\min}}(x) = 1$ on $[0, e_{\min}]$. In addition,

$$\sup_{p_i \in \mathscr{C}_{i,e_{\min}}} \frac{|p_i|^2}{m_i^2} \leqslant \frac{2e_{\min}}{m_i},$$

so that

$$\left\| \partial_{p_{i,\alpha}} \left(\frac{D_{e_{\min},i,1,\alpha'}}{e_{\min}} - \mathscr{D}_{i,1,\alpha'} \right) \right\|_{L^\infty\left(\mathscr{C}_{i,e_{\min}}\right)} \leqslant \left(C^* + \frac{2}{m_i e_{\max}} \left\| f'_{0,e_{\max}} \right\|_{L^\infty([0,e_{\min}])} \right) e_{\min} .$$

When $p_i \in \mathscr{C}_{i,e_{\max}} \backslash \mathscr{C}_{i,e_{\min}}$, we use $\theta'_{e_{\min}}(x) = e_{\max}/(e_{\max} - e_{\min})$ for $x \in [e_{\min}, e_{\max}]$, so that there exists $C_\delta > 0$ such that

$$\sup_{x \in [e_{\min}, e_{\max}]} \left| \frac{\theta'_{e_{\min}}(x) - 1}{e_{\min}} - \frac{1}{e_{\max}} \right| \leqslant C_\delta e_{\min}, \qquad \sup_{x \in [e_{\min}, e_{\max}]} \left| \theta'_{e_{\min}}(x) - 1 \right| \leqslant \frac{1}{e_{\max} - e_{\min}} \leqslant \frac{1}{\delta} . \tag{2.48}$$

Using these bounds as well as the inequality $|\theta_{e_{\min}}(x) - x| \leqslant e_{\min}$ and (2.45) for $n = 1$, it follows

$$\left\| \partial_{p_{i,\alpha}} \left(\frac{D_{e_{\min},i,1,\alpha'}}{e_{\min}} - \mathscr{D}_{i,1,\alpha'} \right) \right\|_{L^\infty(\mathscr{C}_{i,e_{\max}})} \leqslant \left(C^* + \frac{2e_{\max}}{m_i \delta} \left\| f''_{0,e_{\max}} \right\|_{L^\infty} + C_\delta \left\| f'_{0,e_{\max}} \right\| \right) e_{\min} .$$

This concludes the proof of (2.47) for $r = 1$.

Bounds on higher order derivatives are obtained in a similar fashion, relying on the fact that $\partial_x^2 \theta_{e_{\min}}(x) = 0$ except at the singularity points $e_{\min}, e_{\max}$ as well as $\partial_x^2 \tilde{\tau}(x) = 0$ for $x \neq e_{\max}$.

We end this section with a last technical result.

Lemma 2.12. *Fix $e_{\max} > 0$. Then for any $f \in L^1(\mu_0)$, there exist $a_f \in \mathbb{R}$ such that, for $0 < \delta < e_{\max}$,*

$$\begin{aligned} &\forall e_{\min} \in [0, e_{\max} - \delta] , \\ &\int_{\mathbb{R}^d} f(p) \, \mathrm{e}^{-\beta U_{e_{\min}}(p)} dp = \int_{\mathbb{R}^d} f(p) \, \mathrm{e}^{-\beta U_0(p)} dp + a_f e_{\min} + \mathrm{O}\left(e_{\min}^2\right) . \end{aligned} \tag{2.49}$$

Proof. Recall that $U_{e_{\min}}(p) = \sum_{i=1}^N u_{e_{\min},e_{\max}}(p_i)$. Note that

$$u_{e_{\min},e_{\max}}(p_i) - u_{0,e_{\max}}(p_i) = \frac{p_i^2}{2m_i} \left[f_{0,e_{\max}}\left(\frac{p_i^2}{2m_i}\right) - f_{e_{\min},e_{\max}}\left(\frac{p_i^2}{2m_i}\right) \right] .$$

Manipulations similar to the ones used to prove (2.47) allow to show that there exists a function $\mathcal{U} \in C^\infty$ with compact support in $\mathscr{C}_{e_{\max}}$ such that, for $0 < \delta < e_{\max}$ and $r \in \mathbb{N}$, there is $C_{r,\delta} > 0$ for which

$$e_{\min} \in [0, e_{\max} - \delta] , \quad \left\| U_{e_{\min}} - U_0 - e_{\min} \mathcal{U} \right\|_{W^{r,\infty}} \leqslant C_{r,\delta} e_{\min}^2 . \tag{2.50}$$

This allows to write

$$U_{e_{\min}} = U_0 + e_{\min}\mathcal{U} + e_{\min}^2 \widetilde{\mathcal{U}}_{e_{\min}},$$

with $\widetilde{\mathcal{U}}_{e_{\min}}$ uniformly bounded in L^∞. Moreover since $U_{e_{\min}} - U_0 \in C^\infty$ also has a compact support, we easily obtain

$$\frac{\mathrm{e}^{-\beta U_{e_{\min}}} - \mathrm{e}^{-\beta U_0}}{e_{\min}} = \mathrm{e}^{-\beta U_0} \frac{\mathrm{e}^{-\beta e_{\min}\left(\mathcal{U} + e_{\min}\widetilde{\mathcal{U}}_{e_{\min}}\right)} - 1}{e_{\min}} = -\beta \mathcal{U}\, \mathrm{e}^{-\beta U_0} + e_{\min}\, \widehat{\mathcal{U}}_{e_{\min}}\, \mathrm{e}^{-\beta U_0},$$

with $\widehat{\mathcal{U}}_{e_{\min}}$ uniformly bounded in L^∞. Therefore, there exists a constant $R > 0$ such that

$$\left| \frac{\displaystyle\int_{\mathbb{R}^d} f \mathrm{e}^{-\beta U_{e_{\min}}} dp - \int_{\mathbb{R}^d} f \mathrm{e}^{-\beta U_0} dp}{e_{\min}} + \beta \int_{\mathbb{R}^d} f\, \mathcal{U}\, \mathrm{e}^{-\beta U_0} dp \right| \leqslant R e_{\min}\,,$$

so that (2.49) follows with $a_f := -\beta \displaystyle\int_{\mathbb{R}^d} \mathcal{U} f\, \mathrm{e}^{-\beta U_0}\, dp$.

2.5.4.3 Verification of Assumption 2.5

In order to use Lemma 2.3, we need to check that Assumption 2.5 holds with G_ν as small as wanted for appropriate values of $e_{\min}, e_{\max}$. The first condition (2.8) is easy to check, so we concentrate on the last two conditions. The reference kinetic energy function U_ν in Lemma 2.3 is chosen as the standard kinetic energy $U_{\mathrm{std}}(p) = p^T M^{-1} p/2$, so that $\nu = 1/\min_{i=1,\dots,N}$. It therefore remains to check the last condition. An inspection of the proof of Lemma 2.3 reveals that it holds provided $e_{\min}, e_{\max}$ are such that (2.34) holds. Straightforward computations show that

$$\nabla_{p_i}\left(U_{e_{\min}} - U_{\mathrm{std}}\right) = \frac{p_i}{m_i}\left[1 - f_{e_{\min},e_{\max}}\left(\frac{p_i^2}{m_i}\right)\right] - \frac{p_i |p_i|^2}{m_i^2} f'_{e_{\min},e_{\max}}\left(\frac{p_i^2}{m_i}\right),$$

so that, using the fact that $U_{e_{\min},e_{\max}} - U_{\mathrm{std}}$ has compact support in $\mathscr{C}_{e_{\max}}$ (hence $|p_i| \leqslant \sqrt{2 m_i e_{\max}}$) and in view of the expression (2.42) of $f'_{e_{\min},e_{\max}}$, the following bound holds:

$$\left\|\nabla_{p_i}\left(U_{e_{\min},e_{\max}} - U_{\mathrm{std}}\right)\right\|_{L^\infty} \leqslant \sqrt{\frac{2e_{\max}}{m_i}} + \sqrt{\frac{8e_{\max}^3}{m_i}}\, \frac{e_{\max}}{e_{\max} - e_{\min}} \left\|f'_{0,e_{\max}}\right\|_{L^\infty}.$$

Similarly, there exists a constant $C > 0$ (depending on $f'_{0,e_{\max}}$, $f''_{0,e_{\max}}$ and $m_1, \dots, m_N$) such that

$$\left\|\Delta U_{e_{\min},e_{\max}}\right\|_{L^\infty} \leqslant C\left[1 + \left(\frac{e_{\max}^2}{e_{\max} - e_{\min}}\right)^2\right].$$

It is then easy to see that (2.34) holds upon choosing $0 < e_{\min} \leqslant e_{\max}/2$ with $e_{\max} > 0$ sufficiently small.

2.5.4.4 Proof of Lemma 2.8

Denote by $\mathcal{A}$ the operator $\mathcal{L}_0^{-1}\Pi_0\left(D_{e_{\min}}\cdot\tilde{\mathcal{L}}\right)$. By Corollary 2.2, for any $n\geqslant 0$ and $0\leqslant e_{\min}\leqslant e_{\max}/2$, there exists a constant $R_n>0$ such that

$$\forall\,|\alpha|\leqslant n,\qquad \left\|\partial_p^\alpha D_{e_{\min}}\right\|_{L^\infty}\leqslant R_n\,e_{\min}.$$

By the resolvent estimate (2.7), there exists for any $s\in\mathbb{N}^*$ a constant $C_s>0$ such that

$$\forall f\in\widetilde{L^\infty_{\mathcal{K}_s}},\qquad \left\|\mathcal{L}_0^{-1}f\right\|_{L^\infty_{\mathcal{K}_s}}\leqslant C_s\,\|f\|_{L^\infty_{\mathcal{K}_s}}\,.$$

Therefore, choosing an integer s for which $\varphi\in W^{1,\infty}_{\mathcal{K}_s}$, there exists a constant $C>0$ such that

$$\|\mathcal{A}\left(\Pi_0\varphi\right)\|_{L^\infty_{\mathcal{K}_s}}\leqslant C_s\left\|D_{e_{\min}}\cdot\tilde{\mathcal{L}}\left(\Pi_0\varphi\right)\right\|_{L^\infty_{\mathcal{K}_s}}\leqslant C\,\|D_{e_{\min}}\|_{L^\infty}\,\|\varphi\|_{W^{1,\infty}_{\mathcal{K}_s}}\leqslant CR_0\,e_{\min}\,\|\varphi\|_{W^{1,\infty}_{\mathcal{K}_s}}\,.$$

By the same principle, using the fact that, by (2.47), there is for any $r\geqslant 0$ a constant $C_r>0$ such that

$$\|D_{e_{\min}}\|_{W^{r,\infty}}\leqslant C_r e_{\min},$$

and in view of (2.13), there exist, for any $l\geqslant 0$, integers $\alpha\geqslant l$ and $s_l\in\mathbb{N}$ such that, for all $s\geqslant s_l$, there is a constant $C>0$ and an integer $r\in\mathbb{N}$ for which

$$\|\mathcal{A}\left(\Pi_0\varphi\right)\|_{W^{l,\infty}_{\mathcal{K}_s}}\leqslant Ce_{\min}\,\|\varphi\|_{W^{\alpha,\infty}_{\mathcal{K}_r}}\,.$$

By recurrence, there exist, for any $n\geqslant 1$, integers $s_n,l_n\geqslant 0$ such that, for all $s\geqslant s_n$, there is $r\in\mathbb{N}$ and $\widetilde{C}>0$ for which

$$\|\mathcal{A}^n\left(\Pi_0\varphi\right)\|_{L^\infty_{\mathcal{K}_s}}\leqslant\widetilde{C}e_{\min}^n\,\|\varphi\|_{W^{l_n,\infty}_{\mathcal{K}_r}}\,.$$

This gives the claimed result.

2.5.4.5 Proof of Lemma 2.7

We start by writing the difference between the variance (2.37) and the truncated one (2.40):

$$\sigma^2_\varphi(e_{\min})-\sigma^2_{\varphi,n}(e_{\min})=-2\int\left(\Phi_{\varphi,e_{\min}}-\Pi_{e_{\min}}\Phi^n_{\varphi,e_{\min}}\right)\varphi\,d\mu_{e_{\min}}\,. \tag{2.51}$$

A simple computation gives

$$\begin{aligned}&\Pi_{e_{\min}}\mathcal{L}_{e_{\min}}\left(\Phi_{\varphi,e_{\min}}-\Phi^n_{\varphi,e_{\min}}\right)\\&=-\Pi_{e_{\min}}\left(D_{e_{\min}}\cdot\tilde{\mathcal{L}}\right)\left(\mathcal{L}_0^{-1}\Pi_0 D_{e_{\min}}\cdot\tilde{\mathcal{L}}\right)^n\mathcal{L}_0^{-1}\Pi_0\varphi\,.\end{aligned} \tag{2.52}$$

We first use Lemma 2.8: there exist $s_n, l_n \in \mathbb{N}$ such that, for $s \geqslant s_n$, there is $r_n \in \mathbb{N}$ and $C > 0$ such that

$$\left\| \left(\mathcal{L}_0^{-1} \Pi_0 D_{e_{\min}} \cdot \tilde{\mathcal{L}} \right)^n \mathcal{L}_0^{-1} \Pi_0 \varphi \right\|_{W^{1,\infty}_{\mathcal{K}_s}} \leqslant C e_{\min}^n \left\| \varphi \right\|_{W^{l_n,\infty}_{\mathcal{K}_{r_n}}} .$$

Therefore, using (2.43) and (2.52), there exists some constant $R_n > 0$ such that

$$\left\| \Pi_{e_{\min}} \mathcal{L}_{e_{\min}} \left(\Phi_{\varphi,e_{\min}} - \Phi^n_{\varphi,e_{\min}} \right) \right\|_{L^\infty_{\mathcal{K}_s}} \leqslant R_n e_{\min}^{n+1} \left\| \varphi \right\|_{W^{l_n,\infty}_{\mathcal{K}_{r_n}}} .$$

We finally apply $\mathcal{L}^{-1}_{e_{\min}}$ to both sides of (2.52): in view of (2.12), it follows

$$\left\| \Pi_{e_{\min}} \left(\Phi_{\varphi,e_{\min}} - \Phi^n_{\varphi,e_{\min}} \right) \right\|_{L^\infty_{\mathcal{K}_s}} \leqslant \frac{R_n C_s}{\lambda_s} e_{\min}^{n+1} \left\| \varphi \right\|_{W^{l_n,\infty}_{\mathcal{K}_{r_n}}} .$$

The result is then a direct consequence of the equality (2.51).

2.5.4.6 Proof of Proposition 2.2

Looking at (2.40), there are three objects which depend on the parameter $e_{\min}$: the projection $\Pi_{e_{\min}}$, the truncated solution of the Poisson equation $\Phi^n_{\varphi,e_{\min}}$ and the modified measure $\mu_{e_{\min}}$.

We first expand $\Phi^n_{\varphi,e_{\min}}$ in terms of $\Phi_{\varphi,0}$ as

$$\begin{aligned}
\Phi^n_{\varphi,e_{\min}} &= \mathcal{L}_0^{-1} \Pi_0 \varphi + \left(\mathcal{L}_0^{-1} \Pi_0 D_{e_{\min}} \cdot \tilde{\mathcal{L}} \right) \mathcal{L}_0^{-1} \Pi_0 \varphi + \sum_{k=2}^{n} \left(\mathcal{L}_0^{-1} \Pi_0 D_{e_{\min}} \cdot \tilde{\mathcal{L}} \right)^k \mathcal{L}_0^{-1} \Pi_0 \varphi \\
&= \Phi_{\varphi,0} + \left(\mathcal{L}_0^{-1} \Pi_0 D_{e_{\min}} \cdot \tilde{\mathcal{L}} \right) \Phi_{\varphi,0} + \sum_{k=2}^{n} \left(\mathcal{L}_0^{-1} \Pi_0 D_{e_{\min}} \cdot \tilde{\mathcal{L}} \right)^k \Phi_{\varphi,0} .
\end{aligned}$$

Estimates on $\Phi_{\varphi,0}$ and its derivatives in terms of φ can be obtained with (2.13). Lemma 2.8 then allows to estimate the higher order terms in the above equality: there exists $s \in \mathbb{N}$ and $C > 0$ such that

$$\left\| \Phi^n_{\varphi,e_{\min}} - \Phi_{\varphi,0} - \left(\mathcal{L}_0^{-1} \Pi_0 D_{e_{\min}} \cdot \tilde{\mathcal{L}} \right) \Phi_{\varphi,0} \right\|_{L^\infty_{\mathcal{K}_s}} \leqslant C\, e_{\min}^2.$$

By combining these estimates with (2.47), we obtain

$$\Phi^n_{\varphi,e_{\min}} = \Phi_{\varphi,0} + e_{\min} \left(\mathcal{L}_0^{-1} \Pi_0 \mathscr{D} \cdot \tilde{\mathcal{L}} \right) \Phi_{\varphi,0} + e_{\min}^2 \mathcal{R}_{e_{\min}}, \tag{2.53}$$

where $\mathcal{R}_{e_{\min}}$ is uniformly bounded in $L^\infty_{\mathcal{K}_s}$ due to (2.47) for $e_{\min}$ small enough (upon possibly increasing s).

With the notation of Lemma 2.12, for any $f \in L^1(\mu_0)$,

$$\int_{\mathcal{E}} f \, d\mu_{e_{\min}} = \frac{\displaystyle\int_{\mathcal{E}} f \mathrm{e}^{-\beta U_{e_{\min}}}}{\displaystyle\int_{\mathcal{E}} \mathrm{e}^{-\beta U_{e_{\min}}}} = \int_{\mathcal{E}} f \, d\mu_0 + \frac{a_f - a_1 \displaystyle\int_{\mathcal{E}} f \, d\mu_0}{\displaystyle\int_{\mathcal{E}} \mathrm{e}^{-\beta U_0}} \, e_{\min} + \widetilde{\mathscr{R}}_{e_{\min}} e_{\min}^2, \tag{2.54}$$

with $\widetilde{\mathscr{R}}_{e_{\min}}$ uniformly bounded for $e_{\min}$ small enough. Finally, by combining (2.53) and (2.54), we see that there exists $\mathscr{K} \in \mathbb{R}$ such that

$$\sigma^2_{\varphi,n}(e_{\min}) = -2 \int_{\mathcal{E}} \Phi_{\varphi,0}\varphi \, d\mu_0 + \mathscr{K} e_{\min} + \mathrm{O}\left(e^2_{\min}\right). \tag{2.55}$$

3

Stable and accurate schemes for Langevin dynamics with general kinetic energies

Summary. We study Langevin dynamics with a kinetic energy different from the standard, quadratic one in order to accelerate the sampling of the Boltzmann–Gibbs distribution. We consider two cases: kinetic energies which are local perturbations of the standard kinetic energy around the origin, where they vanish (this corresponds to the so-called adaptively restrained Langevin dynamics); and more general non-globally Lipschitz energies. We develop numerical schemes which are stable and of weak order two, by considering splitting strategies where the discretizations of the fluctuation/dissipation are corrected by a Metropolis procedure. We use the newly developed schemes for two applications: optimizing the shape of the kinetic energy for the adaptively restrained Langevin dynamics, and reducing the metastability of some toy models with non-globally Lipschitz kinetic energies that we present in Chapter 5.

The results presented in this chapter are preprinted in [114].

In practice, the Langevin dynamics (2.4) cannot be analytically integrated. Its solution is therefore approximated with a numerical scheme. The numerical analysis of such discretization schemes is by now well-understood when U is the standard quadratic kinetic energy (see Section (1.3.2)).

In this chapter, we consider the discretization of modified Langevin dynamics which improves the sampling of the Boltzmann–Gibbs distribution by introducing a more general kinetic energy function U instead of the standard quadratic one. We have in mind the adaptively restrained Langevin dynamics, although we later apply this approach at the importance sampling strategy in Chapter 5.

The main issue with the situations we consider is the stability of discretized schemes. Several works indicate that explicit discretizations of Langevin-type dynamics with non-globally Lipschitz force fields are often unstable (in the sense that the corresponding Markov chains do not admit invariant measures), see *e.g.* [85]. We face such situations here even for compact position spaces when ∇U is not globally Lipschitz. For adaptively restrained Langevin dynamics, the difficulties arise from the possibly abrupt transition from the region where the kinetic energy vanishes to the region where it coincides with the standard one. Numerical evidence reported in Section 2.4 and Chapter 4 indicates that such a fast transition provides a favorable trade-off between the reduced algorithmic complexity and the increase in the asymptotic variance. Abrupt transitions however lead to large "kinetic" forces $\nabla U(p)$ in some regions and hence limit admissible timesteps. As for the stabilization of the Euler-Maruyama discretization of overdamped Langevin dynamics in [105], we suggest to use a Metropolis acceptance/rejection step [87, 56] in order to ensure the stability of the methods under consideration. Such a stabilization leads to schemes which can be seen as one step Hybrid Monte Carlo (HMC)[1] algorithms [40] with partial refreshment of the momenta, studied for instance in [25] for the standard kinetic energy. Here, in order to obtain a weakly consistent method of order 2 (which is no longer trivial when the fluctuation/dissipation cannot be analytically integrated), we rely on the Metropolis schemes studied in [45].

This chapter is organized as follows. In Section 3.1, which is not contained in [114], we recall possible strategies for the discretization of modified Langevin dynamics (2.4). We describe in Section 3.3 the generalized Hybrid Monte Carlo scheme we consider, and prove that it is weakly consistent of order 2. We next turn to numerical results relying on the stability properties of the Metropolized scheme. Finally, in Section 3.4 we propose, for the AR-Langevin method, a better kinetic energy function than the one originally suggested in [9].

3.1 Discretization of the Langevin dynamics

Throughout this section, we work in a compact position space $\mathcal{D}$. We consider in all this chapter kinetic energies $U \in \mathscr{S}$ and potentials $V \in C^\infty$ which are smooth functions satisfying Assumption 2.1. We denote by

[1] Also called "Hamiltonian Monte-Carlo" in the statistics community.

$$\mathcal{L}_{\mathrm{Ham}} = \nabla U \cdot \nabla_q - \nabla V \cdot \nabla_p, \qquad \mathcal{L}_{\mathrm{FD}} = \gamma \left(-\nabla U \cdot \nabla_p + \frac{1}{\beta} \Delta_p \right), \tag{3.1}$$

such that $\mathcal{L} = \mathcal{L}_{\mathrm{Ham}} + \mathcal{L}_{\mathrm{FD}}$ is the generator of the dynamics (2.4).

As we reviewed in Section 1.3.2.1, one appealing strategy to construct numerical schemes for Langevin dynamics is to resort to a splitting scheme between the Hamiltonian part of the dynamics (typically integrated with a Verlet scheme (3.31)) and the fluctuation/dissipation dynamics on the momenta. The corresponding dynamics reads

$$dp_t = -\gamma \nabla U(p_t)\, dt + \sqrt{\frac{2\gamma}{\beta}}\, dW_t, \tag{3.2}$$

with generator $\mathcal{L}_{\mathrm{FD}}$. The momenta marginal distribution κ given by (1.13) is invariant under this dynamics.

In order to state rigorous results, we work with functions growing at most polynomially. More precisely, introducing the weight function[2] $\mathcal{K}_\alpha(q,p) = 1 + |q|^\alpha + |p|^\alpha$, we recall the following spaces of functions growing at most as $\mathcal{K}_\alpha$ at infinity (already defined in (1.36))

$$L^\infty_{\mathcal{K}_\alpha} = \left\{ f \text{ measurable}, \quad \|f\|_{L^\infty_{\mathcal{K}_\alpha}} = \left\| \frac{f}{\mathcal{K}_\alpha} \right\|_{L^\infty} < +\infty \right\}.$$

In order to make more concise statements, we will simply say that a sequence of functions $f_{\Delta t}$ grows at most polynomially in (q,p) uniformly in Δt when there exist $K, \alpha, \Delta t^* > 0$ such that

$$\sup_{0 < \Delta t \leqslant \Delta t^*} \|f_{\Delta t}\|_{L^\infty_{\mathcal{K}_\alpha}} \leqslant K. \tag{3.3}$$

Recall the vector space $\mathscr{S}$ of smooth functions which, together with all their derivatives, grow at most polynomially.

Under the following assumptions on U the process (3.2) admits solutions for all times $t > 0$ (see for instance [70] and references therein):

Assumption 3.1 *(1) $U \in C^\infty$ grows at most polynomially;*

(2) There exists a bounded function $U_1 \in C^\infty\left(\mathbb{R}^d\right)$ with bounded derivatives and a convex function $U_2 \in C^\infty\left(\mathbb{R}^d\right)$ such that $U = U_1 + U_2$;

(3) There exists strictly positive real numbers κ_1 and κ_2 such that

$$\langle x, \nabla U(x) \rangle \geqslant \kappa_1 |x|^2 - \kappa_2 \quad \forall x \in \mathbb{R}^d;$$

(4) For all $k \in \mathbb{N}$

$$\int_{\mathbb{R}^d} |x|^{2k} \, \mathrm{e}^{-2U(x)} dx < \infty.$$

[2] Note that for a compact space the weight functions reduce to $\mathcal{K}_\alpha(q,p) = 1 + |p|^\alpha$.

When Assumption 3.1 is satisfied, it was shown in [70, Proposition 2.7] that the evolution semigroup $\mathrm{e}^{t\mathcal{L}_{\mathrm{FD}}}$ preserves $\mathscr{S}$.

The dynamics (3.2) cannot be analytically integrated, except for very specific kinetic energies such as the standard kinetic energy (1.7). However, by a simple extension of the results of [78] the splitting schemes (either Lie or Strang) based on a weakly second order consistent discretization of (3.2) and a Verlet scheme for the Hamiltonian part are globally weakly consistent, of weak order 1 for Lie-Trotter-based splittings and of weak order 2 for Strang based splittings. In the case when the kinetic energy is a perturbation of the standard kinetic energy, in the sense of

$$\nabla U - \nabla U_{\mathrm{std}} \in C_0^\infty, \tag{3.4}$$

we show that the numerical schemes admit a unique invariant probability measure $\mu_{\Delta t}$. Note that (3.4) implies Assumption 3.1. Moreover, it is possible to prove exponential convergence rates which are uniform in the timestep Δt and depend only on the physically elapsed time. This allows also to state error estimates on the invariant measure $\mu_{\Delta t}$ and on integrated correlation functions. We obtained such results by adapting the proofs of the corresponding statements in [78], upon replacing $\nabla U_{\mathrm{std}}(p) = M^{-1}p$ with $\nabla U(p) = M^{-1}p + Z(p)$ where $Z \in C_0^\infty$.

On the other hand, when the condition (2.6) is not satisfied, it may not be possible to prove the existence of a unique invariant measure for the splitting schemes. The main obstruction is that the Markov chain corresponding to the discretization of the elementary fluctuation/dissipation dynamics (3.2) may itself be transient. This would be the case for instance for non-globally Lipschitz force fields ∇U and the Euler-Maruyama discretization [105]. This observation motivates resorting to a Metropolis correction in order to ensure the existence of an invariant probability distribution which we present in Section 3.3.

3.1.1 A first order scheme

In this section, we present a discretization scheme of order 1 of the Langevin dynamics (2.4) and prove exponential convergence rates which are uniform in Δt.

The scheme we consider is based on the Lie-Trotter splitting:

$$\begin{cases} \tilde{p}^{n+1} = p^n - \nabla V(q^n)\Delta t \\ q^{n+1} = q^n + \nabla U\left(\tilde{p}^{n+1}\right)\Delta t \\ p^{n+1} = \Phi_{\Delta t}^{\mathrm{FD}}(p^n, G^n), \end{cases} \tag{3.5}$$

where G^n are *i.i.d.* standard d-dimensional Gaussian random variables. We integrate the fluctuation-dissipation dynamics (3.2) by the following first order scheme:

$$p^{n+1} = \Phi_{\Delta t}^{\mathrm{FD}}(p^n, G^n) = \alpha_{\Delta t} p^n + \gamma \Delta t Z(p^n) + \sqrt{\frac{1-\alpha_{\Delta t}^2}{\beta}} M G^n, \tag{3.6}$$

where $\alpha_{\Delta t}$ is defined in (1.56) and the AR-perturbation function is defined as

$$Z(p) := \nabla U(p) - M^{-1}p. \tag{3.7}$$

Note that this scheme is based on the fact that, under condition (2.6), the modified Langevin dynamics can be written as a perturbation of the standard dynamics. The following lemma shows that the scheme (3.6) has a weak error of order 1.

Lemma 3.1. *Suppose that Assumption 2.2 and* (3.4) *hold. The discretization scheme* (3.6) *has a weak error of order 1 in the time step size Δt with the following expansion of the generator: for any smooth test function $\varphi \in \mathscr{S}$, there exist $\Delta t^*, K, \alpha > 0$ such that*

$$P^{\mathrm{FD}}_{\Delta t}\varphi = \varphi + \Delta t \mathcal{L}_{\mathrm{FD}}\varphi + \Delta t^2 R^{\mathrm{FD}}_{\Delta t,\varphi}, \tag{3.8}$$

where $\sup_{0<\Delta t\leqslant \Delta t^*} \|R^{\mathrm{FD}}_{\Delta t,\varphi}\|_{L^\infty_{\mathcal{K}_\alpha}} \leqslant K$. Moreover, $P^{\mathrm{FD}}_{\Delta t}$ maps functions growing at most polynomially into functions growing at most polynomially: for any $\alpha \in \mathbb{N}$, there exist $\alpha' \in \mathbb{N}$ and $C_\alpha > 0$ such that

$$\forall f \in L^\infty_{\mathcal{K}_\alpha}, \qquad \left\| P^{\mathrm{FD}}_{\Delta t} f \right\|_{L^\infty_{\mathcal{K}_\alpha}} \leqslant C_\alpha \|f\|_{L^\infty_{\mathcal{K}_{\alpha'}}}. \tag{3.9}$$

Proof. The scheme (3.6) can be interpreted as a Lie-Trotter splitting of the operator $\mathcal{L}_{\mathrm{FD}}$ such that

$$\mathcal{L}_{\mathrm{FD}} = \mathcal{L}_{\mathrm{FD,std}} + \mathcal{L}_{\mathrm{FD,pert}},$$

where $\mathcal{L}_{\mathrm{FD,std}}$ corresponds to the operator of the fluctuation-dissipation equation in the case of the standard kinetic energy, *i.e.*

$$\mathcal{L}_{\mathrm{FD,std}} = -M^{-1}p \cdot \nabla_p + \frac{1}{\beta}\Delta_p, \tag{3.10}$$

and $\mathcal{L}_{\mathrm{FD,pert}}$ is the perturbation operator, which is given by

$$\mathcal{L}_{\mathrm{FD,pert}} = Z(p) \cdot \nabla_p. \tag{3.11}$$

Recall that $Z \in C^\infty_0$. The dynamics associated with the operator (3.10) can be integrated analytically according to (1.56). We write

$$\mathrm{e}^{\Delta t \mathcal{L}_{\mathrm{FD,std}}}\varphi = \varphi + \Delta t \mathcal{L}_{\mathrm{FD,std}}\varphi + \Delta t^2 R^{\mathrm{std}}_{\Delta t}\varphi$$

with an integral remainder

$$R^{\mathrm{std}}_{\Delta t}\varphi = \int_0^1 (1-\theta)\mathrm{e}^{\theta \Delta t \mathcal{L}_{\mathrm{FD,std}}}\mathcal{L}^2_{\mathrm{FD,std}}\varphi \, d\theta.$$

In [70, Proposition 2.7], the following bounds on $\mathrm{e}^{\Delta t \mathcal{L}_{\mathrm{FD,std}}}$ were proven : for $\varphi \in \mathscr{S}$ there exists a constant $\lambda > 0$ such that for any $k \in \mathbb{N}$ there exist $n_k \in \mathbb{N}$ and $m_k \in \mathbb{N}$ and $C_k > 0$ such that for all $t \geqslant 0$

$$\left\|\partial^k \mathrm{e}^{t\mathcal{L}_{\mathrm{std}}}\varphi\right\|_{L^\infty_{\mathcal{K}_{m_k}}} \leqslant C_k \mathrm{e}^{-\lambda t}\left\|\varphi\right\|_{L^\infty_{\mathcal{K}_{n_k}}}.$$

This implies $\mathrm{e}^{\Delta t\mathcal{L}_{\mathrm{FD,std}}} : \mathscr{S} \to \mathscr{S}$. Therefore, we obtain that $R^{\mathrm{std}}_{\Delta t}\varphi$ grows at most polynomially uniformly in Δt.

The dynamics which corresponds to the operator (3.11) is approximated by a first order scheme with the evolution operator:

$$P^{\mathrm{pert}}_{\Delta t}\varphi(p) = \varphi\left(p + \Delta t Z(p)\right),$$

which satisfies, for any $\varphi \in \mathscr{S}$,

$$P^{\mathrm{pert}}_{\Delta t}\varphi = \varphi + \Delta t Z(p)\cdot\nabla\varphi(p) + \Delta t^2 R^{\mathrm{pert}}_{\Delta t}\varphi \tag{3.12}$$

with an integral remainder

$$R^{\mathrm{pert}}_{\Delta t}\varphi = Z(p)^T\left(\int_0^1 (1-\theta)\nabla^2\varphi(p+\theta\Delta t Z(p))\,d\theta\right)Z(p).$$

Since $Z \in C^\infty_0$, it is easy to see that $R^{\mathrm{pert}}_{\Delta t}\varphi$ grows at most polynomially uniformly in Δt.

Finally, we compute

$$\begin{aligned}
P^{\mathrm{FD}}_{\Delta t}\varphi &= P^{\mathrm{pert}}_{\Delta t}\mathrm{e}^{\Delta t\mathcal{L}_{\mathrm{FD,std}}}\varphi = P^{\mathrm{pert}}_{\Delta t}\left(\varphi + \Delta t\mathcal{L}_{\mathrm{FD,std}}\varphi + \Delta t^2 R^{\mathrm{std}}_{\Delta t}\varphi\right)\\
&= \left(\varphi + \Delta t\mathcal{L}_{\mathrm{FD,std}}\varphi + \Delta t^2 R^{\mathrm{std}}_{\Delta t}\varphi\right) + \Delta t\mathcal{L}_{\mathrm{FD,pert}}\left(\varphi + \Delta t\mathcal{L}_{\mathrm{FD,std}}\varphi + \Delta t^2 R^{\mathrm{std}}_{\Delta t}\varphi\right)\\
&\quad + \Delta t^2 R^{\mathrm{pert}}_{\Delta t}\left(\varphi + \Delta t\mathcal{L}_{\mathrm{FD,std}}\varphi + \Delta t^2 R^{\mathrm{std}}_{\Delta t}\varphi\right)\\
&= \varphi + \Delta t\left(\mathcal{L}_{\mathrm{FD,std}}\varphi + \mathcal{L}_{\mathrm{FD,pert}}\varphi\right) + \Delta t^2\left(R^{\mathrm{std}}_{\Delta t}\varphi + \mathcal{L}_{\mathrm{FD,pert}}\mathcal{L}_{\mathrm{FD,std}}\varphi + R^{\mathrm{pert}}_{\Delta t}\varphi\right)\\
&\quad + \Delta t^3\left(\mathcal{L}_{\mathrm{FD,pert}}R^{\mathrm{std}}_{\Delta t}\varphi + R^{\mathrm{pert}}_{\Delta t}\mathcal{L}_{\mathrm{FD,std}}\varphi\right) + \Delta t^4 R^{\mathrm{pert}}_{\Delta t}R^{\mathrm{std}}_{\Delta t}\varphi
\end{aligned} \tag{3.13}$$

and we conclude with (3.8) as well as to (3.9) since the concatenations of the remainders grow at most polynomially uniformly in Δt.

For the evolution operator of the scheme (3.5) the following expansion holds true:

$$P^{\mathrm{Lie}}_{\Delta t}\varphi = \mathrm{e}^{\Delta t\mathcal{L}}\varphi + \Delta t^2 r_{\Delta t,\varphi},$$

where the remainder $r_{\Delta t,\varphi}$ grows at most polynomially in (q,p) uniformly in Δt. The proof is similar to the proof of Lemma 3.4, we therefore omit this part (see also Section 3.1.2).

The ergodicity was proved for the continuous dynamics under Assumption 2.2 and for compact position spaces $\mathcal{D}$ in Chapter 2 (see Theorem 2.4). Under these assumptions, the ergodicity of the discretized scheme (3.5) can be proven. The following result is based on the approach in [78] by obtaining Lyapunov and minorization conditions. The proof can be read in Section 3.5.1.

Lemma 3.2. *Suppose that Assumption 2.2 holds and that $U \in \mathscr{S}$ is such that $\|Z\|_{L^\infty} \leqslant \mathscr{Z}$. The scheme* (3.5) *is ergodic: for any $\gamma > 0$, there exist Δt^* such that there exists a unique invariant measure $\mu_{\Delta t}$ with finite moments. Moreover, for any $s \geqslant 1$ and $0 < \Delta t < \Delta t^*$,*

$$\int_{\mathcal{E}} \mathcal{K}_s d\mu_{\Delta t} < \infty,$$

and the following exponential convergence holds: there exist $\lambda_s, K_s > 0$ such that for almost all $(q,p) \in \mathcal{E}$ and for all $\varphi \in L^\infty_{\mathcal{K}_s}$ and $0 < \Delta t \leqslant \Delta t^*$,

$$\forall n \geqslant 0, \quad \left\| P^n_{\Delta t}\varphi - \int_{\mathcal{E}} \varphi d\mu_{\Delta t} \right\|_{L^\infty_{\mathcal{K}_s}} \leqslant K_s \mathrm{e}^{-\lambda_s n \Delta t} \|\varphi\|_{L^\infty_{\mathcal{K}_s}} . \tag{3.14}$$

Having this results and (3.8) at hand, it is possible to prove the first order accuracy of averages with respect to the invariant measure (see Theorem 1.8).

Corollary 3.1. *Suppose that Assumption 2.2 holds and that $U \in \mathscr{S}$ is such that $\|Z\|_{L^\infty} \leqslant \mathscr{Z}$. The discretization* (3.5) *has an error on the averages of order 1: there exist a function $f \in \mathscr{S}$ such that for any smooth φ there exist $\Delta t^* > 0$ and $C > 0$ such that, for all $0 < \Delta t \leqslant \Delta t^*$,*

$$\int_{\mathcal{E}} \varphi(q,p) d\mu_{\Delta t} = \int_{\mathcal{E}} \varphi(q,p) d\mu + \Delta t \int_{\mathcal{E}} \varphi(q,p) f(q,p) d\mu_{\Delta t} + R_{\Delta t,\varphi} \Delta t^2,$$

where $|R_{\Delta t,\varphi}| \leqslant C$.

3.1.2 Second order schemes

In this section, we apply results from [2, 78, 82] in order to construct a discretization scheme for (2.4), which has an error on the average properties of order 2 in the timestep. For this purpose we discretize the fluctuation-dissipation equation (3.2) by a modified scheme of weak order 2 and we deduce that the resulting scheme for (2.4), which is obtained via Lie-Trotter or Strang splitting of $\mathcal{L}$ into $\mathcal{L}_{\mathrm{Ham}}$ and $\mathcal{L}_{\mathrm{FD}}$, provides a second order accuracy on the average properties.

The Hamiltonian part with the generator $P^{\mathrm{Ham}}_{\Delta t}$ is usually approximated by a second order splitting, here the Verlet scheme, *i.e.*

$$(q^{n+1}, p^{n+1}) = \Phi^{\mathrm{Verlet}}_{\Delta t}(q^n, p^n),$$

given by (1.8). This corresponds to the evolution operator

$$P^{\mathrm{Ham}}_{\Delta t} = \mathrm{e}^{\Delta t B/2} \mathrm{e}^{\Delta t A} \mathrm{e}^{\Delta t B/2} \tag{3.15}$$

with the operators defined in (1.54). In order to be consistent with the order of the Hamiltonian part, we also need to discretize (3.2) by a scheme of (at least) second order. There are plenty of schemes satisfying this requirement. We could for example simply construct a second order scheme by Strang instead of Lie-Trotter

splitting of the operator $\mathcal{L}_{\mathrm{FD}}$ as done in the proof of Lemma 3.1 with an analytic integral of $\mathcal{L}_{\mathrm{FD,std}}$ and a second order discretization of $\mathcal{L}_{\mathrm{FD,pert}}$.

Motivated by the midpoint scheme in (2.21), we use the approach by modified equations from [1, 132]. We construct a second order scheme by a modification of the following first order scheme, which is based on the first order approximation of the midpoint scheme:

$$p^{n+1} = \Phi_{\mathrm{EM},\Delta\mathrm{t}}(p^n) = p^n - \gamma\nabla U\left(p^n - \gamma\frac{\Delta t}{2}\nabla U\left(p^n\right) + \frac{1}{2}\sqrt{\frac{2\gamma\Delta t}{\beta}}G^n\right)\Delta t + \sqrt{\frac{2\gamma\Delta t}{\beta}}G^n\,. \tag{3.16}$$

The discretized modified equation of weak order 2 (for the proof see [45]) reads

$$p^{n+1} = p^n - \gamma\nabla U\left(p^n - \gamma\frac{\Delta t}{2}\nabla U\left(p^n\right) + \frac{1}{2}\sqrt{\frac{2\gamma\Delta t}{\beta}}G^n\right)\Delta t - \frac{\gamma^2}{4\beta}\,\nabla\left(\Delta U\left(p^n\right)\right)\Delta t^2 + \sqrt{\frac{2\gamma\Delta t}{\beta}}G^n\,. \tag{3.17}$$

We denote by $P_{\Delta t}^{\mathrm{FD},2}$ the associated evolution operator. Note that in the case of the standard kinetic energy U_{std}, the correction term $\nabla\left(\Delta U\right)\left(p^n\right)$ disappears and hence (3.16) already provides a numerical scheme of weak order 2.

Under the assumption $U \in \mathscr{S}$, it is possible to state the following expansion of the evolution operator similarly to the result in [45]:

$$P_{\Delta t}^{\mathrm{FD},2}\varphi = \mathrm{e}^{\Delta t\mathcal{L}_{\mathrm{FD}}}\varphi + \Delta t^3 R_{\Delta t}^{\mathrm{FD},\varphi}, \tag{3.18}$$

with the remainder $R_{\Delta t,\varphi}^{\mathrm{FD}}$ grows at most polynomially in p uniformly in Δt, and $P_{\Delta t}^{\mathrm{FD},2}$ maps functions growing at most polynomially into functions growing at most polynomially, *i.e.* for any $s' \in \mathbb{N}$, there exists $s \in \mathbb{N}$ and $C_s > 0$ such that, for all $\Delta t \leqslant \Delta t^*$,

$$\forall\varphi \in L^\infty_{\mathcal{K}_{s'}}, \quad \left\|P_{\Delta t}^{\mathrm{FD},2}\varphi\right\|_{L^\infty_{\mathcal{K}_s}} \leqslant C_s\left\|\varphi\right\|_{L^\infty_{\mathcal{K}_{s'}}}. \tag{3.19}$$

Remark 3.1. *Note that, in general, the modified equations such as* (3.17) *are not applied to discretize the overdamped Langevin dynamics*

$$dq_t = -\nabla V(q_t)\,dt + \sqrt{\frac{2}{\beta}}\,dW_t,$$

due to the computational effort of evaluation of the higher derivatives of the potential. Here, the computation of the modification term in (3.17) *does not significantly increase the computational complexity, because the kinetic energy function U can be chosen to be separable among the particles, hence equation* (1.55) *reduces to $d = DN$ one-dimensional equations.*

On the other hand, it was proved in [78] that the evolution operator of the Hamiltonian part (3.31) satisfies the following expansion: if $U, V \in \mathscr{S}$, then for all smooth $\varphi \in \mathscr{S}$ and $0 < \Delta t \leqslant \Delta t^*$ small enough,

$$P_{\Delta t}^{\mathrm{Ham}}\varphi = \mathrm{e}^{\Delta t\mathcal{L}_{\mathrm{Ham}}}\varphi + \Delta t^3 R_{\Delta t}^{\mathrm{Ham}}\varphi \tag{3.20}$$

where the remainder grows at most polynomially in (q,p) uniformly Δt. Moreover $P_{\Delta t}^{\mathrm{Ham}}$ satisfies that for any $s' \in \mathbb{N}$, there exists $s \in \mathbb{N}$ and $C_s > 0$ such that, for all $\Delta t \leqslant \Delta t^*$,

$$\forall \varphi \in L^\infty_{\mathcal{K}_{s'}}, \quad \left\| P_{\Delta t}^{\mathrm{Ham}} \varphi \right\|_{L^\infty_{\mathcal{K}_s}} \leqslant C_s \left\| \varphi \right\|_{L^\infty_{\mathcal{K}_{s'}}} . \tag{3.21}$$

In order to numerically integrate (2.4), we consider the Strang splitting between the operators $\mathcal{L}_{\mathrm{Ham}}$ and $\mathcal{L}_{\mathrm{FD}}$ which corresponds to the following evolution operator:

$$P_{\Delta t}^{\mathrm{Strang}} = P_{\Delta t/2}^{\mathrm{FD},2} P_{\Delta t}^{\mathrm{Ham}} P_{\Delta t/2}^{\mathrm{FD},2}. \tag{3.22}$$

Of course, the resulting scheme has weak order 2 with the following expansion: for every $\varphi \in \mathscr{S}$,

$$P_{\Delta t}^{\mathrm{Strang}} \varphi = \varphi + \Delta t \mathcal{L} \varphi + \frac{\Delta t^2}{2} \mathcal{L}^2 \varphi + \Delta t^3 r_{\Delta t, \varphi}, \tag{3.23}$$

with the remainder $r_{\Delta t,\varphi}$ growing at most polynomially in (q,p) uniformly in Δt. The proof of the expansion (3.23) is similar to the proof of Lemma 3.4. By the same arguments it is possible to prove an expansion of the generator obtained by the Lie-Trotter splitting

$$P_{\Delta t}^{\mathrm{GLA}} = P_{\Delta t}^{\mathrm{Ham}} P_{\Delta t}^{\mathrm{FD},2}. \tag{3.24}$$

More precisely, there exist an operator $\mathcal{A}$, such that for every $\varphi \in \mathscr{S}$,

$$P_{\Delta t}^{\mathrm{GLA}} \varphi = \varphi + \Delta t \mathcal{L} \varphi + \Delta t^2 \left(\frac{1}{2} \mathcal{L}^2 + \mathcal{A} \right) \varphi + \Delta t^3 r_{\Delta t, \varphi}, \tag{3.25}$$

with the remainder $r_{\Delta t,\varphi}$ growing at most polynomially in (q,p) uniformly in Δt. The operator $\mathcal{A} = [\mathcal{L}_{\mathrm{Ham}}, \mathcal{L}_{\mathrm{FD}}]$ preserves the invariant measure μ, *i.e.*

$$\int_{\mathcal{E}} \mathcal{A} \varphi d\mu = 0 \, . \tag{3.26}$$

Hence, the Lie-Trotter splitting gives a second order accuracy on the invariant measure (see the corollary below).

Under Assumption 2.2, the dynamics is ergodic with an invariant measure μ (see Theorem 2.4) and, similarly to the first order scheme (3.5), we can prove that the second order schemes with evolution operators $P_{\Delta t}^{\mathrm{Strang}}$ and $P_{\Delta t}^{\mathrm{GLA}}$ are ergodic with respect to some measure $\mu_{\Delta t}$ in the sense of Lemma 3.2. The corresponding proof is a simple modification of the proof from Section 3.5.2.

Using the expansion of the evolution operator (3.23) or (3.25), we deduce the second order error on the invariant measure for both splittings, which is a direct application of Theorem 1.8.

Corollary 3.2. *Suppose Assumption 2.2 holds. The schemes induced by $P_{\Delta t}^{\mathrm{Strang}}$ and $P_{\Delta t}^{\mathrm{GLA}}$ preserve the invariant measure at order 2 in the time step size: there exists a function $f \in \mathscr{S}$ such that for any smooth φ*

there exist $\Delta t^* > 0$ *and* $C > 0$ *such that for* $0 < \Delta t \leqslant \Delta t^*$,

$$\int_{\mathcal{E}} \varphi(q,p) d\mu_{\Delta t} = \int_{\mathcal{E}} \varphi(q,p) d\mu + \Delta t^2 \int_{\mathcal{E}} \varphi(q,p) f(q,p) d\mu_{\Delta t} + R_{\Delta t,\varphi} \Delta t^3,$$

where $|R_{\Delta t,\varphi}| \leqslant C$.

Remark 3.2. *An exchange of the order of the operators in the scheme, for instance considering* $P_{\Delta t}^{\mathrm{Ham}} P_{\Delta t}^{\mathrm{FD}}$ *instead of* $P_{\Delta t}^{\mathrm{FD}} P_{\Delta t}^{\mathrm{Ham}}$*, does not change the order of the scheme. However note that, by an application of the TU-Lemma it is possible to obtain the expression of the invariant measure of one scheme when the expression for another one is given (see [78] for more details).*

Recall that, if the estimate (3.14) holds for a generator $P_{\Delta t}$, we control its resolvent: there exists $C > 0$ such that, for $0 < \Delta t \leqslant \Delta t^*$,

$$\left\| \left(\frac{\mathrm{Id} - P_{\Delta t}}{\Delta t} \right)^{-1} \right\|_{\mathscr{B}\left(\widetilde{L^\infty_{\mathcal{K}_s}}\right)} \leqslant C.$$

Weak error estimates also determine the error on the computation of the transport coefficients. The following corollary is an application of [78, Corollary 2.3], since the expansions (3.23) and (3.25) can be rewritten as

$$-\frac{\mathrm{Id} - P_{\Delta t}}{\Delta t} \varphi = \mathcal{L}\varphi + \frac{\Delta t}{2} \mathcal{L}^2 \varphi + \Delta t^2 r_{\Delta t,\varphi}.$$

It states that for a scheme with weak error of order 2, the properties computed through Green-Kubo formula can be computed with a second-order accuracy when using the trapezoidal rule for integrating the auto-correlation function.

Corollary 3.3. *We consider the scheme given by* $P_{\Delta t}^{\mathrm{Strang}}$*. For two smooth observables* $\varphi, \psi \in \widetilde{\mathscr{S}}$*, there exist* $K > 0$ *and* $\Delta t^* > 0$ *such that for any* $0 < \Delta t \leqslant \Delta t^*$,

$$\begin{aligned} &\int_0^{+\infty} \mathbb{E}\left[\psi\left(q_t, p_t\right) \varphi\left(q_0, p_0\right)\right] \mathrm{d}t \\ &\quad = \frac{\Delta t}{2} \mathbb{E}_{\Delta t}\left(\psi_{\Delta t,0}\left(q^0, p^0\right) \varphi\left(q^0, p^0\right)\right) + \Delta t \sum_{n=1}^{+\infty} \mathbb{E}_{\Delta t}\left(\psi_{\Delta t}\left(q^n, p^n\right) \varphi\left(q^0, p^0\right)\right) + \Delta t^2 r_{\Delta t}^{\psi,\varphi} \end{aligned} \tag{3.27}$$

with $\left| r_{\Delta t}^{\psi,\varphi} \right| \leqslant K$ *and* $\psi_{\Delta t,0} = \psi - \int_{\mathcal{E}} \psi d\mu_{\Delta t}$.

Obviously, dynamical properties of the Langevin dynamics with a general kinetic energy are different from the dynamical properties of the standard Langevin dynamics. The previous corollary characterizes the error due to the discretization by the finite time step size with respect to the continuous dynamics. In order to retrieve dynamical properties of the corresponding standard Langevin dynamics, the modified dynamics should be unbiased (for instance via Girsanov formula [34], an approach which needs to be explored for this dynamics, see perspectives in Chapter 5).

In practical applications, the computation of (3.27) is done by truncating the upper bound in the integral by a sufficiently large time T_{corr}, and by using a trapezoidal rule. We have used this approach for an estimation of the asymptotic variance in (2.22).

Remark 3.3. *If the interest lies only in the configurational sampling from the invariant distribution, a natural extension is to resort to a Generalized Langevin equation [94] by introducing a new variable $R \in \mathbb{R}^d$. This approach is motivated by considering* (1.55) *as the overdamped Langevin equation, which can be seen as a limit in the friction constant γ_{FD} of the following Langevin dynamics:*

$$\begin{cases} dp_t = M_{\mathrm{FD}}^{-1} R_t \, dt, \\ dR_t = -\nabla U(p_t) \, dt - \gamma_{\mathrm{FD}} M_{\mathrm{FD}}^{-1} R_t \, dt + \sqrt{\dfrac{2\gamma_{\mathrm{FD}}}{\beta}} \, dW_t, \end{cases} \tag{3.28}$$

where dW_t is a standard d-dimensional Wiener process and $\gamma_{\mathrm{FD}} > 0$ is a friction constant and $M_{\mathrm{FD}} > 0$. The numerical integration of (3.28) *can be done by a scheme such as* (1.59)*, since the function $W(R) := \frac{R^2}{2M_{\mathrm{FD}}}$ is quadratic and hence the fluctuation-dissipation part can be solved analytically. The splitting strategies for the standard Langevin dynamics [78, 23] provide a second-order accuracy on the invariant measure $\mu_{\mathrm{FD}}(p,R) = Z_{FD,R}^{-1} \mathrm{e}^{-\beta U(p)} \mathrm{e}^{-\beta W(R)} dp \, dR$. Strang splitting between the Hamiltonian part and the fluctuation-dissipation part, formally $P_{\Delta t/2}^{\mathrm{FD,R}} P_{\Delta t}^{\mathrm{Verlet}} P_{\Delta t/2}^{\mathrm{FD,R}}$, gives then a weak error of order 2.*

The Hamiltonian of the whole dynamics, in this case, reads $H_{\mathrm{FD}}(q,p,R) = V(q) + W(R) + U(p)$ with an invariant measure

$$\tilde{\mu}(q,p,R) = \nu(q) \mu_{\mathrm{FD}}(p,R).$$

Recall that, the computational bottleneck is the evaluation of $f(q) = -\nabla V(q)$. Hence the extension into an additional variable which requires only a linear complexity, will not significantly increase the computational cost per time step. On the other hand, when the kinetic energy function is chosen such that it helps to decrease the computational complexity in the forces update (consider for example the AR-Langevin dynamics, or the kinetic energy function from Section 5.1), the total cost of the integration of the whole dynamics or the necessary number of time steps can be reduced.

3.1.3 Numerical results

In Section 3.1.3.1 we illustrate using a simple numerical example that the modified scheme (3.16) for the fluctuation-dissipation equation has second order accuracy for the calculation of averages. We also confirm the predictions of Corollary 3.2: schemes obtained through a Lie-Trotter and Strang splitting between (3.31) and (3.16) provide averages that are accurate at order two in the timestep size.

In order to numerically determine the error order on the invariant measure for a given numerical scheme, we plot the relative error

$$r(\Delta t) = \frac{|\hat{\varphi}_{N_{\mathrm{iter}},\Delta t} - \hat{\varphi}_0|}{|\hat{\varphi}_0|} \tag{3.29}$$

of the estimator $\hat{\varphi}_{N_{\mathrm{iter}},\Delta t}$ given by (1.60) with respect to the exact value $\hat{\varphi}_0$ at $\Delta t = 0$.

3.1.3.1 The fluctuation-dissipation equation

First, we consider only the fluctuation-dissipation equation (3.2) for two AR-kinetic energies with different parameters (see Section 3.4 for the definition of the AR-kinetic energy as given by (3.49) with a C^3 interpolation spline) and a three dimensional system of 27 particles with zero forces, an ideal fluid system[3]. We choose $\gamma = 1$ and $\beta = 1$. We compare the discretizations discussed this chapter: the first order scheme (3.16) and the two second order schemes, which are (3.17) and the GLE-like scheme (3.28) discretized by (1.59). We choose various time step sizes and integrate the dynamics over $N_{\text{iter}} \approx 10^{10}$ time steps. We compute the ergodic average of the kinetic temperature, an observable given by $\mathcal{T}(p) = p \cdot \nabla U(p)$, for which we know the exact value at equilibrium $\mathbb{E}_\mu(\mathcal{T}(p)) = \beta^{-1}$ (see (1.16)). Figure 3.1 shows the relative error over the time step size. The error slopes confirm the theoretical orders of the numerical methods.

3.1.3.2 The Langevin equation

In the next example, we numerically confirm the second order error on average properties as given by Corollary 3.2 for the full Langevin dynamics. We consider the system of $N = 27$ particles in a 3D periodic domain at density 0.3, inverse temperature $\beta = 1$ and friction $\gamma = 1$. Particles are interacting by the WCA potential (1.4) with parameters $\varepsilon_{\text{LJ}} = 1$ and $\sigma_{\text{LJ}} = 1$ truncated at the distance $r_{\text{LJ}} = 2^{1/6}\sigma_{\text{LJ}}$ (the same system as in Section 2.4.2). We consider the AR-kinetic energy function with $e_{\max} = 2$ and $e_{\min} = 1$. We measure the averages of two observables: the kinetic temperature $\mathcal{T}(p)$ and the potential energy $V(q)$. Unlike for the kinetic temperature, we do not know the exact expected value of the potential. In order to obtain an approximation of this value, we interpolate the values obtained over Δt by a linear or quadratic function according to the order of the method. We then evaluate the interpolation function at $\Delta t = 0$ which gives an approximation for $\mathbb{E}_\mu(V(q))$.

We observe in Figure 3.2b that the second order accuracy of the Strang splitting of the Hamiltonian part is destroyed when the fluctuation-dissipation part is integrated by a first order scheme[4] (Lie-Trotter splitting between (3.31) and (3.16), denoted as "GLA 1"). On the other hand, Lie-Trotter and Strang splitting between (3.31) and (3.17) shows second order accuracy ("GLA" and "Strang"). Note in Figure 3.2 where we plot the relative error for the potential energy $V(q)$, we do not observe the first order for GLA 1, all schemes show second order.

[3] The fluctuation-dissipation equations are separable in all dimensions, the 27 particles hence act as parallel replicas/realizations.

[4] Note that a similar scheme was used in [9] to integrate the AR-Langevin dynamics. The fluctuation-dissipation equation was integrated with an Euler-Maruyama scheme, while we use here an explicit-midpoint. Both schemes however are of weak order 1.

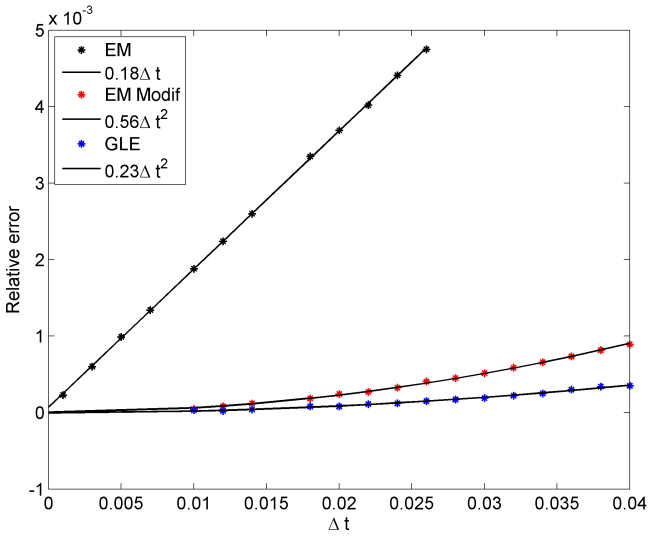

Fig. 3.1: *Error order of the discretization schemes for fluctuation-dissipation equation*. We plot the relative error (3.29) for the kinetic temperature $\mathcal{T}(p)$ over the time step for various discretizations of the fluctuation-dissipation equation (1.55): explicit mid-point scheme (3.16) (EM), its second order modification (3.17) (EM Modif) and the GLE extension (3.28) discretized by (1.59). The AR-kinetic energy is parametrized by $v_{\max} = 2$ and $v_{\min} = 1$.

3.2 Generalized Hybrid Monte-Carlo schemes

We present in this section a generalized Hybrid Monte-Carlo (GHMC) scheme to discretize the Langevin dynamics with non-quadratic kinetic energies. HMC is a Metropolis-Hastings method based on a proposal generated by the integration of the deterministic Hamiltonian dynamics. The proposal is then accepted or rejected according to the Metropolis rule. The rejection of the proposal occurs due to discretization errors. The efficiency of the method is therefore a trade-off between larger simulated physical times (which calls for larger timesteps) and not too large rejection rates (which places an upper limit on possible timesteps).

We metropolize the Langevin dynamics with a general kinetic energy in two steps: first, we metropolize the Hamiltonian part as in the standard single-step HMC method (see Section 3.3.1); in a second step, we add a weakly consistent discretization of the elementary fluctuation/dissipation stabilized by a Metropolis procedure (see Section 3.3.2). The complete algorithm is summarized in Section 3.3.3.

3.3 Generalized Hybrid Monte-Carlo schemes

We present in this section a generalized Hybrid Monte-Carlo (GHMC) scheme to discretize the Langevin dynamics with non-quadratic kinetic energies. For an introduction to HMC and some of its generalizations, we refer for instance the reader to [81, Section 2.2.3]. In essence, HMC is a Metropolis-Hastings method based on a proposal generated by the integration of the deterministic Hamiltonian dynamics. The proposal

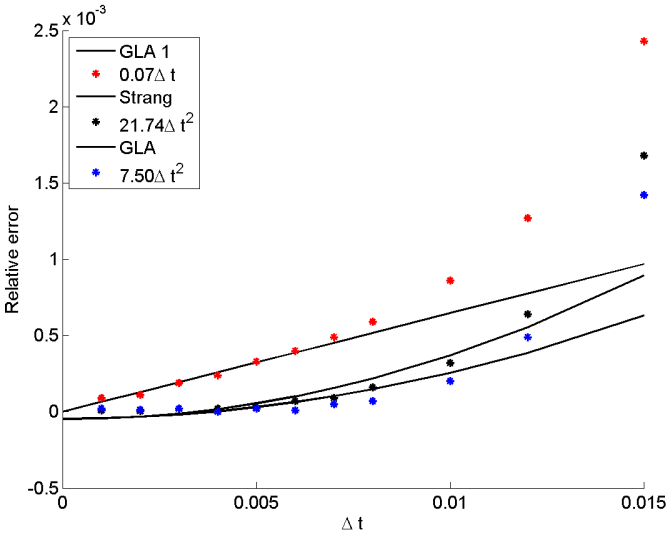

(a) Kinetic temperature

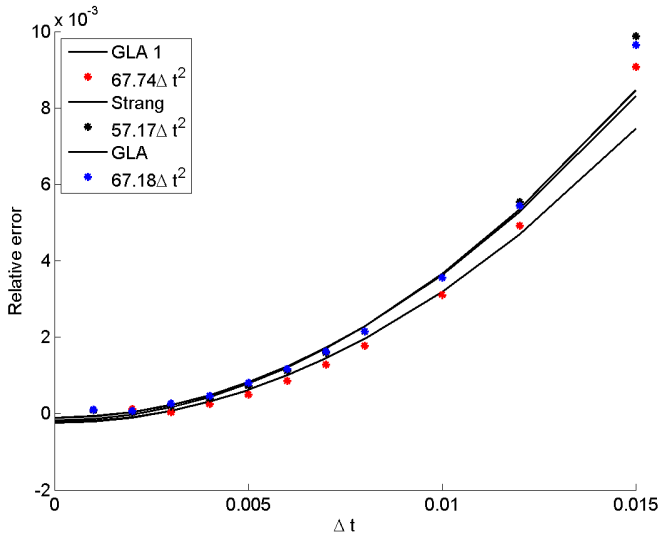

(b) Potential energy

Fig. 3.2: *Illustration of Corollary 3.2.* We consider the potential energy $V(q)$ and the kinetic temperature $\mathcal{T}(p)$ for various integration schemes of the AR- Langevin dynamics with the AR kinetic energy function with parameters $v_{\min} = 1$ and $v_{\max} = 2$ and confirm the predicted error orders on the average properties by plotting the relative error (3.29) over the time step.

is then accepted or rejected according to the Metropolis rule. The rejection of the proposal occurs due to discretization errors. The efficiency of the method is therefore a trade-off between larger simulated physical times (which calls for larger timesteps) and not too large rejection rates (which places an upper limit on possible timesteps).

We metropolize the Langevin dynamics with a general kinetic energy in two steps: first, we metropolize the Hamiltonian part as in the standard single-step HMC method (see Section 3.3.1); in a second step, we add a weakly consistent discretization of the elementary fluctuation/dissipation stabilized by a Metropolis procedure (see Section 3.3.2). The complete algorithm is summarized in Section 3.3.3.

3.3.1 Metropolization of the Hamiltonian part

Let us describe the one-step HMC method we use to discretize the Hamiltonian part of the dynamics:

$$\begin{cases} dq_t = \nabla U(p_t)\, dt, \\ dp_t = -\nabla V(q_t)\, dt. \end{cases} \tag{3.30}$$

Starting from a configuration $(q^n, p^n) \in \mathcal{E}$, a new configuration $(\widetilde{q}^{n+1}, \widetilde{p}^{n+1}) = \Phi_{\Delta t}(q^n, p^n) \in \mathcal{E}$ is proposed using the Verlet scheme

$$\begin{cases} p^{n+1/2} = p^n - \nabla V(q^n)\dfrac{\Delta t}{2}, \\ \widetilde{q}^{n+1} = q^n + \nabla U(p^{n+1/2})\Delta t, \\ \widetilde{p}^{n+1} = p^{n+1/2} - \nabla V(\widetilde{q}^{n+1})\dfrac{\Delta t}{2}. \end{cases} \tag{3.31}$$

The proposal is then accepted with probability

$$A_{\Delta t}^{\mathrm{Ham}}\left(q^n, p^n\right) = \min\left(1, \exp\left(-\beta\Big[H\left(\Phi_{\Delta t}(q^n, p^n)\right) - H\left(q^n, p^n\right)\Big]\right)\right). \tag{3.32}$$

If the proposal is rejected, a momentum reversal is performed and the next configuration is set to $(q^{n+1}, p^{n+1}) = (q^n, -p^n)$ (see the discussion in [81, Section 2.2.3] for a motivation of the momentum reversal). In summary, the new configuration is

$$\begin{aligned} \left(q^{n+1}, p^{n+1}\right) &= \Psi_{\Delta t}^{\mathrm{Ham}}(q^n, p^n, \mathcal{U}^n) \\ &= \mathbb{1}_{\left\{\mathcal{U}^n \leqslant A_{\Delta t}^{\mathrm{Ham}}(q^n, p^n)\right\}} \Phi_{\Delta t}\left(q^n, p^n\right) + \mathbb{1}_{\left\{\mathcal{U}^n > A_{\Delta t}^{\mathrm{Ham}}(q^n, p^n)\right\}}\left(q^n, -p^n\right), \end{aligned} \tag{3.33}$$

where $(\mathcal{U}^n)_{n \geqslant 0}$ is a sequence of independent and identically distributed (i.i.d.) random variables uniformly distributed in $[0, 1]$. A simple proof shows that the canonical measure μ is invariant by the scheme (3.33). The corresponding Markov chain is however of course not ergodic with respect to μ since momenta are not resampled or randomly modified at this stage (this will be done by the discretization of the fluctuation/dissipation, see Section 3.3.3 for the complete GHMC scheme).

Without any discretization error (*i.e.* if the Hamiltonian dynamics was exactly integrated, so that the energy would be constant), the proposal would always be accepted. Since the Verlet scheme is of order 2, we expect the energy difference $H\left(\Phi_{\Delta t}(q^n, p^n)\right) - H\left(q^n, p^n\right)$ to be of order Δt^3. The following lemma makes this intuition rigorous and quantifies the rejection rate $1 - A_{\Delta t}^{\mathrm{Ham}}$ in terms of the timestep Δt and derivatives of the potential and kinetic energy functions.

Lemma 3.3. *Assume that $U, V \in \mathscr{S}$ and that the canonical measure μ admits moments of all order in q, p. Then there exist $K, \Delta t^*, \alpha > 0$ such that the rejection rate of the one-step HMC scheme* (3.33) *admits the following expansion: for any $\Delta t \in (0, \Delta t^*]$,*

$$0 \leqslant 1 - A_{\Delta t}^{\mathrm{Ham}} = \Delta t^3 \xi_+ + \Delta t^4 r_{\Delta t}\,, \tag{3.34}$$

with $\sup_{0<\Delta t\leqslant \Delta t^*} \|r_{\Delta t}\|_{L^\infty_{\mathcal{K}_\alpha}} \leqslant K$. Moreover, the leading order of the rejection rate is given by $\xi_+ := \max(0, \xi)$ with

$$\xi = -\mathcal{L}_{\mathrm{Ham}} H_2, \qquad H_2(q,p) = \frac{1}{12}\left[-\frac{1}{2}\nabla V(q)^T \nabla^2 U(p) \nabla V(q) + \nabla U(p)^T \nabla^2 V(q) \nabla U(p)\right]. \tag{3.35}$$

As discussed in the introduction, the crucial part of the sampling usually is the sampling of the marginal of the canonical measure μ in the position variable. There is therefore some freedom in the choice of U. The expression of the rejection rate (3.35) suggests that U should be chosen such that derivatives of order up to 3 are not too large, in order for $\bar{\xi}$ to be as small as possible. This remark is used in Section 3.4 to improve the kinetic energy functions currently considered in adaptively restrained Langevin dynamics.

Proof. The idea of the proof is that, according to results of backward analysis [53], the first order modified Hamiltonian $H + \Delta t^2 H_2$ should be preserved at order Δt^5 over one timestep. The rejection rate is therefore given, at dominant order, by $-\Delta t^2 [H_2(\Phi_{\Delta t}(q,p)) - H_2(q,p)] \simeq -\Delta t^3 (\mathcal{L}_{\mathrm{Ham}} H_2)(q,p)$.

To identify H_2 and make the previous reasoning rigorous, we write the proposal (3.31) as

$$\Phi_{\Delta t}(q,p) = \begin{pmatrix} q + \nabla U\left(p - \nabla V(q)\dfrac{\Delta t}{2}\right)\Delta t, \\ p - \nabla V(q)\dfrac{\Delta t}{2} - \nabla V\left(q + \nabla U\left(p - \nabla V(q)\dfrac{\Delta t}{2}\right)\Delta t\right)\dfrac{\Delta t}{2} \end{pmatrix},$$

so that

$$\begin{aligned} \Phi_{\Delta t}(q,p) = \begin{pmatrix} q \\ p \end{pmatrix} + \Delta t \begin{pmatrix} \nabla U(p) \\ -\nabla V(q) \end{pmatrix} - \frac{\Delta t^2}{2} \begin{pmatrix} \nabla^2 U(p) \nabla V(q) \\ \nabla^2 V(q) \nabla U(p) \end{pmatrix} \\ + \frac{\Delta t^3}{4} \begin{pmatrix} \dfrac{1}{2} D^3 U(p) : \nabla V(q)^{\otimes 2} \\ \nabla^2 V(q) \nabla^2 U(p) \nabla V(q) - D^3 V(q) : \nabla U(p)^{\otimes 2} \end{pmatrix} + \Delta t^4 R_{\Delta t}(q,p), \end{aligned} \tag{3.36}$$

where the remainder $R_{\Delta t}(q,p)$ grows at most polynomially in (q,p), uniformly in Δt (this is easily seen by performing Taylor expansions with integral remainders). Denoting by $y = (q,p)^T$, we note that the Hamiltonian dynamics (3.30) can be reformulated as

$$\dot{y} = F(y), \qquad F(y) = \begin{pmatrix} \nabla U(p) \\ -\nabla V(q) \end{pmatrix}.$$

This implies that

$$\ddot{y} = DF(y)F(y) = -\begin{pmatrix} \nabla^2 U(p)\nabla V(q) \\ \nabla^2 V(q)\nabla U(p) \end{pmatrix},$$

and

$$\dddot{y} = \begin{pmatrix} D^3U(p) : \nabla V(q)^{\otimes 2} - \nabla^2 U(p)\nabla^2 V(q)\nabla U(p) \\ -D^3V(p) : \nabla U(p)^{\otimes 2} + \nabla^2 V(q)\nabla^2 U(p)\nabla V(q) \end{pmatrix}.$$

Therefore, denoting by ϕ_t the flow of the Hamiltonian dynamics (3.30), it holds

$$\Phi_{\Delta t}(q,p) = \phi_{\Delta t}(q,p) + \Delta t^3 G(q,p) + \Delta t^4 \widetilde{R}_{\Delta t}(q,p), \tag{3.37}$$

where

$$G(q,p) = \frac{1}{12}\begin{pmatrix} -\frac{1}{2}D^3U(p) : \nabla V(q)^{\otimes 2} + 2\nabla^2 U(p)\nabla^2 V(q)\nabla U(p) \\ -D^3V(q) : \nabla U(p)^{\otimes 2} + \nabla^2 V(q)\nabla^2 U(p)\nabla V(q) \end{pmatrix},$$

and the remainder $\widetilde{R}_{\Delta t}(q,p)$ grows at most polynomially in (q,p) uniformly in Δt. A simple computation shows that

$$G = \begin{pmatrix} \nabla_p H_2(q,p) \\ -\nabla_q H_2(q,p) \end{pmatrix},$$

with H_2 defined in (3.35). Note that for the standard kinetic energy U_{std}, this expression reduces to the one derived in [52, 116].

From the error estimate (3.37), we compute

$$\begin{aligned} H(\Phi_{\Delta t}(q,p)) - H(q,p) &= H(\phi_{\Delta t}(q,p)) - H(q,p) + \Delta t^3 G(q,p)\nabla H(q,p) + \Delta t^4 \widehat{R}_{\Delta t}(q,p) \\ &= -\Delta t^3 \mathcal{L}_{\mathrm{Ham}} H_2(q,p) + \Delta t^4 \widehat{R}_{\Delta t}(q,p), \end{aligned}$$

where the remainder $\widehat{R}_{\Delta t}(q,p)$ grows at most polynomially in (q,p) uniformly in Δt. This allows to identify $\xi = -\mathcal{L}_{\mathrm{Ham}} H_2$ as the leading order term of the energy variation over one step. In order to compute the expected rejection rate, we rely on the inequality

$$x_+ - \frac{x_+^2}{2} \leqslant 1 - \min\left(1, \mathrm{e}^{-x}\right) \leqslant x_+, \quad x_+ = \max(0,x).$$

This implies that

$$0 \leqslant A_{\Delta t}^{\mathrm{Ham}}(q^n,p^n) = \Delta t^3 \xi_+(q^n,p^n) + \Delta t^4 \mathscr{R}_{\Delta t}(q^n,p^n), \tag{3.38}$$

where the remainder $\mathscr{R}_{\Delta t}$ grows at most polynomially in (q,p) uniformly in Δt, which concludes the proof.

As a corollary of the estimates (3.34) on the rejection rate and the consistency result (3.37) for the scheme without rejections, we can obtain weak-type expansions for the evolution operator

$$\begin{aligned}\tilde{P}^{\mathrm{Ham}}_{\Delta t}\varphi(q,p) &= \mathbb{E}_{\mathcal{U}}\left[\Psi^{\mathrm{Ham}}_{\Delta t}(q,p,\mathcal{U})\right] \\ &= \varphi\left(\Phi_{\Delta t}(q,p)\right) + \left(1 - A^{\mathrm{Ham}}_{\Delta t}(q,p)\right)\Big(\varphi(q,-p) - \varphi(\Phi_{\Delta t}(q,p))\Big).\end{aligned}$$

Since $A^{\mathrm{Ham}}_{\Delta t}(q,p) \in [0,1]$ and $\Phi_{\Delta t}(q,p)$ grows at most polynomially in (q,p) uniformly in Δt, a direct inspection of the latter expression shows that the operator $\tilde{P}^{\mathrm{Ham}}_{\Delta t}$ maps functions growing at most polynomially into functions growing at most polynomially: for any $\alpha \in \mathbb{N}$, there exist $\alpha' \in \mathbb{N}$ and $C_\alpha > 0$ such that

$$\forall f \in L^\infty_{\mathcal{K}_\alpha}, \qquad \left\|\tilde{P}^{\mathrm{Ham}}_{\Delta t} f\right\|_{L^\infty_{\mathcal{K}_\alpha}} \leqslant C_\alpha \|f\|_{L^\infty_{\mathcal{K}_{\alpha'}}}. \tag{3.39}$$

In order to understand the behavior of the evolution operator for small Δt, we first note that, for instance by the techniques reviewed in [78, Section 4.3], it can be shown that, for any $\varphi \in \mathscr{S}$,

$$\varphi\left(\Phi_{\Delta t}(q,p)\right) = \varphi + \Delta t \mathcal{L}_{\mathrm{Ham}}\varphi + \frac{\Delta t^2}{2}\mathcal{L}^2_{\mathrm{Ham}}\varphi + \Delta t^3 R^{\mathrm{Verlet}}_{\Delta t}\varphi,$$

where $R^{\mathrm{Verlet}}_{\Delta t}\varphi$ grows at most polynomially in (q,p) uniformly in Δt. Therefore, by (3.38),

$$\tilde{P}^{\mathrm{Ham}}_{\Delta t}\varphi = \varphi + \Delta t \mathcal{L}_{\mathrm{Ham}}\varphi + \frac{\Delta t^2}{2}\mathcal{L}^2_{\mathrm{Ham}}\varphi + \Delta t^3 R^{\mathrm{Ham}}_{\Delta t}\varphi, \tag{3.40}$$

where the remainder

$$R^{\mathrm{Ham}}_{\Delta t}\varphi(q,p) = \left(1 - A^{\mathrm{Ham}}_{\Delta t}(q,p)\right)\Big(\varphi(q,-p) - \varphi(\Phi_{\Delta t}(q,p))\Big) + R^{\mathrm{Verlet}}_{\Delta t}\varphi(q,p).$$

grows at most polynomially in (q,p) uniformly in Δt.

3.3.2 Discretization of the fluctuation/dissipation

In order to construct a GHMC scheme for (2.4), we need to generate momenta distributed according to

$$\kappa(dp) = Z_\kappa^{-1} \mathrm{e}^{-\beta U(p)}\, dp, \tag{3.41}$$

which are then used as initial conditions in the Hamiltonian part of the scheme. This can be achieved through a discretization of the fluctuation-dissipation, corrected by a Metropolis procedure.

We use here a scheme proposed in [45] for the elementary dynamics (3.2). The proposal function is given by

$$\widetilde{p}^{n+1} = \Phi^{\mathrm{FD}}_{\Delta t}(p^n, G^n) = p^n - \gamma \nabla U\left(p^n + \frac{1}{2}\sqrt{\frac{2\gamma\Delta t}{\beta}}G^n\right)\Delta t + \sqrt{\frac{2\gamma\Delta t}{\beta}}G^n\,, \tag{3.42}$$

where $(G^n)_{n\geqslant 0}$ is a sequence of i.i.d. standard d-dimensional Gaussian random variables. It seems that the computation of the probability density of going from a given momentum p to a new one p' is difficult since $\Phi^{\mathrm{FD}}_{\Delta t}(p,G)$ depends nonlinearly on G. It turns out however that the proposal (3.42) can itself be interpreted as the output of some one-step HMC scheme, starting from a random conjugate variable $R^n := G^n/\sqrt{\beta} \in \mathbb{R}^d$

and for an effective timestep $h = \sqrt{2\gamma\Delta t}$:

$$\begin{cases} p^{n+1/2} = p^n + R^n \dfrac{h}{2}, \\ R^{n+1} = R^n - \nabla U(p^{n+1/2})h, \\ \widetilde{p}^{n+1} = p^{n+1/2} + R^{n+1}\dfrac{h}{2}. \end{cases} \tag{3.43}$$

The Hamiltonian dynamics which is discretized by this scheme is the one associated with the energy

$$E(p, R) = U(p) + \frac{1}{2}R^2.$$

Therefore, the acceptance rule for the proposal (3.42) is

$$A_{\Delta t}^{\mathrm{FD}}(p^n, G^n) = \min\left(1, \exp\left(-\beta\Big[E\left(\widetilde{p}^{n+1}, R^{n+1}\right) - E(p^n, R^n)\Big]\right)\right).$$

In summary, the new momentum is therefore given by

$$p^{n+1} = \Psi_{\Delta t}^{\mathrm{FD}}(p^n, G^n, \mathcal{U}^n) = p^n + \mathbb{1}_{\left\{\mathcal{U}^n \leqslant A_{\Delta t}^{\mathrm{FD}}(p^n, G^n)\right\}}\left(\Phi_{\Delta t}^{\mathrm{FD}}(p^n, G^n) - p^n\right). \tag{3.44}$$

For the same reason as in Remark 3.1, the efficiency of the Metropolization procedure of the fluctuation/dissipation does not degrade as the dimension increases in the case when the kinetic energy is a sum of individual contributions:

$$U(p) = \sum_{i=1}^{d} u(p_i).$$

In this case, the dynamics in each component can indeed be Metropolized independently of the other components.

In [45], the properties of the scheme (3.42) were studied for compact spaces. It is however possible to adapt some of the results obtained in this work when $U(p)$ and all its derivatives grow at most polynomially, and the marginal κ defined in (3.41) admits moments of all orders. In this case, the rejection rate scales as $\Delta t^{3/2}$ (which in fact can also be obtained directly from Lemma 3.3 for the effective timestep $h = \sqrt{2\gamma\Delta t}$). Moreover, since $\Phi_{\Delta t}^{\mathrm{FD}}(p, G)$ grows at most polynomially in (p, G) uniformly in Δt, the evolution operator

$$\begin{aligned} \tilde{P}_{\Delta t}^{\mathrm{FD}}\varphi(p) &= \mathbb{E}_{\mathcal{U},G}\left[\varphi\left(\Psi_{\Delta t}^{\mathrm{FD}}(p, G, \mathcal{U})\right)\right] \\ &= \mathbb{E}_G\left[A_{\Delta t}^{\mathrm{FD}}(p, G)\varphi\left(\Phi_{\Delta t}^{\mathrm{FD}}(p, G)\right)\right] + \left(1 - \mathbb{E}_G\left[A_{\Delta t}^{\mathrm{FD}}(p, G)\right]\right)\varphi(p), \end{aligned}$$

maps functions growing at most polynomially into functions growing at most polynomially: for any $\alpha \in \mathbb{N}$, there exist $\alpha' \in \mathbb{N}$ and $C_\alpha > 0$ such that

$$\forall f \in L^\infty_{\mathcal{K}_\alpha}, \qquad \left\|\tilde{P}_{\Delta t}^{\mathrm{FD}} f\right\|_{L^\infty_{\mathcal{K}_\alpha}} \leqslant C_\alpha \|f\|_{L^\infty_{\mathcal{K}_{\alpha'}}}. \tag{3.45}$$

Finally, the following weak-type expansion holds true by [45, Lemma 3]: for $\varphi \in \mathscr{S}$,

$$\tilde{P}^{\mathrm{FD}}_{\Delta t}\varphi = \varphi + \Delta t \mathcal{L}_{\mathrm{FD}}\varphi + \frac{\Delta t^2}{2}\mathcal{L}^2_{\mathrm{FD}}\varphi + \Delta t^{5/2} R^{\mathrm{FD}}_{\Delta t}\varphi, \tag{3.46}$$

where the remainder $R^{\mathrm{FD}}_{\Delta t}\varphi$ grows at most polynomially in (q,p) uniformly in Δt.

3.3.3 Complete Generalized Hybrid Monte-Carlo scheme

The complete scheme for the metropolized Langevin dynamics with general kinetic energy is obtained by concatenating the updates (3.33) and (3.44). Depending on whether Lie or Strang splittings are considered, and also on the order in which the operations are performed, several schemes can be considered. For instance, the scheme characterized by the evolution operator $P^{\mathrm{GHMC}}_{\Delta t} = P^{\mathrm{FD}}_{\Delta t} P^{\mathrm{Ham}}_{\Delta t}$ corresponds to first updating the momenta with (3.44), and then updating both positions and momenta according to (3.33).

All such splitting schemes preserve the invariant measure μ by construction. They are also all of weak order at least 1. A second weak order accuracy can however be obtained for Strang splittings, as made precise in the following lemma.

Lemma 3.4. *Consider* $P^{\mathrm{GHMC}}_{\Delta t} = \tilde{P}^{\mathrm{FD}}_{\Delta t/2}\tilde{P}^{\mathrm{Ham}}_{\Delta t}\tilde{P}^{\mathrm{FD}}_{\Delta t/2}$ *or* $P^{\mathrm{GHMC}}_{\Delta t} = \tilde{P}^{\mathrm{Ham}}_{\Delta t/2}\tilde{P}^{\mathrm{FD}}_{\Delta t}\tilde{P}^{\mathrm{Ham}}_{\Delta t/2}$. *Then, for any* $\varphi \in \mathscr{S}$, *there exist* $\Delta t^*, K, \alpha > 0$ *such that*

$$P^{\mathrm{GHMC}}_{\Delta t}\varphi = \varphi + \Delta t \mathcal{L}\varphi + \frac{\Delta t^2}{2}\mathcal{L}^2\varphi + \Delta t^{5/2} r_{\Delta t,\varphi}, \tag{3.47}$$

where $\sup_{0<\Delta t\leqslant \Delta t^*} \|r_{\Delta t,\varphi}\|_{L^\infty_{\mathcal{K}_\alpha}} \leqslant K$.

Proof. This result is a direct consequence of the estimates (3.40)-(3.46). We however sketch the proof for completeness. Fix $\varphi \in \mathscr{S}$. In view of (3.46),

$$\tilde{P}^{\mathrm{FD}}_{\Delta t/2}\tilde{P}^{\mathrm{Ham}}_{\Delta t}\tilde{P}^{\mathrm{FD}}_{\Delta t/2}\varphi = \tilde{P}^{\mathrm{FD}}_{\Delta t/2}\tilde{P}^{\mathrm{Ham}}_{\Delta t}\widetilde{\varphi} + \Delta t^{5/2}\tilde{P}^{\mathrm{FD}}_{\Delta t/2}\tilde{P}^{\mathrm{Ham}}_{\Delta t}R^{\mathrm{FD}}_{\Delta t}\varphi,$$

where

$$\widetilde{\varphi} = \left(\mathrm{Id} + \frac{\Delta t}{2}\mathcal{L}_{\mathrm{FD}} + \frac{\Delta t^2}{8}\mathcal{L}^2_{\mathrm{FD}}\right)\varphi \in \mathscr{S}.$$

The remainder $\tilde{P}^{\mathrm{FD}}_{\Delta t/2}\tilde{P}^{\mathrm{Ham}}_{\Delta t}R^{\mathrm{FD}}_{\Delta t}\varphi$ grows at most polynomially in (q,p) uniformly in Δt by (3.39)- (3.45). We next use (3.40) to write

$$\tilde{P}^{\mathrm{FD}}_{\Delta t/2}\tilde{P}^{\mathrm{Ham}}_{\Delta t}\widetilde{\varphi} = \tilde{P}^{\mathrm{FD}}_{\Delta t/2}\widehat{\varphi} + \Delta t^3\tilde{P}^{\mathrm{FD}}_{\Delta t/2}R^{\mathrm{Ham}}_{\Delta t}\widetilde{\varphi},$$

where

$$\widehat{\varphi} = \left(\mathrm{Id} + \Delta t\mathcal{L}_{\mathrm{Ham}} + \frac{\Delta t^2}{2}\mathcal{L}^2_{\mathrm{Ham}}\right)\left(\mathrm{Id} + \frac{\Delta t}{2}\mathcal{L}_{\mathrm{FD}} + \frac{\Delta t^2}{8}\mathcal{L}^2_{\mathrm{FD}}\right)\varphi \in \mathscr{S}.$$

The remainder $\tilde{P}^{\rm FD}_{\Delta t/2} R^{\rm Ham}_{\Delta t} \widetilde{\varphi}$ grows at most polynomially in (q,p) uniformly in Δt by (3.45). By applying again (3.46), we finally obtain that

$$\tilde{P}^{\rm FD}_{\Delta t/2} \tilde{P}^{\rm Ham}_{\Delta t} \tilde{P}^{\rm FD}_{\Delta t/2} \varphi = \Delta t^{5/2} \mathcal{R}_{\Delta t,\varphi} + \left({\rm Id} + \frac{\Delta t}{2} \mathcal{L}_{\rm FD} + \frac{\Delta t^2}{8} \mathcal{L}^2_{\rm FD} \right) \left({\rm Id} + \Delta t \mathcal{L}_{\rm Ham} + \frac{\Delta t^2}{2} \mathcal{L}^2_{\rm Ham} \right) \left({\rm Id} + \frac{\Delta t}{2} \mathcal{L}_{\rm FD} + \frac{\Delta t^2}{8} \mathcal{L}^2_{\rm FD} \right) \varphi,$$

where the remainder $\mathcal{R}_{\Delta t,\varphi}$ grows at most polynomially in (q,p) uniformly in Δt. The conclusion follows by expanding the last term on the right-hand side, grouping together terms of order Δt and Δt^2, and gathering the higher order terms in the remainder.

As corollary of the weak error expansion (3.47), error estimates on dynamical properties such as integrated correlation functions can be deduced with the techniques from [78] provided an exponential convergence of $(P^{\rm GHMC}_{\Delta t})^n \varphi$ towards $\mathbb{E}_\mu(\varphi)$ is proved in the spaces $L^\infty_{\mathcal{K}_\alpha}$, with a rate depending on the physical time $n\Delta t$, uniformly in Δt. A typical way to obtain such estimates is to establish a Lyapunov condition for the functions $\mathcal{K}_\alpha$ and a minorization condition on a compact space, in order to apply the results from [89, 54]. Although we were able to prove a minorization condition in the case when $U - U_{\rm std}$ is bounded and the position space $\mathcal{D}$ is compact (see Section 3.5.3), we were not able to establish a Lyapunov condition (see Section 3.5.4). The problem is that, even for compact position spaces and standard, quadratic kinetic energies, the rejection rate of the fluctuation/dissipation part of the scheme degenerates as $|p| \to +\infty$. Such difficulties were already encountered in the study of Metropolized Langevin-type algorithms on unbounded spaces, where the problem was taken care of by an appropriate truncation of the accessible space [22].

3.4 Adaptively restrained Langevin dynamics

The aim of this section is to devise better kinetic energy functions for the AR-Langevin dynamics, allowing for larger timesteps in the simulations. In Section 3.4.1, for ease of reading, we recall the kinetic energy function used in the original AR-Langevin dynamics that we have introduced in Section 1.5 and we also propose an alternative kinetic energy function. The relevance of this alternative energy function is studied in Section 3.4.2, where we use the rejection rates of the GHMC algorithm to quantify the stability of the schemes under consideration. In essence, we fix an admissible rejection rate, and find the largest timestep for which the rejection is lower or equal to this tolerance.

3.4.1 Kinetic energy functions for AR Langevin

In AR Langevin, the standard kinetic energy is replaced by a kinetic energy which vanishes for small values of momenta and matches the standard kinetic energy for sufficiently large values of momenta. The transition between these two regions is made in the original model [9] by an interpolation spline $s_{\rm org}$ which ensures the regularity of the transition on the kinetic energy itself. More precisely, introducing two energy parameters $0 < e_{\min} < e_{\max}$,

$$U_{\mathrm{org}}(p) = \sum_{i=1}^{N} u(p_i) \quad \text{where} \quad u(p_i) = \begin{cases} 0 & \text{for} \quad \dfrac{p_i^2}{2m_i} \leqslant e_{\min}, \\ s_{\mathrm{org}}\left(\dfrac{p_i^2}{2m_i}\right) & \text{for} \quad \dfrac{p_i^2}{2m_i} \in [e_{\min}, e_{\max}], \\ \dfrac{p_i^2}{2m_i} & \text{for} \quad \dfrac{p_i^2}{2m_i} \geqslant e_{\max}. \end{cases} \tag{3.48}$$

The function s_{org} is such that $x \mapsto s_{\mathrm{org}}(x)\, \mathbb{1}_{x \in [e_{\min}, e_{\max}]} + x\, \mathbb{1}_{x > e_{\max}}$ is C^2. The original AR-Langevin kinetic energy was motivated by some physical interpretation in terms of momentum-dependent masses. One unpleasant feature of the definition (3.48) is that the derivatives ∇U which appear in the dynamics (2.4) are typically large at the transition points (see Figure 3.3b). Since the dynamics is determined by ∇U, a more satisfactory approach seems to interpolate the kinetic force ∇U between 0 in the region of small momenta and $M^{-1}p$ in the region of large momenta. We introduce to this end a second spline function s_{new} and define, for two velocity parameters $0 < e_{\min} < e_{\max}$,

$$U_{\mathrm{new}}(p) = \sum_{i=1}^{d} u(p_i) \quad \text{where} \quad u(p_i) = \begin{cases} S_{e_{\min} e_{\max}} \text{ for} & \dfrac{|p_i|}{m_i} \leqslant e_{\min}, \\ s_{\mathrm{new}}\,(p_i) \text{ for} & \dfrac{|p_i|}{m_i} \in [e_{\min}, e_{\max}], \\ \dfrac{p_i^2}{2m_i} \text{ for} & \dfrac{|p_i|}{m_i} \geqslant e_{\max} \end{cases} \tag{3.49}$$

where $S_{e_{\min} e_{\max}}$ is a constant ensuring the continuity of the kinetic energy. Figure 3.3a represents the alternative kinetic energy (3.49) as a function of the momenta for various choices of the parameters. Figure 3.3b compares the derivatives of the original and new kinetic energies. Note that the alternative kinetic energy (3.49) leads to a smaller maximal value of the kinetic force ∇U than the original AR kinetic energy (3.48). This is also true for higher order derivatives of U.

It is difficult to directly compare the canonical distributions of momenta associated with U_{org} and U_{new}. For instance, it is not possible in general to ensure that these two distributions coincide for small and large momenta, because of the normalization constant in the probability distribution. In the sequel, we consider $e_{\min} = m_i e_{\min}^2/2$ and $e_{\max} = m_i e_{\max}^2/2$ for the ith particle, in order to have a constant kinetic energy (resp. a standard kinetic energy) in the same energy intervals.

3.4.2 Determining the best kinetic energy function

Since the AR-kinetic energy in general has derivatives larger than the ones of the standard kinetic energy, the timestep should be reduced in order to preserve the stability of the numerical method. We characterize in this section the possible reduction of the timestep due to the modification of the kinetic energy. As described in Section 3.3.3, we metropolize the AR-Langevin dynamics by first integrating the Hamiltonian with (3.33) and then the fluctuation-dissipation part with (3.44). This corresponds to the evolution operator $P_{\Delta t}^{\mathrm{GHMC}} = \tilde{P}_{\Delta t}^{\mathrm{Ham}} \tilde{P}_{\Delta t}^{\mathrm{FD}}$.

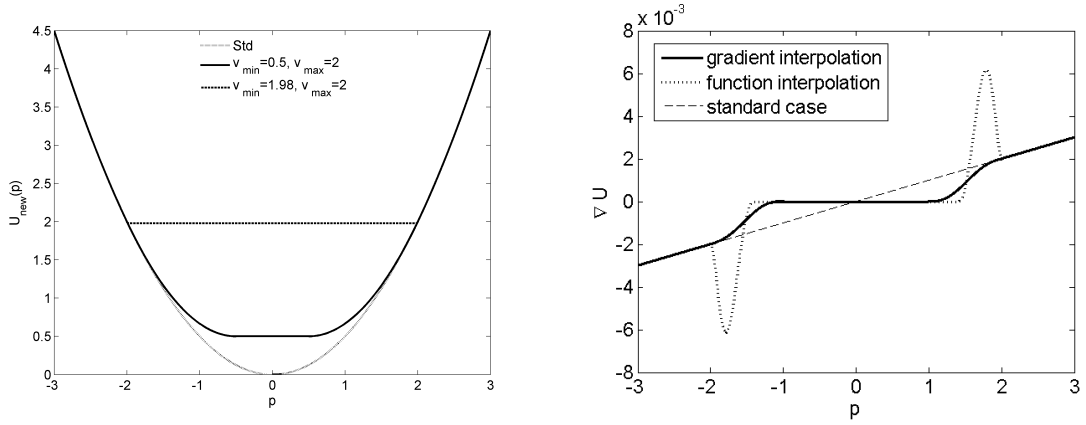

(a) The AR-kinetic energy function (3.49) for various choice of parameters $e_{\min}$ and $e_{\max}$.

(b) Gradient interpolation of the kinetic energy ($U_{\rm new}$) versus function interpolation ($U_{\rm org}$).

Fig. 3.3: Comparison between the AR-kinetic energy function (3.49) and the original AR kinetic energy (3.48).

Recall that the average rejection rate of the Hamiltonian and fluctuation/dissipation parts, namely (with expectations over $(q,p) \sim \mu$ and over the random variables $G, \mathcal{U}$ used in the updates)

$$\mathcal{R}^{\rm Ham}(\Delta t) := \mathbb{E}\left(1 - A^{\rm Ham}_{\Delta t}\right), \qquad \mathcal{R}^{\rm FD}(\Delta t) := \mathbb{E}\left[1 - A^{\rm FD}_{\Delta t}(\Psi(p,G,\mathcal{U}))\right],$$

respectively scale as Δt^3 and $\Delta t^{3/2}$ (see Lemma 3.3). We consider three kinds of AR-kinetic energies: the original function interpolation (3.48), and two interpolation functions (3.49) based on the gradient. More precisely, we either choose a linear spline or a C^2 spline by a polynomial of order 5 on the gradient ∇U. The corresponding kinetic energies are respectively C^2 and C^3. The aim is to check the scaling of the rejection rates in terms of powers of Δt, and to estimates the prefactors for the various kinetic energies.

We consider a system of 64 particles of mass $m_i = 1$ in a three dimensional periodic box with particle density $\rho = 0.56$. The particles interact by a purely repulsive WCA pair potential, which is a truncated Lennard-Jones potential [115]:

$$V_{\rm WCA}(r) = \begin{cases} 4\varepsilon_{\rm LJ}\left[\left(\frac{\sigma_{\rm LJ}}{r}\right)^{12} - \left(\frac{\sigma_{\rm LJ}}{r}\right)^{6}\right] + \varepsilon_{\rm LJ} & \text{if } r \leqslant r_0, \\ 0 & \text{if } r > r_0, \end{cases}$$

where r denotes the distance between two particles, $\varepsilon_{\rm LJ}$ and $\sigma_{\rm LJ}$ are two positive parameters and $r_0 = 2^{1/6}\sigma_{\rm LJ}$. In our simulations the parameters of the potential are set to $\varepsilon_{\rm LJ} = 1, \sigma_{\rm LJ} = 1$, while the parameters of the AR-Langevin dynamics (2.4) are set to $\gamma = 1, \beta = 1$.

Figure 3.4 shows the average rejection rates for the AR parameters $e_{\max} = 2$ and $e_{\min} = 1$ for $U_{\rm new}$, as well as $e_{\max} = 2$ and $e_{\min} = 0.5$ for $U_{\rm org}$. This choice of parameters corresponds to $\sim 30\%$ percent of particles which are frozen for both AR-kinetic energies, *i.e.* which are in the region where ∇U

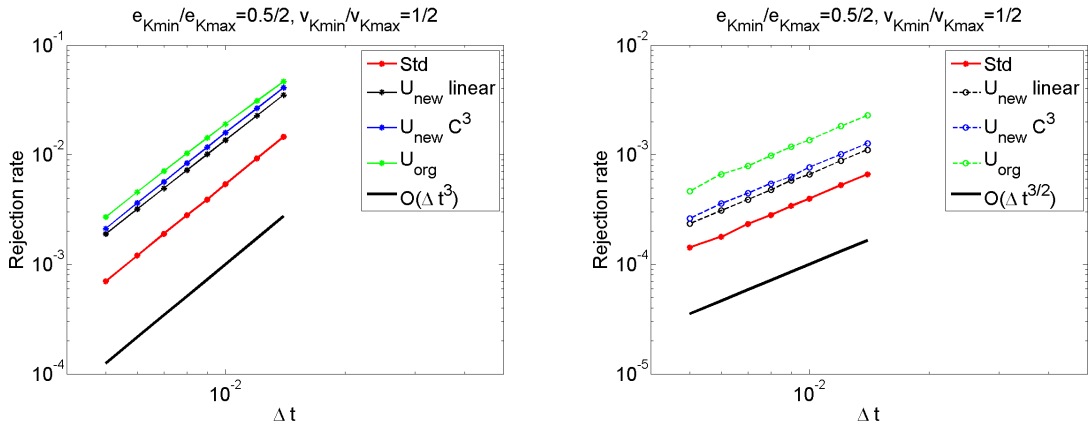

(a) Hamiltonian part

(b) Fluctuation-dissipation part.

Fig. 3.4: Average rejection rates of GHMC as a function of the timestep for various kinetic energies (see text). The scaling of the rejection rates corresponds to the predicted orders, *i.e.* Δt^3 for the Hamiltonian part and $\Delta t^{3/2}$ for the fluctuation-dissipation part.

vanishes (see [120] for a thorough discussion on the link between the percentage of frozen particles and the algorithmic speed-up). Note that the predicted scalings of the rejection rates are recovered in all cases. The prefactor is however larger for the kinetic energy U_{org} from [9] than for U_{new}, especially for the fluctuation-dissipation part. The prefactor is also slightly smaller for the kinetic energy based on the gradient interpolation with a linear function, which is fortunate since ∇U has a lower computational cost than for interpolations based on higher order splines.

In order to quantify the dependence of the prefactors in the rejection rate on the concrete choice of the parameters in the kinetic energy function, we compute the relative deviation of the prefactor from the reference provided by simulations with the standard kinetic energy. Figure 3.5 plots for various values of the parameter e_{min} (for fixed $e_{\text{max}} = 2$) the relative deviation between the prefactors inferred from simulation results such as the ones presented in Figure 3.4. To this end, we perform a least-square fit in a log-log scale to determine the prefactor C such that the rejection rate is approximately equal to $C\Delta t^{\alpha}$ (with $\alpha = 3$ for the Hamiltonian part, and $\alpha = 3/2$ for the fluctuation/dissipation). For each value of the parameters, we compute the relative variation of the prefactor with respect to the reference prefactor C_{std} provided by the rejection rate obtained for the standard kinetic energy:

$$\delta C = \frac{C}{C_{\text{std}}} - 1.$$

The relative variation δC depends on the parameters $e_{\text{min}}, e_{\text{max}}$ (or $e_{\text{min}}, e_{\text{max}}$, depending on the context). As $e_{\text{min}} \to e_{\text{max}}$, the derivatives of the kinetic energy function have larger absolute values (recall Figure 3.3b). The dynamics is therefore less stable, which translates into larger values of the prefactor in the rejection rate as e_{min} increases (see Figure 3.5). Moreover, the relative increase of the prefactor is larger for U_{org} than for

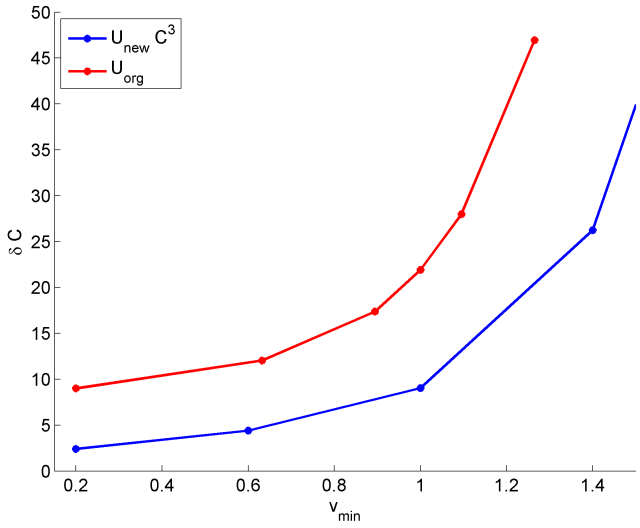

Fig. 3.5: Relative deviation of the prefactor in the scaling of the average rejection for the Hamiltonian part as a function of the timestep Δt. The data is extracted from the results presented in Figure 3.4a.

U_{new}. In conclusion, the new definition of the AR-kinetic energy improves the numerical properties of the method, as demonstrated by a smaller prefactor in the rejection rate of the GHMC scheme.

We are now in a position to determine the variations in the admissible timesteps as a function of the kinetic energies. To this end, we fix a rejection rate for the Hamiltonian part since this subdynamics mixes information in the positions and momenta, and involves the forces $-\nabla V(q)$ which are often the cause of the stability limitations. Similar results are however obtained for the fluctuation/dissipation part, see Figure 3.7.

In our tests, we set the target rejection rate to two values: $\mathcal{R}^{\text{Ham}}(\Delta t) \in \{0.001, 0.5\}$. Figure 3.6 presents the timesteps Δt achieving the desired rejection rates (normalized by Δt_{std}, the timestep corresponding to the given rejection rate for the standard quadratic energy), for the kinetic energy U_{new} (with an interpolation spline such that $U_{\text{new}} \in C^3$) and for various values of the parameters. We observe that the timestep should be reduced with respect to the standard case when the transition becomes somewhat sharper, *i.e.* for δ approaching 1. Surprisingly, we observe that for smaller values of δ, the timestep can in fact be increased compared to standard Langevin dynamics.

3.5 Some additional proofs

3.5.1 Proof of Lemma 3.2

We follow the proof from [78] which is based on a Lyapunov condition which is uniform in the timestep and a minorization condition [85]. We start by proving a Lyapunov condition, *i.e.* for any $s^* \in \mathbb{N}$ there exists $\Delta t > 0$ small enough and constants $C_a, C_b > 0$ such that, for any $1 \leqslant s \leqslant s^*$,

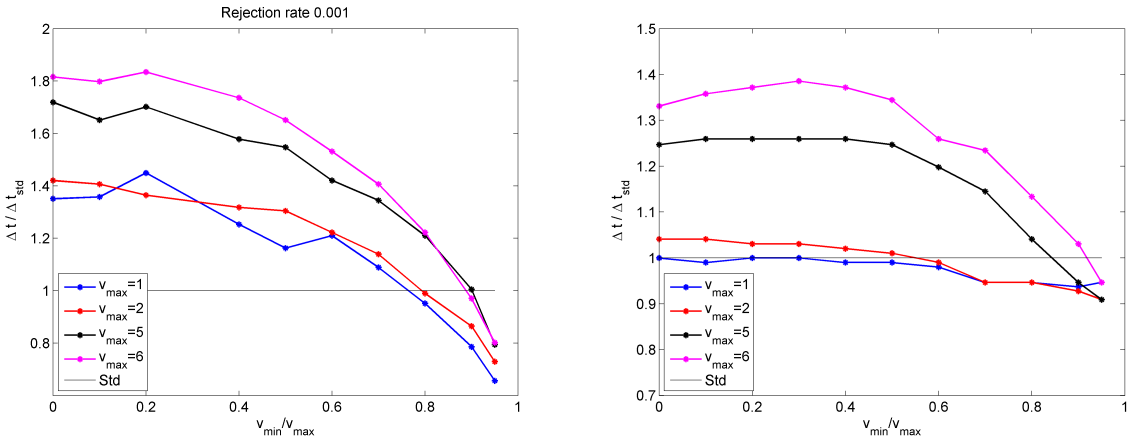

(a) Rejection rate fixed at 0.001

(b) Rejection rate fixed at 0.5

Fig. 3.6: Timesteps normalized by Δt_{std} (the time step corresponding to the same rejection rate for the standard kinetic energy) corresponding to a fixed rejection rate in the Hamiltonian part for various values of $\delta = v_{\min}/v_{\max}$ and the kinetic energy (3.49).

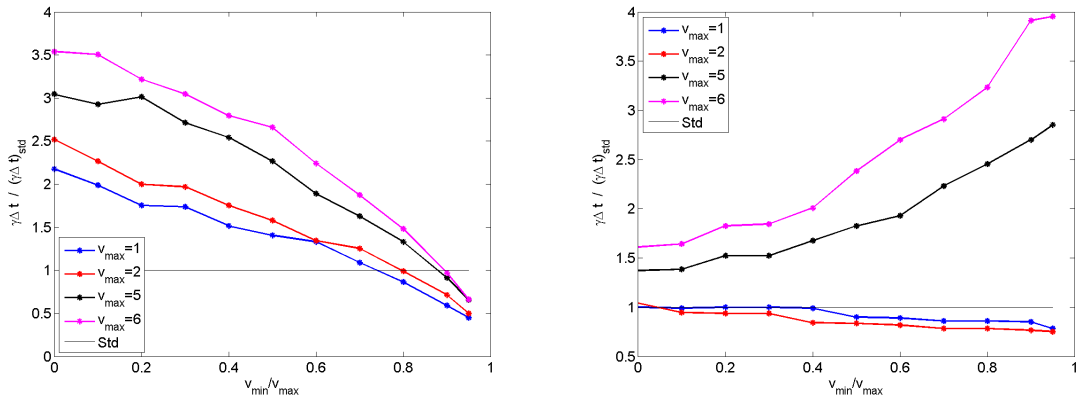

(a) Rejection rate fixed at 0.001

(b) Rejection rate fixed at 0.5

Fig. 3.7: Timesteps corresponding to a fixed rejection rate in the fluctuation-dissipation part for various values of $\delta = v_{\min}/v_{\max}$ and the kinetic energy (3.49).

$$P_{\Delta t}\mathcal{K}_s \leqslant \mathrm{e}^{-C_a\Delta t}\mathcal{K}_s + C_b\Delta t.$$

Recall that Z is such that there exists $\mathscr{Z} > 0$ such that $\|Z\|_{L^\infty} \leqslant \mathscr{Z}$ and that the standard dynamics corresponds to $U_{\mathrm{std}}(p) = p^T M^{-1} p$. We define $m > 0$ such that $m \leqslant M \leqslant m^{-1}$. We compute

$$\begin{aligned}\mathbb{E}\left[\left(p^{n+1}\right)^2\right] &\leqslant \alpha^2 (p^n)^2 + 2\alpha\gamma\mathscr{Z}\Delta t p^n + \gamma^2\mathscr{Z}^2\Delta t^2 + \frac{1}{\beta}\mathrm{Tr}\left[\left(1-\alpha_{\Delta t}^2\right)M^2\right] \\ &\leqslant \left(\varepsilon\gamma\Delta t + \alpha^2\right)(p^n)^2 + \left(\frac{\gamma\Delta t}{\varepsilon}\alpha^2 + \gamma^2\Delta t^2\right)\mathscr{Z}^2 + \frac{1-\alpha_{\Delta t}^2}{\beta m^2}\end{aligned}$$

where we used the Young inequality. The choice $\varepsilon = m$ ensures, for Δt sufficiently small, that

$$\left(\varepsilon\gamma\Delta t + \mathrm{e}^{-2m\gamma\Delta t}\right) \leqslant \mathrm{e}^{-C_a\Delta t}, \text{ with } C_a = \frac{\gamma m}{2}.$$

Moreover, there exists $C_b > 0$ such that

$$\left(\frac{\gamma\Delta t}{m}\alpha^2 + \gamma^2\Delta t^2\right)\mathscr{Z}^2 + \frac{1-\alpha_{\Delta t}^2}{\beta m^2} \leqslant C_b\Delta t.$$

for $C_b > 0$. Hence, there exists $C_a \in (0,1)$ and $C_b > 0$ such that

$$P_{\Delta t}\mathcal{K}_s(p^{n+1}) = \mathbb{E}\left[\mathcal{K}_s(p^{n+1}) \mid \mathcal{F}_n\right] \leqslant \mathrm{e}^{-C_a\Delta t}\mathcal{K}_s + C_b\Delta t. \tag{3.50}$$

Following the same approach as in [78], the corresponding estimates can be obtained for a general power $s \geqslant 2$. We also omit the minorization condition, since it can be obtained by combining the proof for the minorization condition in [78] by using the same approach as in proof of Lemma 2.1, where the minorizing measure is constructed by comparing the modified dynamics with the standard dynamics with zero forces. The key point here is that the additional perturbations $\Delta t\sum_{i=1}^n Z(p_i)$ (for $n\Delta t \leqslant T$) are bounded (see Section 3.5.2.1).

3.5.2 Ergodicity of non-metropolized schemes

We prove the ergodicity of a scheme which is a proposal for the GHMC scheme, because we use it in the proof for the metropolized scheme. More precisely, we consider

$$\begin{cases} p^{n+1/2} = p^n - \nabla V(q^n)\dfrac{\Delta t}{2}, \\ \widetilde{q}^{n+1} = q^n + \nabla U(p^{n+1/2})\Delta t, \\ \widetilde{p}^{n+1} = p^{n+1/2} - \nabla V(\widetilde{q}^{n+1})\dfrac{\Delta t}{2}. \\ p^{n+1} = \widetilde{p}^{n+1} - \gamma\nabla U\left(\widetilde{p}^{n+1} + \dfrac{1}{2}\sqrt{\dfrac{2\gamma\Delta t}{\beta}}G^n\right)\Delta t + \sqrt{\dfrac{2\gamma\Delta t}{\beta}}G^n\,. \end{cases} \tag{3.51}$$

The evolution operator of this scheme reads

$$P_{\Delta t} = P_{\Delta t}^{\mathrm{FD}} P_{\Delta t}^{\mathrm{Ham}}$$

where $P_{\Delta t}^{\mathrm{FD}}$ is the evolution operator of the scheme (3.42) and $P_{\Delta t}^{\mathrm{Ham}}$ corresponds to (3.31). This scheme has order 1 due to the first order scheme used for an integration of the fluctuation-dissipation part. However, the proof can be easily extended in order to prove the ergodicity of a second order scheme such as (3.22), where the fluctuation-dissipation part is integrated by, for instance, (3.17).

3.5.2.1 Minorization condition

Recall the definition of the perturbation function Z in (3.7). The position and momenta updates obtained by the scheme given by (3.42) and (3.31) can be written as

$$\begin{aligned}\tilde{q}^{n+1} &= q^n + \frac{p^n}{m}\Delta t + Z(\tilde{p}^{n+1})\Delta t - \frac{1}{2}\nabla V(q^n)\Delta t \\ &= q^0 + \frac{\Delta t}{m}\sum_{k=0}^{n} p^n + \Delta t \sum_{k=0}^{n} Z(\tilde{p}^{k+1}) - \frac{1}{2}\Delta t \sum_{k=0}^{n} \nabla V(q^k)\end{aligned}$$

and

$$\begin{aligned}\tilde{p}^{n+1} &= \left(1 - \frac{\gamma\Delta t}{m}\right) p^n - \Delta t \left(1 - \frac{\gamma\Delta t}{m}\right) \nabla V\left(q^{n+1}\right) - \gamma\Delta t Z(\hat{p}^{n+1}) + \frac{1}{2}\sqrt{\frac{2\gamma\Delta t}{\beta}}\,(1+\alpha)\,G^n \\ &= \alpha^n p^0 + \Delta t \sum_{k=0}^{n} \alpha^{n-k}\nabla V(q^k) - \gamma\Delta t \sum_{k=0}^{n} \alpha^{n-1-k} Z(\hat{p}^k) + \frac{1}{2}\sqrt{\frac{2\gamma\Delta t}{\beta}}\,(1+\alpha)\sum_{k=0}^{n}\alpha^{n-1-k}G^k,\end{aligned}$$

where we introduced the notation $\alpha := 1 - \frac{\gamma\Delta t}{m}$. We write

$$\tilde{p}^n = \mathscr{P}^n + \mathscr{G}_p^n, \quad \tilde{q}^n = \mathscr{D}^n + \mathscr{G}_q^n, \tag{3.52}$$

with

$$\begin{aligned}\mathscr{P}^n &:= \alpha^n p^0 + \Delta t \sum_{k=0}^{n-1} \alpha^{n-k}\nabla V(q^k) - \gamma\Delta t \sum_{k=0}^{n-1} \alpha^{n-1-k} Z(\hat{p}^k), \\ \mathscr{D}^n &:= q^0 + \frac{\Delta t}{m}\sum_{k=0}^{n-1} \mathscr{P}^k + \Delta t \sum_{k=0}^{n-1} Z(\tilde{p}^{k+1}) - \frac{1}{2}\Delta t \sum_{k=0}^{n-1} \nabla V(q^k),\end{aligned}$$

and the two centered Gaussian variables

$$\begin{aligned}\mathscr{G}_p^n &:= \frac{1}{2}\sqrt{\frac{2\gamma\Delta t}{\beta}}\,(1+\alpha)\sum_{k=0}^{n-1}\alpha^{n-1-k}G^k, \\ \mathscr{G}_q^n &:= \frac{\Delta t}{m}\sum_{k=1}^{n-1}\mathscr{G}_p^k.\end{aligned} \tag{3.53}$$

Note that $\mathscr{P}^n$ and $\mathscr{D}^n$ are uniformly bounded.

The variance of the centered Gaussian vector $(\mathscr{G}_q, \mathscr{G}_p)$ reads

$$\mathcal{V}^n = \mathbb{E}_{G_R}\left[(\mathscr{G}_q, \mathscr{G}_p)^T (\mathscr{G}_q, \mathscr{G}_p)\right] = \begin{pmatrix} \mathcal{V}_{qq}^n & \mathcal{V}_{qp}^n \\ \mathcal{V}_{pq}^n & \mathcal{V}_{pp}^n \end{pmatrix}, \tag{3.54}$$

where

$$\begin{cases} \mathcal{V}_{qq}^n = \xi^2 \dfrac{\Delta t^2}{m^2} \displaystyle\sum_{k=0}^{n-2} \left(\sum_{j=0}^{k} \alpha^j \right)^2 \\ \mathcal{V}_{qp}^n = \xi^2 \dfrac{\Delta t}{m} \dfrac{1}{1-\alpha} \displaystyle\sum_{k=1}^{n-1} \alpha^k - \alpha^{2k-2} \\ \mathcal{V}_{pp}^n = \xi^2 \displaystyle\sum_{k=0}^{n-1} \alpha^{2(n-1-k)}, \end{cases}$$

with $\xi := \frac{1}{2}\sqrt{\frac{2\gamma\Delta t}{\beta}}\,(1+\alpha)$. A simple computation allows to verify that for a fixed $T > 0$ and $n = \lfloor T/\Delta t \rfloor$, the limit $\Delta t \to 0$ corresponds to the variance $\mathcal{V}^{\mathrm{cont}}$ of the limiting continuous process, which is given by (see [78])

$$\begin{cases} \mathcal{V}_{qq}^{\mathrm{cont}} = \dfrac{1}{\beta\gamma}\left(2T - \dfrac{M}{\gamma}\left(3 - 4\tilde{\alpha}_T + \tilde{\alpha}_T^2\right)\right), \\ \mathcal{V}_{qp}^{\mathrm{cont}} = \dfrac{M}{\gamma\beta}\left(1 - \tilde{\alpha}_T\right)^2, \\ \mathcal{V}_{pp}^{\mathrm{cont}} = \dfrac{M}{\beta}\left(1 - \tilde{\alpha}_T^2\right), \end{cases}$$

where we denote $\tilde{\alpha}_T := \mathrm{e}^{-\frac{\gamma T}{m}}$.

There exists $\Delta t^* > 0$ such that for any $0 < \Delta t \leqslant \Delta t^*$ and $n = \lfloor T/\Delta t \rfloor$ the variance $\mathcal{V}^n$ in (3.54) satisfies $\mathcal{V}^n \geqslant \mathcal{V}^{\mathrm{cont}}/2 > 0$. By following the approach from [78] that there exists a probability measure ν and $\kappa > 0$, such that for any Borel set $A \subset \mathcal{E}$,

$$\mathbb{P}\left((\tilde{q}^n, \tilde{p}^n) \in A \middle| \left|p^0\right| \leqslant p^*\right) = \mathbb{P}\left((\mathscr{G}_q^n, \mathscr{G}_p^n) \in \left(A_q - \mathscr{D}^n, A_p^n - \mathscr{P}^n\right) \middle| \left|p^0\right| \leqslant p^*\right) \geqslant \kappa\nu(A). \tag{3.55}$$

3.5.2.2 Lyapunov condition

We prove the Lyapunov condition for the fluctuation-dissipation part: there exists $C_a \in (0,1)$ and $c > 0$ such that

$$P_{\Delta t}\mathcal{K}_s(p^{n+1}) = \mathbb{E}\left[\mathcal{K}_s(p^{n+1}) \mid \mathcal{F}_n\right] \leqslant \mathrm{e}^{-C_a\Delta t}\mathcal{K}_s + c\Delta t. \tag{3.56}$$

We again show the case $s = 2$ only, since the generalization to $s \geqslant 2$ follows by the same arguments as in [78].

We write

$$\mathbb{E}\left(\left(\Phi_{\Delta t}^{\mathrm{FD}}(p, G)\right)^2\right) \leqslant \left[\left(1 - \frac{\gamma\Delta t}{m}\right)^2 + \varepsilon\Delta t\right] p^2 + \frac{2\gamma\Delta t}{\beta} + \gamma^2 \mathscr{Z}^2 \Delta t \left(\frac{9}{4\varepsilon} + \Delta t\right).$$

For the Hamiltonian part, we write

$$\Phi_{\Delta t}^{\mathrm{Ham}}(q,p) = p - \nabla V(q)\frac{\Delta t}{2} - \nabla V\left(q + \left(\left(p - \frac{1}{2}\nabla V(q)\Delta t\right)\frac{1}{m} + Z\left(p - \frac{1}{2}\nabla V(q)\Delta t\right)\right)\Delta t\right)\frac{\Delta t}{2}$$

and we obtain

$$\left(\Phi_{\Delta t}^{\mathrm{Ham}}(q^n,p^n)\right)^2 \leqslant (1+\tilde{\varepsilon}\Delta t)(p^n)^2 + \|\nabla V\|_{L^\infty}^2 \Delta t^2 + \|\nabla V\|_{L^\infty}^2 \Delta t \tilde{\varepsilon}^{-1}$$
$$\leqslant (1+\tilde{\varepsilon}\Delta t)(p^n)^2 + C_{\mathrm{Ham}}\Delta t.$$

We conclude that the Lyapunov condition is satisfied for (3.51) since we find $\varepsilon, \tilde{\varepsilon} > 0$ such that $(1+\tilde{\varepsilon}\Delta t)\mathrm{e}^{-C_a\Delta t} \leqslant \mathrm{e}^{-\tilde{C}_a\Delta t}$ with $\tilde{C}_a > 0$ which gives

$$P_{\Delta t}^{\mathrm{Ham}} P_{\Delta t}^{\mathrm{FD}} \mathcal{K}_2 \leqslant (1+\tilde{\varepsilon}\Delta t) P_{\Delta t}^{\mathrm{FD}} \mathcal{K}_2 + C_{\mathrm{Ham}}\Delta t \leqslant (1+\tilde{\varepsilon}\Delta t)\mathrm{e}^{-C_a\Delta t}\mathcal{K}_2 + C_{\mathrm{Ham}}\Delta t \leqslant \mathrm{e}^{-\tilde{C}_a\Delta t}\mathcal{K}_2 + C_{\mathrm{Ham}}\Delta t$$

for $\mathcal{K}_2(p) := 1 + |p|^2$.

3.5.3 Minorization condition for the GHMC scheme

Recall that the position space $\mathcal{D}$ is compact. For the metropolized scheme, we rely on the minorization condition obtained for the un-metropolized scheme in Section 3.5.2.1. More precisely, starting from $\left|p^0\right| \leqslant p^*$, the probability that a metropolized trajectory reaches the set A in n steps is bounded from below by requiring that no rejection occurs (hence the trajectory is the same as the one obtained without metropolization), and that the momenta remain in a compact set (which allows to uniformly bound the rejection rate). We introduce, for $R \geqslant p^*$,

$$B_R = \left\{ p \in \mathbb{R}^d \,\middle|\, |p| \leqslant R \right\},$$

and denote by $\mathcal{N}_n$ the random variable counting the number of rejections until the nth step (both in the fluctuation/dissipation part and in the Hamiltonian part). For a given measurable set $\mathcal{A}$ and $\left|p^0\right| \leqslant p^*$, we therefore consider a lower bound on the probability $\mathbb{P}\left((q^n,p^n) \in \mathcal{A} \mid \left|p^0\right| \leqslant p^*\right)$ corresponding to the additional conditions $\mathcal{N}_n = 0$ and $p^k \in B_R$ at all steps $0 \leqslant k \leqslant n$:

$$\begin{aligned}
&\mathbb{P}\left((q^n,p^n) \in \mathcal{A} \mid \left|p^0\right| \leqslant p^*\right) \\
&\geqslant \mathbb{P}\left((q^n,p^n) \in \mathcal{A},\, \mathcal{N}_n = 0,\, (p^0,\dots,p^n) \in B_R^{n+1} \,\middle|\, \left|p^0\right| \leqslant p^*\right) \\
&= \mathbb{P}\left((\tilde{q}^n,\tilde{p}^n) \in \mathcal{A},\, \mathcal{N}_n = 0,\, (\tilde{p}^0,\dots,\tilde{p}^n) \in B_R^{n+1} \,\middle|\, \left|p^0\right| \leqslant p^*\right) \\
&= \mathbb{P}\left((\tilde{q}^n,\tilde{p}^n) \in \mathcal{A},\, (\tilde{p}^0,\dots,\tilde{p}^n) \in B_R^{n+1} \,\middle|\, \left|p^0\right| \leqslant p^*\right) \mathbb{P}\left(\mathcal{N}_n = 0 \,\middle|\, (\tilde{q}^n,\tilde{p}^n) \in \mathcal{A},\, (\tilde{p}^0,\dots,\tilde{p}^n) \in B_R^{n+1},\, \left|p^0\right| \leqslant p^*\right).
\end{aligned} \tag{3.57}$$

The last term can be estimated by using the expression of the rejection rate and the fact that the variables remain in a compact set: there exists $C_R \in \mathbb{R}_+$ such that

$$0 \leqslant 1 - \max_{(\tilde{q},\tilde{p}) \in \mathcal{D}\times B_R} A^{\mathrm{FD}}(\tilde{q},\tilde{p}) \leqslant C_R^{\mathrm{FD}} \Delta t^{3/2}.$$

and $C_R^{\mathrm{Ham}} \in \mathbb{R}_+$ such that

$$0 \leqslant 1 - \max_{(\tilde{q},\tilde{p}) \in \mathcal{D}\times B_R} A^{\mathrm{Ham}}(\tilde{q},\tilde{p}) \leqslant C_R^{\mathrm{Ham}} \Delta t^{3}.$$

Then,

$$\mathbb{P}\left(\mathcal{N}_n = 0 \,\middle|\, (\tilde{q}^n, \tilde{p}^n) \in \mathcal{A},\, (\tilde{p}^0, \dots, \tilde{p}^n) \in B_R^{n+1},\, \left|p^0\right| \leqslant p^*\right) \geqslant \left(1 - C_R^{\mathrm{FD}} \Delta t^{3/2}\right)^n \left(1 - C_R^{\mathrm{Ham}} \Delta t^3\right)^n. \tag{3.58}$$

In addition,

$$\begin{aligned}
&\mathbb{P}\left((\tilde{q}^n, \tilde{p}^n) \in \mathcal{A},\, (\tilde{p}^0, \dots, \tilde{p}^n) \in B_R^{n+1} \,\middle|\, \left|p^0\right| \leqslant p^*\right) \\
&= \mathbb{P}\left((\tilde{q}^n, \tilde{p}^n) \in \mathcal{A} \,|\, \left|p^0\right| \leqslant p^*\right) \mathbb{P}\left\{(\tilde{p}^0, \dots, \tilde{p}^n) \in B_R^{n+1} \,\middle|\, \left|p^0\right| \leqslant p^*, (\tilde{q}^n, \tilde{p}^n) \in \mathcal{A}\right\}.
\end{aligned}$$

The first probability is bounded from below by $\kappa\nu(\mathcal{A})$ given by (3.55) using the minorization condition for the un-metropolized dynamics (see (3.55)). Let us prove that the second probability is very close to 1 when $\mathcal{A} \subset \mathcal{D} \times B_{R/4}$ (for R large), which will give us a minorization condition for the probability measure

$$\widetilde{\nu}(E) = \frac{\nu\Big(E \cap (\mathcal{D} \times B_{R/4})\Big)}{\nu(\mathcal{D} \times B_{R/4})},$$

which has support in $\mathcal{D} \times B_{R/4}$.

The first task is to rewrite the probability stated for $\widetilde{p}^k$ in terms of the underlying Gaussian increments. Due to (3.52) we can write

$$\widetilde{p}^{n+1} = P^{n+1} + \alpha^n M_n, \qquad M_n = \frac{1}{2}\sqrt{\frac{2\gamma\Delta t}{\beta}}\,(1+\alpha)\,\alpha \sum_{k=0}^{n} \frac{G^k}{\alpha^{k+1}},$$

with P^{n+1} bounded by $p^* + (n+1)\Delta t(\gamma\mathscr{Z} + \|\nabla V\|_{L^\infty})$. The sequence M_{n+1} is a sequence of martingales with independent increments. It is then possible to apply the Kolmogorov inequality [19, Theorem 22.4] which states that for $X_1, \dots, X_n$ are independent with zero mean and finite variances, the maxima of partial sums satisfy the following inequality, for $\alpha > 0$,

$$\mathbb{P}\left[\max_{1 \leqslant k \leqslant n} |S_k| \geqslant \alpha\right] \leqslant \frac{1}{\alpha^2}\mathrm{Var}\left[S_n\right].$$

In order to do so, we write

$$\begin{aligned}
&\mathbb{P}\left((\tilde{p}^0, \dots, \tilde{p}^n) \in B_R^{n+1} \,\middle|\, \left|p^0\right| \leqslant p^*,\, (\tilde{q}^n, \tilde{p}^n) \in \mathcal{A}\right) \\
&= \mathbb{P}\left\{\left(P^1 + \alpha M_1, \dots, P^n + \alpha^n M_n\right) \in B_R^{n+1} \,\middle|\, \left|p^0\right| \leqslant p^*, (\tilde{q}^n, \tilde{p}^n) \in \mathcal{A}\right\}.
\end{aligned}$$

We now consider $0 \leqslant n \leqslant T/\Delta t$, and choose $R > 0$ sufficiently large so that $p^* + (\gamma\mathscr{Z} + \|\nabla V\|_{L^\infty})T \leqslant R/4$. Note also that $\alpha^n \leqslant 1$. The condition

$$\left|P^k + \alpha^k M_k\right| \geqslant R$$

for some $k \in \{1, \dots, n\}$ then implies $|M_k| \geqslant 3R/4$, so that

$$\begin{aligned}
&\mathbb{P}\left((\tilde{p}^0, \dots, \tilde{p}^n) \in B_R^{n+1} \,\middle|\, \left|p^0\right| \leqslant p^*,\, (\tilde{q}^n, \tilde{p}^n) \in \mathcal{A}\right) \\
&\quad = 1 - \mathbb{P}\left((\tilde{p}^0, \dots, \tilde{p}^n) \notin B_R^{n+1} \,\middle|\, \left|p^0\right| \leqslant p^*,\, (\tilde{q}^n, \tilde{p}^n) \in \mathcal{A}\right) \\
&\quad = 1 - \mathbb{P}\left(\max_{k=1,\dots,n} \left|\tilde{p}^k\right| > R \,\middle|\, \left|p^0\right| \leqslant p^*,\, (\tilde{q}^n, \tilde{p}^n) \in \mathcal{A}\right) \\
&\quad \geqslant 1 - \mathbb{P}\left\{\max_{k=1,\dots,n} |M_k| \geqslant \frac{3R}{4} \,\middle|\, \left|p^0\right| \leqslant p^*,\, (\tilde{q}^n, \tilde{p}^n) \in \mathcal{A}\right\}.
\end{aligned}$$

Since $\widetilde{p}^n \in \mathcal{A} \subset \mathcal{D} \times B_{R/4}$ and hence $|M_n| \leqslant \alpha^{-n}(|P^n| + R/4) \leqslant R/2$, we see that

$$\sup_{k=1,\dots,n} |M_k - M_n| \geqslant \frac{R}{4},$$

which can be rephrased as

$$\sup_{k=1,\dots,n} \left|\sum_{j=k+1}^{n} \frac{G^j}{\alpha^{j+1}}\right| \geqslant \frac{R}{4(1+\alpha)\alpha}\sqrt{\frac{2\beta}{\gamma \Delta t}}.$$

Since the above sum is a sum of independent increment of mean 0, Kolmogorov inequality shows that there exists a constant $C_T > 0$ such that

$$\mathbb{P}\left\{\sup_{k=1,\dots,n} \left|\sum_{j=k+1}^{n} \frac{G^j}{\alpha^{j+1}}\right| \geqslant \frac{R}{4(1+\alpha)\alpha}\sqrt{\frac{2\beta}{\gamma \Delta t}}\right\} \leqslant \frac{C_T}{R^2}.$$

Since this estimate holds irrespectively of the set $\mathcal{A} \subset \mathcal{D} \times B_{R/4}$, we finally obtain

$$\mathbb{P}\left((\tilde{p}^0, \dots, \tilde{p}^n) \in B_R^{n+1} \,\middle|\, \left|p^0\right| \leqslant p^*,\, (\tilde{q}^n, \tilde{p}^n) \in \mathcal{A}\right) \geqslant 1 - \frac{C_T}{R^2}.$$

To conclude the proof, we first choose $R > 0$ sufficiently large (such that $C_T/R^2 \leqslant 1/2$). This determines the constants C_R^{FD} and C_R^{Ham}. Gathering all the estimates, and for $\mathcal{A} \subset \mathcal{D} \times B_{R/4}$, it holds

$$\begin{aligned}
&\mathbb{P}\left(\left(q^{\lceil T/\Delta t \rceil}, p^{\lceil T/\Delta t \rceil}\right) \in \mathcal{A} \,\middle|\, \left|p^0\right| \leqslant p^*\right) \\
&\quad \geqslant \frac{1}{2}\mathbb{P}\left((\tilde{q}^{\lceil T/\Delta t \rceil}, \tilde{p}^{\lceil T/\Delta t \rceil}) \in \mathcal{A} \,\middle|\, \left|p^0\right| \leqslant p^*\right) (1 - C_R^{\mathrm{FD}} \Delta t^{3/2})^{\lceil T/\Delta t \rceil} (1 - C_R^{\mathrm{Ham}} \Delta t^3)^{\lceil T/\Delta t \rceil}.
\end{aligned}$$

The latter two factors converge to 1 as $\Delta t \to 0$, so they remain uniformly positive for Δt sufficiently small. We conclude by obtaining a minorization condition as in (3.55).

3.5.4 Why proving a Lyapunov condition for the Metropolized scheme is difficult

In this section we show why the proof for the Lyapunov condition fails for the Metropolized scheme for the fluctuation-dissipation equation with proposal (3.44). Of course, the same issue appears also in the complete

Metropolized scheme with generator $P_{\Delta t}^{\mathrm{GHMC}}$ introduced in Section 3.3.3. More precisely, we show that the rejection rate degenerates as $|p| \to \infty$ for the standard kinetic energy, *i.e.* the perturbation function $Z \equiv 0$.

We would like to obtain a Lyapunov condition as in (3.56). We recall that for $s \geqslant 0$

$$P_{\Delta t}^{\mathrm{FD}} \mathcal{K}_s(q,p) = 1 + \mathbb{E}_{\mathcal{U}^n, G^n}\left[(p^{n+1})^s\right] \tag{3.59}$$

with p^{n+1} given by (3.44). The expectation with respect to $\mathcal{U}^n$ can be easily computed. Note that the proposal (3.42) simplifies for the standard kinetic energy as

$$\Phi_{\Delta t}^{\mathrm{FD}}(p,G) = (1-\delta)\, p + \sqrt{\frac{2m\delta}{\beta}}\,(1-\delta)\; G.$$

where we defined $\delta := \frac{\gamma \Delta t}{m}$. The acceptance rule for the proposal (3.42) is

$$A_{\Delta t}^{\mathrm{FD}}(p,G) = \min\left(1, \exp\left(-\beta \alpha_{\Delta}(p,G)\right)\right),$$

where the rejection rule is given by

$$\alpha_{\Delta t}\left(p,G\right) := E\left(\Phi_{\Delta t}^{\mathrm{FD,Verlet}}\left(p, G/\sqrt{\beta}\right)\right) - E\left(p, G/\sqrt{\beta}\right)$$

with $\Phi_{\Delta t}^{\mathrm{FD,Verlet}}(p,G)$ defined in (3.43) and $E(p,R) = U_{\mathrm{std}}(p) + \frac{1}{2}R^2$. We next rewrite $\alpha_{\Delta t}$ as

$$\begin{aligned}
\alpha_{\Delta t}\left(p,G\right) &= -\frac{\delta^2}{2\beta}\left(1 - \frac{1}{2}\delta\right) G^2 - \frac{1}{2}\frac{\sqrt{2}\,(1-\delta)\,\delta^{3/2}}{\sqrt{m\beta}} pG + \frac{\delta^2}{2m} p^2 \\
&= \quad -\frac{\delta^2}{2\beta}\left(1 - \frac{1}{2}\delta\right)(G - G_-)(G - G_+),
\end{aligned}$$

with

$$G_- = -\sqrt{\frac{2\beta}{m\delta}}\, p, \quad G_+ = -\frac{\sqrt{2\beta\delta m}}{m\,(2-\delta)}\, p.$$

We decompose the rejection rule according to $\alpha_{\Delta t}(p,G) \geqslant 0$ (which corresponds to $G \in [G_-, G_+]$) or not :

$$\begin{aligned}
\sqrt{2\pi}\,\mathbb{E}_G\left\{\min\left(1, \exp\left(-\beta \alpha_{\Delta t}\left(p^n, G\right)\right)\right)\right\} &= \int_{-\infty}^{G_-} \mathrm{e}^{-g^2/2}\, dg + \int_{G_-}^{G_+} \mathrm{e}^{-\beta \alpha_{\Delta t}(p,g) - g^2/2}\, dg + \int_{G_+}^{+\infty} \mathrm{e}^{-g^2/2}\, dg \\
&= \sqrt{2\pi}\, \mathscr{G}(G_-) + \int_{G_-}^{G_+} \mathrm{e}^{-\beta \alpha_{\Delta t}(p,g) - g^2/2}\, dg + \sqrt{2\pi}\, \mathscr{G}(G_+),
\end{aligned} \tag{3.60}$$

where the error function is bounded by

$$\mathscr{G}(R) = \frac{1}{\sqrt{2\pi}} \int_R^{\infty} \mathrm{e}^{-g^2/2} dg \leqslant C \mathrm{e}^{-|R|^2/2}. \tag{3.61}$$

In order to compute the middle integral, we rewrite

$$\alpha_{\Delta t}(p,G)+\frac{G^2}{2}=a\,(G-b)^2+c$$

where

$$a:=\frac{1}{2}\left(1+\left(\frac{1}{2}\delta-1\right)\frac{\delta^2}{\beta}\right),\quad b:=\sqrt{\frac{2\beta}{m}}\frac{(1-\delta)\,\delta^{3/2}}{(2\beta-2\delta^2+\delta^3)}p$$

and $c:=\tilde{c}|p|^2$ with

$$\tilde{c}=\frac{(2\beta-\delta)\,\delta^2}{2m\,(2\beta-2\delta^2+\delta^3)}.$$

When Δt is sufficiently small, namely $\delta/2<\beta$ and $\delta<1$, the constants $\tilde{c}$ and a are positive. Note that

$$\lim_{\Delta t\to 0}\frac{\tilde{c}}{\Delta t^2}=\frac{1}{2}\frac{\gamma^2}{m^3}.$$

After a change of variables, we transform to a standard Gaussian and compute the middle integral in (3.60):

$$\int_{G_-}^{G_+}\mathrm{e}^{-\alpha_{\Delta t}(p,g)-g^2/2}\,dg=\frac{\sqrt{2\pi}}{\sqrt{a}}\mathrm{e}^{-\tilde{c}|p|^2}\left(\mathscr{G}\left(\sqrt{a}G_-+\sqrt{a}b\right)-\mathscr{G}\left(\sqrt{a}G_++\sqrt{a}b\right)\right).$$

We bound the error functions by

$$\begin{aligned}
&\mathscr{G}\left(\sqrt{a}G_-+\sqrt{a}b\right)\leqslant C_3\mathrm{e}^{-c_3(\delta)\frac{p^2}{4}},\quad c_3(\delta):=\frac{(2\beta-\delta^2)^2}{(+\beta-2\delta^2+\delta^3)\delta m}=\frac{1}{8}\frac{\beta\delta}{m}+O(\delta^2)\\
&\mathscr{G}\left(\sqrt{a}G_++\sqrt{a}b\right)\leqslant C_4\mathrm{e}^{-c_4(\delta)\frac{p^2}{4}},\quad c_4(\delta):=\frac{\delta(2\beta-2\delta+\delta^2)^2}{(2\beta-2\delta^2+\delta^3)m(\delta-2)^2}=\frac{1}{2}\frac{\beta}{m\delta}+O(\delta^2),
\end{aligned}$$

with $C_3,C_4>0$. Since for δ sufficiently small and $\beta>\delta/2$ it holds that $c_3(\delta)>\tilde{c}$ and $c_4(\delta)>\tilde{c}$, we obtain that for some $C_5>0$

$$\int_{G_-}^{G_+}\mathrm{e}^{-\alpha_{\Delta t}(p,g)-g^2/2}\,dg\leqslant\frac{\sqrt{2\pi}}{\sqrt{a}}\mathrm{e}^{-C_5\delta^2|p|^2}.$$

Note that

$$\mathscr{G}(G_-)\leqslant C_1\mathrm{e}^{-\frac{\beta}{\delta m}p^2},\quad \mathscr{G}(G_+)\leqslant C_2\mathrm{e}^{-\frac{\delta\beta}{m(2-\delta)^2}p^2},$$

for some $C_1,C_2>0$ and we conclude by estimating (3.60) by

$$\begin{aligned}
\frac{1}{\sqrt{2\pi}}\mathbb{E}_G A^{\mathrm{FD}}_{\Delta t}(p,G)&\leqslant\sqrt{2\pi}\,C_1\mathrm{e}^{-\frac{\beta}{\delta m}p^2}+\frac{\sqrt{2\pi}}{\sqrt{a}}\mathrm{e}^{-C_5\delta^2|p|^2}+\sqrt{2\pi}\,C_2\mathrm{e}^{-\frac{\delta\beta}{m(2-\delta)^2}p^2}\\
&\leqslant C_6\mathrm{e}^{-C_7\delta^2|p|^2/2},
\end{aligned}\tag{3.62}$$

for $C_6,C_7>0$. The acceptance rate therefore degenerates as $p\gg 1/\Delta t$.

In order to conclude, we consider (3.59) and we write for a polynomial function f,

$$\mathbb{E}_{\mathcal{U},G}(f(p^{n+1}))=\mathbb{E}_G(A^{\mathrm{FD}}_{\Delta t}(p^n,G^n)f(\Phi_{\Delta t}(p^n,G^n)))+(1-\mathbb{E}_G(A^{\mathrm{FD}}_{\Delta t}(p^n,G^n)))f(p^n).$$

For $|p| \to +\infty$, the term $f(\Phi_{\Delta t}(p, G))$ grows polynomially. However, for $|p| \to +\infty$ it holds that $\mathbb{E}_G(A^{\mathrm{FD}}_{\Delta t}(p, G)) \to 0$ exponentially due to estimates (3.62). By similar arguments as above, it follows that $\mathbb{E}_G(A^{\mathrm{FD}}_{\Delta t}(p, G) f(\Phi_{\Delta t}(p, G))) \to 0$ for $|p| \to \infty$. In conclusion, if follows that $E_{\mathcal{U},G}(f(p^{n+1})) \to f(p^n)$ and hence it is not possible to obtain any Lyapunov condition.

4

Estimating the speed-up of Adaptively Restrained Langevin Dynamics

Summary. In this chapter, we analyze the influence of the parameters of the Adaptively Restrained Langevin dynamics on the total achievable speed-up. In particular, we estimate both the algorithmic speed-up, resulting from incremental force updates, and the influence of the change of the dynamics on the asymptotic variance. This allows us to propose a practical strategy for the parametrization of the method. We validate these theoretical results by representative numerical experiments.

This work has been submitted in [120].

In this chapter, we analyze the efficiency of the Adaptively Restrained Langevin dynamics. We study the gain associated with the reduction of the computational complexity of the force update quantified by an algorithmic speed-up factor $S_{\mathrm{a}} \geqslant 1$. On the other hand, as we showed in Chapter 2, the asymptotic variance of time averages σ^2_{AR} given by the Central Limit Theorem, differs from the asymptotic variance σ^2_{std} of the standard Langevin dynamics, since the dynamics is modified. The actual speed-up of the method in terms of wall-clock time is therefore an interplay between the algorithmic speed-up and the variances.

Since the method is parametrized by two constants, it is not obvious how to choose these parameters in order to achieve an optimal speed-up. Of course, the algorithmic speed-up depends on the percentage of restrained particles. The percentage of restrained particles is a non-linear function of the parameters, hence

it is not trivial how to best choose their values. Our aim in this paper is to propose a strategy for choosing the parameters of the AR method.

This chapter is organized as follows: in Section 4.1 we give a definition of speed-up and we introduce a formula for the total speed-up with the AR approach. In the next two sections we analyze how this formula depends on the parametrization: in Section 4.2 we analyze the computational complexity of the method and we express the corresponding algorithmic speed-up. This part is followed by Section 4.3, in which we give a relation between the restraining parameters and the percentage of restrained particles, as well as an approach for obtaining the linear approximation of the variance with respect to the restraining parameters. By combining all the necessary parts, we propose a practical strategy for the parametrization of the method and we illustrate the theoretical results by numerical simulations in Section 4.4.

4.1 Estimating the speed-up

In this section we introduce a framework for the complexity analysis of the AR dynamics in the case of pair-wise interactions, which are the most common interactions in numerous applications. Note that the discussion below can be easily generalized to interactions present in classical force-fields. The force acting on each particle i is a sum of interactions with all other particles.

The information about the state of the particle allows us to lower the computational cost of the computation of pair-wise interactions between the particles. We consider the potential

$$V(q) = \sum_{\substack{j=1 \\ i \neq j}}^{N} v(r_{ij})$$

and the force acting on the particle i which is given by

$$f_i(q) := -\partial_{q_i} V(q) = -\sum_{\substack{j=1 \\ i \neq j}}^{N} v'(r_{ij}) \frac{q_i - q_j}{r_{ij}}, \quad r_{ij} = |q_i - q_j| \,. \tag{4.1}$$

The change of the force between two time steps only depends on active particles that have moved since the last time step with respect to this particle. This allows us to avoid the computation of pair-wise interactions between restrained particles, hence lower the computational complexity. In order to quantify the computational cost of the force update, we define the force function $f : \mathbb{R} \to \mathbb{R}$ such that $f := v'$. Then the *computational cost of the force update* is defined as the number of times the force function f is called. The speed-up of AR dynamics, due to the decreasing of the computational complexity in the force update, with respect to the non-adaptive method which updates all interactions, defines *the algorithmic speed-up*. Since the computational complexity depends on the ratio of restrained particles, which is a quantity that varies at each time step, we consider averages over the whole simulation. More precisely, we denote by $C_{\mathrm{AR},n}$ the computational cost of the force update in the AR-method at time step n and by $C_{\mathrm{std},n}$ the computational cost

of a standard, non-adaptive method. We denote by $N_{\text{iter}} = T/\Delta t$ the number of time steps in the simulation. Then *the algorithmic speed-up* S_{a} is the ratio of the average computational cost $\widehat{C}_{\text{std}} := \mathbb{E}_{\mu_{\text{std}}}[C_{\text{std}}]$ in the standard method and the average computational cost $\widehat{C}_{\text{AR}} := \mathbb{E}_{\mu_{\text{AR}}}[C_{\text{AR}}]$ in the AR method:

$$S_{\text{a}} := \frac{\lim_{N_{\text{iter}}\to\infty} \frac{1}{N_{\text{iter}}} \sum_{n=0}^{N_{\text{iter}}} C_{\text{std},n}}{\lim_{N_{\text{iter}}\to\infty} \frac{1}{N_{\text{iter}}} \sum_{n=0}^{N_{\text{iter}}} C_{\text{AR},n}} = \frac{\widehat{C}_{\text{std}}}{\widehat{C}_{\text{AR}}}. \tag{4.2}$$

Note that the computational complexities in both cases are bounded functions of the number of particles and, due to the ergodicity of the dynamics, which was proved in Chapter 2 the averages in (4.2) almost surely converge.

However, the important point is the reduction of the error for a given wall-clock duration. We focus here on the statistical error, which is often the dominant source of errors. In order to express the total speed-up with respect to the standard method, we need to consider not only the algorithmic speed-up, but also the modification of the asymptotic variance which depends on the concrete choice of the kinetic energy (see expression (1.67)). We define *the total speed-up* S_{total} as a ratio of the wall-clock time, which is needed by using the AR-method in order to achieve some statistical precision, and the wall-clock time needed for reaching the same precision by the standard method:

$$S_{\text{total}} := \frac{T^{\text{wlck}}_{\text{std}}}{T^{\text{wlck}}_{\text{AR}}}. \tag{4.3}$$

Recall that, for an observable φ, we denoted by $\sigma^2_{\Delta t}$ the asymptotic variance of the sampling from the discretized dynamics and by σ^2 the asymptotic variance of the continuous dynamics. From the Central Limit Theorem, the statistical error at time T is given by

$$\widehat{\varphi}_T = \mathbb{E}_\mu(\varphi) + \varepsilon_T \mathcal{G},$$

where ε_T is of order $\frac{\sigma}{\sqrt{T}}$ and $\mathcal{G} \sim \mathcal{N}(0,1)$. Hence the number of time steps $N_{\text{iter}} = T/\Delta t$ needed in order to have a statistical error of order ε_T is

$$N_{\text{iter}} = \frac{\sigma^2_{\Delta t}}{\varepsilon_T^2}.$$

The corresponding wall-clock time is therefore obtained by considering the average cost $\widehat{C}$ as

$$T^{\text{wlck}} = N_{\text{iter}} \widehat{C}.$$

Taking into account that $\Delta t \sigma^2_{\Delta t} \sim \sigma^2$ (for time steps small enough, recall Section 1.3.2.5), the total speed-up S_{total} defined in (4.3) can be expressed as

$$S_{\text{total}} = \frac{\widehat{C}_{\text{std}}}{\widehat{C}_{\text{AR}}} \frac{\sigma^2_{\text{std},\Delta t}}{\sigma^2_{\text{AR},\Delta t}} = S_{\text{a}} \frac{\sigma^2_{\text{std},\Delta t}}{\sigma^2_{\text{AR},\Delta t}} \approx S_{\text{a}} \frac{\sigma^2_{\text{std}}}{\sigma^2_{\text{AR}}} \frac{\Delta t_{\text{AR}}}{\Delta t_{\text{std}}} \,. \tag{4.4}$$

The last two terms in (4.4) become equal for small values of Δt and it is therefore sufficient to study the variance of the continuous process σ^2_{std} and σ^2_{AR}. As we have already mentioned, the choice of the modified kinetic energy should not change the stability properties of the standard dynamics. This would otherwise require us to choose a smaller time step size Δt_{AR}, which would lead to a smaller total speed-up S_{total}. Unfortunately, this is the case of the kinetic energy defined in [9]. Still, the stability can be significantly improved by using the kinetic energy given by (3.49) instead. In this case, the stability properties become comparable to the ones of the standard dynamics (see Chapter 3). We therefore assume in this chapter that $\Delta t_{\text{std}} = \Delta t_{\text{AR}}$.

The computation in (4.4) shows the trade-off between the algorithmic speed-up and the change in variance. Both the algorithmic speed-up S_{a} and the AR variance σ^2_{AR} depend on the parameters of the AR dynamics. As already showed in [9], in some applications, the restraining parameters can be chosen such that the total speed-up satisfies $S_{\text{total}} > 1$. Therefore, there are systems for which this method can be efficient, even though this might be counter-intuitive since one could suggest that in order to accelerate the sampling, the system should move "faster" and not be restrained. Note however that the wall-clock duration of the force update step depends on the implementation and on the complexity of the evaluation of φ. Hence, the same physical model with variance σ^2, can have various algorithmic speed-ups S_{a}. Finally, an interesting observation is, that due to the separability of the Hamiltonian, the algorithmic speed-up does not depend on the potential.

4.2 Algorithmic speed-up

The goal of this section is to propose a methodology to analyze the algorithmic speed-up S_{a} (defined in (4.2)) of AR dynamics as a function of the percentage of restrained particles. We first describe the adaptive algorithm for computing forces, and we estimate the corresponding computational cost. In the last part, we also consider the effort for updating neighbor lists used for updating of short-ranged interactions and we obtain an estimation of the algorithmic speed-up per time step.

4.2.1 Description of the AR force update algorithm

For simplicity, we consider a system of N particles where only pair-wise interactions take place. In AR dynamics, this sum can be split into three kinds of interactions depending on the state of the two interacting particles: active-active, active-restrained and restrained-restrained. We define the set of indices of active particles I_{A} and restrained particles I_{R}. Then, sum (4.1) can be re-written as

$$f_i = \sum_{\substack{j \in I_{\text{A}} \\ j \neq i}} f_{ij} + \sum_{\substack{j \in I_{\text{R}} \\ j \neq i}} f_{ij} \,. \tag{4.5}$$

The force acting on particle i in the next time step $n+1$ can be formally obtained using the old position q^n:

$$f_i^{\text{new}} = f_i^{\text{old}} + \left(f_i^{\text{new}} - f_i^{\text{old}}\right), \quad f_i^{\text{old}} = \sum_j f_{ij}(q^n), \quad f_i^{\text{new}} = \sum_j f_{ij}(q^{n+1}). \tag{4.6}$$

Since, for the set of restrained particles, positions have not changed since the previous time step, one can easily see that

$$\forall i \in I_R, \quad \sum_{\substack{j \in I_{\text{R}} \\ j \neq i}} f_{ij}^{\text{new}} - f_{ij}^{\text{old}} = 0\,.$$

The computation in (4.6) is therefore reduced to subtracting the old and adding the new active-restrained and active-active interactions. This simple remark provides in fact a key point for the reduced complexity of the AR algorithm.

In a standard simulation, when taking into account Newton's third law $f_{ij} = -f_{ji}$, the computational cost of pair-wise interactions is $\frac{N(N-1)}{2}$. The resulting quadratic complexity in the number of particles is not favorable due to the system size, and therefore neighbor lists are usually introduced (see Section 1.1.1.3). Neighbor lists can be used in systems where forces vanish after a certain cut-off distance, so that each particle only interacts with a relatively limited number of neighbors. For simplicity, we consider a homogenous system where we assume that the number of neighbors C of a particle is the same for each particle. Taking into account that, for each pair (i, j), we may only compute the force f_{ij} and deduce f_{ji} thanks to Newton's third law, the number of interactions reduces to $\frac{NC}{2}$.

We take as an example the first order discretization scheme (3.5) which can be formalized in the following way:

Input: Initial conditions p^0, q^0
Output: p^n, q^n
for *each time step and each particle* **do**
    B: Update momenta ;
    A: Update positions ;
        Update neighbor-lists ;
        Update forces ;
    O: Update momenta in fluctuation-dissipation part (FD) ;
end

Algorithm 1: Algorithm for (3.5) in the case of the standard dynamics.

In AR dynamics, the information about which particles are going to move after the position update is already available after updating the momenta B, since the kinetic energy will not change anymore. The algorithm above may thus be modified in the following way:

Input: Initial conditions p^0, q^0
Output: p^n, q^n
For each particle i, initialize force f_i;
for *each time step and each particle* **do**
    B: Update momenta;
        Create lists of active and restrained particles;
        Subtract active-active and active-restrained interactions;
    A: Update positions;
        Update neighbor-lists;
        Add active-active and active-restrained interactions;
    O: Update momenta in FD;
end

Algorithm 2: Algorithm for (3.5) using adaptive forces updates.

Updating neighbor lists normally consists in re-assigning each particle to a specific grid cell (in our implementation we used a combination of Verlet lists and linked-cell lists. In AR dynamics, restrained particles do not have to be re-assigned, and neighbor lists may be updated more efficiently. More precisely, the complexity of updating the neighbor lists goes from $O(N)$ the number of particles, to $O(K)$, where K is the number of active particles.

Note that the force function f is called in both AR force updates (subtract and add steps), since we need to evaluate forces for positions at the previous time step. It would be possible to avoid updating forces twice by saving all pairwise forces, but this may result in a quadratic space complexity. We will not analyze this case, although it would result in a larger algorithmic speed-up and lead to less restrictive conditions on the efficiency of AR dynamics.

Note that there is a slight overhead due to computing the AR kinetic energy functions ∇U, which is more complicated than in the standard case. Still, this involves $O(N)$ additional operations, and can be neglected compared to the cost of the force update in practical applications. Furthermore, the overhead mostly comes from the transition regime since ∇U vanishes for restrained particles and becomes $M^{-1}p$ for the full-dynamics state.

Note that a similar strategy for incremental force update may be applied to other splitting schemes of the modified Langevin equations. However, the status of a particle (active, in transition or restrained) depends on the state of the momenta before the position update, and hence this status should not be destroyed by updating momenta between two position updates. Using the same notation as in Section 1.3.2.1 (with $\mathrm{O} := \gamma\mathcal{L}_{\mathrm{FD}}$), this implies that the second order splittings BAOAB[1] and OABAO are not directly suited for a modification by the AR dynamics algorithm, since between the two position updates A, the momentum changes by either O or B step. On the other hand, ABOBA, BOAOB, OBABO and AOBOA can be used,

[1] BAOAB denotes a scheme with the evolution operator $\mathrm{e}^{\Delta t B/2}\mathrm{e}^{\Delta t A/2}\mathrm{e}^{\Delta t \gamma \mathcal{L}_{\mathrm{FD}}}\mathrm{e}^{\Delta t A/2}\mathrm{e}^{\Delta t B/2}$.

since the lists of active particles can be created before the position update A and hence active-active and active-restrained interactions can be subtracted and added after the position update A.

4.2.2 Complexity analysis

At each time step, the computational cost of the force update depends on the percentage of restrained particles. Let us denote the number of active particles by $K = \alpha N$, where $\alpha \in [0, 1]$ is the average ratio of active particles. The number of restrained particles is then $N - K$. We are going to formalize the computational complexity of the force update as a function of the ratio of restrained particles, denoted by $\rho := 1 - \alpha$.

We recall that we have considered the average computational cost over the whole trajectory in equation (4.2), since the instantaneous computational cost may vary at each time step. Because, in the algorithm analyzed in this chapter, we add and subtract pairwise forces, the computational complexity of the force update in an AR simulation is lower than a regular force update if and only if a sufficient number of particles is restrained. We are thus going to analyze which conditions on the number of restrained particles are sufficient to obtain a speed-up larger than one, when a standard simulation has a linear or quadratic complexity[2]. This analysis can be extended to other force update algorithms.

4.2.2.1 Quadratic complexity

Let us first consider a standard (non-adaptive) simulation with a quadratic-complexity force update algorithm, i.e. when no neighbor-lists are used. In this case, the number of interactions computed at every time step is $C_{\mathrm{std}} := \frac{N(N-1)}{2}$. In AR dynamics, we do not need to recompute interactions between restrained particles, hence we only update interactions involving active particles, either with other active particles, or with restrained particles. As a result, the computational cost for the AR force update is[3]:

$$C_{\mathrm{AR}} := 2\left(\frac{K(K-1)}{2} + K(N-K)\right) = (2N - \alpha N - 1)\, N\alpha\,.$$

and $C_{\mathrm{std}} > C_{\mathrm{AR}}$ is satisfied for

$$\alpha < 0.29 \tag{4.7}$$

and $N > \frac{1-2\alpha}{2\alpha^2-4\alpha+1}$. The inferior bound on the number of particles is not a restrictive condition for molecular dynamics, where the number of particles is usually much bigger. (For example, for $\alpha = 0.28$, the number of particles N must be larger than 12.) More importantly, this implies that at least 71% of particles must be restrained in order for this force update algorithm to be beneficial, in which case the algorithmic speed-up is:

$$S_{\mathrm{a},1} = \frac{C_{\mathrm{std}}}{C_{\mathrm{AR}}} = \frac{N-1}{2(N\rho + N - 1)(1-\rho)}\,.$$

[2] The quadratic complexity corresponds to bonded interactions and the linear complexity to non-bonded, in which case the neighbor lists can be applied.

[3] The factor of 2 comes from the need to subtract old forces (with previous positions) and add new forces (with current positions).

When the number of particles tends to infinity, this becomes

$$S_{\mathrm{a},1}^{\infty} = \lim_{N\to\infty} S_{\mathrm{a}}(N) = \frac{1}{2(\rho+1)(1-\rho)}\,. \tag{4.8}$$

Note that if the double computation of forces can be avoided (for example by storing previous pairwise forces), the complexity becomes

$$C_{\mathrm{AR},2} := \frac{C_{\mathrm{AR}}}{2}\,,$$

so that $C_{\mathrm{AR},2} > C_{\mathrm{std}}$ is achieved for any $\alpha < 1$ and $N > \frac{1}{1-\alpha}$, resulting in the following speed-up:

$$S_{\mathrm{a},2} = \frac{N-1}{(N\rho+N-1)\,(1-\rho)}, \quad S_{\mathrm{a},2}^{\infty} = \frac{1}{(\rho+1)(1-\rho)}\,.$$

4.2.2.2 Linear complexity

Let us now consider the (much more frequent) case where the complexity of the force update is linear, e.g. when forces become sufficiently small after a given cutoff distance r_{cut}, and neighbor lists may be used to efficiently determine which particles are interacting. The reference complexity is therefore $C_{\mathrm{std,NL}} = \frac{NC}{2}$, where C is the (average) number of neighbors. The algorithm for the adaptive force update is as follows: for all active particles compute interactions with their neighbors, and between the active neighbors use $f_{ij} = -f_{ji}$. The total number of interactions to be updated in the AR dynamics algorithm is then:

$$C_{\mathrm{AR,NL}} := 2\left(\sum_{i=1}^{K}\sum_{j\in L_A(i)} 1 + \sum_{i=1}^{K}\sum_{j\in L_R(i)} 1\right) = 2\left(\frac{KC_A}{2} + KC_R\right) = \left(1-\frac{\alpha}{2}\right)\alpha CN\,, \tag{4.9}$$

where the set $L_A(i) \subset I_A$ contains the indices of the active neighbors of the particle i, $L_R(i) \subset I_R$ contains the indices of the restrained neighbors, $C_A = \alpha C$ and $C_R = \rho C$. The necessary condition for $C_{\mathrm{std,NL}} > C_{\mathrm{AR,NL}}$ is then

$$\alpha < 0.293\,. \tag{4.10}$$

Note that this condition does not depend on N, nor on C. The AR dynamics algorithm is more efficient in number of operations for forces update if and only if the percentage of restrained particles is bigger than $70,7\%$. The algorithmic speed-up is hence

$$S_{\mathrm{NL}} := \frac{C_{\mathrm{std}}}{C_{\mathrm{AR,NL}}} = \frac{1}{2\alpha(2-\alpha)} = \frac{1}{2(1-\rho^2)}\,. \tag{4.11}$$

Again, avoiding the double re-computation of force components from the old positions for the active particles, removes a factor of 2 from $C_{\mathrm{AR,NL}}$ and the computational cost becomes $C_{\mathrm{AR,NL}} = \left(\frac{1}{2}-\alpha\right)\alpha CN$, which implies an unconditional algorithmic speed-up $S_{\mathrm{a}} = \left(1-\rho^2\right)^{-1}$.

An important conclusion is that an incremental force update is computationally beneficial if the percentage of restrained particles is larger than a threshold $\mathcal{R}$. We may thus modify Algorithm 2 as follows:

Input: Initial conditions p^0, q^0. **Output**: p^n, q^n

For each particle i, initialize the force f_i;

for *each time step and each particle* **do**

  B: Update momenta;

  Create lists of active and restrained particles;

  if $\rho > \mathcal{R}$ **then**

    Subtract active-active and active-restrained interactions;

    A: Update positions;

    Add active-active and active-restrained interactions;

  else

    A: Update positions;

    Update forces with the standard approach;

  end

  Update neighbor-lists;

  O: Update momenta in FD;

end

Algorithm 3: Improvement of Algorithm 2 by using the condition on the ratio of restrained particles ρ given by the constant $\mathcal{R} \geqslant 0$.

Finally, we consider the case where the neighbor lists are updated at each time step[4]. This is not usually done in practical applications, where neighbor lists are updated only after a certain time period which can be computed from the maximal velocity of the particles. The cost per time step then extends in re-assigning N particles into the grid, which gives order of $NC/2 + N$ operations. In the AR simulation, only active particles need to be re-assigned into the grid. Therefore, the cost per time step computed in (4.9) becomes

$$C_{\mathrm{AR,NL}} := \left(1 - \frac{\alpha}{2}\right) \alpha C N + \alpha N \,.$$

Assuming that there are C neighbors in average, the resulting speed-up is:

$$S_{\mathrm{a}} = \frac{C + 2}{2(1-\rho)(C\rho + C + 1)} \,. \tag{4.12}$$

4.3 Total speed-up

As explained above, the total speed-up (4.2) reachable by AR dynamics when estimating observables depends on both the computational complexity of the force update, and the variance of the AR dynamics.

In this section, we first analyze how the percentage of restrained particles depends on the restraining parameters $e_{\min}$ and $e_{\max}$. Then, we approximate the variance of the AR dynamics by a linear function. Combining both, we finally express the total speed-up as a function of $e_{\min}$ and $e_{\max}$.

[4] Note that this can be easily modified in order to express the update of neighbor-lists every time period T.

4.3.1 Percentage of restrained particles

The percentage of restrained particles can be computed from the average occupation of the restrained state of each particle. In other words, it is the probability that the momenta of one particle belong to the restrained region of phase space. For the AR kinetic energy function (3.49), the average occupation of the restrained state $R(v_{\min}, v_{\max})$ of particle i with parameters $v_{\min}$ and $v_{\max}$ is the expected value of the indicator function of the absolute values of all momenta components of one particle being smaller than the restraining parameter $v_{\min}$.

We denote by $\mu_{v_{\min},v_{\max}}$ the invariant measure which corresponds to the AR kinetic energy function with parameters $v_{\min}$ and $v_{\max}$ and we compute

$$R(v_{\min}, v_{\max}) = \int_{\mathbb{R}^d} \mathbb{1}_{\left\{\frac{|p_i|}{m_i} \leqslant v_{\min}\right\}} \mu_{v_{\min},v_{\max}} = \frac{(2v_{\min}m_i)^D \exp\left(-\beta D S_{v_{\min},v_{\max}}\right)}{Z_p(v_{\min}, v_{\max})}\,, \tag{4.13}$$

where the momenta normalization constant of the particle i is simply $Z_p = z^D$, with

$$\begin{aligned} z(v_{\min}, v_{\max}) &= \int_{\left\{\frac{|p_i|}{m_i} \leqslant v_{\min}\right\}} \mathrm{e}^{-\beta S_{v_{\min},v_{\max}}}\, dp + \int_{\left\{\frac{|p_i|}{m_i} \geqslant v_{\max}\right\}} \mathrm{e}^{-\beta \frac{p_i^2}{2m_i}}\, dp \\ &\quad + \int_{\left\{\frac{|p_i|}{m_i} \in [v_{\min},v_{\max}]\right\}} \mathrm{e}^{-\beta s(p_i)} dp \\ &= (2v_{\min}m_i)\, \mathrm{e}^{-\beta S_{v_{\min},v_{\max}}} + \sqrt{2\pi m_i \beta^{-1}} - 2\int_0^{m_i v_{\max}} \mathrm{e}^{-\beta \frac{p^2}{2m_i}} dp \\ &\quad + \int_{m_i v_{\min}}^{m_i v_{\max}} \mathrm{e}^{-\beta s(p_i)} dp + \int_{-m_i v_{\max}}^{-m_i v_{\min}} \mathrm{e}^{-\beta s(p_i)} dp\,. \end{aligned} \tag{4.14}$$

Note that in the standard dynamics $Z_p = (2\pi m_i/\beta)^{3/2}$.

Finally, considering a system consisting of particles with various restraining parameters $v^i_{\min}$ and $v^i_{\max}$, the total average percentage of restrained particles can be computed as an average over the individual values $R(v^i_{\min}, v^i_{\max})$ of each particle. Denoting by $N_{v_{\min},v_{\max}}$ the number of particles with parameters $v_{\min}$ and $v_{\max}$ and by $\mathcal{N}$ the set of all chosen pairs $(v_{\min}, v_{\max})$, the total average percentage of restrained particles[5] $R_{\text{total}} \in [0,1]$ is given by

$$R_{\text{total}} = \frac{1}{N} \sum_{(v_{\min},v_{\max}) \in \mathcal{N}} N_{v_{\min},v_{\max}} R(v_{\min}, v_{\max})\,. \tag{4.15}$$

For example, the percentage of restrained particles for a system consisting of a dimer that follows standard dynamics and that is surrounded by solvent particles following AR dynamics with non-zero parameters $v_{\min}$ and $v_{\max}$ is:

$$R^{\text{DS}}_{\text{total}} = \frac{N_{\text{Solv}}}{N_{\text{total}}} R_{\text{Solv}}(v_{\min}, v_{\max})\,,$$

[5] Note that this corresponds to the notation $\rho = R_{\text{total}}$ in Section 4.2.

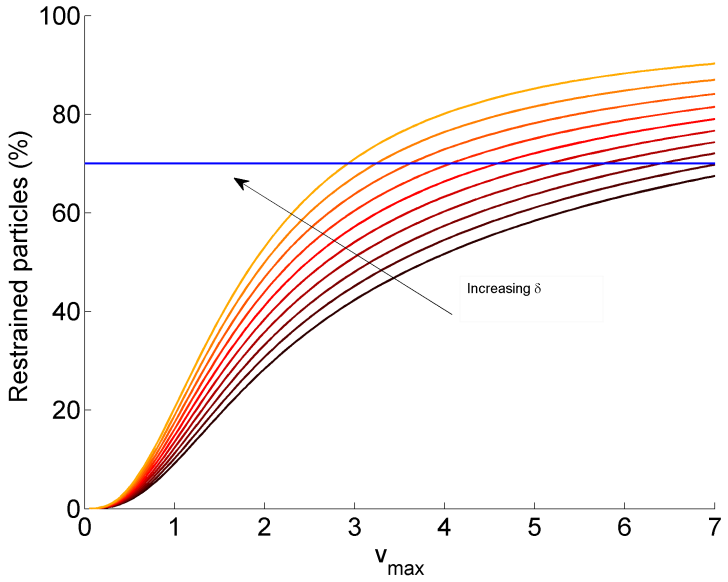

Fig. 4.1: *Average occupation of the restrained state with respect to the parameter ratio.* We computed $R_{\text{total}} = R(v_{\min}, v_{\max})$ for one particle in 3D according to (4.13) for various $v_{\max}$ and various values of the parameter ratio $\delta \in [0.7, 0.98]$ (black to orange or bottom to top lines) such that $v_{\min} = \delta v_{\max}$. The blue line is the value 70% of restrained particles which corresponds to the necessary condition for $S_{\text{a}} > 1$.

since, in standard dynamics, the average occupation of the restrained state is zero and $R_{\text{Dimer}} = 0$.

In conclusion, the algorithmic speed-up S_{a} can be estimated using the computational complexity of the algorithm (see Section 4.2) with the speed-up being a function of $\rho = R_{\text{total}}$.

Figure 4.1 shows, for U defined in (3.49), the average occupation of the restrained state $R(v_{\min}, v_{\max})$ as a function of $v_{\max}$ for various $\delta \in [0.5, 0.98]$ such that $v_{\max} = \delta v_{\min}$ in dimension three. We depicted also the value 70% of restrained particles which corresponds to the necessary condition for $S_{\text{a}} > 1$ (given by (4.7) or (4.10)). We observe on this figure that the bigger δ, the bigger average occupation of the restrained state. Figure 4.2 shows the dependence of $R(v_{\min}, v_{\max})$ on the temperature. This suggests that the restraining parameters should be scaled with respect to the temperature $k_B T$.

Finally, Figure 4.3 shows $R_{\text{total}}(v_{\min}, v_{\max})$ as a function of both parameters. Note that the highest value of percentage of restrained particles is located close to the diagonal, *i.e.* when the gap between the parameters $v_{\min}$ and $v_{\max}$ is small.

4.3.2 Linear approximation of the variance

In Chapter 2, we proved that there exists a regime in which the variance from the AR dynamics simulations can be approximated by a linear function of the restraining parameters: for a given observable, there exists $v^*_{\max}$ small enough such that for $v_{\max} < v^*_{\max}$ there exist constants $c_1, c_2 \in \mathbb{R}$ such that for $v_{\min} \in [0, v_{\max}]$

$$\sigma^2_{\text{AR}}(v_{\min} + \zeta, v_{\max} + \eta) = \sigma^2_{\text{AR}}(v_{\min}, v_{\max}) + c_1\zeta + c_2\eta + \mathrm{O}\left(\zeta^2 + \eta^2\right). \tag{4.16}$$

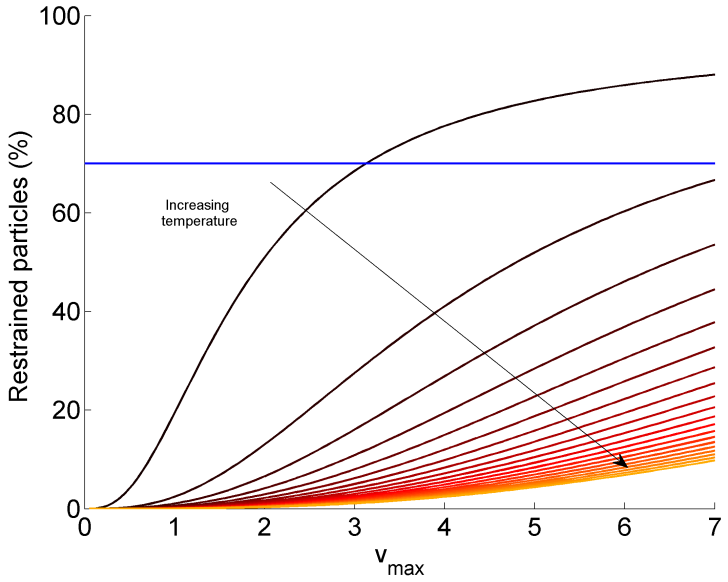

Fig. 4.2: *Average occupation of the restrained state with respect to the temperature.* We computed $R_{\text{total}} = R(v_{\min}, v_{\max})$ of a particle in 3D according to (4.13) for $v_{\max}$ and $v_{\min} = 0.95 v_{\max}$ and for various temperatures $k_B T = [1, 100]$ (black to orange or top to bottom lines).

The total speed-up of the wall-clock time needed to reach a certain statistical precision (4.4) can hence be expressed in terms of the restraining parameters using (4.16) as

$$\begin{aligned} S_{\text{total}} &\approx S_{\text{a}}(v_{\min}, v_{\max}) \frac{\sigma^2(0,0)}{\sigma^2(0,0) + c_1 v_{\min} + c_2 v_{\max}} \\ &= S_{\text{a}}(v_{\min}, v_{\max}) \frac{1}{1 + \frac{c_1}{\sigma^2(0,0)} v_{\min} + \frac{c_2}{\sigma^2(0,0)} v_{\max}}. \end{aligned} \tag{4.17}$$

The gap between the restraining parameters $v_{\min}$ and $v_{\max}$ should be big enough to ensure a smooth transition between the full and the restrained dynamics and prevent numerical instabilities. Note, however, that in the numerical experiments performed in Section 2.4, where the variance was computed for a simple 1D system, it was shown that the relative increase of the variance with respect to the full-dynamics parameter $v_{\max}$ is more significant than with respect to the restraining parameter $v_{\min}$. This result is not surprising, since the gap between the parameters smooths out the dynamics, which translates into an increase of correlations. This implies that the optimal strategy is to choose the gap between the parameters as small as possible while still maintaining the numerical stability and keeping the systematical error sufficiently low (i.e. the error on the computed averages, arising from the fact that $\mu \neq \mu_{\Delta t}$). At the same time, the restraining parameters should give the desired percentage of restrained particles R_{total}. For example, in the case when $\delta = v_{\min}/v_{\max} = 0.98$, the relative derivative of the restrained energy of one particle $R(v_{\min}, v_{\max})$ with respect to $v_{\max}$, almost vanishes after the value $v_{\max} = 5$. Hence this is a critical value after which the growth of function $R(v_{\min}, v_{\max})$ slows down (see again Figure 4.1). Having in mind that the variance

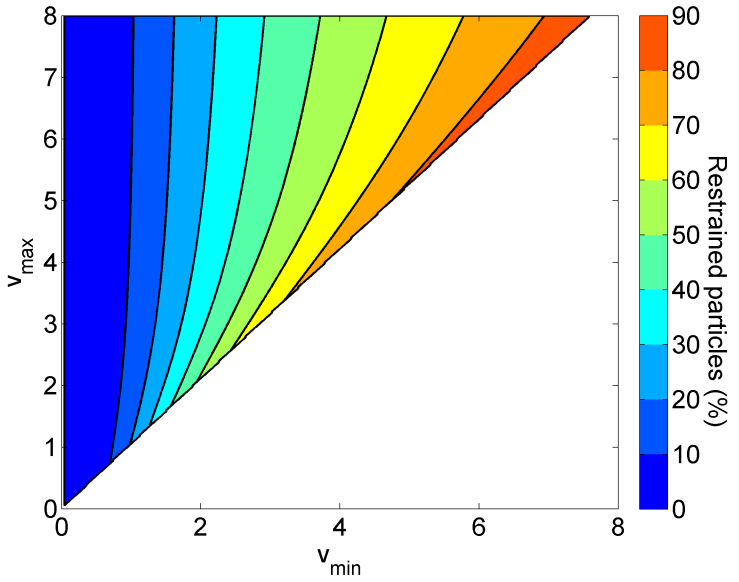

Fig. 4.3: *Percentage of restrained particles over* $v_{\min}$ *and* $v_{\max}$. We considered the system described in Section 4.4 with the AR kinetic energy function chosen according to (3.49). We computed the percentage of restrained particles (4.15) for various values $0 \leqslant v_{\min} \leqslant 0.95 v_{\max}$.

locally increases with respect to $v_{\max}$, this implies that, in this region, the efficiency of the algorithmic speed-up does not grow fast enough with increasing $v_{\max}$, while the variance might be still growing. In this case, either the gap δ should be chosen smaller, or one must ensure that the variance does not grow too fast, in order to compensate the variance growth with the algorithmic speed-up.

It is easy to estimate the algorithmic speed-up S_{a}. The problematic part is to estimate the sensitivity of the variance of a given observable with respect to the modification by the restrained dynamics, i.e. the estimation of c_1 and c_2 in (4.17). This can be done by a linear interpolation in the pre-processing part, which should involve at least three AR dynamics simulations in order to estimate the constants c_1 and c_2. Finally, (4.17) allows to have a complete expression for the total speed-up as a function of the parameters $v_{\min}$ and $v_{\max}$. Choosing $\delta = v_{\min}/v_{\max}$ as small as possible, one can find the optimal $v_{\max}$ which produces the highest total speed-up (see Section 4.4 for a numerical example).

We thus propose the following guidelines to estimate the total speed-up S_{total} with respect to the parameters $v_{\min}$ and $v_{\max}$:

(1) Choose the order (scale) of the restraining parameters $v_{\min}$ and $v_{\max}$ for each particle according to its mass, its role in the system and the temperature $k_B T$.
(2) Choose the minimal gap δ between $v_{\min}$ and $v_{\max}$ with respect to the numerical stability.
(3) Compute the percentage of restrained particles R_{total} according to (4.13), (4.14) and (4.15).
(4) Compute the algorithmic speed-up S_{a} according to the implementation algorithm according to Section 4.2.

(5) Estimate the linear approximation of the variance $\sigma^2_{\mathrm{AR}}(\delta v_{\max}, v_{\max})$ for the observable A.
(6) Find the optimal value of $v_{\max}$ (with $v_{\min} = \delta v_{\max}$) by maximizing $S_{\mathrm{total}}(v_{\min}, v_{\max})$.

4.4 Numerical illustration

In order to illustrate the theoretical results from the previous section, we consider a system of $N = 64$ particles consisting of a dimer (q_1, q_2) surrounded by 62 solvent particles $(q_3, \ldots, q_N)$ in space dimension $D = 3$. This model is representative of many systems, where the macroscopic property only depends on a small part of the simulated system.

We use periodic boundary conditions with box-length such that the density is 0.4. We consider reduced units such that particles have identical masses $m_i = 1$ and the temperature is chosen so that $\beta = 1$. The friction constant in the Langevin equations is $\gamma = 1$. Solvent particles interact with each other and with the dimer particles by a WCA potential (1.4) with parameters $\varepsilon_{\mathrm{LJ}} = 1$ and $\sigma_{\mathrm{LJ}} = 1$ with a cut-off distance $r_{\mathrm{LJ}} = 2^{1/6}$. Dimer particles interact with each-other with a double-well potential (1.1) with width $w = 1$ and height $h = 1$. This system is the same as the one in Section 2.4. We discretize the modified Langevin equations (2.4) by a second-order scheme (OBABO) with time step size $\Delta t = 0.001$ and perform $N_{\mathrm{iter}} \approx 10^9$ time steps.

We use neighbor-lists based on the cut-off distance of the Lennard-Jones potential r_{LJ}, according to Algorithm 3. The average number of neighbors is estimated as $C = 0.25$. We run one reference simulation in the standard dynamics.

In the AR simulations, we consider non-zero restraining parameters on the solvent only, and we let dimer particles follow the standard dynamics. In order to demonstrate the dependence of the total speed-up S_{total} on the restraining parameters $v_{\min}$ and $v_{\max}$, we consider the following observables: the dimer distance $A_D(q_1, q_2) = |q_1 - q_2|$, the dimer potential $A_V(q_1, q_2) = V_{DW}(|q_1 - q_2|)$ and the kinetic temperature $\mathcal{T}(p) = p \cdot \nabla U(p)$. The first two observables only depend on the positions of the dimer particles, hence we expect that the variance will not be much modified even for large restraining parameters. The function $\mathcal{T}(p)$ depends on the momenta of all particles p and satisfies $\langle \mathcal{T} \rangle_{\mu_{v_{\min}, v_{\max}}} = k_B T$. The knowledge of the exact average allows us to verify that the time step size Δt is chosen sufficiently small in order to make the systematic error on the averages smaller than 1% even for $v_{\max} = 10$. The asymptotic variance σ^2 of a time average for a given observable A is estimated by approximating the integrated auto-correlation function by a trapezoidal rule as (2.22).

First, we confirm theoretical predictions for the algorithmic speed-up S_{a}. In our simulations, we measure the time per force update, as well as the time per time step. We compare the measured speed-up, which is a ratio of the measured time in the standard dynamics and the AR dynamics, with the estimated speed-up in the force update (4.11) and for the overall time step (4.12). Figure 4.4 shows that the predicted algorithmic speed-up corresponds to the measured algorithmic speed-up in our simulation.

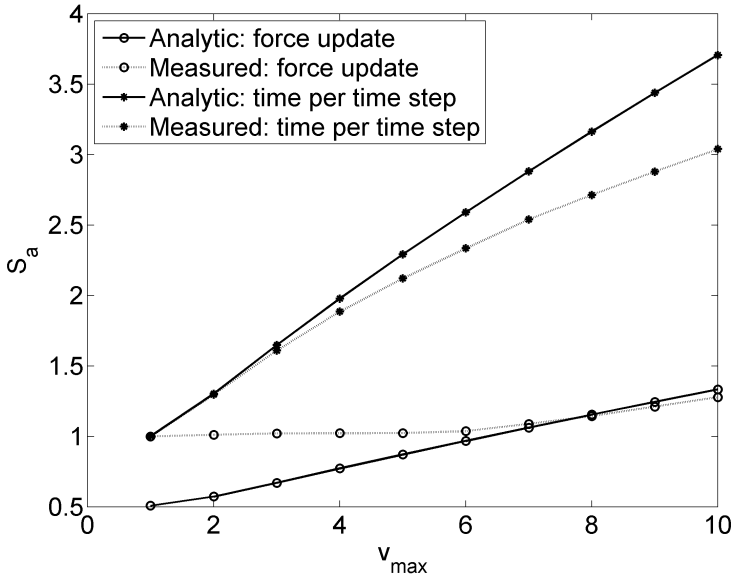

Fig. 4.4: *Comparison of the analytically estimated algorithmic speed-up with the measured one.* We considered a system described in Section 4.4. We measured the algorithmic speed-up S_a of the forces update function and the total time step, with respect to the parameters v_max and $v_\mathrm{min} = 0.8 v_\mathrm{max}$. The computed speed up in forces update (4.11) corresponds to the measured one, as well as the algorithmic speed-up per time step (4.12). Note that the measured S_a of the forces update is equal to one for small values of v_max, which is due to the implementation of the condition on the adaptive forces update as proposed in Algorithm 3 which assures $S_\mathrm{a} \geqslant 1$.

Figure 4.5 plots the estimated relative variation of the variance of three observables as a function of the parameters v_max for $v_\mathrm{min} = \delta v_\mathrm{max}$ with $\delta = 0.5$. The variance of $\mathcal{T}$ is modified more drastically than the variance of observables measured on the dimer with growing v_max.

Finally, combining the algorithmic speed-up $S_\mathrm{a}(v_\mathrm{min}, v_\mathrm{max})$ with the variance $\sigma^2(v_\mathrm{min}, v_\mathrm{max})$, we estimate the total speed-up according to (4.4). This is depicted on Figure 4.6. We again consider $\delta_k \in \{0.5, 0.8, 0.9\}$ in order to demonstrate the impact of the gap between the parameters $\delta = v_\mathrm{min}/v_\mathrm{max}$ on the total speed-up S_total: the smaller the gap, the larger S_total becomes. Also, it holds that $S_\mathrm{total} > 1$ for the dimer observables only (up to 4), and not for the global observable $\mathcal{T}$. This supports the idea that we can speed-up the computation of macroscopic properties that depend on unrestrained degrees of freedom, i.e. those of the dimer in this example.

It is easy to compute the algorithmic speed-up S_a. The problematic part is the determination of the sensitivity of the observable on the restraining parameters (see again Figure 4.5). Since the variance can be approximated by a linear function of the restraining parameters at least locally, we can compute the slopes c_{v_max} such that[6] $\sigma^2(v_\mathrm{min}, v_\mathrm{max}) \approx \sigma^2(v_\mathrm{min}, v_\mathrm{max}) + c_{v_\mathrm{max}} v_\mathrm{max}$ from three AR simulations with parameters $(v^1_\mathrm{min}, v^1_\mathrm{max}), (v^1_\mathrm{min}, v^2_\mathrm{max}), (v^2_\mathrm{min}, v^1_\mathrm{max})$. More precisely, this allows us to approximate the total speed-up as

[6] Note that, in this linear approximation, we consider a fixed ratio δ such that $v_\mathrm{min} = \delta v_\mathrm{max}$.

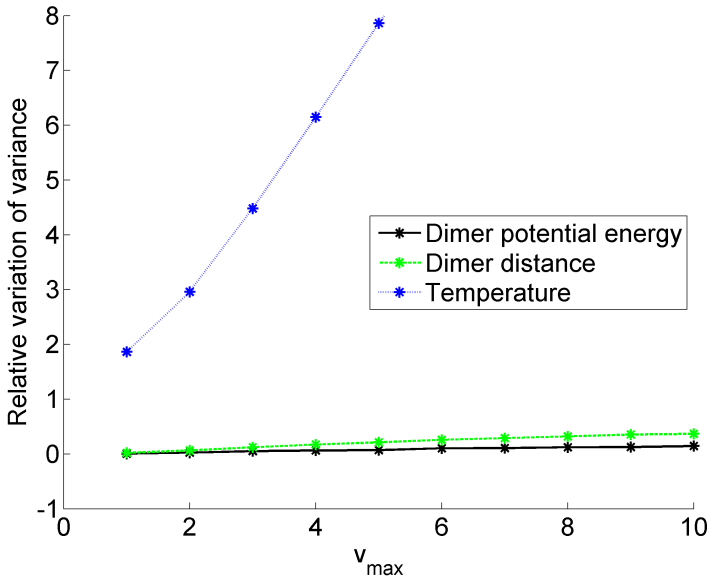

Fig. 4.5: *Relative deviation of the asymptotic variance from the variance in the standard dynamics.* We considered a system of described in Section 4.4. We measured the variance of the dimer distance A_D (green), the dimer potential A_{DW} (black) and the temperature $\mathcal{T}$ (blue) in various parametrization of the AR dynamics. We plotted the relative deviation of the variance from the variance in the standard dynamics for parameters $v_{\max}$ with $\delta = 0.8$. Note that the variance is more perturbed for $\mathcal{T}$ than for the other two observables, which depend only on the dimer particles.

$$S_{\text{total}}(v_{\min}, v_{\max}) \approx S_{\text{a}}(v_{\min}, v_{\max}) \frac{1}{1 + \frac{c_{v_{\max}}}{\sigma^2(0,0)} v_{\max}} \,. \tag{4.18}$$

We choose $(v_{\min}, v_{\max}) \in \{(3,6), (3,7), (2,6)\}$ and we estimate the slope $c_{v_{\max}}$. Table 4.1 shows the comparison with the slope directly obtained from simulations with fixed $\delta = 0.9$ and $\delta = 0.8$ for $v_{\max} \in [1, 10]$ (see Figure 4.5). This confirms that it is possible to capture the quantitative behavior of the relative slope

$c_{v_{\max}}/\sigma^2_{A_i}(0,0)$	$\delta = 0.9$: 3 points	$\delta = 0.9$: $v_{\max} \in [0, 10]$
A_{DW}	0.017863	0.016452
A_D	0.043855	0.042729
	$\delta = 0.8$: 3 points	$\delta = 0.8$: $v_{\max} \in [0, 10]$
A_{DW}	0.016426	0.015028
A_D	0.039587	0.039787

Table 4.1: Comparison of the relative deviation of the variance, obtained from linear interpolation of three points and the interpolation of values obtained from many simulations.

$c_{v_{\max}}/\sigma^2_{\varphi}(0,0)$ from only three AR simulations. Note that the same approach could be used to determine

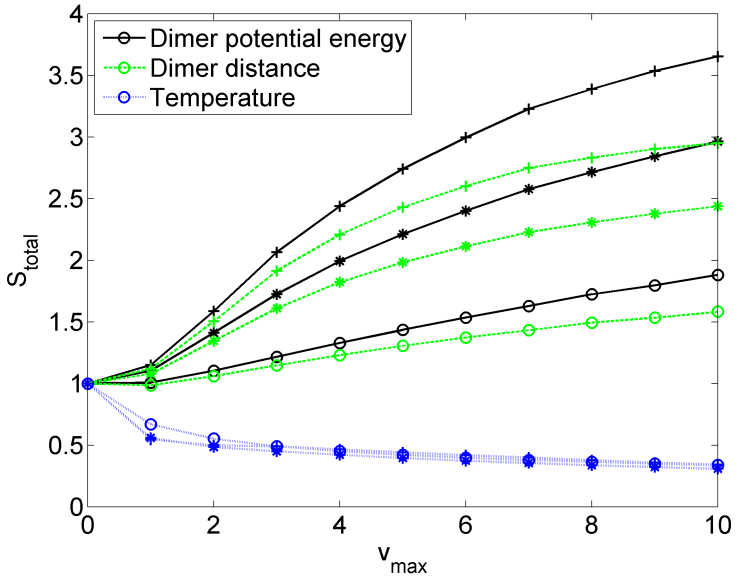

Fig. 4.6: *Numerical estimation of the total speed-up depending on the parameters ratio.* We estimated the total speed-up S_{total} given by (4.4) for system described in Section 4.4. The algorithmic speed-up as well as the variance (see Figure 4.5) were obtained directly from the measurements in the simulation, *i.e.* not from the analytical formula. On the plot the results are showed for three observables (various color and line styles). The various markers correspond to different value of δ: the marker "open circles" corresponds to $\delta = 0.5$, the marker "star" corresponds to $\delta = 0.8$ and the marker "plus sign" corresponds to $\delta = 0.9$, such that $\delta = v_{\min}/v_{\max}$. The bigger is δ, the more particles are restrained and hence the bigger is the algorithmic speed-up.

the behavior of the variance as a function of different temperatures by measuring the variance only at a few points.

We have obtained an estimation of the variance $\sigma^2(v_{\min}, v_{\max})$. This allows us to express the total speed-up S_{total} as a function of $v_{\min}$ and $v_{\max}$, which is depicted on Figure 4.7 for A_D.

Remark 4.1. *It would be possible to push the parameters in Figure 4.7 in order to achieve a higher speed-up, up to the moment when the variance increase would start countering the algorithmic speed-up. Since the total speed-up depends on the simulated system and a concrete observable function, it does not make much sense to try and find the limit for our toy model. Moreover, for large parameters values, it is difficult to converge the quadratures in* (4.14) *and computationally too expensive to obtain the estimates numerically in the sense of Figure 4.7. Nevertheless, we believe Figure 4.7 provides a good understanding of the qualitative behavior of the total speed-up.*

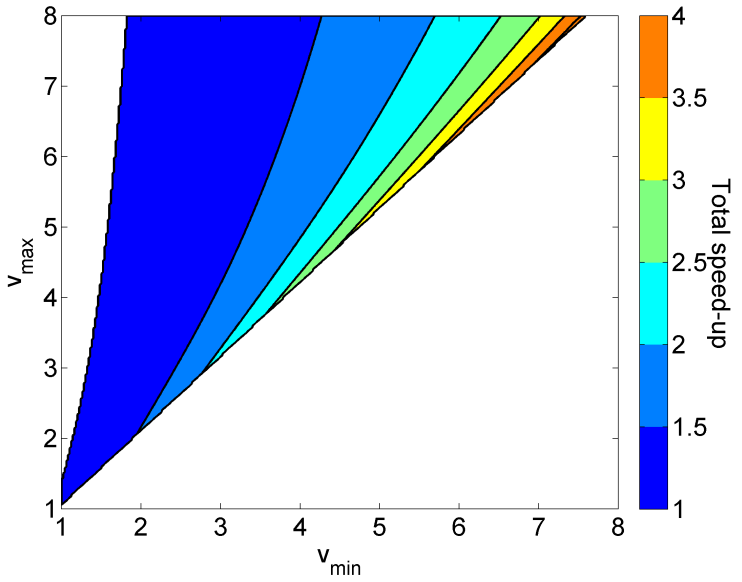

Fig. 4.7: *Analytical estimation of the total speed-up.* We estimated the expected total speed-up S_{total} for the observable dimer distance A_D with respect to parameters v_{min} and v_{max} ($v_{\mathrm{max}} \leqslant 0.95 v_{\mathrm{max}}$). The variance was estimated from three points as a linear function of v_{min} and v_{max} and we used the analytical estimation of S_{a} according to (4.12). Only $S_{\mathrm{total}} > 1$ is plotted.

5

Extensions and perspectives

Summary. This chapter presents several works on progress. The aim of the first one is to find kinetic energy functions which allow to reduce the metastability of standard Langevin dynamics. We discuss also other extensions such as the unbiasing of the dynamical properties of the modified Langevin dynamics through appropriate Girsanov weights; and present some ideas to compare the convergence rates between various Langevin dynamics in quantitative way by a recently introduced hypocoercive approach.

5.1 Decreasing metastability with modified kinetic energies

In this section we present work on progress on the reduction of metastability by introducing specific kinetic energy functions. These preliminary results have been preprinted as [114].

We consider Langevin dynamics with kinetic energies growing more than quadratically at infinity, in an attempt to reduce the metastability. Recall indeed that the crucial part of the sampling of the canonical measure is the position marginal $\nu(dq) = Z_\nu^{-1} \mathrm{e}^{-\beta V(q)}\, dq$. The marginal distribution of μ in the variable q is always ν, whatever the choice of the kinetic energy U. The extra freedom provided by U can be used in order to reduce the metastability of the dynamics.

According to our preliminary results, we propose to choose the kinetic energy similar to the potential energy. We demonstrate on a simple low-dimensional example that such a modification of the dynamics can

lead to a faster exploration of the phase-space and hence to improved convergence rates in wall-clock time. An exploration of this idea for high dimensional problems requires further work.

In the following numerical experiments, we discretize the Langevin dynamics (2.4) by the GHMC scheme summarized in Section 3.3.3 with $\gamma = 1$, $m = 1$ and $\Delta t = 0.001$.

5.1.1 Energy barrier in 1D

In the first example, we consider a 1D system, described by the multi-well potential

$$V(q) = h\,\left(|q-1|^{-2} + |q+1|^{-2} + |q-2|^{-2} + |q+2|^{-2}\right)^{-1},$$

see Figure 5.1(Left) for an illustration. There are three energetic barriers, which separate the four metastable regions in which the particle spends more time. We choose the prefactor $h = 10$ and perform simulations at the inverse temperature $\beta = 1$. For the same realization of Brownian motion, we consider five different kinetic energy functions:

(1) the standard one $U_1(p) = p^2/2$;
(2) a higher order polynomial function with shift $U_2(p) = |2p-4|^4/4$;
(3) the same kinetic energy function as the potential energy function $U_3 \equiv V$;
(4) a double-well function $U_4(p) = \left(|x-1|^{-2} + |x+1|^{-2}\right)^{-1}$;
(5) and a "heavy tail" function $U_5(p) = |p|^{5/4}\,(5/4)^{-1}$.

On Figure 5.1(Right) we plot instantaneous positions (left) and momenta (right) over the number of time steps for kinetic energies U_i with $i = 1, \dots 5$ (top to bottom). We observe that for the standard kinetic energy positions q switch between the two biggest metastable states separated at zero only twice during the $N_{\text{iter}} = 10^6$ time steps. On the other hand, we observe that the dynamics exhibits more transitions for any other choice of the kinetic energy as described above. The most numerous transitions are obtained with the kinetic energies U_2 and U_3.

5.1.2 Energy barrier in 2D

In order to confirm the findings of the previous section in a two-dimensional system (*i.e* $q = (x, y) \in \mathbb{R}^2$), we consider the potential already considered in [81]:

$$V(x,y) = \frac{1}{6}\left(4\left(-x^2 - y^2 + w\right)^2 + 2h\left(x^2-2\right)^2 + \left((x+y)^2 - w\right)^2 + \left((x-y)^2 - w\right)^2\right), \qquad (5.1)$$

where we choose $w = 1$ and $h = 5$. This potential can be seen as some effective double well potential in the x direction (see Figure 5.2 for contour plots). The metastability of Langevin dynamics is caused by some energetic barrier in this direction at $x = 0$.

Various kinetic energies can be considered. We focus on the following ones:

(1) the standard kinetic energy $U_1(x, y) = (x^2 + y^2)/2$;

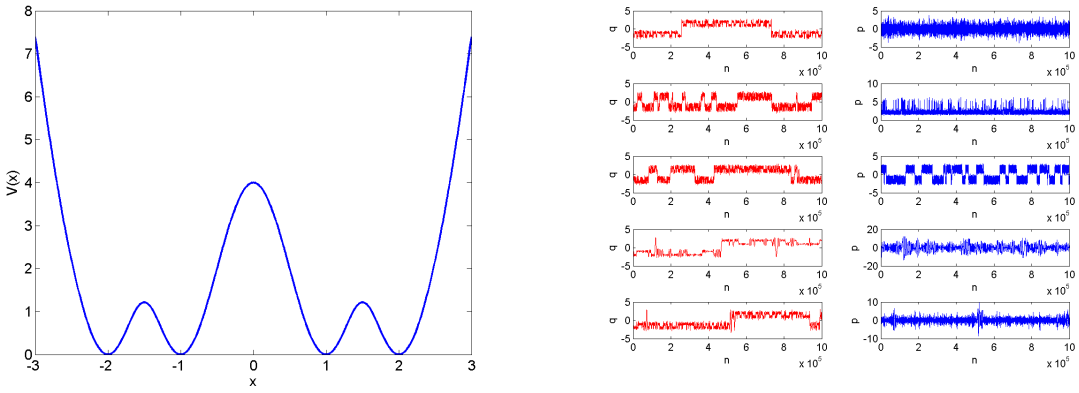

Fig. 5.1: (Right) Instantaneous values of positions and momenta with five kinetic energy functions and the multi-well potential (left). Kinetic energy functions (from top to bottom): standard one, *i.e.* $U_1(p) = p^2/2$; higher order polynomial function with shift, *i.e.* $U_2(p) = |2p-4|^4/4$; multi-well, *i.e.* the kinetic energy function is the same one as the potential energy function $U_3 \equiv V$; double-well function $U_4(p) = \left(|x-1|^{-2} + |x+1|^{-2}\right)^{-1}$; and "heavy tail" function, *i.e.* $U_5(p) = |p|^{5/4}(5/4)^{-1}$.

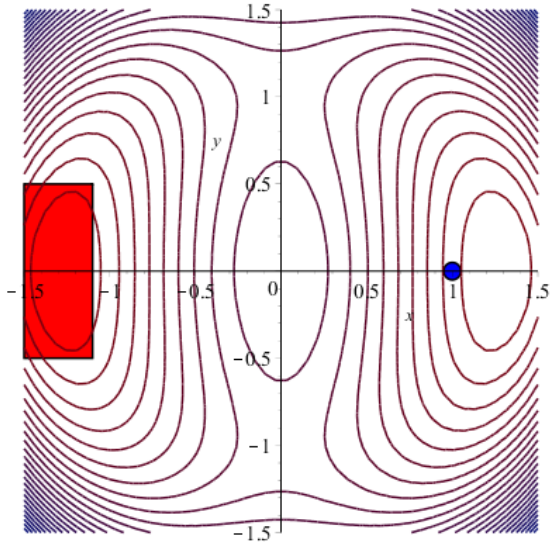

Fig. 5.2: Two dimensional double-well potential (5.1). We compute expected exit times between the starting configuration $A := (1,0)$ and the target set $B := \{(x,y) : x \leqslant -1 \text{ and } |y| \leqslant 0.5\}$.

(2) a fifth order polynomial in both directions $U_2(x,y) = \left(|x|^5 + |y|^5\right)/5$, which provides an example of light-tailed distribution of momenta;

(3) a heavy tailed function distribution of momenta, corresponding to the choice

$$U_3(x,y) = \frac{4}{5}\left[|x|^{5/4} + |y|^{5/4}\right];$$

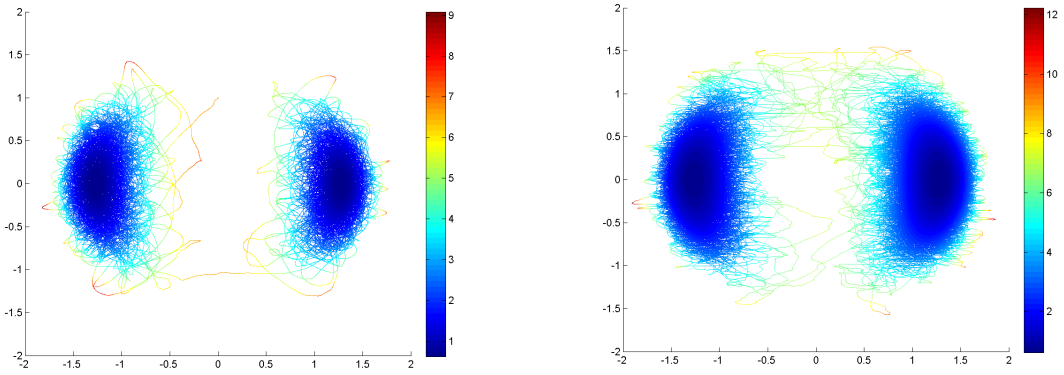

(a) Standard kinetic energy function.

(b) Same kinetic energy function as the potential energy function, *i.e.* $U \equiv V$.

Fig. 5.3: Positions as a function of time for the modified Langevin dynamics with the two-dimensional double well potential (5.1), and two different kinetic energy functions. The simulation time is $T = 1000$, and the same realization of the Brownian motion is used in both cases. For the same number of simulation steps, there are more crossings between the wells for the dynamics with the modified kinetic energy (Right) than for the standard one (Left). The coloring corresponds to the values of the potential energy.

(4) the same function as the potential function $U_4 \equiv V$;

(5) a double-well function in the x-direction and a quadratic function in the $y-$direction:

$$U_5(x,y) = V_{\mathrm{DW}}(x) + \frac{y^2}{2}, \qquad V_{\mathrm{DW}}(x) = \left(|x-1|^{-2} + |x+1|^{-2}\right)^{-1}.$$

This function somewhat approximates V, so we expect the distribution of momenta under the canonical measure associated with U_5 to be close to the one associated with U_4;

Figure 5.3 presents two realizations for a physical time $T = 1000$ and an inverse temperature $\beta = 1$, for the choices U_1 and U_4 above. Note that, for the standard kinetic energy U_1, there is only one crossing from one well to the other during the simulation time. On the other hand, there are many more crossings for U_4.

In order to quantify the reduction of the metastability gained by modifying the kinetic energy function, we numerically estimate the expected hitting time between two sets separated by the energetic barrier. We start in fact from a given initial condition, which corresponds to the initial set $A := \{(1,0)\}$. We then compute the number of simulation steps necessary to reach the set $B := \{(x,y) : x \leqslant -1 \text{ and } |y| \leqslant 0.5\}$ (see Figure 5.2 for an illustration). The expected hitting time is estimated by an average over 1000 independent realizations of the exit process. We report in Table 5.1 the average physical time needed to reach the set B for each choice of the kinetic energy function, as well as the speed-up relative to the results obtained with the standard kinetic energy. Note that the exit time is almost three time smaller with U_4. Intuitively, heavy tailed distributions of momenta (corresponding to U_3 here) could be thought of as being interesting since they allow for larger velocities, which may facilitate the transition from one well to the other. This is howe-

Kinetic energy	$U_1 = U_{\text{std}}$	U_2	U_3	U_4	U_5
T_{hit}	297.2 [±9.5]	259.2 [±7.8]	307.0 [±9.6]	101.7 [±3.2]	203.4 [±6.3]
Speed up $T_{\text{hit}}/T_{\text{std}}$	1	1.155	0.97	2.92	1.46

Table 5.1: Expected hitting times according to the choice of the kinetic energy functions U_i (see text). Errors bars determined by 95% confidence intervals are reported in brackets.

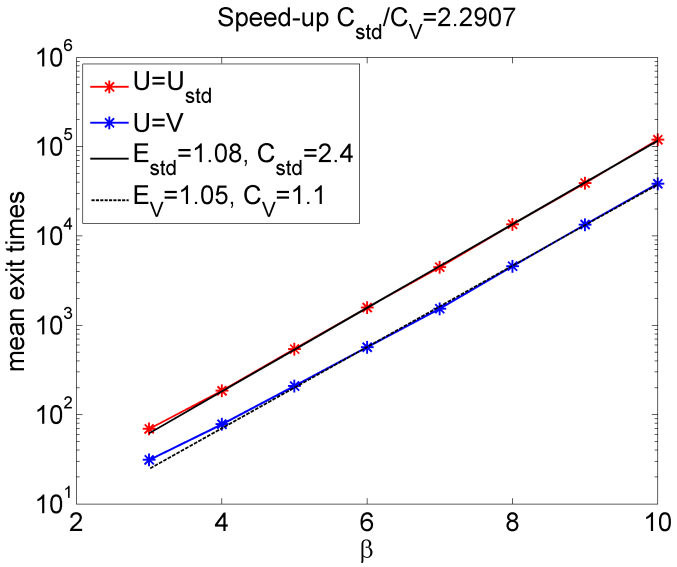

Fig. 5.4: Mean exit times over 2000 realizations as a function of $\beta \in \{3, 4, 5, 6, 7, 8, 9, 10\}$.

ver not the case. On the other hand, we observe that the double-well-like functions (U_4 and U_5) are most helpful to reduce the metastability of the dynamics and allow for more transitions from the region around $x = -1$ to the region around $x = 1$. Note that the exit time is almost three time smaller with U_4. Moreover, in Figure 5.4, we plot the average physical time needed to reach the set B as a function of the inverse temperature β. We observe an exponential growth of the hitting time with respect to β which is characteristic for metastability caused by energetic barriers in the low temperature limit by the Eyring-Kramers law (see for instance the presentation and the references in [14, 82]). We fit the hitting times as

$$T_{\text{hit}}(\beta) = C\mathrm{e}^{\beta E},$$

for some energy level E. For the results presented in Figure 5.4, the energy level E is the same for all kinetic energies, but the prefactor C is different; in fact smaller for the modified kinetic energy U_5 than for the standard kinetic energy U_1.

5.1.3 Higher dimensions

The excellent reduction in metastability we obtain on the simple low-dimensional systems above motivates us to test the relevance of this approach for higher dimensional systems.

5.1.3.1 Biasing reaction coordinates

A first track is to modify only the kinetic energy on the velocity of some reaction coordinate summarizing slow degrees of freedom, keeping the standard kinetic energy for faster degrees of freedom.

More precisely, we aim at performing numerical simulations of a dimer-solvent system described in Section 1.1.1.1. The reaction coordinate $\xi : \mathcal{D} \to [0,1]$ describing the transition between the compact and stretched state of the dimer is given by (for more details see [81, Section 1.3.2.4])

$$\xi(q) = \frac{|q_1 - q_2| - r_0}{2w}.$$

The results from the previous section suggest that we can choose the kinetic energy of the dimer particles the same as the potential energy. On the other hand, we can use the standard kinetic energy for the solvent particles (see also the discussion about the solvent particles below). More precisely, an appealing idea is to consider a double-well energy on the relative momentum $(p_1 - p_2) \cdot e_{12}$, where

$$e_{12} = \frac{q_1 - q_2}{|q_1 - q_2|}$$

is the unit vector is the direction of the line of centers of the particles; the remaining components of the relative momentum, as well as $p_1 + p_2$, having quadratic kinetic energies.

Let us discuss some tracks to further generalize this approach, for a reaction coordinate which is a function $\xi : \mathbb{R}^d \to \mathbb{R}^{\tilde{d}}$ with $\tilde{d} \leqslant d$, such that $(\xi_{q_t}))_{t \geqslant 0}$ is a metastable process. A key quantity to this end is the effective velocity of the reaction coordinate:

$$v_\xi(q,p) = \nabla \xi(q)^T M^{-1} p,$$

see [81, Section 3.3.1.3] for an interpretation of this quantity. When an approximation $\overline{v}_\xi(p)$ of this function as a function of the momenta only is available, the kinetic energy can be chosen to be

$$U(p) = u_{\mathrm{mod}}(\overline{v}_\xi(p)) + \widetilde{U}_{\mathrm{std}}(p_\xi^\perp),$$

where $p_\xi^\perp$ is the component of p in the direction orthogonal to $\overline{v}_\xi(p)$, *i.e.*

$$p_\xi^\perp = p - \frac{p \cdot \overline{v}_\xi(p)}{|\overline{v}_\xi(p)|^2},$$

and $\widetilde{U}_{\mathrm{std}}$ is a quadratic kinetic energy in dimension $d - \widetilde{d}$.

5.1.3.2 Solvent-solute models

Since the kinetic energy can be chosen separately for each particle, we can choose also a specific kinetic energy for the solvent particles when a solvent-solute model is considered. Basically, we can consider two

options which can reduce the wall-clock time. The first option is to use a parametrization of AR kinetic energy which gives a high percentage of restrained solvent particles and hence significantly decreases the computational cost per time step. Alternatively, we can increase the maximal admissible time step by the following strategy: we have demonstrated that for some specific values the AR-Langevin dynamics is more stable and allows to take a bigger integration time step (Figures 3.6). This suggests to choose a specific AR kinetic energy according to the vibrational frequencies of particles (a characterization already used for methods like RESPA in order to integrate slower and faster degrees of freedom separately [121]). We expect, that this effect is similar to increasing the effective mass of fast vibrational modes. More precisely, light particles (for instance atoms of hydrogen in water molecules) can have AR kinetic energy with parameters $v_{\min} = 0$ and $v_{\max}$ big enough and heavier particles could have the standard kinetic energy. For instance, the results presented in Figure 3.6 suggest that for the values $v_{\min} = 0$ and $v_{\max} = 6$ the dynamics admits a timestep 1.8 times bigger than for the standard dynamics. Since the maximal time step in the simulation is limited by the highest vibrational frequencies, we believe that this idea might help to increase the maximal time step of the discretized dynamics. Note that a change of the kinetic energy function is easy to implement and does not require a much higher computational cost. Again, a trade off between the maximal time step size and the variance should be considered in order to confirm the variance reduction in the wall-clock time.

Remark 5.1. *In order to slow down the dynamics and to increase the maximal admissible time step size Δt, the relativistic kinetic energy was suggested*[1] *for the Langevin dynamics. The relativistic kinetic energy reads*

$$U_{\mathrm{rel}}(p) = \sqrt{|p|^2 c^2 + m^2 c^4},$$

where c is the maximal speed (i.e. the speed of light in the relativistic theory). This can be understood also as an automatic way of tuning the mass according to the speed of the particle. Even though this approach allows to increase the maximal time step, its efficiency is not clear since the asymptotic variance increases significantly.

5.2 Retrieving correct dynamical properties

In this thesis, we focused on the computation of the ergodic averages with respect to μ. Langevin dynamics are however also used to predict dynamical properties such as transport coefficients or exit times. Of course, a non-standard the kinetic energy changes the dynamical behavior of the dynamics. However, many methods are used to accelerate the sampling of reactive paths change the original dynamics (for instance, simulations at different temperatures are combined in parallel tempering method [50]). As already explored in [34], a possible remedy in order to retrieve correct physical dynamical properties of modified dynamics is to introduce Girsanov weights on the samples.

Let us recall that in the case of the AR-Langevin dynamics, we have studied the asymptotic variance, which already is a dynamical property since it can be interpreted as some integrated autocorrelation function.

[1] An idea suggested by Ralf Everaers at a summer-school at Ecole de Physique des Houches in May 2015.

We expect that it is possible to extend the results of Proposition 2.1, which shows linear expansion in the AR parameters of the asymptotic variance, to other dynamical properties.

5.3 Quantifying convergence rates in $L^2(\mu)$

The numerical results from Section 5.1 suggest that some kinetic energy functions might reduce the metastability of the dynamics. It may also be possible to compare in quantitative fashion explicit upper bounds on the convergence rate obtained by the modified hypocoercive approach introduced in [38, 39]. This would allow to state rigorous results on the choice of the best kinetic energy.

Let us describe the approach of Dolbeault, Mouhot and Schmeiser [39] in a few words. It is based on the introduction of a modified entropy functional

$$\mathcal{H}(g) = \frac{1}{2} \|g\|_{L^2(\mu)} + \varepsilon \langle Ag, g \rangle_{L^2(\mu)},$$

for some (small) $\varepsilon > 0$ and where the (bounded) operator A reads

$$A = -\left(1 - \Pi \mathcal{L}_{\mathrm{Ham}}^2 \Pi\right)^{-1} \Pi \mathcal{L}_{\mathrm{Ham}}, \quad (\Pi g)(q) = \int_{\mathbb{R}^d} g(q,p)\kappa(p).$$

It turns out that $\mathcal{H}(g)$ induces a norm equivalent to the $L^2(\mu)$ norm. In addition, when the marginal measures ν and κ satisfy Poincare inequalities, it is possible to obtain a functional inequality similar to a Poincare inequality in the norm induced by $\mathcal{H}$. This can then be translated into an exponential convergence of the semigroup: there exist $C, \lambda > 0$ such that, for $\varphi \in L^2(\mu)$ with average 0 with respect to μ,

$$\left\| \mathrm{e}^{t\mathcal{L}} \varphi \right\|_{L^2(\mu)} \leqslant C \mathrm{e}^{-\lambda t} \|\varphi\|_{L^2(\mu)}.$$

The proof in [39] is currently written only for a quadratic kinetic energy. The aim would be to extend it to more general choices $U(p)$, and to quantify as precisely as possible the dependence on U of the convergence rate λ and the prefactor C in the above inequality.

References

[1] A. Abdulle, D. Cohen, G. Vilmart, and K.C. Zygalakis. High weak order methods for stochastic differential equations based on modified equations. *SIAM J. Sci. Comput.*, 34(3):A1800–A1823, 2012.

[2] A. Abdulle, G. Vilmart, and K. C. Zygalakis. High order numerical approximation of the invariant measure of ergodic SDEs. *SIAM J. Num. Anal.*, 52(4):1600–1622, 2014.

[3] A. Abdulle, G. Vilmart, and K. C. Zygalakis. Long time accuracy of Lie–Trotter splitting methods for Langevin dynamics. *SIAM J. Num. Anal.*, 53(1):1–16, 2015.

[4] C. Abrams and G. Bussi. Enhanced sampling in molecular dynamics using metadynamics, replica-exchange, and temperature-acceleration. *Entropy*, 16(1):163–199, 2013.

[5] B. J. Alder and T. E. Wainwright. Phase transition for a hard sphere system. *J. Comput. Phys.*, 27(5):1208, 1957.

[6] M. P. Allen and D. J. Tildesley. *Computer simulation of liquids*. Oxford University Press, 1989.

[7] H. C. Andersen. Molecular dynamics simulations at constant pressure and/or temperature. *J. Chem. Phys.*, 72(4):2384–2393, 1980.

[8] S. Andradóttir, D. P. Heyman, and T. J. Ott. Variance reduction through smoothing and control variates for Markov chain simulations. *ACM Trans. Model. Comput. Simul.*, 3(3):167–189, 1993.

[9] S. Artemova and S. Redon. Adaptively restrained particle simulations. *Phys. Rev. Lett.*, 109(19):190201, 2012.

[10] R. Assaraf and M. Caffarel. Zero-variance principle for Monte Carlo algorithms. *Phys. Rev. Lett.*, 83(23):4682, 1999.

[11] D. J. Auerbach, W. Paul, A. F. Bakker, C. Lutz, W. E. Rudge, and F. F. Abraham. A special purpose parallel computer for molecular dynamics: Motivation, design, implementation, and application. *J. Phys. Chem.*, 91(19):4881–4890, 1987.

[12] R. Balian. *From microphysics to macrophysics: methods and applications of statistical physics*, volume 2. Springer Science & Business Media, 2006.

[13] C. H. Bennett. Mass tensor molecular dynamics. *J. Comput. Phys.*, 19(3):267–279, 1975.

[14] N. Berglund. Kramers' law: Validity, derivations and generalisations. *Markov Process. Rel. Fields*, 19:459–490, 2013.

[15] B. J. Berne, M. Borkovec, and J. E. Straub. Classical and modern methods in reaction rate theory. *J. Phys. Chem.*, 92(13):3711–3725, 1988.

[16] A. Beskos, N. Pillai, G. Roberts, J. M. Sanz-Serna, and A. Stuart. Optimal tuning of the hybrid Monte Carlo algorithm. *Bernoulli*, 19(5A):1501–1534, 2013.

[17] R. N. Bhattacharya. On the functional Central Limit theorem and the law of the iterated logarithm for Markov processes. *Z. Wahrscheinlichkeit.*, 60(2):185–201, 1982.

[18] J. Bierkens. Non-reversible Metropolis-Hastings. *Statistics and Computing*, 26(6):1213–1228, 2016.

[19] P. Billingsley. *Measure and Probability*. John Wiley & Sons, 1995.

[20] M. Bosson, S. Grudinin, X. Bouju, and S. Redon. Interactive physically-based structural modeling of hydrocarbon systems. *J. Comput. Phys.*, 231(6):2581 – 2598, 2012.

[21] M. Bosson, S. Grudinin, and S. Redon. Block-adaptive quantum mechanics: an adaptive divide-and-conquer approach to interactive quantum chemistry. *J. Comp. Chem.*, 34(6):492–504, 2013.

[22] N. Bou-Rabee and M. Hairer. Nonasymptotic mixing of the MALA algorithm. *IMA J. Num. Anal.*, 33:80–110, 2012.

[23] N. Bou-Rabee and H. Owhadi. Long-run accuracy of variational integrators in the stochastic context. *SIAM J. Num. Anal.*, 48(1):278–297, 2010.

[24] N. Bou-Rabee and J. M. Sanz-Serna. Randomized Hamiltonian Monte Carlo. *arXiv preprint arXiv:1511.09382*, 2015.

[25] N. Bou-Rabee and E. Vanden-Eijnden. Pathwise accuracy and ergodicity of metropolized integrators for SDEs. *Commun. Pure Appl. Math.*, 63(5):655–696, 2009.

[26] N. Bou-Rabee and E. Vanden-Eijnden. A patch that imparts unconditional stability to explicit integrators for Langevin-like equations. *J. Comput. Phys.*, 231(6):2565–2580, 2012.

[27] C. Le Bris. Computational chemistry from the perspective of numerical analysis. *Acta Numerica*, 14:363–444, 2005.

[28] A. Brünger, C. L. Brooks, and M. Karplus. Stochastic boundary conditions for molecular dynamics simulations of ST2 water. *Chem. Phys. Lett.*, 105(5):495–500, 1984.

[29] R. E. Caflisch. Monte Carlo and quasi-Monte Carlo methods. *Acta Numerica*, 7:1–49, 1998.

[30] E. Cancès, M. Defranceschi, W. Kutzelnigg, C. Le Bris, and Y. Maday. Computational quantum chemistry: a primer. *Handbook of numerical analysis*, 10:3–270, 2003.

[31] E. Cancès, F. Legoll, and G. Stoltz. Theoretical and numerical comparison of some sampling methods for molecular dynamics. *ESAIM: Math. Mod. Num. Anal.*, 41(2):351–389, 2007.

[32] E. A. Carter, G. Ciccotti, J. T. Hynes, and R. Kapral. Constrained reaction coordinate dynamics for the simulation of rare events. *Chem. Phys. Lett.*, 156(5):472–477, 1989.

[33] M. Chen and Q. Shao. On Monte Carlo methods for estimating ratios of normalizing constants. *Ann. Stat.*, 25(4):1563–1594, 1997.

[34] J. D. Chodera, W. C. Swope, F. Noé, J.H. Prinz, M. R. Shirts, and V. S. Pande. Dynamical reweighting: Improved estimates of dynamical properties from simulations at multiple temperatures. *J. Chem. Phys.*, 134(24):244107, 2011.

[35] G. Ciccotti and M. Ferrario. Rare events by constrained molecular dynamics. *J. Molec. Liq.*, 89(1):1–18, 2000.

[36] C. Dellago, P. G. Bolhuis, and D. Chandler. On the calculation of reaction rate constants in the transition path ensemble. *J. Comput. Phys.*, 110(14):6617–6625, 1999.

[37] B. Devkota, A. S. Petrov, S. Lemieux, M. B. Boz, L. Tang, A. Schneemann, J. E. Johnson, and S. C. Harvey. Structural and electrostatic characterization of pariacoto virus: implications for viral assembly. *Biopolymers*, 91(7):530–538, 2009.

[38] J. Dolbeault, A. Klar, C. Mouhot, and C. Schmeiser. Hypocoercivity and a Fokker–Planck equation for fiber lay-down. *Appl. Math. Res. Exp*, pages 165–175, 2013.

[39] J. Dolbeault, C. Mouhot, and C. Schmeiser. Hypocoercivity for linear kinetic equations conserving mass. *Transact. A. Math. Soc.*, 367(6):3807–3828, 2015.

[40] S. Duane, A. D. Kennedy, B. J. Pendleton, and D. Roweth. Hybrid Monte Carlo. *Phys. Lett. B*, 195(2):216–222, 1987.

[41] A. B. Duncan, T. Lelievre, and G. A. Pavliotis. Variance reduction using nonreversible Langevin samplers. *J. Stat. Phys.*, 163(3):457–491, 2016.

[42] J. D. Durrant and J. A. McCammon. Molecular dynamics simulations and drug discovery. *BMC biology*, 9(1):1, 2011.

[43] P. Español, R. Delgado-Buscalioni, R. Everaers, R. Potestio, D. Donadio, and K. Kremer. Statistical mechanics of Hamiltonian adaptive resolution simulations. *J. Comput. Phys.*, 142(6):064115, 2015.

[44] P. Espanol and P. Warren. Statistical mechanics of dissipative particle dynamics. *Europhys. Lett.*, 30(4):191, 1995.

[45] M. Fathi and G. Stoltz. Improving dynamical properties of stabilized discretizations of overdamped Langevin dynamics. *arXiv preprint 1505.04905*, 2015.

[46] S. E. Feller, Y. Zhang, R. W. Pastor, and B. R. Brooks. Constant pressure molecular dynamics simulation: the Langevin piston method. *J. Chem. Phys.*, 103(11):4613–4621, 1995.

[47] M. I. Freidlin and A. D. Wentzell. *Random Perturbations*, pages 15–43. Springer US, New York, NY, 1984.

[48] D. Frenkel and B. Smit. *Understanding molecular simulation: from algorithms to applications*. Elsevier, 2002.

[49] C. J. Geyer. Estimating normalizing constants and reweighting mixtures in Markov chain Monte Carlo. Technical report 565, School of Statistics, University of Minnesota, 1994.

[50] C. J. Geyer and E. A. Thompson. Annealing Markov chain Monte Carlo with applications to ancestral inference. *J. Am. Stat. Assoc.*, 90(431):909–920, 1995.

[51] S. Goel, X. Luo, A. Agrawal, and R. L. Reuben. Diamond machining of silicon: a review of advances in molecular dynamics simulation. *Int. J. Mach. T. Manuf.*, 88:131–164, 2015.

[52] E. Hairer, C. Lubich, and G. Wanner. Geometric numerical integration illustrated by the Störmer–Verlet method. *Acta Numerica*, 12:399–450, 2003.

[53] E. Hairer, C. Lubich, and G. Wanner. *Geometric numerical integration: structure-preserving algorithms for ordinary differential equations*, volume 31. Springer Science & Business Media, 2006.

[54] M. Hairer and J.C. Mattingly. Yet another look at Harris' ergodic theorem for Markov chains. *Seminar on Stochastic Analysis, Random Fields and Applications VI*, 63:109–117, 2011.

[55] M. Hairer and G. Pavliotis. From ballistic to diffusive behavior in periodic potentials. *J. Stat. Phys.*, 131:175–202, 2008.

[56] W. K. Hastings. Monte Carlo sampling methods using Markov chains and their applications. *Biometrika*, 57:97–109, 1970.

[57] S. G. Henderson. Variance reduction via an approximating Markov process. PhD thesis, Department of Operations Research, Stanford University, 1997.

[58] R. W. Hockney and J. W. Eastwood. *Computer simulation using particles*. CRC Press, 1988.

[59] P. J. Hoogerbrugge and J. M. V. A. Koelman. Simulating microscopic hydrodynamic phenomena with Dissipative Particle Dynamics. *Europhys. Lett.*, 19(3):155, 1992.

[60] W. G. Hoover. Canonical dynamics: equilibrium phase-space distributions. *Phys. Rev. A*, 31(3):1695, 1985.

[61] L. Hörmander. Hypoelliptic second order differential equations. *Acta Mathematica*, 119(1):147–171, 1967.

[62] L. Hörmander. *The Analysis of Linear Partial Differential Operators. I-IV*. Springer, 1985.

[63] J. A. Izaguirre and S. S. Hampton. Shadow hybrid Monte Carlo: an efficient propagator in phase space of macromolecules. *J. Comput. Phys.*, 200(2):581–604, 2004.

[64] R. Joubaud, G. A. Pavliotis, and G. Stoltz. Langevin dynamics with space-time periodic nonequilibrium forcing. *J. Stat. Phys.*, 158(1):1–36, 2015.

[65] M. Karplus and J. A. McCammon. Molecular dynamics simulations of biomolecules. *Nat. Struct. & Molec. Bio.*, 9(9):646–652, 2002.

[66] I. G. Kevrekidis and G. Samaey. Equation-free multiscale computation: Algorithms and applications. *Ann. Rev.Phys .Chem.*, 60:321–344, 2009.

[67] W. Kliemann. Recurrence and invariant measures for degenerate diffusions. *Ann. Probab.*, 15(2):690–707, 1987.

[68] P. E. Kloden and E. Platen. *Numerical Solution of Stochastic Differential Equations*. Springer, 1992.

[69] A. Kong, P. McCullagh, X. Meng, D. Nicolae, and Z. Tan. A theory of statistical models for Monte Carlo integration. *J. R .Stat. Soc.: Series B (Stat. Method.)*, 65(3):585–604, 2003.

[70] M. Kopec. Weak backward error analysis for overdamped Langevin processes. *IMA J. Numer. Anal.*, 55:1057–1103, 2014.

[71] M. Kopec. Weak backward error analysis for Langevin process. *BIT Numerical Mathematics*, 55(4):1057–1103, 2015.

[72] J. C. Latorre, G. A. Pavliotis, and P. R. Kramer. Corrections to Einstein's relation for Brownian motion in a tilted periodic potential. *J. Stat. Phys.*, 150(4):776–803, 2013.

[73] F. Legoll, M. Luskin, and R. Moeckel. Non-ergodicity of the Nosé–Hoover thermostatted harmonic oscillator. *Arch. Rat. Mech. Anal.*, 184(3):449–463, 2007.

[74] B. Leimkuhler and C. Matthews. Rational construction of stochastic numerical methods for molecular sampling. *App. Math. Res. eXpr.*, 2013(1):34–56, 2013.

[75] B. Leimkuhler and C. Matthews. Robust and efficient configurational molecular sampling via Langevin dynamics. *J. Comput. Phys.*, 138(17):174102, 2013.

[76] B. Leimkuhler and C. Matthews. *Molecular Dynamics*. Springer, 2015.

[77] B. Leimkuhler and C. Matthews. Efficient molecular dynamics using geodesic integration and solvent–solute splitting. *Proc. R. Soc. A*, 472(2189):20160138, 2016.

[78] B. Leimkuhler, C. Matthews, and G. Stoltz. The computation of averages from equilibrium and nonequilibrium Langevin molecular dynamics. *IMA J. Num. Anal.*, 36(1):13–79, 2016.

[79] B. Leimkuhler, E. Noorizadeh, and F. Theil. A gentle stochastic thermostat for molecular dynamics. *J. Stat. Phys.*, 135(2):261–277, 2009.

[80] T. Lelièvre. *Two Mathematical Tools to Analyze Metastable Stochastic Processes*, pages 791–810. In *Numerical Mathematics and Advanced Applications, 2011* (A. Cangiani, R. L. Davidchack, E. Georgoulis, A. N. Gorban, J. Levesley and M. V. Tretyakov, eds), Springer.

[81] T. Lelièvre, M. Rousset, and G. Stoltz. *Free Energy Computations: A Mathematical Perspective*. Imperial College Press, 2010.

[82] T. Lelièvre and G. Stoltz. Partial differential equations and stochastic methods in molecular dynamics. *Acta Numerica*, 25:681–880, 2016.

[83] Jerzy Leszczynski. *Handbook of computational chemistry*, volume 2. Springer Science & Business Media, 2012.

[84] S. Livingstone, M. Betancourt, S. Byrne, and M. Girolami. On the geometric ergodicity of Hamiltonian Monte Carlo. *arXiv:1601.08057*, 2016.

[85] J. C. Mattingly, A. M. Stuart, and D. J. Higham. Ergodicity for SDEs and approximations: locally Lipschitz vector fields and degenerate noise. *Stoch. Proc. Appl.*, 101(2):185–232, 2002.

[86] X. Meng and W. Wong. Simulating ratios of normalizing constants via a simple identity: a theoretical exploration. *Statistica Sinica*, 6(4):831–860, 1996.

[87] N. Metropolis, A. W. Rosenbluth, M. N. Rosenbluth, A. H. Teller, and E. Teller. Equations of state calculations by fast computing machines. *J. Chem. Phys.*, 21(6):1087–1091, 1953.

[88] S. P. Meyn and R. L. Tweedie. Stability of Markovian processes. II. Continuous-time processes and sampled chains. *Adv. Appl. Probab.*, 25:487–517, 1993.

[89] S. P. Meyn and R. L. Tweedie. *Markov Chains and Stochastic Stability*. Springer, 2012.

[90] G. N. Milstein and M. V. Tretyakov. *Stochastic Numerics for Mathematical Physics*. Springer Science & Business Media, 2013.

[91] S. Nosé. A molecular dynamics method for simulations in the canonical ensemble. *Molecular physics*, 52(2):255–268, 1984.

[92] S. Nosé. A unified formulation of the constant temperature molecular dynamics methods. *J. Comput. Phys.*, 81(1):511–519, 1984.

[93] S. Nosé. Constant temperature molecular dynamics methods. *Progr. Theor. Phys. Suppl.*, 103:1–46, 1991.

[94] M. Ottobre and G.A. Pavliotis. Asymptotic analysis for the generalized Langevin equation. *Nonlinearity*, 24(5):1629, 2011.

[95] P. Plechac and M. Rousset. Implicit mass-matrix penalization of Hamiltonian dynamics with application to exact sampling of stiff systems. *Multiscale Model. Sim.*, 8(2):498–539, 2010.

[96] M. Praprotnik, L. Delle Site, and K. Kremer. Multiscale simulation of soft matter: From scale bridging to adaptive resolution. *Annu. Rev. Phys. Chem.*, 59:545–571, 2008.

[97] D. C. Rapaport. *The art of molecular dynamics simulation*. Cambridge university press, 2004.

[98] S. Redon, G. Stoltz, and Z. Trstanova. Error analysis of modified Langevin dynamics. *J. Stat. Phys.*, 164(4):735–771, 2016.

[99] L. Rey-Bellet. *Ergodic Properties of Markov Processes*, pages 1–39. Springer Berlin Heidelberg, 2006.

[100] L. Rey-Bellet and K. Spiliopoulos. Irreversible Langevin samplers and variance reduction: a large deviations approach. *Nonlinearity*, 28(7):2081, 2015.

[101] H. Risken. *Fokker-Planck Equation*. Springer, 1984.

[102] G. O . Roberts and R. L. Tweedie. Exponential convergence of Langevin distributions and their discrete approximations. *Bernoulli*, pages 341–363, 1996.

[103] G. O. Roberts, A. Gelman, and W. R. Gilks. Weak convergence and optimal scaling of random walk metropolis algorithms. *Ann. Appl. Proba.*, 7(1):110–120, 1997.

[104] G. O. Roberts and J.S. Rosenthal. Optimal scaling of discrete approximations to Langevin diffusions. *J. R .Stat. Soc.: Series B (Stat. Method.)*, 60(1):255–268, 1998.

[105] G. O. Roberts and R. L. Tweedie. Exponential convergence of Langevin distributions and their discrete approximations. *Bernoulli*, 2(4):341–363, 1996.

[106] M. A. Rohrdanz, W. Zheng, M. Maggioni, and C. Clementi. Determination of reaction coordinates via locally scaled diffusion map. *J. Comput. Phys.*, 134(12):124116, 2011.

[107] R. Rossi, M. Isorce, S. Morin, J. Flocard, K. Arumugam, S. Crouzy, M. Vivaudou, and S. Redon. Adaptive torsion-angle quasi-statics: a general simulation method with applications to protein structure analysis and design. *Bioinformatics*, 23(13), 2007.

[108] P. J. Rossky, J. D. Doll, and HL H. L. Friedman. Brownian dynamics as smart Monte Carlo simulation. *J. Comput. Phys.*, 69(10):4628–4633, 1978.

[109] A. A. Samoletov, C. P. Dettmann, and M. A. J. Chaplain. Thermostats for "slow" configurational modes. *J. Stat. Phys.*, 128(6):1321–1336, 2007.

[110] T. Schlick. *Molecular Modeling and Simulation: An Interdisciplinary Guide*, volume 21. Springer Science & Business Media, 2010.

[111] Ch. Schütte. Conformational dynamics: Modelling, theory, algorithm, and application to biomolecules. Habilitation thesis in mathematics. Freie Universität Berlin. 1999.

[112] M. R. Shirts and J. D. Chodera. Statistically optimal analysis of samples from multiple equilibrium states. *J. Comput. Phys.*, 129(12):124105, 2008.

[113] M. R. Sorensen and A. F. Voter. Temperature-accelerated dynamics for simulation of infrequent events. *J. Comput. Phys.*, 112(21):9599–9606, 2000.

[114] G. Stoltz and Z. Trstanova. Stable and accurate schemes for Langevin dynamics with general kinetic energies. *arXiv:1609.02891*, 2016.

[115] J. E. Straub, M. Borkovec, and B. J. Berne. Molecular-dynamics study of an isomerizing diatomic in a Lennard-Jones fluid. *J. Chem. Phys.*, 89(8):4833–4847, 1988.

[116] C. R. Sweet, S. S. Hampton, R. D. Skeel, and J. A. Izaguirre. A separable shadow Hamiltonian hybrid Monte Carlo method. *J. Chem. Phys.*, 131(17):174106, 2009.

[117] D. Talay. Stochastic Hamiltonian dissipative systems: exponential convergence to the invariant measure, and discretization by the implicit Euler scheme. *Markov Proc. Rel. Fields*, 8:163–198, 2002.

[118] D. Talay and L.Tubaro. Expansion of the global error for numerical schemes solving stochastic differential equations. *Stoch. An. Appl.*, 8(4):483–509, 1990.

[119] L. Tang, K. N. Johnson, L. A. Ball, T. Lin, M. Yeager, and J. E. Johnson. The structure of pariacoto virus reveals a dodecahedral cage of duplex RNA. *Nat. Struct. & Molec. Bio.*, 8(1):77–83, 2001.

[120] Z. Trstanova and S. Redon. Estimating the speed-up of Adaptively Restrained Langevin dynamics. *arXiv:1607.01489*, 2016.

[121] M. E. Tuckerman. *Statistical Mechanics: Theory and Molecular Simulation*. Oxford University Press, 2010.

[122] M. E. Tuckerman and B. J. Berne. Molecular dynamics in systems with multiple time scales: Systems with stiff and soft degrees of freedom and with short and long range forces. *J. Comput. Phys.*, 95(11):8362–8364, 1991.

[123] M. E. Tuckerman, B. J. Berne, and G. J. Martyna. Molecular dynamics algorithm for multiple time scales: Systems with long range forces. *J. Comput. Phys.*, 94(10):6811–6815, 1991.

[124] M. E. Tuckerman, B. J. Berne, and G. J. Martyna. Reversible multiple time scale molecular dynamics. *J. Comput. Phys.*, 97(3):1990–2001, 1992.

[125] M. E. Tuckerman, B. J. Berne, and A. Rossi. Molecular dynamics algorithm for multiple time scales: Systems with disparate masses. *J. Chem. Phys.*, 94(2):1465–1469, 1991.

[126] L. Verlet. Computer "experiments" on classical fluids. I. Thermodynamical properties of Lennard-Jones molecules. *Phys. Rev.*, 159(1):98, 1967.

[127] C. Villani. Hypocoercivity. *Mem. Amer. Math. Soc.*, 202(950), 2009.

[128] A. F. Voter. Hyperdynamics: Accelerated molecular dynamics of infrequent events. *Phys. Rev. Lett.*, 78(20):3908, 1997.

[129] A. F. Voter. Parallel replica method for dynamics of infrequent events. *Phys. Rev. B*, 57(22):R13985, 1998.

[130] A. F. Voter, F. Montalenti, and T. C. Germann. Extending the time scale in atomistic simulation of materials. *Ann. Rev. Mat. Res.*, 32(1):321–346, 2002.

[131] A. Warshel and M. Levitt. Theoretical studies of enzymic reactions: dielectric, electrostatic and steric stabilization of the carbonium ion in the reaction of lysozyme. *J. Mol. Bio.*, 103(2):227–249, 1976.

[132] K. C. Zygalakis. On the existence and the applications of modified equations for stochastic differential equations. *SIAM J. Sc. Comp.*, 33(1):102–130, 2011.